



AN ABSTRACT OF THE DISSERTATION OF

Narumol Jariyasopit for the degree of Doctor of Philosophy in Chemistry presented on May 17, 2013.

Title: The Atmospheric Chemistry of Particulate-bound Polycyclic Aromatic Hydrocarbons: Concentration, Prediction, Laboratory Studies, and Mutagenicity

Abstract approved:

---

Staci L. Massey Simonich

The trans-Pacific atmospheric transport of particulate matter (PM)-bound polycyclic aromatic hydrocarbons (PAHs) to remote sites in western North America has been well documented and has triggered research questions regarding to atmospheric transformation of PM-bound PAHs and the potential impacts on human health from their inhalation exposure. In this dissertation, field measurements, theoretical studies, laboratory experiments, and mutagenicity studies were used to begin the address the questions as to whether PM-bound PAHs undergo atmospheric transformation into mutagenic nitro-PAHs (NPAHs) during trans-Pacific atmospheric transport. PM extracts were tested in the Salmonella mutagenicity assay, using *Salmonella typhimurium* strain TA98 (with and without metabolic activation), to determine the mutagenic activities in relation to the chemical composition of the extracts.

The sampling of atmospheric PM with diameter  $< 2.5 \mu\text{m}$  ( $\text{PM}_{2.5}$ ) before, during, and after the Olympic Games 2008 in Beijing provided some insights into the concentrations, chemical composition, photochemistry, and mutagenicity at the source of emission. The PAH, NPAH and OPAH composition of the  $\text{PM}_{2.5}$  was similar throughout the sampling periods, which included the period when a wide range of combustion sources were controlled. In addition, it showed that PAHs were associated with both local and regional emissions, while the NPAH and OPAH concentrations were only correlated with the NO concentrations, indicating that the NPAH and OPAH were primarily associated with local emissions. The characteristic NPAH ratios suggested a predominance of photochemical formation of NPAHs through OH radical-initiated reactions in the atmosphere.

Subsequently, the heterogeneous reactions of PAHs bound to Beijing ambient PM with various oxidants, including  $\text{NO}_3/\text{N}_2\text{O}_5$ , OH radical and  $\text{O}_3$ , were studied using an environmental reaction chamber under simulated trans-Pacific transport conditions. In addition, PM collected from Riverside, CA was simultaneously exposed along with the Beijing PM in order to allow us to compare the reactivity between two different sites. In general,  $\text{O}_3$  was most effective in degrading PM-bound PAHs with more than five rings, except for benzo[a]pyrene which was degraded by  $\text{O}_3$  and  $\text{NO}_3/\text{N}_2\text{O}_5$  equally well. However, the NPAHs were most effectively formed during the  $\text{NO}_3/\text{N}_2\text{O}_5$  exposure. The reactivity of the PM could be explained by the degree to which the PM had been photochemically aged because the accumulation of degradation products on the surface of PM appeared to inhibit further atmospheric degradation of parent PAHs. For the

NO<sub>3</sub>/N<sub>2</sub>O<sub>5</sub> exposure, the increase in direct-acting mutagenicity was associated with the formation of mutagenic NPAHs.

Additional laboratory experiments were carried out in order to identify NPAH products of 5- to 6-ring PAHs through the heterogeneous reactions of surface-bound PAHs with NO<sub>2</sub>, NO<sub>3</sub>/N<sub>2</sub>O<sub>5</sub>, O<sub>3</sub>, and OH radicals. Five PAHs, benzo[a]pyrene-d<sub>12</sub>, benzo[k]fluoranthene-d<sub>12</sub>, benzo[g,h,i]perylene-d<sub>12</sub>, dibenzo(a,i)pyrene-d<sub>14</sub>, and dibenzo[a,l]pyrene, were spiked onto quartz fiber filters and exposed in the chamber. Some of the identified NPAH products have not yet been measured in the environment. In parallel to the laboratory experiments, a theoretical study was conducted to assist in predicting the formation of NPAH isomers based on the gas-phase OH radical-initiated reaction. This study has shown that NO<sub>2</sub> and NO<sub>3</sub>/N<sub>2</sub>O<sub>5</sub> were effective oxidizing agents in transforming PAHs deposited on filters to NPAHs, under these experimental conditions. The lighter of the PAHs studied, including benzo[a]pyrene-d<sub>12</sub>, benzo[k]fluoranthene-d<sub>12</sub> and benzo[ghi]perylene-d<sub>12</sub>, yielded more than one mono-nitro isomer product, whereas dibenzo[a,l]pyrene and dibenzo[a,i]pyrene-d<sub>14</sub> resulted in the formation of only one mono-nitro isomer product. The direct-acting mutagenicity increased the most after NO<sub>3</sub>/N<sub>2</sub>O<sub>5</sub> exposure, particularly for benzo[k]fluoranthene-d<sub>12</sub> in which dinitro PAHs were observed.



©Copyright by Narumol Jariyasopit  
May 17, 2013  
All Rights Reserved

The Atmospheric Chemistry of Particulate-bound Polycyclic Aromatic Hydrocarbons:  
Concentration, Prediction, Laboratory Studies, and Mutagenicity

by

Narumol Jariyasopit

A DISSERTATION

submitted to

Oregon State University

in partial fulfillment of

the requirements for the

degree of

Doctor of Philosophy

Presented May 17, 2013

Commencement June 2013

Doctor of Philosophy dissertation of Narumol Jariyasopit presented on May 17, 2013

APPROVED :

---

Major Professor, representing Chemistry

---

Chair of the Department of Chemistry

---

Dean of the Graduate School

I understand that my dissertation will become part of the permanent collection of Oregon State University libraries. My signature below authorizes release of my dissertation to any reader upon request.

---

Narumol Jariyasopit, Author

## ACKNOWLEDGEMENTS

I wish to express my sincere thanks to my major advisor, Dr. Staci Simonich for her advice, guidance, support, and patience over the years. I am grateful to her for this precious opportunity to work on this project. I would also like to thank my committee members, Dr. William Baird, Dr. Jennifer Field, Dr. Claudia Maier and Dr. Fredrick Prah, Dr. Paul Ha-Yeon Cheong for sharing your expertise and time on this research. I wish to thank Dr. Janet Arey and Dr. Roger Atkinson, for their profound scientific perspectives, advice, precious time, and resources. Also, I thank their last Ph.D. student, Dr. Kathryn Zimmermann for her assistance and input in our collaborative projects. I would like to thank Dr. Paul Ha-Yeon Cheong for teaching and advising on the computational project. I thank Dr. Shu Tao and his graduate students at Peking University for sample collection. I would also like to thank Dr. Joseph Nibler, my undergraduate research advisor, for introducing me to scientific research and his mentorship. I thank Dr. David Yu for teaching me the Salmonella mutagenicity assay and providing the service.

I wish to express my thanks to my fellow laboratory members (Jill, Wentao, Leah G., Carlos, Jing, Julie, Rita, Oleksii, Yuling, Leah C., Christopher, Scott, Melissa, Pun, Kevin, Shelby, Anna), and friends in Corvallis for their encouragement and support, especially when my right hand did not want to work. I am grateful to Jill, Nathan, and Peter for editing my drafts. I appreciate all the help from the staff in the Chemistry and Environmental and Molecular Toxicology departments at Oregon State University.

I am extremely thankful to my family and friends in Thailand for their infinite support and sincerely tough criticisms. Lastly, I thank all the misfortune and failures that have happened or will happen, I welcome them.

## CONTRIBUTION OF AUTHORS

Dr. Staci L. Massey Simonich from Oregon State University provided advice and support in all aspects of this dissertation.

For all the following studies, Dr. Tian-Wei Yu and Dr. Roderick H. Dashwood provided advice and service in the Salmonella mutagenicity assay. Jill Schrlau assisted in sample preparation and analysis and provided guidance in instrumental use and maintenance. Dr. Shu Tao provided assistance in air sample collection.

Chapter 2. Dr. Shu Tao, Dr. Wentao Wang, Wei Zhang, Xuejun Wang from Peking University provided assistance in air sample collection. Dr. Wentao Wang also assisted in the particulate matter sample method development, sample preparation, and sample analysis. Dr. Yuling Jia provided the high molecular weight polycyclic aromatic hydrocarbon data.

Chapter 3. Melissa McIntosh synthesized the nitrated polycyclic aromatic hydrocarbon standards. Dr. Rich Carter provided advice during the syntheses. Dr. Paul Ha-Yeon Cheong provided advice and support in computational studies.

Chapter 3 and 4. Dr. Janet Arey, Dr. Roger Atkinson and Dr. Kathryn Zimmermann from University of California, Riverside, provided Riverside particulate matter samples, advice on experimental design, and technical support in environmental chamber studies which were carried out at the Air Pollution Research Center, University of California, Riverside. Additionally they also provided advice in data interpretation.

## TABLE OF CONTENTS

	<u>Page</u>
<b>CHAPTER 1. INTRODUCTION</b>	
1.1 Sources of Polycyclic Aromatic Hydrocarbons, Nitrated PAHs and Oxygenated PAHs.....	1
1.2 Nitration Reactions of Gas-phase PAHs in the Atmosphere.....	2
1.3 Heterogeneous Nitration Reactions of Particle-bound PAHs.....	4
1.4 Toxicity of PAHs, NPAHs and OPAHs.....	5
1.5 Scope and significance.....	6
1.6 References.....	14
<b>CHAPTER 2. CONCENTRATION AND PHOTOCHEMISTRY OF PAHs, NPAHs, AND OPAHs AND TOXICITY OF PM<sub>2.5</sub> DURING THE BEIJING OLYMPIC GAMES</b>	
ABSTRACT.....	19
2.1 Introduction.....	20
2.2 Materials and Methods	
2.2.1 Sampling.....	21
2.2.2 Black and Organic Carbon Measurement.....	22
2.2.3 Chemicals.....	22
2.2.4 Sample extraction and Analysis.....	23
2.2.5 Toxicology Studies.....	26
2.2.6 Gas Pollutant Data.....	28
2.3 Results and Discussion	
2.3.1 Effect of Source Control Measures on BC, OC, and Parent PAH Concentrations.....	28
2.3.2 Effect of Source Control Measures on NPAH and OPAH Concentrations.....	32
2.3.3 Parent PAH, NPAH and OPAH Sources.....	32
2.3.4 Role of PAH Photochemistry.....	35
2.3.5 Toxicity of the PM Extracts.....	36
2.4 Acknowledgements.....	39
2.5 References.....	41

TABLE OF CONTENTS (Continued)

	<u>Page</u>
<b>CHAPTER 3. NITRO-PAH PRODUCT FORMATION FROM HETEROGENEOUS REACTIONS OF PAHs WITH NO<sub>2</sub>, NO<sub>3</sub>/N<sub>2</sub>O<sub>5</sub>, O<sub>3</sub> AND OH RADICALS: PREDICTION, LABORATORY STUDIES AND TOXICITY</b>	
ABSTRACT.....	46
3.1 Introduction.....	47
3.2 Experimental	
3.2.1 Chemicals and Materials.....	49
3.2.2 Spiked Filter Preparation and Exposures.....	50
3.2.3 Sample Extraction and Analysis.....	52
3.2.4 Theoretical Study.....	52
3.2.5 Salmonella Mutagenicity Assay.....	53
3.3 Results and Discussion	
3.3.1 Theoretical Studies.....	53
3.3.2 NPAH Product Identification.....	55
3.3.3 Salmonella Mutagenicity Assay.....	67
3.4 Acknowledgements.....	77
3.5 References.....	78
<b>CHAPTER 4. HETEROGENEOUS REACTIONS OF PM-BOUND PAHs AND NPAHs WITH NO<sub>3</sub>/N<sub>2</sub>O<sub>5</sub>, OH RADICALS, AND O<sub>3</sub> UNDER SIMULATED LONG-RANGE ATMOSPHERIC TRANSPORT CONDITIONS: REACTIVITY AND MUTAGENICITY</b>	
ABSTRACT.....	83
4.1 Introduction.....	84
4.2 Experimental	
4.2.1 Chemicals.....	85
4.2.2 Sampling.....	86
4.2.3 Filter Preparation and Exposures.....	87
4.2.4 Sample Extraction and Analysis.....	89
4.2.5 Salmonella Mutagenicity Assay.....	90



## TABLE OF CONTENTS (Continued)

	<u>Page</u>
4.3 Results and Discussion	
4.3.1 Chemical Study.....	91
4.3.2 Mutagenicity Study.....	102
4.4 Acknowledgements.....	107
4.5 References.....	108
<b>CHAPTER 5. CONCLUSIONS.....</b>	<b>113</b>
<b>APPENDICES</b>	
APPENDIX A.....	127
APPENDIX B.....	131
APPENDIX C.....	163
APPENDIX D.....	171

## LIST OF FIGURES

	<u>Page</u>
2.1 Temporal variation of the (A) PM <sub>2.5</sub> , OC, BC, OC/BC and (B) ΣPAH <sub>51</sub> , ΣNPAH, and ΣOPAH concentrations.....	29
2.2 Mean (± standard deviation) of the percent of (A) total MW<300 PAHs, (B) total MW 302 PAHs, and (C) sum of NPAH and OPAH concentrations during the source control, non-source control, Olympic and non-Olympic periods.....	34
2.3 Correlation of ΣPAH <sub>28</sub> , Σ302PAH and sum of ΣNPAH and ΣOPAH with direct-acting and indirect-acting mutagen densities during the source control and non-source control periods.....	38
3.1 Overlaid full scan NCI chromatograms of unexposed BaP-d <sub>12</sub> and exposed BaP-d <sub>12</sub> with A) NO <sub>2</sub> B) NO <sub>3</sub> /N <sub>2</sub> O <sub>5</sub> C) O <sub>3</sub> and D) OH radicals.....	58
3.2 Overlaid full scan NCI chromatograms of unexposed BkF-d <sub>12</sub> and exposed BkF-d <sub>12</sub> with A) NO <sub>2</sub> B) NO <sub>3</sub> /N <sub>2</sub> O <sub>5</sub> C) O <sub>3</sub> and D) OH radicals.....	60
3.3 Overlaid full scan NCI chromatograms of unexposed BghiP-d <sub>12</sub> and exposed BghiP-d <sub>12</sub> with A) NO <sub>2</sub> B) NO <sub>3</sub> /N <sub>2</sub> O <sub>5</sub> C) O <sub>3</sub> and D) OH radical....	63
3.4 Overlaid full scan NCI chromatograms of unexposed DaiP-d <sub>14</sub> and exposed DaiP-d <sub>14</sub> with A) NO <sub>2</sub> B) NO <sub>3</sub> /N <sub>2</sub> O <sub>5</sub> C) O <sub>3</sub> and D) OH radicals....	65
3.5 Overlaid full scan NCI chromatograms of unexposed DalP and exposed DalP with A) NO <sub>2</sub> B) NO <sub>3</sub> /N <sub>2</sub> O <sub>5</sub> C) O <sub>3</sub> and D) OH radicals.....	66
3.6 Mean (± standard error) of A. direct-acting and B. indirect-acting mutagenicities (revertants/plate) of filter extracts. All extracts were tested in triplicate for mutagenicity activity.....	69
3.7 Mean (±95% confidence interval) direct- and indirect-acting mutagenic activities of BaP vs BaP-d <sub>12</sub> and 6-NBaP vs 6-NBaP-d <sub>11</sub> .....	74
3.8 Mean (±95% confidence interval) direct- and indirect-acting mutagenic activities of PYR vs PYR-d <sub>10</sub> and 1-NP vs 1-NP-d <sub>9</sub> .....	75
4.1 A. PAH <sub>exposed</sub> /PAH <sub>unexposed</sub> and B. NPAH <sub>exposed</sub> /NPAH <sub>unexposed</sub> of Beijing PM filters (n=3) used for the chemical study. An asterisk denotes the statistically significant difference between the unexposed and exposed masses.....	93

LIST OF FIGURES (Continued)

	<u>Page</u>
4.2 Correlation between reactivity of the Beijing and Riverside PM samples exposed to $\text{NO}_3/\text{N}_2\text{O}_5$ to $2\text{-NF}_{\text{unexposed}}$ concentrations normalized to $\text{BeP}_{\text{unexposed}}$ .....	99
4.3 A. $\text{PAH}_{\text{exposed}}/\text{PAH}_{\text{unexposed}}$ and B. $\text{NPAH}_{\text{exposed}}/\text{NPAH}_{\text{unexposed}}$ of Riverside PM filters (n=3) used for the chemical study. An asterisk denotes the statistically significant difference between the unexposed and exposed masses.....	101
4.4 Comparison of A. direct-acting mutagenicity, total NPAH concentration and B. indirect-acting mutagenicity, total PAH and NPAH concentrations of exposed and unexposed Beijing PM samples.....	103

## LIST OF TABLES

	<u>Page</u>
1.1 Free energies (Kcal/mol) of OH-PAH adduct and predicted dominant NPAHs formed via gas-phase OH radical-initiated reactions.....	10
2.1 List of MW<300 parent PAHs, MW 302 PAHs, NPAHs and OPAHs (and their abbreviations) measured in this study.....	24
3.1 Free energies ( $\Delta G_{\text{rxn}}$ ) of OH-PAH adducts calculated using density functional theory (B3LYP) and the 6-31G(d) basis set. NPAH isomers are listed in order of predicted stability.....	56

## LIST OF SCHEME

	<u>Page</u>
1.1 General mechanism for the nitration of PAHs via gas-phase reaction with OH radical.....	3

# **THE ATMOSPHERIC CHEMISTRY OF PARTICULATE-BOUND POLYCYCLIC AROMATIC HYDROCARBONS: CONCENTRATION, PREDICTION, LABORATORY STUDIES, AND MUTAGENICITY**

## **CHAPTER 1. INTRODUCTION**

### **1.1 Sources of Polycyclic Aromatic Hydrocarbons (PAHs), Nitrated PAHs and Oxygenated PAHs**

Polycyclic aromatic hydrocarbons (PAHs) are ubiquitous in the environment and have been studied for decades. PAHs largely originate from two sources – petrogenic and pyrogenic sources. The petrogenic source is a direct contribution of fossil fuel, while pyrogenic source includes the combustion of carbon containing fuels. Petrogenic and pyrogenic sources of PAHs give distinctive chemical fingerprints. The petroleum-based fingerprint predominantly contain low molecular weight and alkylated PAHs<sup>1</sup>. In the past two decades, PAHs, especially lower-ring PAHs, were found to be released from biological sources including plants and termites<sup>2,3</sup>.

In the atmosphere, PAHs partition between the gas and particulate phases depending on their vapor pressure and ambient temperature. In general, PAHs with more than four rings are measured primarily in the particulate-phase<sup>4</sup> and are less likely to degrade in the atmosphere, allowing them to undergo long range transport.

Similar to PAHs, nitrated-PAHs (NPAHs) are released from incomplete combustion but are also formed by atmospheric reactions of gas- and particulate-phase PAHs with oxidants, including OH radicals, NO<sub>3</sub> radicals and N<sub>2</sub>O<sub>5</sub>. NPAHs have been primarily detected in airborne particles<sup>5-9</sup>, but their presence in other environmental

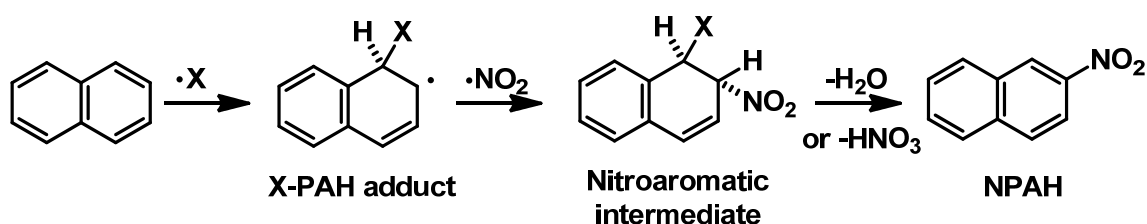
compartments, including, soils<sup>10</sup>, sediments<sup>11</sup>, water<sup>12</sup>, biota<sup>13</sup> and foods<sup>14</sup> has been observed. In general, NPAH concentrations are higher in urban areas. However, their concentrations are significantly lower than PAH concentrations<sup>5, 6, 8, 15</sup>. The PAH and NPAH concentrations measured in the same area, generally differ by an order of magnitude. The NPAH distribution in the particulate phase is primarily dominated by the NPAHs formed by atmospheric gas-phase reactions<sup>8</sup>.

Similar to NPAHs, oxygenated-PAHs (OPAHs), defined as PAHs containing one or more carbonylic oxygen(s), are emitted as products of incomplete combustion and formed by the secondary emission through oxidation of PAHs. In the atmosphere, they can be formed by photooxidation of PAHs<sup>16</sup>, including reactions of PAHs with OH radicals, NO<sub>3</sub> radicals or O<sub>3</sub><sup>17</sup>. Moreover, they have been recognized as dead-end products of soil remediation processes and biological transformations<sup>18-20</sup>. In general, the OPAH concentrations measured, in atmospheric particulate matter and soils, are generally comparable to those of PAHs in the same samples. The significant OPAH concentrations in soils may contribute to the total toxicity of some PAH-contaminated sites<sup>21-23</sup>.

## 1.2 Nitration Reactions of Gas-phase PAHs in the Atmosphere

The atmospheric chemistry of PAH gas-phase nitration reactions have been investigated intensively and the mechanisms of gas-phase radical-initiated reactions of PAHs were well understood<sup>4, 24, 25</sup>. Gas-phase nitration reactions occur in multiple steps illustrated in Scheme 1.1<sup>25</sup>. Initially, OH radicals or NO<sub>3</sub> radicals attack an aromatic carbon forming hydroxycyclohexadienyl radical (OH-PAH adduct) or nitratocyclohexadienyl radical (NO<sub>3</sub>-PAH adduct) intermediates. Studies on naphthalene

have showed that the OH-naphthalene adduct is thermally stable<sup>26</sup>. In contrast, the NO<sub>3</sub>-naphthalene adduct undergoes competition between reaction with NO<sub>2</sub> and decomposition to the starting material<sup>26</sup>. The reaction of these intermediates with NO<sub>2</sub> (ortho addition of NO<sub>2</sub>) yields the nitroaromatic intermediates, followed by the subsequent loss of H<sub>2</sub>O or HNO<sub>3</sub>.



**Scheme 1.1** General mechanism for the nitration of PAHs via gas-phase reaction with OH radical (X represents OH or NO<sub>3</sub> radical).

Even for the simplest PAH compound like naphthalene, the complete set of degradation products have yet to be identified. A study by Sasaki et al. determined total yields of  $\sim 0.67$  for gas-phase OH radical and  $\geq 0.40$  for NO<sub>3</sub> radical-initiated reactions of naphthalene<sup>26</sup>. In the same study, it should be noted that the reported product formation yields were corrected for secondary reactions of observed products. However, the total yield of NO<sub>3</sub> radical-initiated reaction included an expected highly reactive product that could not be quantified. A more recent study attempted to identify 23 products, mostly OPAHs, from the reaction of naphthalene with OH radicals; however, no percent yields were given<sup>27</sup>. This shows that NPAHs were minor products of the reaction of PAHs with OH radicals. Other products may form by reaction of OH-PAH adduct or NO<sub>3</sub>-PAH adduct with O<sub>2</sub>. Nonetheless, future studies are needed to identify unknown PAH degradation products that may pose a threat to humans and/or the environment.



### 1.3 Heterogeneous Nitration Reactions of Particle-bound PAHs

Although the kinetics and product identification regarding heterogeneous reactions of surface-bound PAHs with  $\text{NO}_2$ <sup>28-35</sup>, OH radicals<sup>30, 33, 36</sup>,  $\text{N}_2\text{O}_5$ <sup>37</sup>,  $\text{NO}_3$ <sup>38</sup>,  $\text{O}_3$ <sup>35, 39, 40</sup>, and  $\text{NO}^{33}$  have been previously studied to some degree using various substances as atmospheric particle models. It has been shown that the NPAH isomer distribution resulting from the reactions of fluoranthene and pyrene with  $\text{N}_2\text{O}_5$  in the gas phase is different from that in the adsorbed state<sup>25, 41-43</sup>. Such isomer distribution differences were thought to be caused by the state of  $\text{N}_2\text{O}_5$ , whether  $\text{N}_2\text{O}_5$  exists as ionic or covalent forms<sup>42</sup>. Zielinska et al.<sup>42</sup>, showed that in the gas phase, when covalent  $\text{N}_2\text{O}_5$  exists in equilibrium with  $\text{NO}_3$  and  $\text{NO}_2$ ,  $\text{NO}_3$  radicals initiate the reaction with unsubstituted PAHs, followed by *ortho* addition of  $\text{NO}_2$ . On the other hand, the NPAH isomer distribution resulting from the reaction of surface-adsorbed fluoranthene with gaseous  $\text{N}_2\text{O}_5$  resembled that resulting from the reaction of fluoranthene with  $\text{N}_2\text{O}_5$  in  $\text{CCl}_4$  at low temperature and in a polar solvent. The nitration mechanism in the solution was believed to occur by  $\text{NO}_2^+$  through electrophilic nitration, implying that the mechanism of heterogeneous reaction was ionic.

In the study by Ghigo et al., two nitration pathways of benzene with  $\text{N}_2\text{O}_5$  were studied theoretically which were 1) the syn-1,2-addition of  $\text{NO}_3$  and  $\text{NO}_2$  moieties (partially connected) and 2) the hydrogen abstraction by  $\text{NO}_3$ , followed by the  $\text{NO}_2$  addition on the same carbon. The authors noted that  $\text{N}_2\text{O}_5$  was not likely to be an important gas-phase nitrating agent, at least for benzene, due to the high energy barriers corresponding to both pathways.

The heterogeneous nitration reaction of PAHs with  $\text{NO}_2$  was also found to give the same major nitro isomers as the nitration reaction with  $\text{N}_2\text{O}_5$ <sup>28, 44</sup>. The mechanism was thought to involve the  $\text{HNO}_3$  because no NPAHs were observed when  $\text{HNO}_3$  was removed from the system<sup>45</sup>. But the reaction with  $\text{HNO}_3$  alone did not yield NPAHs<sup>44</sup>.

#### **1.4 Toxicity of PAHs, NPAHs and OPAHs**

The summary of the International Agency for Research on Cancer (IARC) classification of the toxicity of PAHs, NPAHs and OPAHs are listed in Appendix A.1 In the recent monographs, benzo[a]pyrene was upgraded to Group 1 (carcinogenic to humans) and cyclopenta[cd]pyrene, dibenz[a,h]anthracene, dibenzo[a,l]pyrene, 1-nitropyrene and 6-nitrochrysene were upgraded to Group 2A (probably carcinogenic to humans). In addition, a number of PAHs, NPAHs and OPAHs are classified as probably and possibly carcinogenic to humans.

The widely accepted short-term assay, the Salmonella mutagenicity assay, uses bacteria as an indicator for DNA damage leading to gene mutation which could be linked to cancer. Parent PAHs are indirect-acting mutagens, requiring metabolic activation system to convert them into active forms<sup>46</sup>. The most commonly used system is “S9”enzyme, prepared from the livers of rodents. Most NPAHs are direct-acting mutagens, independent of metabolic activation, with an exception of 6-nitrobenz[a]pyrene and 1-nitrocoronene<sup>47</sup>. Some NPAHs were found to be more toxic than their parent PAHs<sup>48, 49</sup>. For example, dinitropyrenes were found to be very powerful direct-acting mutagens, with mutagenic activities (revertants per nmol) greatly exceeding that of pyrene<sup>48</sup>. Therefore, only small concentrations of some NPAHs in the environment are needed to make a large contribution to total mutagenicity. Although the

mutagenic activity of dinitropyrenes were found to be greater than that of benzo[a]pyrene<sup>48</sup>, which is classified as “carcinogenic to humans”, the lack of dinitropyrene carcinogenicity studies on humans resulted in dinitropyrenes being classified as “possibly carcinogenic to humans” by IARC. There is a need for additional toxicological studies on NPAHs and the results may affect cancer risk assessment.

Although OPAHs have been determined to be the dominant degradation products of PAHs in various environmental media, the mutagenicity of OPAHs have been much less reported. The mutagenicity of OPAHs was found to be both dependent and independent of metabolic activation. A mutagenicity study of Salmonella TA97 strain with lower-ring OPAHs (naphthoquinone, anthraquinone, and 2-methylanthraquinone) showed they were mutagenic in the presence of S9<sup>50</sup>. However, the highly mutagenic quinones containing more than 4 rings (1,6-pyrenequinone and 1,8-pyrenequinone) gave similar responses in the presence or absence of S9<sup>50</sup>. It was reported that quinones may undergo redox cycling, catalyzed by NADPH-cytochrome P-450 reductase, generating oxygen radicals which can lead to oxidative stress<sup>51</sup>. A study of the mutagenicity of quinones found that the metabolic pathways could be complex when cytochrome P-450 converted phenanthrenequinone to a non-mutagenic metabolite, whereas it converted danthron to a powerful mutagenic metabolite<sup>51</sup>.

### **1.5 Scope and Significance**

The significance of research was essentially built on the trans-Pacific atmospheric transport of PAHs which hypothesizes that PAHs undergo long range atmospheric transport to North America on PM, affecting the mutagenicity of PM in the Western U.S. The evidence of long range transport across Pacific was first documented by Jaffe et al.<sup>52</sup>

and has since been documented by our laboratory for PAHs and other semivolatile organic compounds<sup>53, 54</sup>. These studies indicate that the trans-Pacific transport can occur in 5-7 days during the spring. The consequences of the trans-Pacific transport of Asian PM, and atmospheric transformation of particulate-bound PAHs, are our main focus of this research. This research spans from field measurements of PAHs in China during the 2008 Beijing Olympic Games to chamber studies of the atmospheric heterogeneous reactions of particle-bound PAHs with  $\text{NO}_3/\text{N}_2\text{O}_5$ ,  $\text{NO}_2$ ,  $\text{O}_3$  and OH radicals to the mutagenicity of PM extracts to the computational chemistry of PAHs.

Based on 2004 data, China is the world's largest emitter atmospheric PAHs (114 Gg y<sup>-1</sup>)<sup>55</sup>. Biomass was ranked first in PAH emission sources in China, followed by coke production. Coal combustion is a major source of energy, and accounts for 60% of the energy consumption in China<sup>55</sup>. In 2011, China was the second largest oil consumer, with more than a twofold increase in the consumption compared to 2001<sup>56</sup>. In contrast, the same reports show that the trends of oil consumption in North America and Europe have been declining for the past few years. This implies that PAH emissions in China will continue to increase. Not only will an increase in PAH emissions in China have a significant impact on human health in China from the inhalation exposure of carcinogenic PAHs, but may also, to a lesser extent, affect human health in the countries downwind of China.

In this research, atmospheric particulate matter with diameter  $< 2.5 \mu\text{m}$  ( $\text{PM}_{2.5}$ ) was collected during a series of sampling campaigns in China in order to 1) characterize the chemical composition of Chinese PM, 2) be tested in subsequent heterogeneous reaction studies using an indoor reaction chamber, and 3) assess the change in

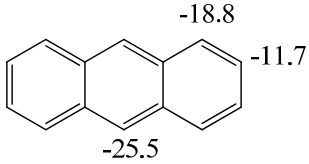
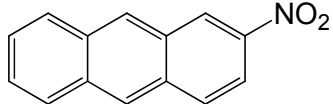
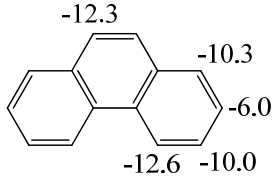
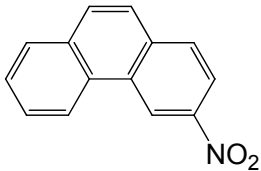
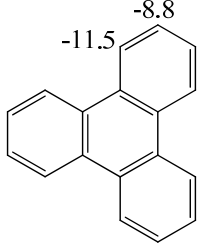
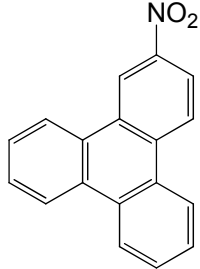
mutagenicity of the PM. Chapter 2 describes the first sampling campaign conducted during the 2008 Olympic Games, when stringent combustion source control measures were implemented. The objectives were to 1) measure PAH, NPAH and OPAH concentrations and the associated mutagenicity, using the Salmonella assay and human lung cell-based Comet assays, 2) use ratios of NPAHs to characterize the influence of photochemistry on the formation of PAH derivatives, and 3) assess the influence of source control measures on chemical concentrations and toxicity.

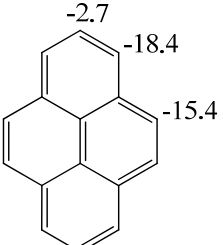
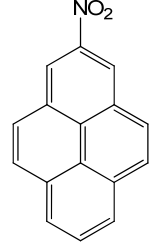
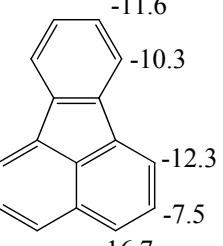
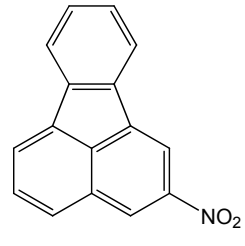
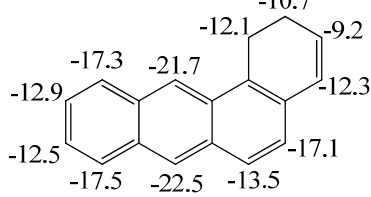
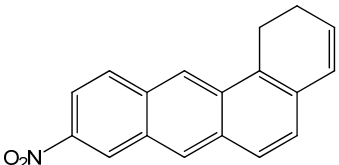
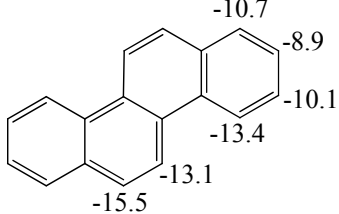
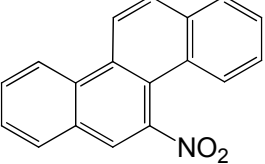
Subsequently, heterogeneous reactions of surface-bound PAHs with atmospheric oxidants, including OH radicals,  $\text{NO}_3/\text{N}_2\text{O}_5$ ,  $\text{O}_3$  and  $\text{NO}_2$ , were studied under a simulated environment. The experiments were carried out at the Air Pollution Research Center at University of California, Riverside which houses an indoor reaction chamber. The experiments were divided into two parts which consisted of exposures of 1) surface-bound PAHs (Part 1) and 2) PM-bound PAHs (Part 2). Described in Chapter 3, Part 1 aimed to identify nitro derivatives of relatively higher molecular weight PAHs by exposing quartz fiber filters spiked with PAHs to  $\text{NO}_2$ ,  $\text{NO}_3/\text{N}_2\text{O}_5$ ,  $\text{O}_3$ , and OH radicals. Five PAHs, including benzo[a]pyrene- $\text{d}_{12}$  (BaP- $\text{d}_{12}$ ), benzo[k]fluoranthene- $\text{d}_{12}$  (BkF- $\text{d}_{12}$ ), benzo[ghi]perylene- $\text{d}_{12}$  (BghiP- $\text{d}_{12}$ ), dibenzo[a,i]pyrene- $\text{d}_{14}$  (DaiP- $\text{d}_{14}$ ), and dibenzo[a,l]pyrene (DalP) were selected for testing in order to identify nitrated products after exposure to atmospheric oxidants. To compensate for several NPAH standards not being commercially available, a computational method, using Gaussian03, was used to predict which NPAH isomers were likely to form. The computational approach was based on the gas-phase OH radical-initiated reaction to find the most thermodynamically stable OH-PAH adducts which determine the position for  $\text{NO}_2$  addition through the

heterogeneous reaction. The preliminary calculations were carried out on selected PAHs (not shown in Chapter 3). A comparison between the theoretical and experimental (chamber studies) NPAH products for the OH-radical initiated reaction is shown in Table 1.1. There was good agreement between the theoretical and experimental result for anthracene, phenanthrene, pyrene and fluoranthene. The other products could not be confirmed because of the lack of laboratory studies for these PAHs. The agreement between the theoretical and experimental results showed that our computational method was reliable for predicting the dominant nitro-products formed by gas-phase and heterogeneous nitration of PAHs. In Chapter 3, nitro products could be identified in the chamber studies after  $\text{NO}_3/\text{N}_2\text{O}_5$  and  $\text{NO}_2$  exposures for the studied PAHs. The heterogeneous reaction of benzo[a]pyrene-d<sub>12</sub>, benzo[ghi]perylene-d<sub>12</sub>, and benzo[k]fluoranthene-d<sub>12</sub> yielded multiple nitro isomers, while that of dibenzo[a,i]pyrene-d<sub>14</sub> (DaiP-d<sub>14</sub>) and dibenzo[a,l]pyrene (DaIP) resulted in a single nitro product. Moreover, the extracts were tested for mutagenicity activity in the Salmonella assay. The results may potentially bring to light the presence of the NPAHs in the environment and the evaluation of their health risk.

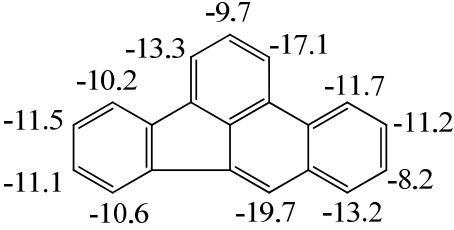
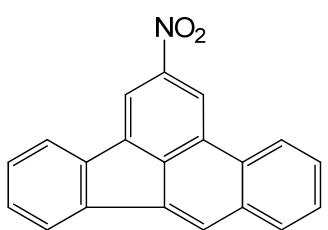
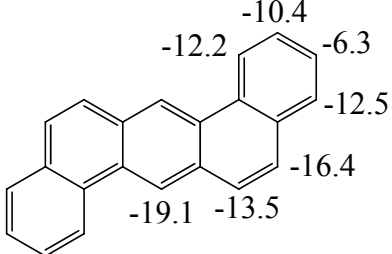
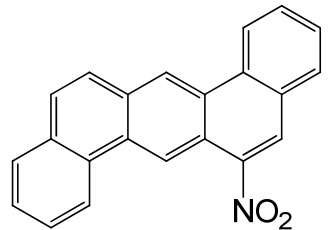
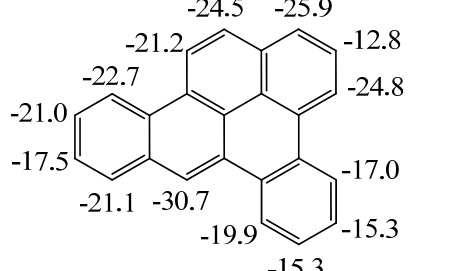
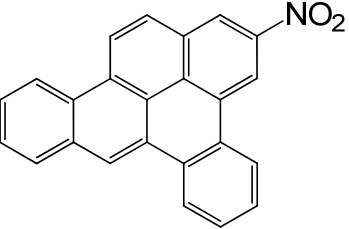
Chapter 4 describes Part 2 of the chamber studies which aimed at measuring changes in the chemical composition and mutagenicity due to atmospheric transformation of PM-bound PAHs. The PM, collected at two sites with different dominant emission sources (Beijing, China and Riverside, CA), was exposed to  $\text{NO}_3/\text{N}_2\text{O}_5$ , OH radicals, and  $\text{O}_3$  in order to simulate heterogeneous reactions that may occur during trans-Pacific

**Table 1.1. Free energies (Kcal/mol) of OH-PAH adduct and predicted dominant NPAHs formed via gas-phase OH radical-initiated reactions.**

Parent PAH	OH-PAH-Adduct $\Delta G_{\text{rxn}}$ (Kcal/mol)	Theoretical NPAH formed	Chamber NPAH measured <sup>1</sup>
1. Anthracene			1-nitroanthracene (low yield) 2-nitroanthracene (low yield)
2. Phenanthrene			Two isomers (not 9-nitrophenanthrene) in trace yield.
3. Triphenylene			No data available

Parent PAH	OH-PAH-Adduct $\Delta G_{rxn}$ (Kcal/mol)	Theoretical NPAH formed	Chamber NPAH measured <sup>1</sup>
4.Pyrene			2-nitropyrene (~0.5%) 4-nitropyrene (~0.06%)
5.Fluoranthene			2-nitrofluoranthene (~3%) 7-nitrofluoranthene (~1%) 8-nitrofluoranthene (~0.3%)
6.Benzo[a]anthracene			No data available
7.Chrysene			No data available



Parent PAH	OH-PAH-Adduct $\Delta G_{rxn}$ (Kcal/mol)	Theoretical NPAH formed	Chamber NPAH measured <sup>1</sup>
8. Benzo[b]fluoranthene			No data available
9. Dibenzo[a,h]anthracene			No data available
10. Dibenzo[a,e]pyrene			No data available

atmospheric transport. Black carbon and organic carbon concentrations were measured in atmospheric PM filters. The changes in unexposed and exposed filters were measured for PAH, NPAH and OPAH concentrations. Chapter 4 discusses changes in NPAH and OPAH distributions and changes in associated mutagenic activity of the PM after  $\text{NO}_3/\text{N}_2\text{O}_5$ , OH radical, and  $\text{O}_3$  exposures. The significance of the transformation PM-bound PAHs during long range atmospheric transport is also discussed in Chapter 4 of the thesis. This research will increase our understanding of the impact of trans-Pacific atmospheric transport of particle-bound PAH on human health. The information will be relevant to our ongoing field studies at Mt. Bachelor, Oregon, where the influence of Asian air masses continues to be monitored. In addition, the newly identified NPAHs from the chamber studies may initiate additional research regarding their presence in the environment and their associated toxicity and potential impact on human health.

## 1.6 References

1. Lichtfouse, E.; Budzinski, H.; Garrigues, P.; Eglinton, T. I., Ancient polycyclic aromatic hydrocarbons in modern soils:  $^{13}\text{C}$ ,  $^{14}\text{C}$  and biomarker evidence. *Org. Geochem.* **1997**, *26*, 353-359.
2. Azuma, H.; Toyota, M.; Asakawa, Y.; Kawano, S., Naphthalene - a constituent of Magnolia flowers. *Phytochemistry* **1996**, *42* (4), 999-1004.
3. Chen, J.; Henderson, G.; Grimm, C.; Lloyd, S.; Laine, R., Termites fumigate their nests with naphthalene. *Nature* **1998**, *392*, 558-559.
4. Atkinson, R.; Arey, J., Atmospheric Chemistry of Gas-Phase Polycyclic Aromatic Hydrocarbons: Formation of Atmospheric Mutagens. *Environ. Health Perspect.* **1994**, *102*, 117-126.
5. Albinet, A.; Leoz-Garziandia, E.; Budzinski, H.; Villenave, E., Polycyclic aromatic hydrocarbons (PAHs), nitrated PAHs and oxygenated PAHs in ambient air of the Marseilles area (South of France): Concentrations and sources. *Sci. Total Environ.* **2007**, *384* (1-3), 280-292.
6. Bamford, H. A.; Baker, J. E., Nitro-polycyclic aromatic hydrocarbon concentrations and sources in urban and suburban atmospheres of the Mid-Atlantic region. *Atmos. Environ.* **2003**, *37* (15), 2077-2091.
7. Dimashki, M.; Harrad, S.; Harrison, R. M., Measurements of nitro-PAH in the atmospheres of two cities. *Atmos. Environ.* **2000**, *34* (15), 2459-2469.
8. Reisen, F.; Arey, J., Atmospheric Reactions Influence Seasonal PAH and Nitro-PAH Concentrations in the Los Angeles Basin. *Environ. Sci. Technol.* **2004**, *39* (1), 64-73.
9. Wang, W.; Jariyasopit, N.; Schrlau, J.; Jia, Y.; Tao, S.; Yu, T.-W.; Dashwood, R. H.; Zhang, W.; Wang, X.; Simonich, S. L. M., Concentration and Photochemistry of PAHs, NPAHs, and OPAHs and Toxicity of PM<sub>2.5</sub> during the Beijing Olympic Games. *Environ. Sci. Technol.* **2011**, *45* (16), 6887-6895.
10. Niederer, M., Determination of polycyclic aromatic hydrocarbons and substitutes (nitro-, oxy-PAHs) in urban soil and airborne particulate by GC-MS and NCI-MS/MS. *Environmental Science and Pollution Research* **1998**, *5* (4), 209-216.
11. Sato, T.; Kato, K.; Ose, Y.; Nagase, H.; Ishikawa, T., Nitroarenes in Suimon river sediment. *Mutation Research/Genetic Toxicology* **1985**, *157* (2), 135-143.
12. Ohe, T.; Nukaya, H., Genotoxic activity of 1-nitropyrene in water from the Yodo River, Japan. *Sci. Total Environ.* **1996**, *181* (1), 7-12.
13. Uno, S.; Tanaka, H.; Miki, S.; Kokushi, E.; Ito, K.; Yamamoto, M.; Koyama, J., Bioaccumulation of nitroarenes in bivalves at Osaka Bay, Japan. *Mar. Pollut. Bull.* **2011**, *63* (5), 477-481.
14. Schlemitz, S.; Pfannhauser, W., Monitoring of nitropolycyclic aromatic hydrocarbons in food using gas chromatography. *Zeitschrift für Lebensmitteluntersuchung und-Forschung A* **1996**, *203* (1), 61-64.
15. Hattori, T.; Tang, N.; Tamura, K.; Hokoda, A.; Yang, X.; Igarashi, K.; Ohno, M.; Okada, Y.; Kameda, T.; Toriba, A., Particulate polycyclic aromatic hydrocarbons and their nitrated derivatives in three cities in Liaoning Province, China. *Environmental Forensics* **2007**, *8* (1-2), 165-172.

16. Barbas, J. T.; Sigman, M. E.; Dabestani, R., Photochemical oxidation of phenanthrene sorbed on silica gel. *Environ. Sci. Technol.* **1996**, *30* (5), 1776-1780.
17. Wang, L.; Atkinson, R.; Arey, J., Formation of 9, 10-phenanthrenequinone by atmospheric gas-phase reactions of phenanthrene. *Atmos. Environ.* **2007**, *41* (10), 2025-2035.
18. Lundstedt, S.; White, P. A.; Lemieux, C. L.; Lynes, K. D.; Lambert, I. B.; Öberg, L.; Haglund, P.; Tysklind, M., Sources, Fate, and Toxic Hazards of Oxygenated Polycyclic Aromatic Hydrocarbons (PAHs) at PAH- contaminated Sites. *AMBIO: A Journal of the Human Environment* **2007**, *36* (6), 475-485.
19. Lundstedt, S.; Persson, Y.; Öberg, L., Transformation of PAHs during ethanol-Fenton treatment of an aged gasworks' soil. *Chemosphere* **2006**, *65* (8), 1288-1294.
20. Cerniglia, C. E., Fungal metabolism of polycyclic aromatic hydrocarbons: past, present and future applications in bioremediation. *J. Ind. Microbiol. Biotechnol.* **1997**, *19* (5), 324-333.
21. Lundstedt, S.; Haglund, P.; Öberg, L., Degradation and formation of polycyclic aromatic compounds during bioslurry treatment of an aged gasworks soil. *Environ. Toxicol. Chem.* **2003**, *22* (7), 1413-1420.
22. Meyer, S.; Cartellieri, S.; Steinhart, H., Simultaneous Determination of PAHs, Hetero-PAHs (N, S, O), and Their Degradation Products in Creosote-Contaminated Soils. Method Development, Validation, and Application to Hazardous Waste Sites. *Anal. Chem.* **1999**, *71* (18), 4023-4029.
23. Bandowe, B. A. M.; Wilcke, W., Analysis of Polycyclic Aromatic Hydrocarbons and Their Oxygen-Containing Derivatives and Metabolites in Soils. *J. Environ. Qual.* **2010**, *39* (4), 1349-1358.
24. Atkinson, R.; Arey, J., Mechanisms of the gas-phase reactions of aromatic hydrocarbons and PAHs with OH and NO<sub>3</sub> radicals. *Polycyclic Aromat. Compd.* **2007**, *27* (1), 15-40.
25. Atkinson, R.; Arey, J.; Zielinska, B.; Aschmann, S. M., Kinetics and Nitro-Products of the Gas-Phase OH and NO<sub>3</sub> Radical-Initiated Reactions of Naphthalene-d<sub>8</sub>, Fluoranthene-d<sub>10</sub>, and Pyrene. *Int. J. Chem. Kinet.* **1990**, *22*, 999-1014.
26. Sasaki, J.; Aschmann, S. M.; Kwok, E. S. C.; Atkinson, R.; Arey, J., Products of the Gas-Phase OH and NO<sub>3</sub> Radical-Initiated Reactions of Naphthalene. *Environ. Sci. Technol.* **1997**, *31* (11), 3173-3179.
27. Lee, J.; Lane, D. A., Formation of oxidized products from the reaction of gaseous phenanthrene with the OH radical in a reaction chamber. *Atmos. Environ.* **2010**, *44* (20), 2469-2477.
28. Miet, K.; Le Menach, K.; Flaud, P. M.; Budzinski, H.; Villenave, E., Heterogeneous reactivity of pyrene and 1-nitropyrene with NO<sub>2</sub>: Kinetics, product yields and mechanism. *Atmos. Environ.* **2009**, *43* (4), 837-843.
29. Carrara, M.; Wolf, J.-C.; Niessner, R., Nitro-PAH formation studied by interacting artificially PAH-coated soot aerosol with NO<sub>2</sub> in the temperature range of 295-523 K. *Atmos. Environ.* **2010**, *44* (32), 3878-3885.
30. Esteve, W.; Budzinski, H.; Villenave, E., Relative rate constants for the heterogeneous reactions of NO<sub>2</sub> and OH radicals with polycyclic aromatic hydrocarbons adsorbed on carbonaceous particles. Part 2: PAHs adsorbed on diesel particulate exhaust SRM 1650a. *Atmos. Environ.* **2006**, *40* (2), 201-211.

31. Ma, J.; Liu, Y.; He, H., Heterogeneous reactions between NO<sub>2</sub> and anthracene adsorbed on SiO<sub>2</sub> and MgO. *Atmos. Environ.* **2011**, *45* (4), 917-924.
32. Jäger, J.; Hanus, V., Reaction of solid carrier-adsorbed polycyclic aromatic hydrocarbons with gaseous low-concentrated nitrogen dioxide. *J. Hyg. Epidemiol. Microbiol. Immunol* **1980**, *24*, 1-12.
33. Esteve, W.; Budzinski, H.; Villenave, E., Relative rate constants for the heterogeneous reactions of OH, NO<sub>2</sub> and NO radicals with polycyclic aromatic hydrocarbons adsorbed on carbonaceous particles. Part 1: PAHs adsorbed on 1-2 μm calibrated graphite particles. *Atmos. Environ.* **2004**, *38* (35), 6063-6072.
34. Nguyen, M.; Bedjanian, Y.; Guilloteau, A., Kinetics of the reactions of soot surface-bound polycyclic aromatic hydrocarbons with NO<sub>2</sub>. *J. Atmos. Chem.* **2009**, *62* (2), 139-150.
35. Pöschl, U., Formation and decomposition of hazardous chemical components contained in atmospheric aerosol particles. *Journal of aerosol medicine* **2002**, *15* (2), 203-212.
36. Bedjanian, Y.; Nguyen, M. L.; Le Bras, G., Kinetics of the reactions of soot surface-bound polycyclic aromatic hydrocarbons with the OH radicals. *Atmos. Environ.* **2010**, *44* (14), 1754-1760.
37. Kamens, R. M.; Guo, J.; Guo, Z.; McDow, S. R., Polynuclear aromatic hydrocarbon degradation by heterogeneous reactions with N<sub>2</sub>O<sub>5</sub> on atmospheric particles. *Atmospheric Environment. Part A. General Topics* **1990**, *24* (5), 1161-1173.
38. Zhang, Y.; Yang, B.; Gan, J.; Liu, C.; Shu, X.; Shu, J., Nitration of particle-associated PAHs and their derivatives (nitro-, oxy-, and hydroxy-PAHs) with NO<sub>3</sub> radicals. *Atmos. Environ.* **2011**, *45* (15), 2515-2521.
39. Miet, K.; Le Menach, K.; Flaud, P. M.; Budzinski, H.; Villenave, E., Heterogeneous reactions of ozone with pyrene, 1-hydroxypyrene and 1-nitropyrene adsorbed on particles. *Atmos. Environ.* **2009**, *43* (24), 3699-3707.
40. Bedjanian, Y.; Nguyen, M. L., Kinetics of the reactions of soot surface-bound polycyclic aromatic hydrocarbons with O<sub>3</sub>. *Chemosphere* **2010**, *79* (4), 387-393.
41. Pitts, J. N.; Sweetman, J. A.; Zielinska, B.; Atkinson, R.; Winer, A. M.; Harger, W. P., Formation of nitroarenes from the reaction of polycyclic aromatic hydrocarbons with dinitrogen pentoxide. *Environ. Sci. Technol.* **1985**, *19* (11), 1115-1121.
42. Zielinska, B.; Arey, J.; Atkinson, R.; Ramdahl, T.; Winer, A. M.; Pitts, J. N., Reaction of dinitrogen pentoxide with fluoranthene. *J. Am. Chem. Soc.* **1986**, *108* (14), 4126-4132.
43. Pitts Jr, J. N.; Zielinska, B.; Sweetman, J. A.; Atkinson, R.; Winer, A. M., Reactions of adsorbed pyrene and perylene with gaseous N<sub>2</sub>O<sub>5</sub> under simulated atmospheric conditions. *Atmos. Environ.* **1985**, *19*, 911-915.
44. Pitts Jr, J. N.; Zielinska, B.; Sweetman, J. A.; Atkinson, R.; Winer, A. M., Reactions of adsorbed pyrene and perylene with gaseous N<sub>2</sub>O<sub>5</sub> under simulated atmospheric conditions. *Atmospheric Environment (1967)* **1985**, *19* (6), 911-915.
45. Van Cauwenberghe, K.; Van Vaeck, L.; Pitts, J., Physical and chemical transformations of organic pollutants during aerosol sampling. **1980**.
46. McCann, J.; Choi, E.; Yamasaki, E.; Ames, B. N., Detection of carcinogens as mutagens in the Salmonella/microsome test: assay of 300 chemicals. *Proceedings of the National Academy of Sciences* **1975**, *72* (12), 5135-5139.

47. Rosenkranz, H. S.; Mermelstein, R., The mutagenic and carcinogenic properties of nitrated polycyclic aromatic hydrocarbons. White, C. M., Ed. Huethig: Heidelberg, 1985; pp 267-297.
48. Yang, X.-Y.; Igarashi, K.; Tang, N.; Lin, J.-M.; Wang, W.; Kameda, T.; Toriba, A.; Hayakawa, K., Indirect- and direct-acting mutagenicity of diesel, coal and wood burning-derived particulates and contribution of polycyclic aromatic hydrocarbons and nitropolycyclic aromatic hydrocarbons. *Mutation Research/Genetic Toxicology and Environmental Mutagenesis* **2010**, 695 (1-2), 29-34.
49. Purohit, V.; Basu, A. K., Mutagenicity of Nitroaromatic Compounds. *Chem. Res. Toxicol.* **2000**, 13 (8), 673-692.
50. Sakai, M.; Yoshida, D.; Mizusaki, S., Mutagenicity of polycyclic aromatic hydrocarbons and quinones on *Salmonella typhimurium* TA97. *Mutation Research/Genetic Toxicology* **1985**, 156 (1), 61-67.
51. Chesis, P. L.; Levin, D. E.; Smith, M. T.; Ernster, L.; Ames, B. N., Mutagenicity of quinones: pathways of metabolic activation and detoxification. *Proceedings of the National Academy of Sciences* **1984**, 81 (6), 1696-1700.
52. Jaffe, D.; Anderson, T.; Cover, D.; Kotchenruther, R.; Trost, B.; Danielson, J.; Simpson, W.; Bernstein, T.; Karlsdottir, S.; Blake, D.; Harris, J.; Carmichael, G.; Uno, I., Transport of Asian Air Pollution to North America. *Geophys. Res. Lett.* **1999**, 26 (6), 711-714.
53. Primbs, T.; Simonich, S.; Schmedding, D.; Wilson, G.; Jaffe, D.; Takami, A.; Kato, S.; Hatakeyama, S.; Kajii, Y., Atmospheric Outflow of Anthropogenic Semivolatile Organic Compounds from East Asia in Spring 2004. *Environ. Sci. Technol.* **2007**, 41 (10), 3551-3558.
54. Primbs, T.; Piekarz, A.; Wilson, G.; Schmedding, D.; Higginbotham, C.; Field, J.; Simonich, S. M., Influence of Asian and Western United States Urban Areas and Fires on the Atmospheric Transport of Polycyclic Aromatic Hydrocarbons, Polychlorinated Biphenyls, and Fluorotelomer Alcohols in the Western United States. *Environ. Sci. Technol.* **2008**, 42 (17), 6385-6391.
55. Zhang, Y. X.; Tao, S.; Shen, H. Z.; Ma, J. M., Inhalation exposure to ambient polycyclic aromatic hydrocarbons and lung cancer risk of Chinese population. *Proc. Natl. Acad. Sci. U. S. A.* **2009**, 106 (50), 21063-21067.
56. Petroleum, B. BP Statistical Review. [www.bp.com/statisticalreview](http://www.bp.com/statisticalreview) (accessed 1/3/13).

**CHAPTER 2. CONCENTRATION AND PHOTOCHEMISTRY OF PAHs, NPAHs, AND OPAHs AND TOXICITY OF PM<sub>2.5</sub> DURING THE BEIJING OLYMPIC GAMES**

NARUMOL JARIYASOPIT<sup>1</sup>, WENTAO WANG<sup>2</sup>, JILL SCHRLAU<sup>3</sup>, YULING JIA<sup>3</sup>, SHU TAO<sup>2</sup>, TIAN-WEI YU<sup>4</sup>, RODERICK H. DASHWOOD<sup>4</sup>, WEI ZHANG<sup>2</sup>, XUEJUN WANG<sup>2</sup>, STACI L. MASSEY SIMONICH<sup>3,\*</sup>

<sup>1</sup>Department of Chemistry, Oregon State University, Corvallis, Oregon USA 97331;

<sup>2</sup>College of Urban and Environmental Science, Peking University, Beijing, China, 100871;

<sup>3</sup>Environmental and Molecular Toxicology, Oregon State University, Corvallis, Oregon, United States, 97331;

<sup>4</sup>Linus Pauling Institute, Oregon State University, Corvallis, Oregon, United States. 97331.

Environ. Sci. Technol. 2011, 45, 6887–6895  
DOI: 10.1021/es201443z  
Copyright ©2011 American Chemical Society

\*Corresponding author, E-mail: [staci.simonich@oregonstate.edu](mailto:staci.simonich@oregonstate.edu), fax: 541-737-0497.

## ABSTRACT

Atmospheric particulate matter with diameter  $<2.5$   $\mu\text{m}$  ( $\text{PM}_{2.5}$ ) was collected at Peking University (PKU) in Beijing, China before, during, and after the 2008 Olympics and analyzed for black carbon (BC), organic carbon (OC), lower molecular weight ( $\text{MW}<300$ ) and  $\text{MW}302$  Polycyclic Aromatic Hydrocarbons (PAHs), nitrated PAHs (NPAHs) and oxygenated PAHs (OPAHs). In addition, the direct and indirect acting mutagenicity of the  $\text{PM}_{2.5}$  and the potential for DNA damage to human lung cells were also measured. Significant reductions in BC (45%), OC (31%),  $\text{MW}<300$  PAH (26% - 73%),  $\text{MW}302$  PAH (22% - 77%), NPAH (15% - 68%) and OPAH (25% - 53%) concentrations were measured during the source control and Olympic periods. However, the mutagenicity of the  $\text{PM}_{2.5}$  was significantly reduced only during the Olympic period. The PAH, NPAH, and OPAH composition of the  $\text{PM}_{2.5}$  was similar throughout the study, suggesting similar sources during the different periods. During the source control period, the parent PAH concentrations were correlated with  $\text{NO}$ ,  $\text{CO}$ , and  $\text{SO}_2$  concentrations, indicating that these PAHs were associated with both local and regional emissions. However, the NPAH and OPAH concentrations were only correlated with the  $\text{NO}$  concentrations, indicating that the NPAH and OPAH were primarily associated with local emissions. The relatively high 2-nitrofluoranthene/1-nitropyrene ratio (25 - 46) and 2-nitrofluoranthene/2-nitropyrene ratio (3.4 - 4.8), suggested a predominance of photochemical formation of NPAHs through OH-radical-initiated reactions in the atmosphere. On average, the  $\Sigma\text{NPAH}$  and  $\Sigma\text{OPAH}$  concentrations were 8% of the parent PAH concentrations, while the direct-acting mutagenicity (due to the NPAH and OPAH) was 200% higher than the indirect-acting mutagenicity (due to the PAH). This suggests



that NPAH and OPAH make up a significant portion of the overall mutagenicity of PM<sub>2.5</sub> in Beijing.

## 2.1 Introduction

There was an unprecedented effort by the Beijing municipal government to improve air quality for the 2008 Beijing Olympics. A wide range of combustion sources, including vehicles, trucks, factories, and coal combustion for power generation, were controlled leading up to the Olympics, with the most stringent combustion source control measures occurring during the Olympic period (August 8-24, 2008)<sup>1-4</sup>. From July 20-August 7, 2008, traffic was reduced, with license plates ending in even (odd) numbers allowed on the roads on even (odd) numbered calendar days, construction sites were closed, and the operation of coal fired power plants were strictly limited<sup>1-3</sup>. From August 8-24, 2008 (the Olympic period), additional restrictions on coal-combustion were implemented<sup>1-4</sup>. It has been estimated that the traffic volume of typical roads in Beijing was reduced by ~32% during the Olympic period<sup>4-6</sup>. From August 25-September 20, 2008 the source control measures were less strictly implemented<sup>1</sup>. As a result, significant reductions in carbon monoxide (CO), nitrogen oxide (NO<sub>x</sub>), sulfur dioxide (SO<sub>2</sub>), ozone (O<sub>3</sub>), volatile organic compound (VOC), and particulate matter (PM) emissions and concentrations have been reported in Beijing, particularly during August 8-24, 2008<sup>1-17</sup>. In addition to source control measures, the fluctuations in Beijing PM concentration during the source control period have also been attributed to regional transport and meteorology<sup>1, 4, 7, 9, 10</sup>.

Black carbon (BC) and organic carbon (OC) are emitted into the atmosphere on fine, respirable PM, including PM<sub>2.5</sub>, during incomplete combustion and contribute to climate change, decreased visibility, and health effects<sup>18, 19</sup>. Polycyclic aromatic

hydrocarbons (PAHs) are components of OC on PM<sub>2.5</sub> and are mutagenic products of incomplete combustion<sup>20, 21</sup>. China is currently the world's largest emitter of BC<sup>19</sup>, OC<sup>19</sup> and PAHs<sup>20</sup> and human exposure to these air pollutants has been predicted to be a major health concern in China now and in the future<sup>17, 18, 21</sup>.

The significant effort to reduce combustion emissions in Beijing during the Olympic period provided a unique opportunity to study the PM<sub>2.5</sub>-bound PAH, NPAH and OPAH concentrations, as well as the associated toxicity, in correspondence with the implementation and removal of source control measures. The objectives of this study were to: 1) measure the PM<sub>2.5</sub>-bound PAH, NPAH, and OPAH concentrations and toxicity in Beijing before, during, and after the Olympics; 2) characterize the influence of photochemistry on the formation of NPAH and OPAH; and 3) assess the influence of sources and source control measures on the PM<sub>2.5</sub>-bound PAH, NPAH, and OPAH concentrations and, in turn, mutagenicity and potential for DNA damage.

## **2.2 Materials and Methods**

### **2.2.1 Sampling**

The sampling site and sample collection have been previously described in detail<sup>7</sup>. In brief, the sampling site was located on the roof of the 7-story Geology Building on the PKU campus, about 25 meters above ground. PKU is located in a primarily residential and commercial area in Northwestern Beijing. Local BC and PAH emission sources, within 1 km of PKU, include vehicular traffic and fuel combustion for cooking. Several 2008 Olympic events took place on or near the PKU campus.

PM<sub>2.5</sub> was collected using a High Volume Cascade Impactor (Series 230, Tisch Environmental, Cleves, OH) that operated in accordance with procedures established by

USEPA (CFR40, Part 50.11, Appendix B, July 1, 1975, pages 12-16) and ASTM Specification D2009<sup>7</sup>. Sixty-three PM<sub>2.5</sub> samples were collected over 24 h periods (~1500 m<sup>3</sup> of air) from July 28 to September 3, 2008 and from September 13 to October 7, 2008. The source control period includes samples from July 28-September 20, 2008, while the non-source control period includes samples from September 21-October 7, 2008<sup>7</sup>. The Olympic period includes samples from August 8-August 24, 2008, while the non-Olympic period includes samples from July 28-August 7, 2008 and August 26-October 7, 2008<sup>7</sup>.

Six field blanks were also collected during these periods. Samples were not collected from September 4 to 12, 2008 because of sampler motor failure. Pre-baked (350°C) quartz fiber filters (No.1851-865, Tisch Environmental, Cleves, OH) were used for sample collection. The filters were weighed before and after sample collection for PM<sub>2.5</sub> mass<sup>7</sup>.

### **2.2.2 Black and Organic Carbon Measurement**

The black carbon (BC) and organic carbon (OC) concentrations were measured using a Sunset EC/OC analyzer (Sunset Lab, USA)<sup>22</sup>. There is debate as to whether thermal-optically measured elemental carbon (EC) should be referred to as BC. However, based on previous studies<sup>19, 23, 24</sup>, we refer to the measured EC concentration as BC concentration.

### **2.2.3 Chemicals**

All of the MW<300 parent PAHs, MW 302 PAHs, NPAHs and OPAHs are listed in Table 2.1. Deuterium-labeled PAHs and NPAHs were purchased from CDN Isotopes (Point-Claire, Quebec, Canada) and Cambridge Isotope Laboratories (Andover, MA).

The isotopically labeled recovery PAH and NPAH surrogates included d<sub>10</sub>-fluorene, d<sub>10</sub>-phenanthrene, d<sub>10</sub>-pyrene, d<sub>12</sub>-triphenylene, d<sub>12</sub>-benzo[a]pyrene, d<sub>12</sub>-benzo[ghi]perylene, d<sub>7</sub>-1-nitronaphthalene, d<sub>9</sub>-5-nitroacenaphthene, d<sub>9</sub>-9-nitroanthracene, d<sub>9</sub>-3-nitrofluoranthene, d<sub>9</sub>-1-nitropyrene and d<sub>11</sub>-6-nitrochrysene. The labeled PAH and NPAH internal standards included d<sub>10</sub>-acenaphthene, d<sub>10</sub>-fluoranthene, d<sub>12</sub>-benzo[k]fluoranthene, d<sub>9</sub>-2-nitrobiphenyl and d<sub>9</sub>-2-nitrofluorene.

#### **2.2.4 Sample extraction and Analysis**

Using the extraction method previously described in detail<sup>25-27</sup>, the PM<sub>2.5</sub> filters were extracted twice using pressurized liquid extraction with dichloromethane. The extracts were combined and divided into two halves by weight. One half of the extract was prepared for toxicity testing by evaporating the extract to dryness under a stream of N<sub>2</sub> with a Turbovap II (Caliper Life Sciences, MA). The residue was dissolved in 500 µl of dimethyl sulfoxide (DMSO). For chemical analysis, the other half of the extract was spiked with perdeuterated PAH and NPAH surrogates. It should be noted that the surrogates were spiked after extraction to avoid any interference of the surrogates with the subsequent toxicological testing of the extracts. For chemical analysis, the extracts were then purified using 20-g silica columns (Mega BE-SI, Agilent Technologies, New Castle, DE), eluted with dichloromethane, and spiked with perdeuterated PAH and NPAH internal standards. The analysis of parent PAHs was conducted using gas chromatographic mass spectrometry (Agilent 6890 GC coupled with an Agilent 5973N MSD) in selected ion monitoring mode using electron impact ionization<sup>25, 27, 28</sup>, while the analysis of NPAH and OPAHs was conducted using electron capture negative ionization (ECNI) with a programmed temperature vaporization (PTV) inlet (Gerstel, Germany).

**Table 2.1** List of MW<300 parent PAHs, MW 302 PAHs, NPAHs and OPAHs (and their abbreviations) measured in this study.

#	Compound	Abbreviation	#	Compound	Abbreviation
<b>MW&lt;300 PAHs<sup>1</sup></b>					
1	naphthalene	NAP	12	benzo[b]perylene	BbPer
2	2-methylnaphthalene	2-MNAP	13	dibenzo[a,i]pyrene	DBaiP
3	1-methylnaphthalene	1-MNAP	14	dibenzo[a,e]pyrene	DBaeP
4	2,6-dimethylnaphthalene	2,6-DMNAP	15	dibenzo[a,l]pyrene	DBalP
5	1,3-dimethylnaphthalene	1,3-DMNAP	16	dibenzo[a,h]pyrene	DBahP
6	acenaphthylene	ACY			
7	fluorene	FLO	<b>NPAHs<sup>3</sup></b>		
8	phenanthrene	PHE	1	1-nitronaphthalene	1-NN
9	anthracene	ANT	2	2-nitronaphthalene	2-NN
10	2-methylphenanthrene	2-MPHE	3	2-nitrobiphenyl	2-NBP
11	2-methylanthracene	2-MANT	4	3-nitrobiphenyl	3-NBP
12	1-methylphenanthrene	1-MPHE	5	4-nitrobiphenyl	4-NBP
13	3,6-dimethylphenanthrene	3,6-DMPHE	6	3-nitrodibenzofuran	3-NBF
14	dibenzothiophene	DBT	7	5-nitroacenaphthalene	5-NAC
15	fluoranthene	FLA	8	2-nitrofluorene	2-NFL
16	pyrene	PYR	9	9-nitroanthracene	9-NAN
17	retene	RET	10	9-nitrophenanthrene	9-NPH
18	1-methylpyrene	1-MPYR	11	2-nitrodibenzothiophene	2-NDB
19	benz[a]anthracene	BaA	12	3-nitrophenanthrene	3-NPH
20	chrysene + triphylene	CHR+TRI	13	2-nitroanthracene	2-NAN
21	6-methylchrysene	6-MCHR	14	2-nitrofluoranthene	2-NF
22	benzo(b)fluoranthene	BbF	15	3-nitrofluoranthene	3-NF
23	benzo(k)fluoranthene	BkF	16	1-nitropyrene	1-NP
24	benzo[e]pyrene	BeP	17	2-nitropyrene	2-NP
25	benzo[a]pyrene	BaP	18	7-nitrobenz(a)anthracene	7-NBaA
26	indeno[1,2,3-cd]pyrene	IcdP	19	2,8-dinitrodibenzothiophene	2,8-DNDB
27	dibenz[a,h]anthracene	DahA	20	6-nitrochrysene	6-NCH
28	benzo[g,h,i]perylene	BghiP	21	3-nitrobenzathrone	3-NBENZ
			22	1,3-dinitropyrene	1,3-DNP
<b>MW 302 PAH<sup>2</sup></b>					
			23	1,6-dinitropyrene	1,6-DNP
1	naphtho[2,3-a]pyrene	N23aP	24	1,8-dinitropyrene	1,8-DNP
2	naphtho[2,3-e]pyrene	N23eP	25	6-nitrobenzo[a]pyrene	6-NBaP
3	naphtho[1,2-b]fluoranthene	N12bF			
4	dibenzo[a,e]fluoranthene	DBaeF	<b>OPAHs<sup>3</sup></b>		
5	dibenzo[b,k]fluoranthene	DBbkF	1	9-fluorenone	9-FLU
6	dibenzo[e,l]pyrene	DBelP	2	9,10-anthraquinone	ANQ
7	dibenzo[a,k]fluoranthene	DBakF	3	2-methyl-9,10-anthraquinone	2-MANQ
8	dibenzo[j,l]fluoranthene	DBjlF	4	benzanthrone	BEN
9	naphtho[2,3-j]fluoranthene	N23jF	5	benz[a]anthracene-7,12-dione	BaAD
10	naphtho[2,3-b]fluoranthene	N23bF			
11	naphtho[2,3-k]fluoranthene	N23kF			

<sup>1</sup>Purchased from AccuStandard (New Haven, CT) and Chem Service (West Chester, PA)

<sup>2</sup>Purchased from Chiron AS (Trondheim, Norway) and AccuStandard (New Haven, CT)

<sup>3</sup>Purchased from Chiron AS (Norway), AccuStandard (New Haven, CT), Chem Service (West Chester, PA) and Sigma-Aldrich Corp.

A 5% phenyl substituted methylpolysiloxane GC column (DB-5MS, 30m×0.25mm I.D., 0.25 µm film thickness, J&W Scientific, USA) was used to measure the MW<300 parent PAHs and the majority of NPAHs and OPAHs. A 50% phenyl substituted methylpolysiloxane GC column (DB-17MS, 30m×0.25mm I.D., 0.25 µm film thickness, J&W Scientific, USA) was used to resolve 2-NF and 3-NF, and a similar column (DB-17MS, 60m×0.25mm I.D., 0.25 µm film thickness, J&W Scientific, USA) was used to measure the MW 302 parent PAHs<sup>17</sup>. Additional information on the analysis and method recovery of MW 302 parent PAH, NPAH, and OPAH is given in the Appendix B.1 to Appendix B.5.

The MW<300 parent PAH concentrations are reported as individual PAH concentrations as well as the sum of NAP, 2-MNAP, 1-MNAP, 2,6-DMNAP, and 1,3-DMNAP, ACY, FLO and DBT concentrations ( $\Sigma\text{PAH}_{2\text{ring}}$ ), the sum of PHE, ANT, 2-MPHE, 2-MANT, 1-MPHE, and 3,6-DMPHE concentrations ( $\Sigma\text{PAH}_{3\text{ring}}$ ), the sum of FLA, PYR, RET, 1-MPYR, BaA, CHR+TRI, and 6-MCHR concentrations ( $\Sigma\text{PAH}_{4\text{ring}}$ ), the sum of BbF, BkF, BeP, BaP, IcdP, DahA, and BghiP concentrations ( $\Sigma\text{PAH}_{5\text{ring}}$ ), the sum of NAP, ACY, FLO, PHE, ANT, FLA, PYR, BaA, CHR, BbF, BkF, BaP, IcdP, DahA, and BghiP concentrations ( $\Sigma\text{PAH}_{\text{US-Priority}}$ ), and the sum of all 28 individual MW<300 parent PAH concentrations ( $\Sigma\text{PAH}_{28}$ ). The MW 302 parent PAH concentrations are reported as individual PAH concentrations as well as the sum of DBaeP, DBaiP, DBalP, and DBahP ( $\Sigma\text{DBP}$ ), the sum of N12kF, N23bF, DBaeF/DBbkF, DBakF, DBalP, N23eP, DBaeP, DBelP, N23aP, DBaiP, DBahP, DBbeF, and N21aP that have been reported as human mutagens in literature<sup>29-31</sup> ( $\Sigma\text{302PAH}_{\text{mut}}$ ), and the sum of all individual MW 302 PAHs ( $\Sigma\text{302PAH}$ ). The NPAH and OPAH concentrations are reported as individual PAH

concentration as well as the sum of all individual NPAH concentrations ( $\Sigma$ NPAH) and the sum of all individual OPAH concentrations ( $\Sigma$ OPAH). The sum of  $\Sigma$ PAH<sub>28</sub> and  $\Sigma$ 302PAH are reported as  $\Sigma$ PAH<sub>51</sub>.

### 2.2.5 Toxicology Studies

***Bacteria for Ames Assays*** The basic method follows that reported by Maron and Ames<sup>32</sup>. Salmonella strains TA98 were used in the study. Salmonella tester strain TA98 was originally purchased from Xenometrix, Inc.

***Ames Assays*** Briefly, 2 ml molten top agar (45°C), 30  $\mu$ l samples in DMSO, 0.5 ml of phosphate buffered saline or rat S9 mix (an exogenous metabolic activation system based on rat liver enzymes), and 0.1 ml of bacteria were quickly mixed in a sterile disposable tube and the mixture was poured onto a Vogel-Bonner minimal agar plate. After the bacteria-containing agar was solidified, the plates were incubated at 37°C in inverse position for 48 hr. The histidine revertant colonies were counted with a Sorcerer Colony Counter (Perceptive Instruments, Haverhill, Suffolk, UK). All air samples were tested in triplicate. The positive control (4-nitro-1,2-phenylenediamine) and negative control (DMSO) doses were 20  $\mu$ g and 50  $\mu$ l, respectively. With respect to cytotoxicity, no adverse effects were seen on the background lawn.

***Human A549 lung carcinoma cells and treatment for Comet Assays*** Human A549 lung carcinoma cells were originally purchased from American Type Culture Collection (ATCC, Manassas, VA). ATCC protocols were followed for cell culture and maintenance. The cell line was maintained in F-12K medium supplemented with 10% fetal bovine serum in a 5% CO<sub>2</sub> incubator at 37°C. On the day of Comet treatment, cells in a T25 flask (~90% confluence) were trypsinized and re-suspended in growth medium.

Approximately 20,000 cells were treated with the 10  $\mu$ l air sample extract in DMSO and with 990  $\mu$ l growth medium for 1 hr at 37°C.

**Comet Assays** The single cell gel electrophoresis ('comet') assay was used to assess levels of DNA damage in A549 cells. The assay was modified based on the protocol of Singh et al.<sup>33</sup>. Briefly, cells in 60  $\mu$ l of 0.5% low melting point agarose (LMPA) were spread onto a dry, pre-coated slide (with 1% normal melting point agarose) with a coverglass, and then placed onto a 4°C surface for 20 min. The coverglass was removed and another layer of cell-free LMPA (70- $\mu$ l) was spread over the cell-containing layer using a second coverglass. After the layer of agarose had hardened for 15 min, the coverglass was removed and the slide was immersed overnight in cold lysing solution (2.5 M NaCl, 100 mM EDTA disodium salt, 10 mM Tris, pH 10, containing 1% Triton X-100 and 10% DMSO, added just before use). Slides were rinsed in cold deionized water and placed in a horizontal gel electrophoresis tank containing fresh cold electrophoresis solution (300 mM NaOH and 1 mM Na EDTA, pH >13) for 30 min, followed by electrophoresis at 0.8 V/cm for 30 min. Upon completion of the electrophoresis, slides were rinsed briefly in deionized water and neutralized using 0.4 M Tris-HCl buffer, pH 7.4. The slide was stained with 60  $\mu$ l of 10  $\mu$ g/ml ethidium bromide, covered with a coverglass, and 25 randomly chosen nuclei per duplicate slide were analyzed using a Nikon E400 fluorescence microscope linked to Comet Assay III software (Perspective Instruments, Suffolk, UK), as reported elsewhere<sup>34</sup>. Statistical analyses were performed for 'Percent DNA in the Tail' (the percentage of DNA in the "Comet" tail area in the assay and an indicator of the degree of DNA damage in the cells). With regard to cytotoxicity, none of the treatments reduced cell viability below 90%, as measured by the



trypan blue exclusion assay.

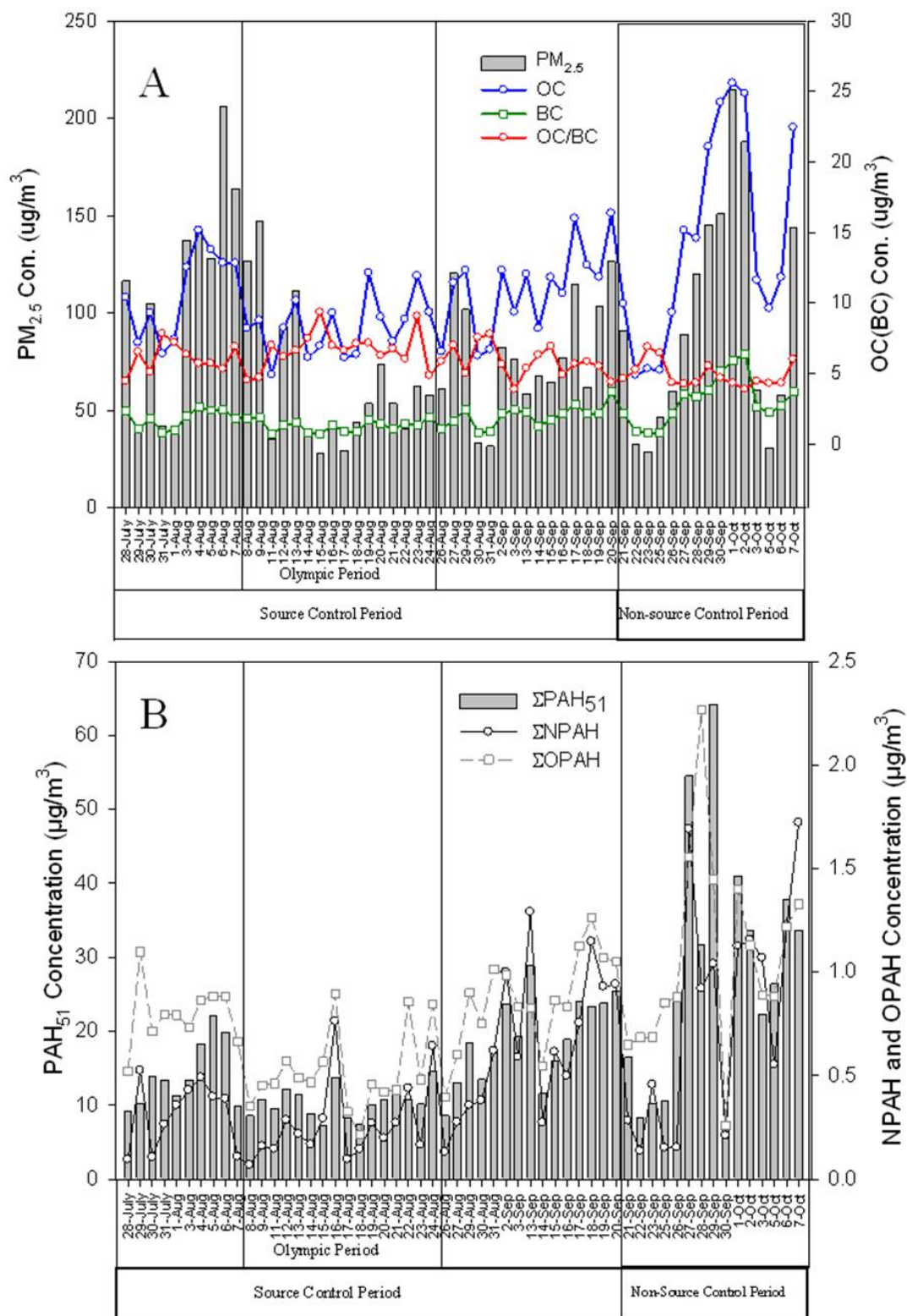
**2.2.6 Gas Pollutant Data** The NO, NO<sub>2</sub>, NO<sub>x</sub>, SO<sub>2</sub>, CO and O<sub>3</sub> concentrations were measured by Zhang et al<sup>1</sup> at the China Meteorological Administration (CMA) in Beijing. This site was at approximately 20 m above ground and 5 km south of Peking University where the PAH samples were collected.

## 2.3 Results and Discussion

### 2.3.1 Effect of Source Control Measures on BC, OC, and Parent PAH Concentrations

Because PAHs are an important part of the OC, it is useful to understand the relationship between BC, OC and PAH concentrations. The mean  $\pm$  standard deviation of the BC, OC, MW<300 parent PAH, and MW 302 parent PAH concentrations during the non-source control and source control periods are given in Appendix B.6, while their concentrations during the non-Olympic and Olympic periods are given in Appendix B.7. In addition, Figure 2.1A shows the temporal variation in the PM<sub>2.5</sub>, OC, and BC concentrations, as well as the OC/BC ratio, while Figure 2.1B shows the variation in  $\Sigma$ PAH<sub>51</sub> concentration. The mean BC and OC concentrations were statistically different ( $p < 0.05$ ) during the non-source control and source control periods and the non-Olympic and Olympic periods (Appendix B.6 and Appendix B.7). The BC and OC concentrations ranged from 0.8-6.4  $\mu\text{g}/\text{m}^3$  and 4.9-25.6  $\mu\text{g}/\text{m}^3$ , respectively, during the non-source control period and from 0.7-3.7  $\mu\text{g}/\text{m}^3$  and 4.9-16.3  $\mu\text{g}/\text{m}^3$ , respectively, during the source control period, with a mean reduction in concentrations of 1.4  $\mu\text{g}/\text{m}^3$  (45.5%) and 4.5  $\mu\text{g}/\text{m}^3$  (31.1%), respectively. During the non-Olympic and Olympic periods, the mean BC and OC concentrations were reduced by 1.1  $\mu\text{g}/\text{m}^3$  (44.8%) and 3.8  $\mu\text{g}/\text{m}^3$  (31.5%),

**Figure 2.1** Temporal variation of the (A)  $PM_{2.5}$ , OC, BC, OC/BC and (B)  $\Sigma PAH_{51}$ ,  $\Sigma NPAH$ , and  $\Sigma OPAH$  concentrations. The source control, non-source control, and the Olympic periods are indicated by labels and lines.



respectively. Other authors have reported BC concentrations in the range of 2-6  $\mu\text{g}/\text{m}^3$  and a reduction of 12-50% during the Olympic period (Appendix B.8)<sup>1-3</sup>. In addition, we measured relatively high OC to BC ratios (up to 9) during all periods, with a mean ratio of  $5.88 \pm 1.28$  for all periods (Appendix B.8).

Twenty-five of the 28 individual MW<300 parent PAH concentrations were significantly different between non-source control and source control periods, with concentration reductions of 26.6% to 77.9% ( $p < 0.05$ ) during the source control period (Appendix B.6). Only 1-MNAP, 2,6-DMNAP, and 1,3-DMNAP concentrations were not significantly different. Similarly, 22 of the 28 individual PAH concentrations were statistically different between the non-Olympic and Olympic periods, with concentration ( $\text{ng}/\text{m}^3$ ) reductions of 26.0% to 72.4% ( $p < 0.05$ ) during the Olympic period (Appendix B.7). In addition to 1-MNAP, 2,6-DMNAP, and 1,3-DMNAP concentrations, NAP, 2-MNAP, and ANT concentrations were not significantly different. This is likely because naphthalenes are emitted from a wide variety of consumer products (including personal care products, household products, adhesives, sealants, pesticides, and coatings)<sup>20</sup>, as well as incomplete combustion, and emissions from consumer products were not controlled in Beijing during this time period. In addition, the lower molecular weight PAHs, including naphthalenes, exist primarily in the atmospheric gas phase. Because only the particulate-phase was sampled, their total concentration in the atmosphere was significantly (but consistently) underestimated. Like the majority of the individual PAHs,  $\sum\text{PAH}_{28}$ ,  $\sum\text{PAH}_{2\text{ring}}$ ,  $\sum\text{PAH}_{3\text{ring}}$ ,  $\sum\text{PAH}_{4\text{ring}}$ ,  $\sum\text{PAH}_{56\text{ring}}$  and  $\sum\text{PAH}_{16\text{-US priority}}$  concentrations were all significantly different between non-source control and source control periods and between non-Olympic and Olympic periods, with concentration reductions of 32.4% to

60.0% and 22.8% to 58.3% ( $p < 0.05$ ), respectively.

Significant reductions were also observed for all measured MW 302 PAH isomers during the source control period compared to the non-source control period, ranging from 22% to 77% (Appendix B.6 and Appendix B.7) ( $p < 0.05$ ). Concentrations of  $\Sigma 302\text{PAH}$ ,  $\Sigma 302\text{PAH}_{\text{mut}}$ , and  $\Sigma\text{DBP}$  were reduced by 32% ( $4.6 \pm 2.3$  to  $3.2 \pm 1.2$   $\text{ng}/\text{m}^3$ ,  $p < 0.001$ ), 31% ( $2.9 \pm 1.4$  to  $2.0 \pm 0.8$   $\text{ng}/\text{m}^3$ ,  $p = 0.001$ ), and 39% ( $0.44 \pm 0.22$  to  $0.27 \pm 0.11$   $\text{ng}/\text{m}^3$ ,  $p < 0.001$ ), respectively. Similar and further reductions were observed during the Olympic period compared to the non-Olympic period, with individual MW302 PAH isomers reduced by 32% to 67%, and  $\Sigma 302\text{PAH}$ ,  $\Sigma 302\text{PAH}_{\text{mut}}$ , and  $\Sigma\text{DBP}$  reduced by 43-44% ( $p < 0.001$ ). The significant reductions in the MW 302 PAH concentrations were consistent with our findings for the majority of the lower molecular weight parent PAHs.

In general, for the MW<300 parent PAHs, the individual PAH concentrations were strongly positively correlated with the concentrations of other individual PAHs and with the  $\Sigma\text{PAH}_{28}$  and  $\Sigma\text{PAH}_{16\text{-US priority}}$  concentrations ( $p < 0.01$ ) (Appendix B.9). However, 1-MNAP, 2,6-DMNAP, and 1,3-DMNAP concentrations had less or no correlation with the other individual PAH,  $\Sigma\text{PAH}_{28}$ , and  $\Sigma\text{PAH}_{16\text{-US priority}}$  concentrations. However, these individual NAP concentrations were highly correlated with each other. This suggests that the naphthalenes are coming from a different source than the other individual PAHs, including consumer products<sup>20</sup>. Concentrations of ANT, one of the most photoreactive PAHs, were not as highly correlated with other individual PAH,  $\Sigma\text{PAH}_{28}$ , or  $\Sigma\text{PAH}_{16\text{-US priority}}$  concentrations. This may suggest that PAHs, especially ANT, undergo photodegradation enroute from regional and local sources to our sampling site.

### 2.3.2 Effect of Source Control Measures on NPAH and OPAH Concentrations

The mean  $\pm$  standard deviation of the individual NPAHs and OPAHs detected during the non-source control and source control periods, and during the non-Olympic and Olympic periods, are given in Appendix B.6 and Appendix B.7, respectively. Figure 2.1B shows the temporal variation in the  $\Sigma$ NPAH and  $\Sigma$ OPAH concentrations. Five of the 11 individual NPAH concentrations, and 2 of the 5 OPAH concentrations were significantly different between the source control and non-source control periods, with concentration reductions of 15.1% to 56.6% and 24.8% to 46.6%, respectively. During the Olympic period, 3-NBP, 3-NBF, 5-NAc and 1-NP concentrations were detectable, but below the limit of quantitation. Excluding these compounds, six of the 11 individual NPAH and all of the individual OPAH concentrations were statistically different between the Olympic and non-Olympic periods, with concentration reductions of 28.0% to 68.1% and 36.5% to 49.7%, respectively.

Except for 3-NBP, 3-NBF and 5-NAC, the individual NPAH and OPAH concentrations were strongly positively correlated to other NPAH and OPAH concentrations (Appendix B.11 and Appendix B.12).

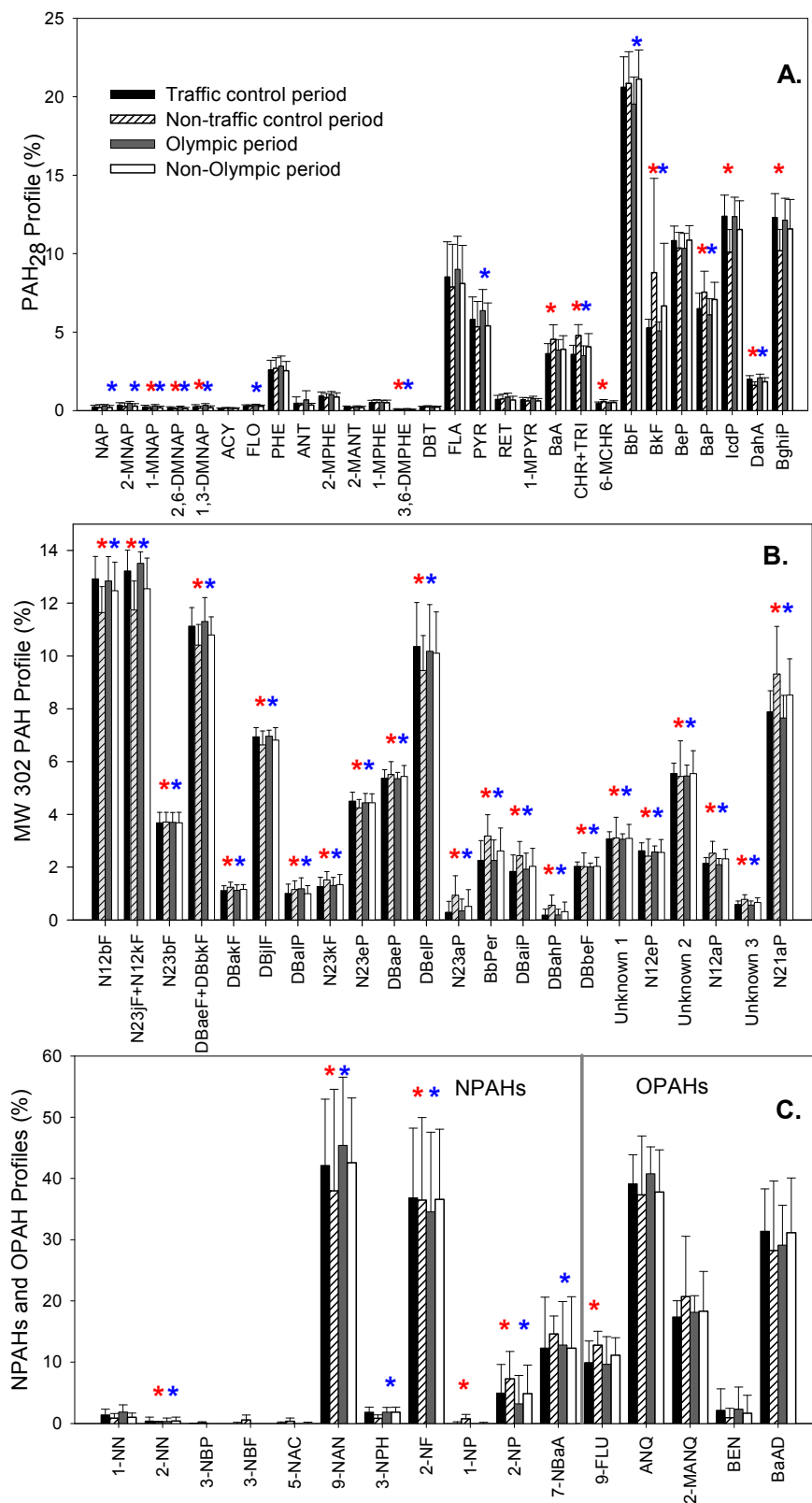
### 2.3.3 Parent PAH, NPAH and OPAH Sources

Appendix B.13 shows the correlation of individual parent PAH, NPAH, OPAH,  $\Sigma$ PAH<sub>28</sub>,  $\Sigma$ PAH<sub>2ring</sub>,  $\Sigma$ PAH<sub>3ring</sub>,  $\Sigma$ PAH<sub>4ring</sub>,  $\Sigma$ PAH<sub>56ring</sub>,  $\Sigma$ PAH<sub>16-US</sub> priority,  $\Sigma$ 302PAH,  $\Sigma$ 302PAH<sub>mut</sub>,  $\Sigma$ NPAH and  $\Sigma$ OPAH with NO, NO<sub>2</sub>, NO<sub>x</sub>, CO, SO<sub>2</sub>, and O<sub>3</sub> concentrations measured on the same days, during the source control period, when the PAH and gas-phase pollutant sampling overlapped<sup>1</sup>. Most of the individual parent PAH, NPAH and OPAH concentrations were positively correlated with NO and NO<sub>2</sub>

concentrations. NO is a short-lived species, with atmospheric residence time of 1 day<sup>35</sup>, and is an effective tracer for local traffic emissions<sup>36</sup>. However, only the individual parent PAH concentrations, and not the NPAH and OPAH concentrations, were correlated with CO and SO<sub>2</sub> concentrations. CO has an atmospheric residence time of 37 days<sup>35</sup>, and has been reported to undergo long-range transport<sup>37</sup>. This suggests that the parent PAHs are associated with both regional and local emissions, while the NPAH and OPAHs are primarily associated with local emissions and local photochemical formation. In addition, the CO and PM<sub>2.5</sub> mass concentrations were correlated with air masses from the south of Beijing ( $p < 0.001$ )<sup>7</sup>, where there are significant regional combustion sources, while the NO, NO<sub>2</sub> and NO<sub>x</sub> concentrations were not.

Figure 2.2A shows the mean ( $\pm$  standard deviation) profile of the 28 individual MW<300 parent PAHs (percent of total 28 MW<300 parent PAH concentration) during the source control, non-source control, Olympic, and non-Olympic periods. For all periods, the general trend in concentrations was: BbF > BeP  $\simeq$  IcdP  $\simeq$  BghiP > FLA > PYR  $\sim$  BkF  $\sim$  BaP > CHR+TRI  $\sim$  BaA. The lower molecular weight PAHs, those with 2 or 3 rings, had lower concentrations on PM<sub>2.5</sub> because they exist primarily in the atmospheric gas phase. However, the 4-ring PAHs, such as fluoranthene and pyrene, are distributed between the gas- and particulate-phases and the 5-ring (and higher) PAHs exist primarily in the particulate-phase. Because only the particulate-phase was measured in this study, the 5-ring PAHs, such as BbF and BeP were most abundant. Most individual MW<300 parent PAHs made up a similar percentage of the total MW<300 parent PAH concentration during the different periods. However, the 1-MNAP, 2,6-DMNAP, 1,3-DMNAP, 3,6-DMPHE, and DahA concentrations were slightly enhanced

**Figure 2.2** Mean ( $\pm$  standard deviation) of the percent of (A) total MW<300 PAHs, (B) total MW 302 PAHs, and (C) sum of NPAH and OPAH concentrations during the source control, non-source control, Olympic and non-Olympic periods. Red asterisks indicate a significant difference ( $p < 0.05$ ) between the source control and non-source control periods and blue asterisks indicate a significant difference ( $p < 0.05$ ) between the Olympic and non-Olympic periods.



in both the source control and Olympic periods, relative to the other MW<300 parent PAHs. In contrast, the CHR+TRI, BkF, and BaP concentrations were slightly enhanced in both the non-source control and non-Olympic periods. Furthermore, the FLA/ (FLA + PYR); IcdP/ (IcdP + BghiP); BeP/(BeP + BaP); and IcdP/ (IcdP + BeP) concentration ratios are consistent with local traffic emissions (Appendix B.14)<sup>38</sup>.

The mean profile of the MW 302 parent PAHs, NPAHs, and OPAHs was similar between the source control and non-source control periods and between the Olympic and non-Olympic periods (Figure 2.2B and 2.2C). This indicates that the combustion sources of these PAHs were similar among the different periods. For the MW 302 parent PAHs, N12bF, N23jF/N12kF, DBaEF/DBbkF, and DBelP were the most abundant species, accounting for 34% to 57% of the total measured MW 302 parent PAH concentration. Together, 2-NF and 9-NAN were the most abundant NPAHs, accounting for 74% to 80% of the total NPAH concentration, while ANQ and BaAD were the most abundant OPAHs, accounting for 63% - 68% of the total OPAH concentration.

### **2.3.4 Role of PAH Photochemistry**

To assess the contribution of primary emission (direct emission) and secondary emission (photochemical formation) of NPAH and OPAH, the 2-NF/1-NP concentration ratio was calculated. 2-NF is formed photochemically from the reaction of FLA with OH radical and NO<sub>3</sub> radical, while 1-NP is emitted from primary emissions<sup>39, 40</sup>. A 2-NF/1-NP ratio of 5 or greater indicates a dominance of photochemical formation, while a ratio of less than 5 indicates a dominance of direct emissions<sup>41, 42</sup>. The mean 2-NF/1-NP ratios during the source control, non-source control, non-Olympic periods were greater than 5 and ranged from 25-46 (Appendix B.6 and Appendix B.7). This suggests that there was a



dominance of photochemical formation during all periods. There was also a statistical difference in the 2-NF/1-NP ratio between the source control and non-source control periods and Olympic and non-Olympic periods, with lower ratios measured during the source control ( $38.7 \pm 15.2$ ) and Olympic periods (25.2). 1-NP was near the limit of quantitation on some of the source control and Olympic days because of the reduced direct emissions. Combined, these ratios indicate that there was greater photochemical formation of NPAHs during the non-source control and non-Olympic periods. This was the result of both meteorological conditions<sup>7</sup> and increased traffic emissions.

The 2-NF/2-NP concentration ratio has been used to estimate the relative importance of OH radical initiated reaction vs. NO<sub>3</sub> radical initiated reaction in the photochemical formation of NPAHs in the atmosphere<sup>41, 43</sup>. During daytime, fluoranthene and pyrene react with OH radical in the presence of NO<sub>2</sub> to form 2-NF and 2-NP, respectively<sup>40, 43</sup>. During nighttime, fluoranthene and pyrene react with NO<sub>3</sub> radicals to form predominantly 2-NF and negligible amounts of 2-NP<sup>40, 43</sup>. A 2-NF/2-NP concentration ratio close to 10 indicates the OH radical-initiated reaction is dominant, while a ratio closer to 100 indicates the NO<sub>3</sub> radical-initiated reaction is dominant<sup>43</sup>. During all periods, the mean 2-NF/2-NP concentration ratio was consistently below 10 (Appendix B.6 and Appendix B.7), ranging from 3.4 to 4.8, suggesting a dominance of daytime OH radical-initiated reaction for NPAH formation. This observation is consistent with previous ambient measurements<sup>41, 42</sup>.

### **2.3.5 Toxicity of the PM extracts**

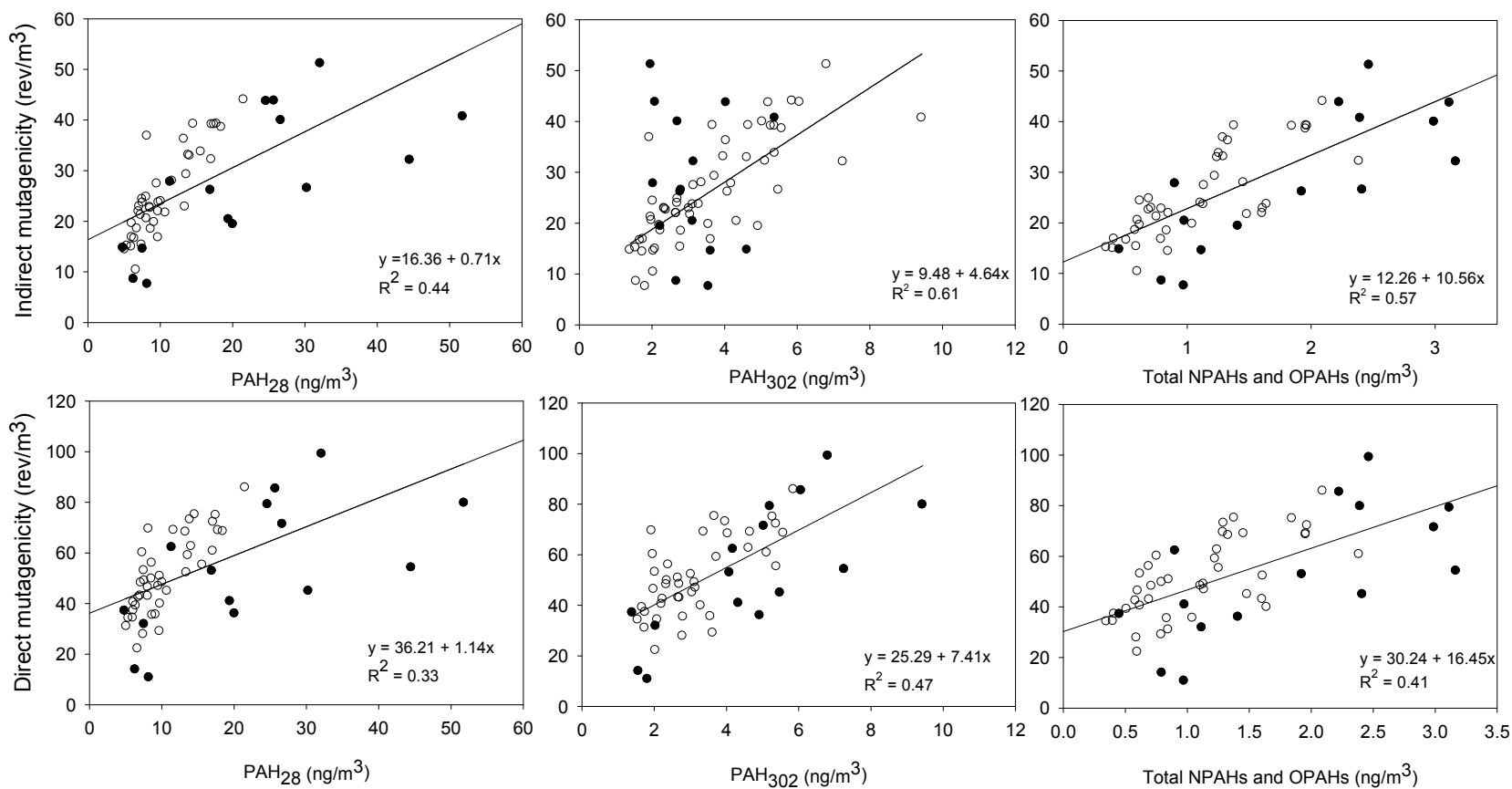
We have previously reported the estimated reduction in PAH-related inhalation cancer risk due to source control measures during the Beijing Olympics using a point-

estimate approach based on relative potency factors<sup>17</sup>. In this study, the PM<sub>2.5</sub> crude extracts were assayed by the Ames test using the *Salmonella typhimurium* TA98 strain with and without S9 mix. The mutagen density (revertants per volume of air) and the corresponding  $\Sigma$ PAH<sub>28</sub>,  $\Sigma$ 302PAH,  $\Sigma$ NPAH, and  $\Sigma$ OPAH concentrations are reported in Appendix B.15. Because the crude extracts were not fractionated, the direct-acting NPAH mutagenicity may have been suppressed by the presence of indirect-acting parent PAHs<sup>44</sup>. Nonetheless, the crude extracts are representative of the PAH, NPAH, and OPAH mixture that Beijing residents are exposed to in ambient air.

The correlations of  $\Sigma$ PAH<sub>28</sub>,  $\Sigma$ 302PAH and sum of  $\Sigma$ NPAH and  $\Sigma$ OPAH concentrations with direct-acting and indirect-acting mutagen densities are shown in Figure 2.3. The parent PAHs, including  $\Sigma$ PAH<sub>28</sub>,  $\Sigma$ 302PAH and the sum of  $\Sigma$ NPAH and  $\Sigma$ OPAH were well correlated with the indirect-acting mutagen density, with R<sup>2</sup> values of 0.44, 0.61 and 0.57 (p-values < 0.0001), respectively. The correlation of the sum of  $\Sigma$ NPAH and  $\Sigma$ OPAH concentrations with direct-acting mutagen density was less significant (R<sup>2</sup> of 0.41, p-value < 0.001). This may be due to the presence of parent PAHs in the crude extract<sup>44</sup>. On average, the  $\Sigma$ NPAH and  $\Sigma$ OPAH concentrations were 8% of the parent PAH concentrations, while the direct-acting mutagenicity (due to NPAH and OPAH) was 200% higher than the indirect-acting mutagenicity (due to parent PAH). This suggests that NPAH and OPAH make up a significant portion of the overall mutagenicity of PM<sub>2.5</sub> in Beijing. The lowest mean mutagen density was associated with the Olympic period, which is consistent with statistically significant decreases in  $\Sigma$ PAH<sub>28</sub>,  $\Sigma$ 302PAH, and sum of  $\Sigma$ NPAH and  $\Sigma$ OPAH concentrations.

Human cell assays were carried out on the PM<sub>2.5</sub> crude extracts in order to

**Figure 2.3** Correlation of  $\Sigma\text{PAH}_{28}$ ,  $\Sigma 302\text{PAH}$  and sum of  $\Sigma\text{NPAH}$  and  $\Sigma\text{OPAH}$  with direct-acting and indirect-acting mutagen densities during the source control (○) and non-source control periods (●).



associate the bacteria-based toxicity with human cell-based toxicity. Appendix B.15 shows the median percent DNA damage of human A549 lung carcinoma cells dosed with the daily PM extracts in the Comet assay. The toxicity of PM, including direct and indirect mutagenicities and percent DNA damage in the Comet assay, were not statistically different between the source control and non-source control periods. However, the mutagenicity of the PM<sub>2.5</sub> was significantly reduced during the Olympic period. This suggests that the source control measures did not result in as significant a reduction in PM toxicity as  $\Sigma$ PAH<sub>28</sub>,  $\Sigma$ 302PAH,  $\Sigma$ NPAH and  $\Sigma$ OPAH concentrations. This may be because pollutants other than those measured here contributed to the overall toxicity of the PM<sub>2.5</sub> crude extracts and may not have been reduced in concentration due to the source control measures.

Appendix B.16 shows the Spearman correlation between mutagenic activities in the Ames bacterial assays and levels of DNA damage in human cell assays for all of the PM<sub>2.5</sub> extracts. There was a strong correlation ( $r = 0.77$ ,  $p < 0.0001$ ) between the results of the two different assays. Previous studies questioned the comparison of mutagenic activities of unsubstituted and substituted PAHs in bacterial assays with human cell assays, calling into question the relevance of bacterial assays<sup>45</sup>). However, our results suggest that there is a significant correlation between the bacterial assay results and the human cell assay results.

## **2.4 Acknowledgements**

Funding for this research was provided by the China Scholarship Council (to Wentao Wang), the U.S. National Science Foundation (ATM-0841165), and National Scientific Foundation of China (40710019001 and 40730737). This publication was

made possible in part by grant number P30ES00210 from the National Institute of Environmental Health Sciences (NIEHS), NIH and NIEHS Grant P42 ES016465. We also thank Xiao Ye Zhang from Chinese Academy of Meteorological Sciences for providing us the gas pollutant data. Its contents are solely the responsibility of the authors and do not necessarily represent the official view of the NIEHS, NIH.

### **Supporting Information Available**

Details of the concentrations during the different periods, correlation analysis, and temporal variation in concentrations with meteorological parameters are provided in the Supporting Information. This material is available free of charge via the Internet at <http://pubs.acs.org>.

## 2.5 References

1. Zhang, X. Y.; Wang, Y. Q.; Lin, W. L.; Zhang, Y. M.; Zhang, X. C.; Gong, S.; Zhao, P.; Yang, Y. Q.; Wang, J. Z.; Hou, Q.; Zhang, X. L.; Che, H. Z.; Guo, J. P.; Li, Y., Changes of atmospheric composition and optical properties over Beijing. *Bulletin of the American Meteorological Society* **2009**, *90*, (11), 1633-1651.
2. Wang, M.; Zhu, T.; Zheng, J.; Zhang, R. Y.; Zhang, S. Q.; Xie, X. X.; Han, Y. Q.; Li, Y., Use of a mobile laboratory to evaluate changes in on-road air pollutants during the Beijing 2008 Summer Olympics. *Atmos. Chem. Phys. Discuss.* **2009**, *9*, (21), 8247-8263.
3. Wang, X.; Westerdahl, D.; Chen, L. C.; Wu, Y.; Hao, J.; Pan, X.; Guo, X.; Zhang, K. M., Evaluating the air quality impacts of the 2008 Beijing Olympic Games: On-road emission factors and black carbon profiles. *Atmos. Environ.* **2009**, *43*, (30), 4535-4543.
4. Wang, S.; Zhao, M.; Xing, J.; Wu, Y.; Zhou, Y.; Lei, Y.; He, K.; Fu, L.; Hao, J., Quantifying the Air Pollutants Emission Reduction during the 2008 Olympic Games in Beijing. *Environ. Sci. Technol.* **2010**, *44*, (7), 2490-2496.
5. Shou-bin, F.; Gang, T.; Gang, L.; Yu-hu, H.; Jian-ping, Q.; Shui-yuan, C., Road fugitive dust emission characteristics in Beijing during Olympics Game 2008 in Beijing, China. *Atmos. Environ.* **2009**, *43*, (38), 6003-6010.
6. Wang, T.; Xie, S., Assessment of traffic-related air pollution in the urban streets before and during the 2008 Beijing Olympic Games traffic control period. *Atmos. Environ.* **2009**, *43*, (35), 5682-5690.
7. Wang, W.; Primbs, T.; Tao, S.; Simonich, S. L. M., Atmospheric Particulate Matter Pollution during the 2008 Beijing Olympics. *Environ. Sci. Technol.* **2009**, *43*, (14), 5314-5320.
8. Zhou, Y.; Wu, Y.; Yang, L.; Fu, L.; He, K.; Wang, S.; Hao, J.; Chen, J.; Li, C., The impact of transportation control measures on emission reductions during the 2008 Olympic Games in Beijing, China. *Atmos. Environ.* **2010**, *44*, (3), 285-293.
9. Cermak, J.; Knutti, R., Beijing Olympics as an aerosol field experiment. *Geophys. Res. Lett.* **2009**, *36*, (10), L10806.
10. Xin, J.; Wang, Y.; Tang, G.; Wang, L.; Sun, Y.; Wang, Y.; Hu, B.; Song, T.; Ji, D.; Wang, W.; Li, L.; Liu, G., Variability and reduction of atmospheric pollutants in Beijing and its surrounding area during the Beijing 2008 Olympic Games. *Chin. Sci. Bull.* **2010**, *55*, (18), 1937-1944.
11. Li, Y.; Wang, W.; Kan, H. D.; Xu, X. H.; Chen, B. H., Air quality and outpatient visits for asthma in adults during the 2008 Summer Olympic Games in Beijing. *Sci. Total Environ.* **2010**, *408*, (5), 1226-1227.
12. Li, Y.; Shao, M.; Lu, S.; Chang, C.-C.; Dasgupta, P. K., Variations and sources of ambient formaldehyde for the 2008 Beijing Olympic games. *Atmos. Environ.* **2010**, *44*, (21-22), 2632-2639.
13. Wang, Y.; Hao, J.; McElroy, M. B.; Munger, J. W.; Ma, H.; Chen, D.; Nielsen, C. P., Ozone air quality during the 2008 Beijing Olympics: effectiveness of emission restrictions. *Atmos. Chem. Phys.* **2009**, *9*, 5237-5251.
14. Witte, J. C.; Schoeberl, M. R.; Douglass, A. R.; Gleason, J. F.; Krotkov, N. A.; Gille, J. C.; Pickering, K. E.; Livesey, N., Satellite observations of changes in air quality during the 2008 Beijing Olympics and Paralympics. *Geophys. Res. Lett.* **2009**, *36*, (17), L17803.

15. Mijling, B.; van der A, R. J.; Boersma, K. F.; Van Roozendaal, M.; De Smedt, I.; Kelder, H. M., Reductions of NO<sub>2</sub> detected from space during the 2008 Beijing Olympic Games. *Geophys. Res. Lett.* **2009**, *36*, (13), L13801.
16. Wang, B.; Shao, M.; Lu, S. H.; Yuan, B.; Zhao, Y.; Wang, M.; Zhang, S. Q.; Wu, D., Variation of ambient non-methane hydrocarbons in Beijing city in summer 2008. *Atmos. Chem. Phys.* **2010**, *10*, (13), 5911-5923.
17. Jia, Y.; Stone, D.; Wang, W.; Schrlau, J.; Tao, S.; Massey Simonich, S. L., Estimated Reduction in Cancer Risk due to PAH Exposures if Source Control Measures during the 2008 Beijing Olympics were Sustained. *Environ. Health Perspect.* **2011**.
18. Saikawa, E.; Naik, V.; Horowitz, L. W.; Liu, J. F.; Mauzerall, D. L., Present and potential future contributions of sulfate, black and organic carbon aerosols from China to global air quality, premature mortality and, radiative forcing. *Atmos. Environ.* **2009**, *43*, (17), 2814-2822.
19. Bond, T. C.; Streets, D. G.; Yarber, K. F.; Nelson, S. M.; Woo, J.-H.; Klimont, Z., A technology-based global inventory of black and organic carbon emissions from combustion. *J. Geophys. Res.* **2004**, *109*, (D14), D14203.
20. Zhang, Y.; Tao, S., Global atmospheric emission inventory of polycyclic aromatic hydrocarbons (PAHs) for 2004. *Atmos. Environ.* **2009**, *43*, (4), 812-819.
21. Zhang, Y. X.; Tao, S.; Shen, H. Z.; Ma, J. M., Inhalation exposure to ambient polycyclic aromatic hydrocarbons and lung cancer risk of Chinese population. *Proc. Natl. Acad. Sci. U. S. A.* **2009**, *106*, (50), 21063-21067.
22. Birch, M. E.; Cary, R. A., Elemental Carbon-Based Method for Monitoring Occupational Exposures to Particulate Diesel Exhaust. *Aerosol Sci. Technol.* **1996**, *25*, (3), 221 - 241.
23. Chen, Y. J.; Sheng, G. Y.; Bi, X. H.; Feng, Y. L.; Mai, B. X.; Fu, J. M., Emission factors for carbonaceous particles and polycyclic aromatic hydrocarbons from residential coal combustion in China. *Environ. Sci. Technol.* **2005**, *39*, (6), 1861-1867.
24. Shen, G.; Yang, Y.; Wang, W.; Tao, S.; Zhu, C.; Min, Y.; Xue, M.; Ding, J.; Wang, B.; Wang, R.; Shen, H.; Li, W.; Wang, X.; Russell, A. G., Emission Factors of Particulate Matter and Elemental Carbon for Crop Residues and Coals Burned in Typical Household Stoves in China. *Environ. Sci. Technol.* **2010**, *44*, (18), 7157-7162.
25. Primbs, T.; Simonich, S.; Schmedding, D.; Wilson, G.; Jaffe, D.; Takami, A.; Kato, S.; Hatakeyama, S.; Kajii, Y., Atmospheric Outflow of Anthropogenic Semivolatile Organic Compounds from East Asia in Spring 2004. *Environ. Sci. Technol.* **2007**, *41*, (10), 3551-3558.
26. Primbs, T.; Genualdi, S.; Simonich, S. M., Solvent selection for pressurized liquid extraction of polymeric sorbents used in air sampling. *Environ. Toxicol. Chem.* **2008**, *27*, (6), 1267-1272.
27. Primbs, T.; Piekarz, A.; Wilson, G.; Schmedding, D.; Higginbotham, C.; Field, J.; Simonich, S. M., Influence of Asian and Western United States Urban Areas and Fires on the Atmospheric Transport of Polycyclic Aromatic Hydrocarbons, Polychlorinated Biphenyls, and Fluorotelomer Alcohols in the Western United States. *Environ. Sci. Technol.* **2008**, *42*, (17), 6385-6391.
28. Usenko, S.; Hageman, K. J.; Schmedding, D. W.; Wilson, G. R.; Simonich, S. L., Trace analysis of semivolatile organic compounds in large volume samples of snow, lake water, and groundwater. *Environ. Sci. Technol.* **2005**, *39*, (16), 6006-6015.

29. Durant, J. L.; Busby, W. F.; Lafleur, A. L.; Penman, B. W.; Crespi, C. L., Human cell mutagenicity of oxygenated, nitrated and unsubstituted polycyclic aromatic hydrocarbons associated with urban aerosols. *Mutation Research/Genetic Toxicology* **1996**, *371*, (3-4), 123-157.
30. Durant, J. L.; Lafleur, A. L.; Plummer, E. F.; Taghizadeh, K.; Busby, W. F.; Thilly, W. G., Human Lymphoblast Mutagens in Urban Airborne Particles. *Environ. Sci. Technol.* **1998**, *32*, (13), 1894-1906.
31. Durant, J. L.; Lafleur, A. L.; Busby, W. F.; Donhoffner, L. L.; Penman, B. W.; Crespi, C. L., Mutagenicity of C<sub>24</sub>H<sub>14</sub> PAH in human cells expressing CYP1A1. *Mutation Research/Genetic Toxicology and Environmental Mutagenesis* **1999**, *446*, (1), 1-14.
32. Maron, D. M.; Ames, B. N., Revised methods for the Salmonella mutagenicity test. *Mutation Research/Environmental Mutagenesis and Related Subjects* **1983**, *113*, (3-4), 173-215.
33. Singh, N. P.; McCoy, M. T.; Tice, R. R.; Schneider, E. L., A simple technique for quantitation of low levels of DNA damage in individual cells. *Exp. Cell Res.* **1988**, *175*, (1), 184-191.
34. Mastaloudis, A.; Yu, T.-W.; O'Donnell, R. P.; Frei, B.; Dashwood, R. H.; Traber, M. G., Endurance exercise results in DNA damage as detected by the comet assay. *Free Radical Biol. Med.* **2004**, *36*, (8), 966-975.
35. Brimblecombe, P., *Air composition & chemistry*. second ed.; Cambridge University Press: Cambridge, UK, 1996.
36. Janhäll, S.; M. Jonsson, Å.; Molnár, P.; A. Svensson, E.; Hallquist, M., Size resolved traffic emission factors of submicrometer particles. *Atmos. Environ.* **2004**, *38*, (26), 4331-4340.
37. Peng, L.; Zhao, C.; Lin, Y.; Zheng, X.; Tie, X.; Chan, L.-Y., Analysis of carbon monoxide budget in North China. *Chemosphere* **2007**, *66*, (8), 1383-1389.
38. van Pinxteren, D.; Brüggemann, E.; Gnauk, T.; Iinuma, Y.; Müller, K.; Nowak, A.; Achtert, P.; Wiedensohler, A.; Herrmann, H., Size- and time-resolved chemical particle characterization during CAREBeijing-2006: Different pollution regimes and diurnal profiles. *Journal of Geophysical Research-Atmospheres* **2009**, *114*, D00G09.
39. Schuetzle, D., Sampling of vehicle emissions for chemical analysis and biological testing. *Environ. Health Perspect.* **1983**, *47*, 65-80.
40. Atkinson, R.; Arey, J.; Zielinska, B.; Aschmann, S. M., Kinetics and Nitro-Products of the Gas-Phase OH and NO<sub>3</sub> Radical-Initiated Reactions of Naphthalene-d<sub>8</sub>, Fluoranthene-d<sub>10</sub>, and Pyrene. *Int. J. Chem. Kinet.* **1990**, *22*, 999-1014.
41. Ciccioli, P.; Cecinato, A.; Brancaleoni, E.; Frattoni, M.; Zacchei, P.; Miguel, A. H.; Vasconcellos, P. d. C., Formation and transport of 2-nitrofluoranthene and 2-nitropyrene of photochemical origin in the troposphere. *J. Geophys. Res.* **1996**, *101*, (D14), 19567-19581.
42. Albinet, A.; Leoz-Garziandia, E.; Budzinski, H.; Villenave, E.; Jaffrezo, J. L., Nitrated and oxygenated derivatives of polycyclic aromatic hydrocarbons in the ambient air of two French alpine valleys: Part 1: Concentrations, sources and gas/particle partitioning. *Atmos. Environ.* **2008**, *42*, (1), 43-54.
43. Arey, J.; Zielinska, B.; Atkinson, R.; Aschmann, S. M., Nitroarene Products from the Gas-Phase Reactions of Volatile Polycyclic Aromatic Hydrocarbons with the OH



Radical and N<sub>2</sub>O<sub>5</sub>. *Int. J. Chem. Kinet.* **1989**, *21*, 775-799.

44. Hayakawa, K.; Nakamura, A.; Terai, N.; Kizu, R.; Ando, K., Nitroarene Concentration and Direct-acting Mutagenicity of Diesel Exhaust Particulates Fractionated by Silica-Gel Column Chromatography. *Chem. Pharm. Bull.* **1997**, *45*, (11), 1820-1822.

45. Hannigan, M. P.; Cass, G. R.; Penman, B. W.; Crespi, C. L.; Lafleur, A. L.; Busby, W. F.; Thilly, W. G., Human Cell Mutagens in Los Angeles Air. *Environ. Sci. Technol.* **1997**, *31*, (2), 438-447.

**CHAPTER 3. NITRO-PAH PRODUCT FORMATION FROM  
HETEROGENEOUS REACTIONS OF PAHS WITH NO<sub>2</sub>, NO<sub>3</sub>/N<sub>2</sub>O<sub>5</sub>,  
O<sub>3</sub> AND OH RADICALS: PREDICTION, LABORATORY STUDIES  
AND MUTAGENICITY**

NARUMOL JARIYASOPIT<sup>1</sup>, MELISSA MC INTOSH<sup>1</sup>, KATHRYN  
ZIMMERMANN<sup>2</sup>, JANET AREY<sup>2</sup>, ROGER ATKINSON<sup>2</sup>, PAUL HA-YEON  
CHEONG<sup>1</sup>, RICH G. CARTER<sup>1</sup>, TIAN-WEI YU<sup>3</sup>, RODERICK H. DASHWOOD<sup>3,4</sup>,  
STACI L. MASSEY SIMONICH<sup>1,4\*</sup>

<sup>1</sup>Department of Chemistry, Oregon State University, Corvallis, Oregon USA 97331;

<sup>2</sup>Air Pollution Research Center, University of California, Riverside;

<sup>3</sup>Linus Pauling Institute, Oregon State University, Corvallis, Oregon USA, 97331;

<sup>4</sup>Environmental and Molecular Toxicology, Oregon State University, Corvallis, Oregon,  
USA, 97331.

\*Corresponding author e-mail: [staci.simonich@orst.edu](mailto:staci.simonich@orst.edu); phone: (541) 737-9194; fax:  
(541) 737-0497

## ABSTRACT

The heterogeneous reaction of benzo[a]pyrene-d<sub>12</sub>, benzo[k]fluoranthene-d<sub>12</sub>, benzo[ghi]perylene-d<sub>12</sub>, dibenzo[a,i]pyrene-d<sub>14</sub>, and dibenzo[a,l]pyrene, with atmospheric oxidants, including NO<sub>2</sub>, NO<sub>3</sub>/N<sub>2</sub>O<sub>5</sub>, O<sub>3</sub>, and OH radicals, were investigated at room temperature and atmospheric pressure in a Teflon chamber. Quartz fiber filters (QFF) were used as a reaction surface and substrate. The analyses of parent polycyclic aromatic hydrocarbons (PAHs) and nitro products in the analytical extracts were conducted using gas chromatographic mass spectrometry. In addition, the filter extracts were tested in the Salmonella mutagenicity assay, using *Salmonella typhimurium* strain TA98 (with and without metabolic activation), to determine changes in mutagenic activities upon exposures. In parallel to the laboratory experiments, a theoretical study was conducted to assist in determining the formation of NPAH isomers based on the OH radical-initiated reaction. The computed thermodynamic stability of OH-PAH intermediates was used to predict the selectivity of OH radical addition. This study has shown that the NO<sub>2</sub> and NO<sub>3</sub>/N<sub>2</sub>O<sub>5</sub> were effective oxidizing agents in transforming PAHs deposited on filters to nitrated-PAHs (NPAHs), under these experimental conditions with benzo[a]pyrene-d<sub>12</sub> being the most readily nitrated. The relatively lower molecular weight PAHs studied, including benzo[a]pyrene-d<sub>12</sub>, benzo[k]fluoranthene-d<sub>12</sub> and benzo[ghi]perylene-d<sub>12</sub>, yielded more than one mono-nitro isomer product, whereas the higher molecular weight PAHs studied, dibenzo[a,i]pyrene-d<sub>14</sub> and dibenzo[a,l]pyrene, resulted in the formation of only one mono-nitro isomer product. The direct-acting mutagenicity increased the most after NO<sub>3</sub>/N<sub>2</sub>O<sub>5</sub> exposure, particularly for benzo[k]fluoranthene-d<sub>12</sub> in which dinitro PAHs were observed. Deuterium isotope effect study suggested that substitution of deuterium for hydrogen lowered the mutagenicity. The magnitude of mutagenicity could

be underestimated because the nitro products were deuterated.

### 3.1 Introduction

Polycyclic aromatic hydrocarbons (PAHs) have been intensively studied because of their ubiquitous presence in the environment and toxicity. In the atmosphere, PAHs with 2-4 rings partition primarily into the gas phase<sup>1</sup>, while PAHs with more than four rings are partitioned primarily to the particulate phase. Once emitted from combustion sources, hydrophobic PAHs undergo atmospheric transformation reactions converting them to the more hydrophilic compounds, such as nitro-PAHs (NPAHs) and oxy-PAHs (OPAHs). The gas-phase and particle-phase PAHs may undergo wet and dry deposition, direct photolysis, reaction with ozone and radical-initiated reactions, such as OH-radical and NO<sub>3</sub>-radical initiated reactions. Gas-phase radical initiated reactions are thought to be a significant removal process for gas-phase PAHs<sup>1</sup>.

NPAHs are PAH derivatives emitted directly to the atmosphere from combustion sources and/or formed from atmospheric transformation via gas-phase OH- and NO<sub>3</sub>-radical initiated reactions of PAHs<sup>1</sup>, and some NPAHs are more toxic than the parent PAHs<sup>2,3</sup>. Gas-phase reactions of PAHs to form NPAHs are initiated by either OH or NO<sub>3</sub> radical attack at the position of highest electron density on the aromatic ring, followed by NO<sub>2</sub> addition. In contrast, the heterogeneous nitration follows different mechanism as previous studies have shown that heterogeneous reactions of pyrene and fluoranthene with NO<sub>3</sub>/N<sub>2</sub>O<sub>5</sub> yield different dominant nitropyrene and nitrofluoranthene isomers than the corresponding gas-phase reactions<sup>4-6</sup>. The kinetics of heterogeneous reactions were found to highly vary due to the inherent complexity of heterogeneous reactions caused by the characteristics of substrates, surface chemistry and the substrate-specific kinetics

of heterogeneous reactions<sup>7-9</sup>. The formation of NPAHs from the heterogeneous reactions of PAHs containing two to five rings have been studied with NO<sub>2</sub>, N<sub>2</sub>O<sub>5</sub><sup>5, 6, 8, 10-13</sup>, whereas a limited number of studies have investigated the formation of NPAHs from the heterogeneous reaction of PAHs with greater than five rings<sup>14</sup>. In field studies, nitrobenzopyrenes and nitroperylene (MW297) were the highest molecular weight NPAHs detected in the atmosphere<sup>15-17</sup>. Deuterated PAHs were used, except for dibenzo[a,l]pyrene, for which the deuterated analog was not commercially available. Deuterated PAHs were chosen because they are not significantly abundant in the environment, attributing the formation of deuterated nitro PAH products solely to reactions in the chamber. Because mutagenicity of deuterated nitro PAH products may differ from non-deuterated analogs, a deuterium isotope effect study was carried out to investigate the effect on mutagenicity.

The objectives of this study were to 1) identify NPAHs formed from the heterogeneous reaction of filter-adsorbed perdeuterated PAHs with NO<sub>2</sub>, NO<sub>3</sub>/N<sub>2</sub>O<sub>5</sub>, O<sub>3</sub>, and OH radicals using laboratory experiments and theoretical calculations and 2) associate NPAH formation in the laboratory experiments with the mutagenicity of the extracts. Five higher molecular weight PAHs, including benzo[a]pyrene-d<sub>12</sub> (BaP-d<sub>12</sub>), benzo[ghi]perylene-d<sub>12</sub> (BghiP-d<sub>12</sub>), benzo[k]fluoranthene-d<sub>12</sub> (BkF-d<sub>12</sub>), dibenzo[a,i]pyrene-d<sub>14</sub> (DaiP-d<sub>14</sub>), and dibenzo[a,l]pyrene (DaIP) were selected for this research because of their mutagenicity and the lack of data on their formation of NPAH products during heterogeneous reactions. To our knowledge, the NPAH products of DaIP and DaiP have not been previously identified.

## 3.2 Experimental

### 3.2.1 Chemicals and Materials

Perdeuterated BaP-d<sub>12</sub>, BkF-d<sub>12</sub>, BghiP-d<sub>12</sub>, and DaiP-d<sub>14</sub> were purchased from CDN Isotopes (Point-Claire, Quebec, Canada) and Cambridge Isotope Laboratories (Andover, MA). Because perdeuterated DalP was not commercially available we purchased the non-deuterated DalP from Cambridge Isotope Laboratories (Andover, MA). Dichloromethane, ethyl acetate and dimethyl sulfoxide were purchased from Fisher Scientific (Santa Clara, CA) and EMD Chemicals (Gibbstown, NJ). Salmonella tester strain TA98 was originally purchased from Xenometrix, Inc. Of the mono-NO<sub>2</sub>-PAH and di-NO<sub>2</sub>-PAH products identified in this study, only 6-NO<sub>2</sub>-BaP-d<sub>11</sub> was commercially available and was purchased from Chiron AS (Trondheim, Norway).

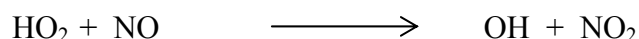
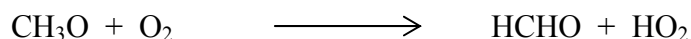
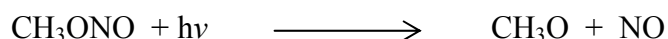
Synthesis of standards that were not commercially available was accomplished through direct nitration of the parent PAH with nitric acid in acetic anhydride following conditions provided by Cho et al.<sup>18</sup>. Nitration of benzo[k]fluoranthene provided 7-nitrobenzo[k]fluoranthene<sup>19, 20</sup> and 3,7-dinitrobenzo[k]fluoranthene as major and minor compounds respectively. Nitration of benzo[ghi]perylene provided 7-nitrobenzo[ghi]perylene and 5-nitrobenzo[ghi]perylene<sup>21</sup>. These compounds were characterized by 1D <sup>1</sup>H and <sup>13</sup>C NMR, 2D <sup>1</sup>H-<sup>1</sup>H Correlation Spectroscopy (COSY), 2D <sup>1</sup>H-<sup>13</sup>C Heteronuclear Single-Quantum Correlation and Multiple-Bond Correlation (HSQC and HMBC) NMR, Infrared, GCMS, and High Resolution Mass Spectrometry. The structure of 3,7-dinitrobenzo[k]fluoranthene was elucidated using the techniques described above along with 1D Nuclear Overhauser Effect (NOE) NMR spectroscopy.

### 3.2.2 Spiked Filter Preparation and Exposures

The quartz fiber filters (QFFs) (8 in x 10 in, No.1851-865, Tisch Environmental, Cleves, OH) were pre-baked (350°C) before use. Each clean QFF was divided into 4 quarters. Ten µg of the individual PAHs in ethyl acetate were deposited separately onto each quarter of the QFFs with a pipette and placed in the laboratory fume hood, allowing ethyl acetate to evaporate at room temperature for approximately 30 minutes. A quarter of clean, unspiked QFF was also placed in the chamber during each experiment as a negative control for toxicological and chemical studies.

Laboratory experiments were carried out in ~7000 L indoor collapsible Teflon chamber equipped with two parallel banks of blacklamps and a Teflon-coated fan at room temperature (~297 K) and ~740 Torr<sup>6</sup>. All the filters were placed on a standing, rotating apparatus inside the Teflon chambers.

*OH radical Exposure.* OH radicals were generated by the photolysis of methylnitrite (CH<sub>3</sub>ONO) at wavelength of > 300 nm in the presence of added NO<sup>22, 23</sup>.



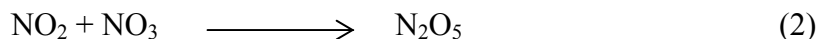
Approximately 1 ppm of CH<sub>3</sub>ONO and NO were flushed into the chamber every hour, leading to average OH radical concentration in the chamber of  $2 \times 10^7$  molecule cm<sup>-3</sup> (~0.8 ppt). The chamber was operated in the flush mode to avoid the build-up of NO<sub>2</sub> and HNO<sub>3</sub> in the chamber. However, a minor amount of HNO<sub>3</sub> was expected to

form and could have nitrated the PAHs. Irradiations were carried out at 20% of the maximum light intensity for 140 minutes. Two additions of 1 ppm CH<sub>3</sub>ONO and NO were made to maintain the OH radical concentration throughout the course of 140 minute exposure.

*NO<sub>3</sub>/N<sub>2</sub>O<sub>5</sub> Exposure.* The NO<sub>3</sub>/N<sub>2</sub>O<sub>5</sub> exposure was carried out in the dark and NO<sub>3</sub> radicals were generated by the thermal decomposition of N<sub>2</sub>O<sub>5</sub><sup>24,25</sup>:



The generated NO<sub>3</sub> also reacts with NO<sub>2</sub> to form N<sub>2</sub>O<sub>5</sub>:



Under ambient conditions, NO<sub>2</sub>, NO<sub>3</sub> and N<sub>2</sub>O<sub>5</sub> are present at equilibrium concentrations and the NO<sub>3</sub> concentration can be calculated based on the experimental rate constants of reactions (1) and (2)<sup>26</sup>. One addition of approximately 0.44 and 0.75 ppm of N<sub>2</sub>O<sub>5</sub> and NO<sub>2</sub>, respectively, were made every hour, with a total of two additions over the entire 165 minutes of exposure, by flushing into the chamber with a stream of N<sub>2</sub>. The chamber was continually flushed. The amount of NO<sub>2</sub> added was proportional to the N<sub>2</sub>O<sub>5</sub> concentration in order to control the NO<sub>3</sub> formation and ensure that the NO<sub>3</sub>-PAH adduct reacted only with NO<sub>2</sub><sup>25</sup>. This resulted in an average NO<sub>3</sub> concentration of ~ 658 ppt over the course of exposure.

*O<sub>3</sub> and NO<sub>2</sub> Exposures.* The O<sub>3</sub> and NO<sub>2</sub> experiments were conducted in the dark and operated in the flush-off mode. Ozone was generated using a Welsbach T-408 O<sub>3</sub> generator and added to the chamber so that the concentration was ~945 ppb over the entire 210 minutes of exposure. NO<sub>2</sub> was generated by oxidation of NO with O<sub>2</sub> and



introduced to the chamber. The average NO<sub>2</sub> concentration was ~4.9 ppm over the entire 238 minutes of exposure.

### **3.2.3 Sample extraction and Analysis**

Using the extraction method previously described in detail<sup>27</sup>, the QFFs were extracted twice (both extracts were combined) using pressurized liquid extraction with dichloromethane. The extracts subjected to chemical analysis were evaporated and solvent-exchanged to ethyl acetate under a purified N<sub>2</sub> stream with a Turbovap II (Caliper Life Sciences, MA). The extracts subjected to the Salmonella assay were evaporated to the dryness under a stream of N<sub>2</sub> and the residue was dissolved in 500 µl of dimethylsulfoxide (DMSO). Only for the unexposed filters spiked with individual PAHs tested, the extracts were divided into two halves by weight. One half of the extract was prepared for mutagenicity testing and the other half was prepared for chemical analysis as described.

The analyses of parent PAHs and NPAHs in the analytical extracts was conducted using gas chromatographic mass spectrometry (GCMS, Agilent 6890 GC coupled with an Agilent 5973N MSD) in selected ion monitoring (SIM) and scan modes using both electron impact (EI) and negative chemical ionization (NCI) (using CH<sub>4</sub>), with a programmed temperature vaporization (PTV) inlet (Gerstel, Germany). A 5% phenyl substituted methylpolysiloxane GC column (DB-5MS, 30m×0.25mm I.D., 0.25 µm film thickness, J&W Scientific, USA) was used to separate the parent PAHs and NPAHs.

### **3.2.4 Theoretical Study**

In parallel to the laboratory experiments, a theoretical study was conducted using Density Functional Theory (DFT), with the B3LYP functional and the 6-31G(d) basis set, as implemented in Gaussian03. The thermodynamic stability of the OH-PAH intermediates was used to rationalize the formation of NPAH isomers. From our computations, the positions of OH addition that gave the most thermodynamically stable OH-PAH intermediates corresponded to the positions where the electrophilic nitration would occur (see discussion below).

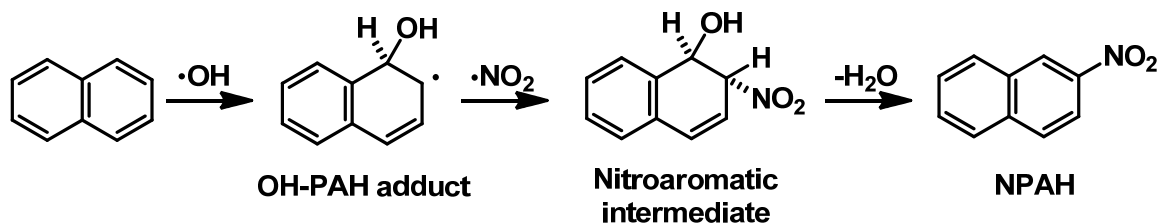
### 3.2.5 Salmonella Mutagenicity Assay

The basic method followed that reported by Maron and Ames<sup>28</sup> and *Salmonella typhimurium* strain TA98 was used in the study. The experimental details have been described elsewhere<sup>27</sup>. The positive control doses were 2 µg of 2-aminoanthracene (2-AA) and 20 µg of 4-nitro-1,2-phenylenediamine (NPD) for assays with and without metabolic activation (rat S9 mix), respectively. The negative control (DMSO) dose was 30 µl. All filter extracts were tested in triplicate.

## 3.3 Results and Discussion

### 3.3.1 Theoretical Studies

The mechanism of gas-phase OH radical-initiated reaction with PAHs to give NPAH has been previously described<sup>29</sup>. Scheme 3.1 shows that, in the gas-phase, the initial addition of OH radical to an aromatic ring leads to an OH-PAH adduct. This radical further can further react with NO<sub>2</sub> to yield a nitrocyclohexadienyl radical intermediate, which is followed by water elimination to form the NPAH. Alternatively, in ambient atmospheres, the OH-PAH adduct can also react with O<sub>2</sub> to give other degradation products<sup>30</sup>.



**Scheme 3.1.** General mechanism for the nitration of PAHs via gas-phase reaction with OH radical.

To verify our computation strategy, computations for pyrene and fluoranthene were carried out and compared with nitro products identified in a previous gas-phase OH-radical chamber study<sup>4</sup> (Appendix C.1). Positions 1 and 3 on pyrene and fluoranthene, respectively, were found to yield the most thermodynamically stable OH-PAH adduct intermediates (pyrene:  $\Delta G_{\text{rxn}} = -18.4$  Kcal/mol and fluoranthene:  $\Delta G_{\text{rxn}} = -16.7$  Kcal/mol) (Appendix C.1). Followed by  $\text{NO}_2$  addition to the *ortho* position, the reactions were predicted to yield 2-nitropyrene and 2-nitrofluoranthene as major products from the OH radical-initiated gas-phase reaction of pyrene and fluoranthene, respectively. Because our theoretical results for pyrene and fluoranthene were in good agreement with the experimental results<sup>4</sup>, this suggested that the thermodynamic stability of the OH-PAH adducts in the first step of the gas-phase OH radical-initiated reaction, which involves loss of aromaticity of the PAH system, could be used to predict the formation of NPAHs in the gas-phase.

The strong thermodynamic stability of intermediates formed from addition to 1 and 3 positions on pyrene and fluoranthene, respectively, dictates all reactions. Therefore, addition of  $\text{NO}_2$  by direct nitration reactions should also occur at the same positions. Unlike the gas-phase radical-initiated reactions, the heterogeneous nitration of

pyrene and fluoranthene with  $\text{N}_2\text{O}_5$ <sup>5, 11</sup> and  $\text{NO}_2$ <sup>31</sup> formed 1-nitropyrene and 3-nitrofluoranthene as dominant isomers. Table 3.1 shows the calculated free energies of the OH-PAH adducts for all possible OH radical attack positions at peripheral aromatic carbons and predicts the NPAHs formed from heterogeneous reaction of BaP, BkF, BghiP, DaiP, and DalP.

### 3.3.2 NPAH Product Identification

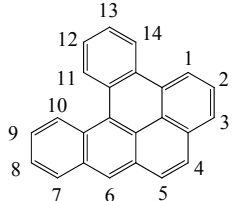
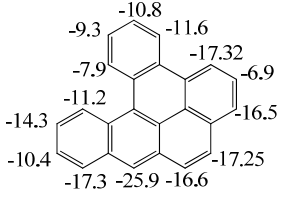
All major NPAH product isomers were identified based on the GC retention time, full scan EI and/or NCI mass spectra of the standards when they were available. For NPAH isomers without commercially available standards, a previously published method was used to predict their GC retention time orders<sup>32</sup>. White et al. found that the dipole moment of mono-nitro PAH isomers predicted their GC retention time order on a non-polar SE-52 GC column, a 5% phenyl substituted methylpolysiloxane stationary phase, with the NPAH isomers eluting in order of increasing dipole moment<sup>32</sup>. In this study, we predicted the GC retention time orders of the most stable mono-nitro PAH isomers products listed in Table 3.1 by calculating their dipole moments using Gaussian with B3LYP/6-31G(d) (Appendix C.2) and predicted the molecular ion of the NCI mass spectra based on their molecular weight.

***Benzo[a]pyrene*** Figures 3.1A-D show the NCI full scan chromatograms of BaP-d<sub>12</sub> exposed to  $\text{NO}_2$ ,  $\text{NO}_3/\text{N}_2\text{O}_5$ ,  $\text{O}_3$  and OH radical overlaid with the chromatogram of the unexposed BaP-d<sub>12</sub>. The m/z 264 peak is the molecular ion of BaP-d<sub>12</sub>. BaP-d<sub>12</sub> reacted with  $\text{NO}_2$  and  $\text{NO}_3/\text{N}_2\text{O}_5$  (Figures 3.1A and 3.1B) and yielded significant amounts of mono  $\text{NO}_2$ -BaPs. In contrast, after the  $\text{O}_3$  and OH radical exposures, no apparent mono  $\text{NO}_2$ -BaP-d<sub>11</sub> products and noticeably lower amounts of mono  $\text{NO}_2$ -BaP-d<sub>11</sub> products

**Table 3.1.** Free energies ( $\Delta G_{\text{rxn}}$ ) of OH-PAH adducts calculated using density functional theory (B3LYP) and the 6-31G(d) basis set. NPAH isomers are listed in order of predicted stability.

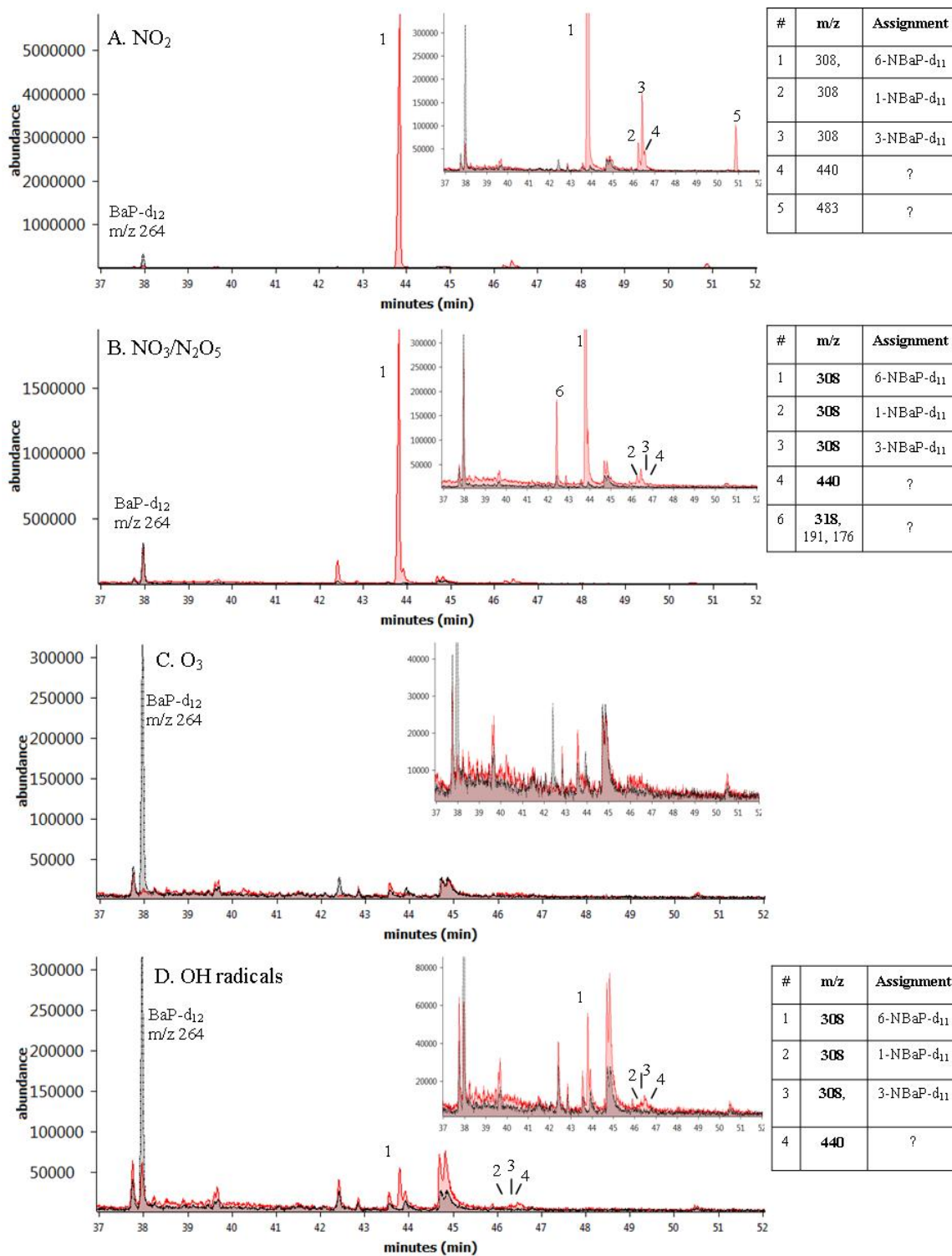
PAH	Numbering Scheme	OH-PAH-Adduct $\Delta G_{\text{rxn}}$ (Kcal/mol)	NPAH identified in this study	Identified in	Detected in environment?
Benzo[a]pyrene			6-nitrobenzo[a]pyrene <sup>ψ</sup> 1-nitrobenzo[a]pyrene 3-nitrobenzo[a]pyrene	NO <sub>2</sub> , NO <sub>3</sub> /N <sub>2</sub> O <sub>5</sub> , OH NO <sub>2</sub> , NO <sub>3</sub> /N <sub>2</sub> O <sub>5</sub> , OH NO <sub>2</sub> , NO <sub>3</sub> /N <sub>2</sub> O <sub>5</sub> , OH	Y <sup>15-17, 33</sup> Y <sup>34</sup> Y <sup>34</sup>
Benzo[k]fluoranthene			3-nitrobenzo[k]fluoranthene <sup>θ</sup> 7-nitrobenzo[k]fluoranthene <sup>θ</sup> 8-nitrobenzo[k]fluoranthene <sup>θ</sup> 1-nitrobenzo[k]fluoranthene <sup>θ</sup> 9-nitrobenzo[k]fluoranthene <sup>θ</sup> 3,7-dinitrobenzo[k]fluoranthene <sup>θ</sup> 4 dinitrobenzo[k]fluoranthenes	NO <sub>2</sub> , NO <sub>3</sub> /N <sub>2</sub> O <sub>5</sub> , OH NO <sub>2</sub> , NO <sub>3</sub> /N <sub>2</sub> O <sub>5</sub> , O <sub>3</sub> , OH NO <sub>3</sub> /N <sub>2</sub> O <sub>5</sub> , OH NO <sub>3</sub> /N <sub>2</sub> O <sub>5</sub> , O <sub>3</sub> , OH NO <sub>3</sub> /N <sub>2</sub> O <sub>5</sub> NO <sub>3</sub> /N <sub>2</sub> O <sub>5</sub> NO <sub>3</sub> /N <sub>2</sub> O <sub>5</sub>	N N N N N N N
Benzo[ghi]perylene			5-nitrobenzo[ghi]perylene <sup>θ</sup> 7-nitrobenzo[ghi]perylene <sup>θ</sup> 4-nitrobenzo[ghi]perylene	NO <sub>3</sub> /N <sub>2</sub> O <sub>5</sub> , OH NO <sub>3</sub> /N <sub>2</sub> O <sub>5</sub> NO <sub>3</sub> /N <sub>2</sub> O <sub>5</sub>	N N N
Dibenzo[a,i]pyrene			5-nitrodibenzo[a,i]pyrene	NO <sub>2</sub> , NO <sub>3</sub> /N <sub>2</sub> O <sub>5</sub>	N

**Table 3.1 (Continued)**

PAH	Numbering Scheme	OH-PAH-Adduct $\Delta G_{rxn}$ (Kcal/mol)	NPAH identified in this study	Identified in	Detected in environment?
Dibenzo[a,l]pyrene			6-nitrodibenzo[a,l]pyrene	NO <sub>2</sub> , NO <sub>3</sub> /N <sub>2</sub> O <sub>5</sub> , OH	N

<sup>ψ</sup> verified with deuterated standard. <sup>θ</sup> verified with non-deuterated standard.

**Figure 3.1.** Overlaid full scan NCI chromatograms of unexposed BaP-d<sub>12</sub> and exposed BaP-d<sub>12</sub> with A) NO<sub>2</sub> B) NO<sub>3</sub>/N<sub>2</sub>O<sub>5</sub> C) O<sub>3</sub> and D) OH radicals. Inset chromatograms are zoomed in at full chromatograms. All chromatograms are NCI full scan. A *m/z* ion in bold indicates a base peak. ( - - - Unexposed BaP-d<sub>12</sub> , — Exposed BaP-d<sub>12</sub>)

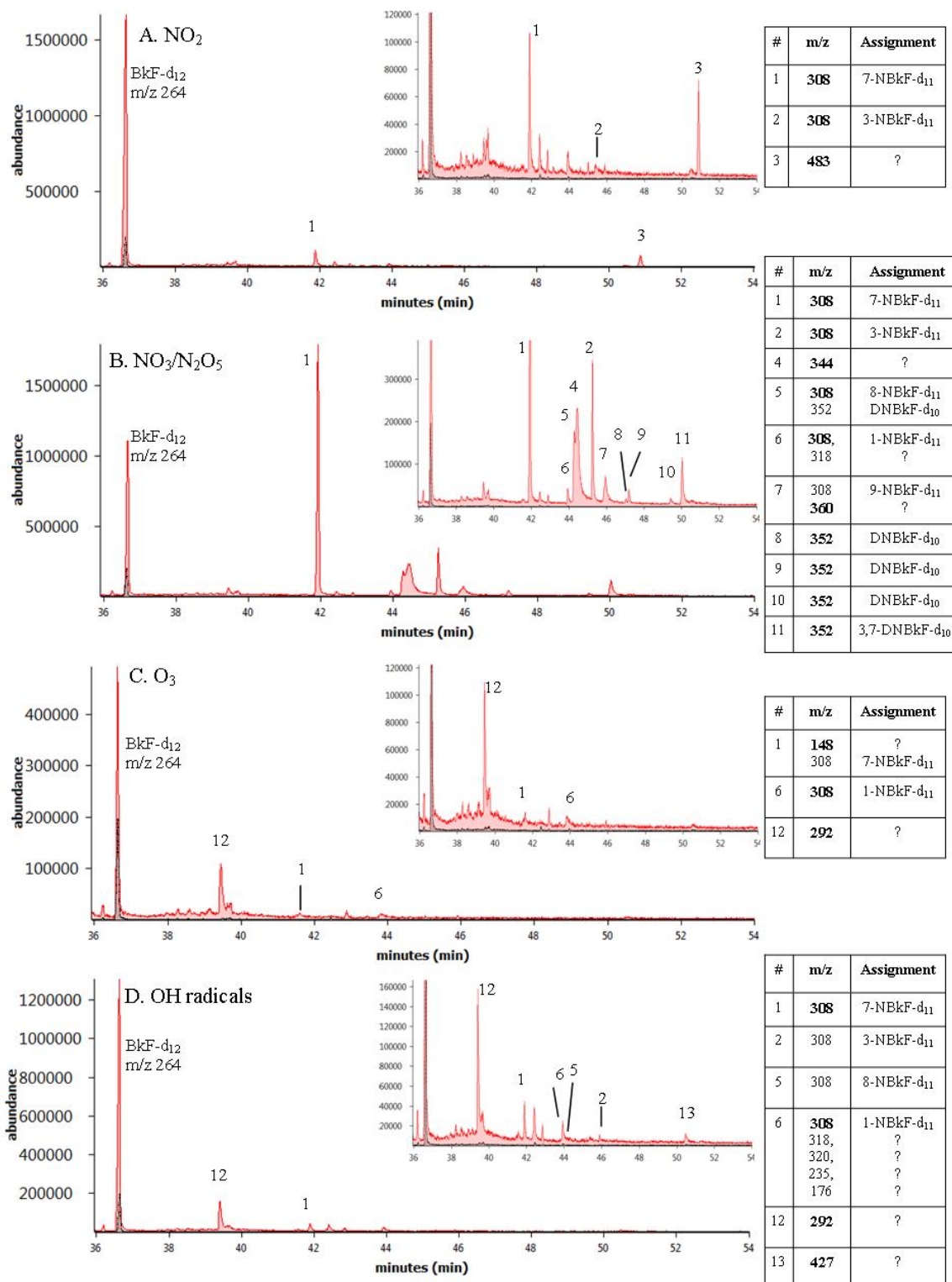


were formed, respectively (Figures 3.1C and 3.1D). Three mono NO<sub>2</sub>-BaP isomers (Figure 3.1A, 3.1B and 3.1D, peaks 1-3) were identified from the reaction of BaP-d<sub>12</sub> with NO<sub>2</sub>, NO<sub>3</sub>/N<sub>2</sub>O<sub>5</sub>, and OH radicals. No dinitro PAH isomers were identified in the exposures. Based on the ΔG values shown in Table 3.1, we predicted that the most reactive position for OH attack of BaP is 6, followed by 1 and 3, respectively. This prediction is consistent with a previous study which determined the distribution of NO<sub>2</sub>-BaP isomers based on the calculated reactivity numbers<sup>35</sup>. The calculated dipole moments of these isomers suggested a GC retention time order of 6-, 1- and 3-NO<sub>2</sub>-BaP-d<sub>11</sub> (Appendix C.2) and this same retention order was previously observed for these isomers using the same type of nonpolar GC column<sup>36</sup>. Therefore, the earliest eluting peak with m/z 308 (Figure 3.1A-B, peak 1) was identified as 6-NO<sub>2</sub>-BaP-d<sub>11</sub> and its retention time confirmed with a standard of 6-NO<sub>2</sub>-BaP-d<sub>11</sub>. This peak also had the highest intensity, corresponding to the highest stability of the calculated 6-OH-BaP adduct. In addition, 6-NO<sub>2</sub>-BaP was recently identified as a major product from the heterogeneous reaction of BaP coated soot particles with NO<sub>2</sub><sup>13</sup>. A slight difference in dipole moments of 1- and 3-NO<sub>2</sub>-BaP-d<sub>11</sub> (6.06 and 6.16 Debye, respectively) predicts close GC retention times for these two isomers and peaks 2 and 3 (both with m/z 308) were tentatively assigned to 1- and 3-NO<sub>2</sub>-BaP-d<sub>11</sub>, respectively. 1- and 3-NO<sub>2</sub>-BaP were previously found to be minor products from a study of heterogeneous reaction of BaP with NO<sub>2</sub> and N<sub>2</sub>O<sub>5</sub><sup>7, 11</sup>.

***Benzo[k]fluoranthene*** Figures 3.2A-D show the NCI full scan chromatograms of BkF-d<sub>12</sub> exposed to NO<sub>2</sub>, NO<sub>3</sub>/N<sub>2</sub>O<sub>5</sub>, O<sub>3</sub> and OH radical overlaid with the chromatogram of the unexposed BkF-d<sub>12</sub>. The m/z 264 peak is the molecular ion of BkF-d<sub>12</sub>. Two mono NO<sub>2</sub>-BkF-d<sub>11</sub> peaks (m/z 308), 3- and 7-NO<sub>2</sub>-BkF-d<sub>11</sub>, were identified from the reaction of BkF-d<sub>12</sub> with NO<sub>2</sub> (Figure 3.2A) based on the ΔG



**Figure 3.2.** Overlaid full scan NCI chromatograms of unexposed BkF-d<sub>12</sub> and exposed BkF-d<sub>12</sub> with A) NO<sub>2</sub> B) NO<sub>3</sub>/N<sub>2</sub>O<sub>5</sub> C) O<sub>3</sub> and D) OH radicals. Inset chromatograms are zoomed in at full chromatograms. All chromatograms are NCI full scan. A m/z ion in bold indicates a base peak. ( --- Unexposed BkF-d<sub>12</sub> , — Exposed BkF-d<sub>12</sub>)



values shown in Table 3.1. The weaker calculated dipole moment of 7-NO<sub>2</sub>-BkF-d<sub>11</sub>, relative to 3-NO<sub>2</sub>-BkF-d<sub>11</sub>, suggested it would elute first, and comparison with the synthesized standard confirmed this. Therefore, peaks 1 and 2 were identified as 7-NO<sub>2</sub>-BkF-d<sub>11</sub> and 3-NO<sub>2</sub>-BkF-d<sub>11</sub>, respectively. The formation of 3-NO<sub>2</sub>-BkF-d<sub>11</sub> was expected to be more favorable than 7-NO<sub>2</sub>-BkF-d<sub>11</sub> based on the stability of the various OH-BkF adducts (Table 3.1). However, the intensity of the 3-NO<sub>2</sub>-BkF-d<sub>11</sub> peak was significantly lower than that of 7-NO<sub>2</sub>-BkF-d<sub>11</sub>. The same observation was made in the EI full scan chromatogram and may suggest that 3-NO<sub>2</sub>-BkF-d<sub>11</sub> was more prone to further nitration, yielding di-NO<sub>2</sub>-BkF-d<sub>10</sub>, compared to 7-NO<sub>2</sub>-BkF-d<sub>11</sub>. The retention time of 7-NO<sub>2</sub>-BkF-d<sub>11</sub> was confirmed with the non-deuterated 7-NO<sub>2</sub>-BkF standard, noting a slight difference in retention times due to deuterium isotope effect was observed.

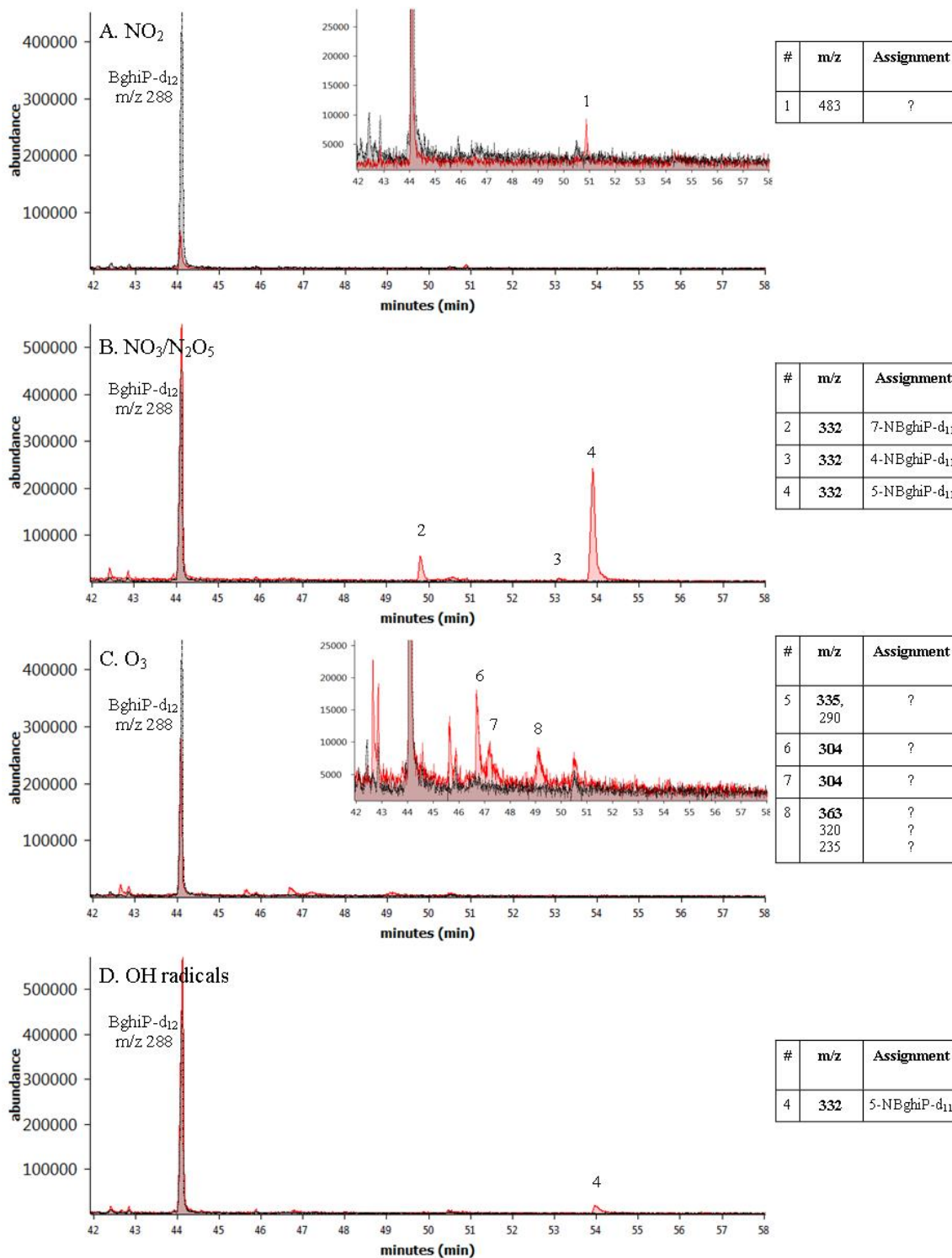
BkF-d<sub>12</sub> was nitrated during the NO<sub>3</sub>/N<sub>2</sub>O<sub>5</sub> exposure and five mono-NO<sub>2</sub>-BkF-d<sub>11</sub> products (m/z 308) were identified in the NCI full scan chromatogram (Figure 3.2B). As shown in Table 3.1, the predicted order of product stability, based on the thermodynamic stability of the OH-BkF adducts, was: 3, 7, 8, 1 and 9 positions of mono-NO<sub>2</sub>-BkF-d<sub>11</sub>. Based on the calculated dipole moments of these compounds, the predicted GC retention time elution order was: 7-, 1-, 8-, 3- and 9-NO<sub>2</sub>-BkF-d<sub>11</sub> (Appendix C.2). In addition to the mono-NO<sub>2</sub>-BkF-d<sub>11</sub> products, we also identified di-NO<sub>2</sub>-BkF-d<sub>10</sub> products (m/z 352) after the NO<sub>3</sub>/N<sub>2</sub>O<sub>5</sub> exposure (Figure 3.2B). Dinitro-PAHs are believed to form from reaction of mono-nitro PAHs with the oxidizing agent<sup>12, 37</sup> and, therefore, the most stable mono-NO<sub>2</sub>-BkF-d<sub>11</sub> product (3-NO<sub>2</sub>-BkF-d<sub>11</sub>) is likely to react further with an oxidizing agent. To predict the most likely di-NO<sub>2</sub>-BkF-d<sub>10</sub> products, we calculated the thermodynamic stability of the OH-3-NO<sub>2</sub>-BkF-d<sub>10</sub> adducts. If 3-NO<sub>2</sub>-BkF-d<sub>11</sub> were the only mono-NO<sub>2</sub>-BkF-d<sub>11</sub> isomer that

underwent further nitration, the five dominant di-NO<sub>2</sub>-BkF-d<sub>10</sub> products were predicted to be: 3,12-, 3,7-, 3,4-, 3,6- and 3,8-NO<sub>2</sub>-BkF-d<sub>10</sub> (Appendix C.3). Because 3-NO<sub>2</sub>-BkF-d<sub>11</sub> was not the only mono-NO<sub>2</sub>-BkF-d<sub>11</sub> product formed, other di-nitro-BkF-d<sub>10</sub> isomers may also have been formed. The positive identification of the di-NO<sub>2</sub>-BkF-d<sub>10</sub> products would require authentic standards which are not currently commercially available. Only 3,7-NO<sub>2</sub>-BkF-d<sub>10</sub> (peak 11) was verified with the non-deuterated 3,7-NO<sub>2</sub>-BkF standard.

Only two small mono-NO<sub>2</sub>-BkF-d<sub>11</sub> peaks, 1-NO<sub>2</sub>-BkF-d<sub>11</sub> and 7-NO<sub>2</sub>-BkF-d<sub>11</sub>, were identified in the O<sub>3</sub> exposure chromatograms (Figure 3.2C). However, the OH radical exposure chromatograms indicated the presence of 7, 3, 8, and 1-NO<sub>2</sub>-BkF-d<sub>11</sub> but not 9-NO<sub>2</sub>-BkF-d<sub>11</sub> (Figure 3.2D). The NCI full scan chromatograms for both O<sub>3</sub> and OH radical exposures showed traces of other degradation products, possibly oxygenated PAHs, mostly eluting before the mono-NO<sub>2</sub>-BkF-d<sub>11</sub> and di-NO<sub>2</sub>-BkF-d<sub>10</sub> isomers (Figures 3.2C and D).

***Benzo[ghi]perylene*** Unlike the other PAHs, BghiP-d<sub>12</sub> was not effectively nitrated by NO<sub>2</sub> and only one small unidentified peak (m/z 483) was observed in the NCI full scan chromatogram (Figure 3.3A). In contrast, after NO<sub>3</sub>/N<sub>2</sub>O<sub>5</sub> exposure, three apparent mono-NO<sub>2</sub>-BghiP-d<sub>11</sub> isomers (m/z 332) were identified (Figure 3.3B). Based on the ΔG values shown in Table 3.1, we predicted that 5-, 7-, and 4-NO<sub>2</sub>-BghiP-d<sub>11</sub> would be the most stable mono-NO<sub>2</sub>-BghiP-d<sub>11</sub> products. A previous study also identified 5-NO<sub>2</sub>-BghiP as a dominant nitro product formed from the reaction of BghiP adsorbed on silica gel particles with NO<sub>2</sub><sup>14</sup>. The calculated dipole moments for these isomers suggested an elution order of 7-, 4-, and 5-NO<sub>2</sub>-BghiP-d<sub>11</sub> (Appendix C.2). No NO<sub>2</sub>-BghiP-d<sub>11</sub> products were identified after O<sub>3</sub> exposure, however, other unidentified products were formed (Figure 3.3C). After OH radical exposure, only 5-

**Figure 3.3.** Overlaid full scan NCI chromatograms of unexposed BghiP-d<sub>12</sub> and exposed BghiP-d<sub>12</sub> with A) NO<sub>2</sub> B) NO<sub>3</sub>/N<sub>2</sub>O<sub>5</sub> C) O<sub>3</sub> and D) OH radicals. Inset chromatograms are zoomed in at full chromatograms. All chromatograms are NCI full scan. A m/z ion in bold indicates a base peak. ( --- Unexposed BghiP-d<sub>12</sub>, — Exposed BghiP-d<sub>12</sub>)



NO<sub>2</sub>-BghiP-d<sub>11</sub>, the most stable NO<sub>2</sub>-BghiP-d<sub>11</sub> isomer, was identified in the NCI full scan chromatogram (Figure 3.3D).

**Dibenzo[a,i]pyrene** As shown in Figures 3.4A and B, the NO<sub>2</sub> and NO<sub>3</sub>/N<sub>2</sub>O<sub>5</sub> exposures resulted in only one mono-NO<sub>2</sub>-DaiP-d<sub>13</sub> product (m/z 360). Based on the ΔG values shown in Table 3.1, we predicted that 5-NO<sub>2</sub>-DaiP-d<sub>13</sub> would be the most stable mono-NO<sub>2</sub>-DaiP-d<sub>13</sub> product. The exposure of DaiP-d<sub>14</sub> to O<sub>3</sub> and OH radicals did not result in any mono-NO<sub>2</sub>-DaiP-d<sub>13</sub> products (Figures 3.4C and D).

**Dibenzo[a,l]pyrene** Because a perdeuterated DalP standard was not commercially available, we used a nondeuterated DalP standard for our experiments. The presence of DalP in the purified air in the chamber was below the detection limit. A single mono-NO<sub>2</sub>-DalP peak (m/z 347) was observed after the NO<sub>2</sub> and NO<sub>3</sub>/N<sub>2</sub>O<sub>5</sub> exposures (Figure 3.5A and B). Based on the ΔG values shown in Table 3.1, we predicted that 6-NO<sub>2</sub>-DalP would be the most stable mono-NO<sub>2</sub>-DalP product. Similarly, OH radical exposure also resulted in the formation of 6-NO<sub>2</sub>-DalP, but to a much lesser extent than the NO<sub>2</sub> and NO<sub>3</sub>/N<sub>2</sub>O<sub>5</sub> exposures (Figure 3.5D). Even though the DalP peak (m/z 302) was significantly reduced after O<sub>3</sub> exposure, no mono-NO<sub>2</sub>-DalP products were formed (Figure 3.5C) and no other degradation products could be identified from the EI or NCI full scan chromatograms. It should be noted that the GC oven temperatures and run times were extended to look for additional DalP and DaiP-d<sub>14</sub> products. The absence of DalP degradation products upon O<sub>3</sub> exposure in the GC chromatograms may be the result of low vapor pressure of the DalP degradation products and/or strong interaction with the GC stationary phase.

Overall, the mono-NO<sub>2</sub>-PAH products of these heterogeneous reactions could be predicted based on free energies of the intermediates from radical initiated

**Figure 3.4.** Overlaid full scan NCI chromatograms of unexposed DaiP-d<sub>14</sub> and exposed DaiP-d<sub>14</sub> with A) NO<sub>2</sub> B) NO<sub>3</sub>/N<sub>2</sub>O<sub>5</sub> C) O<sub>3</sub> and D) OH radicals. Inset chromatograms are zoomed in at full chromatograms. All chromatograms are NCI full scan. A m/z ion in bold indicates a base peak. ( --- Unexposed DaiP-d<sub>14</sub>, — Exposed DaiP-d<sub>14</sub>)

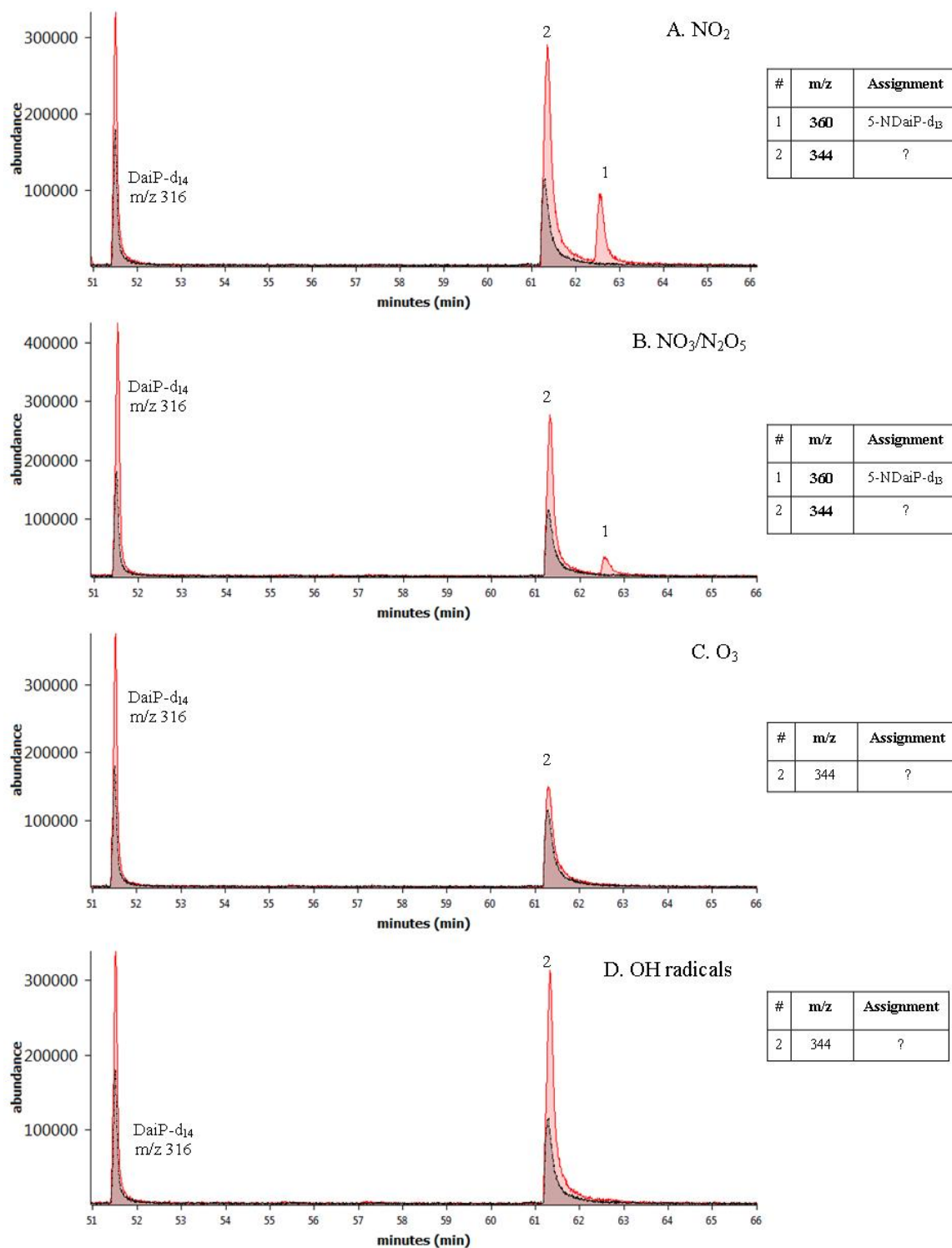
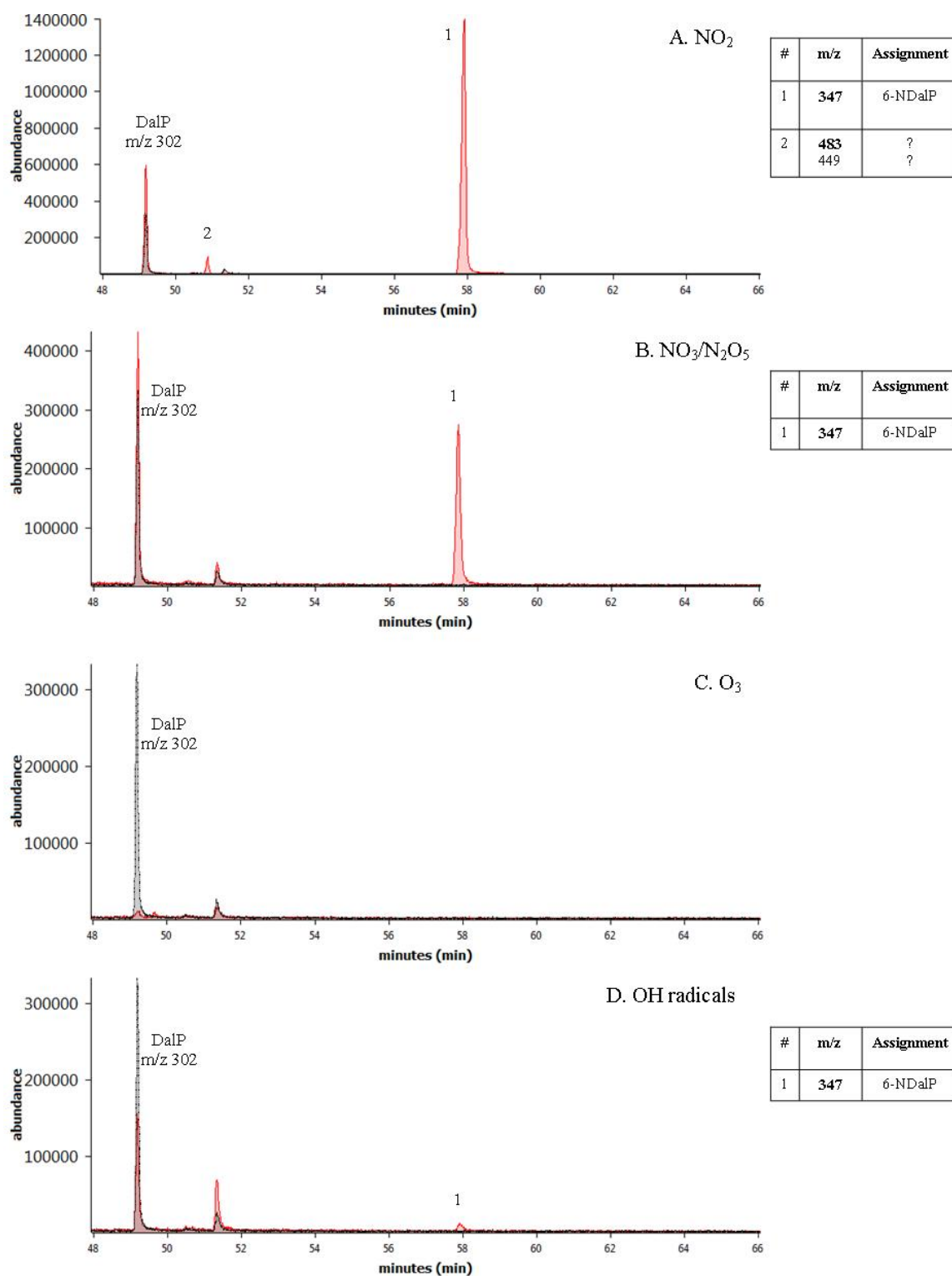


**Figure 3.5.** Overlaid full-scan NCI chromatograms of unexposed DalP and exposed DalP with A)  $\text{NO}_2$  B)  $\text{NO}_3/\text{N}_2\text{O}_5$  C)  $\text{O}_3$  and D) OH radicals. Inset chromatograms are zoomed in at full chromatograms. All chromatograms are NCI full scan. A m/z ion in bold indicates a base peak. ( --- Unexposed DalP, — Exposed DalP)



reactions. These favorable OH radical attack sites are likely to be nitrated in heterogeneous reactions and, in the case of pyrene and fluoranthene, result in different nitro-isomer products that are formed by gas phase radical-initiated reactions. In this study, more than one mono-nitro isomer product was measured after heterogeneous reaction of the lower molecular weight PAHs, including BaP-d<sub>12</sub>, BkF-d<sub>12</sub> and BghiP-d<sub>12</sub>. However, heterogeneous reaction of the higher molecular weight PAHs, DaiP-d<sub>14</sub> and DalP, resulted in the formation of only one mono-nitro isomer product. Larger differences in the free energy of the first and the second favorable OH-attack positions, 8.6 and 4.9 Kcal/mol for DalP and DaiP-d<sub>14</sub>, respectively, may result in nitration of only the most favorable position.

The estimated percent of NPAH product formation relative to the amount of unexposed parent PAH was used to estimate the effectiveness of nitration for the different PAHs tested under the various exposure conditions (Appendix C.4). It should be noted that the objective of this study was to qualitatively identify nitro products. Therefore, the extracts were not prepared for quantitative analysis and there was no surrogate addition. However, we estimated the percent of nitro product formation from the sum of identified NPAH product peak areas (in exposed extracts) to its parent PAH peak area (in unexposed extracts) from the EI full scan chromatograms (Appendix C.4). For NO<sub>2</sub>, NO<sub>3</sub>/N<sub>2</sub>O<sub>5</sub> and OH radical exposures, BaP-d<sub>12</sub> was most readily nitrated in comparison to the other PAHs (181%, 82%, and 40%, respectively), while BghiP-d<sub>12</sub> was the least effectively nitrated (Appendix C.4). Among the various exposures, the percent NPAH product formation was highest for the NO<sub>2</sub> exposure.

### **3.3.3 Salmonella Mutagenicity Assay**

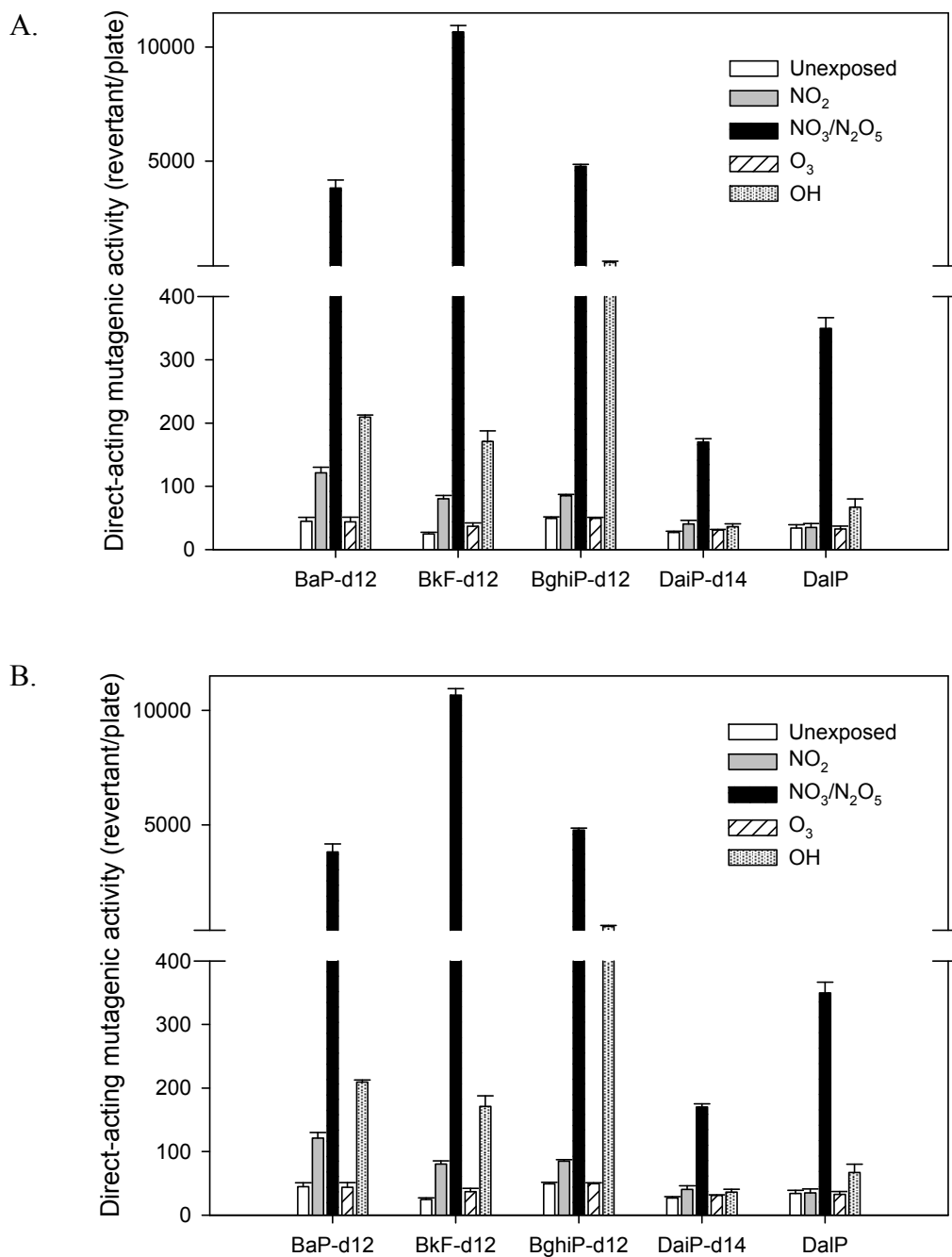
Because the objective of the experiments was to study changes in mutagenicity of extracts with respect to different oxidizing agent exposures,



mutagenic activities determined do not represent the absolute mutagenic potency of the selected PAHs or NPAHs. For the non-metabolic activation assays, the positive control, 20  $\mu\text{g}$  NPD, gave a mean revertant count of  $\sim 3500$ /plate. For the metabolic activation assays, 2  $\mu\text{g}$  of 2-AA was tested and gave a mean revertant counts of  $\sim 1000$ /plate. Spontaneous revertant counts of DMSO (30  $\mu\text{l}$ ) alone were  $\sim 25$ /plate for both assays. The mutagenicity of chamber air system was tested by placing clean filters in all chamber experiments. In the assays without S9, the revertant counts for the blank filters were 27, 38, 28 and 23 revertants/plate for  $\text{NO}_2$ ,  $\text{NO}_2/\text{N}_2\text{O}_5$ , OH and  $\text{O}_3$  exposures, respectively. In the assays with S9, the revertant counts for the blank filters were 44, 42, 35, and 29 revertants/plate for  $\text{NO}_2$ ,  $\text{NO}_2/\text{N}_2\text{O}_5$ , OH and  $\text{O}_3$  exposures, respectively. Overall, they were comparable to the spontaneous revertant counts. This shows that the chamber environment and our sample preparation process had no substantial effects on the toxicology studies. Mutagenic activities of the unexposed extracts reflected responses to  $\sim 1$  nmol of the PAHs tested (Figure 3.6).

***Direct-acting mutagenicity*** Figure 3.6A shows the means and standard errors of direct-acting mutagenicity of the various exposure extracts. Overall, the  $\text{O}_3$  exposure did not change the direct-acting mutagenicity profiles of PAHs tested. Apart from the small amounts or the absence of NPAH products after the  $\text{O}_3$  exposure, this result suggests that other possible products that may have formed, such as oxygenated PAHs, do not exhibit significant direct-acting mutagenicity or that their concentrations were too low. The direct-acting mutagenicity increased the most after  $\text{NO}_3/\text{N}_2\text{O}_5$  exposure, particularly for BkF-d<sub>12</sub>. For all of the PAHs tested, the  $\text{NO}_3/\text{N}_2\text{O}_5$  exposure resulted in 6- to 432-fold increase in direct-acting mutagenicity. The sharp increase in the direct-acting mutagenicity of  $\text{NO}_3/\text{N}_2\text{O}_5$  exposed BkF-d<sub>12</sub> (432-fold) extract may correspond to the formation of di- $\text{NO}_2$ -BkF-d<sub>11</sub> products. Dose-response profiles of

**Figure 3.6.** Mean ( $\pm$  standard error) of A. direct-acting and B. indirect-acting mutagenicities (revertants/plate) of filter extracts. All extracts were tested in triplicate for mutagenicity activity.



two non-deuterated NO<sub>2</sub>-BkF standards indicate that 3,7-NO<sub>2</sub>-BkF is a strong direct-acting mutagen, whereas 7-NO<sub>2</sub>-BkF is not (Appendix C.5A). Higher mutagenic activities of di-NO<sub>2</sub>-PAH-d<sub>11</sub> products, in comparison to mono-nitro isomers, were reported for dinitropyrenes in which their direct-acting mutagenicity, in TA98, was 272- to 467-fold higher than that of 1-nitropyrene<sup>38</sup>.

The direct-acting mutagenicity of BaP-d<sub>12</sub> was similar before and after exposure to NO<sub>2</sub>, O<sub>3</sub>, and OH radical (Figure 3.6A). However, the direct-acting mutagenicity of the BaP-d<sub>12</sub> extract was 43 times higher after exposure to NO<sub>3</sub>/N<sub>2</sub>O<sub>5</sub> than the unexposed extract (Figure 3.6A) due to the formation of 1- and 3-NO<sub>2</sub>-BaP-d<sub>11</sub> products, rather than the formation of 6-NO<sub>2</sub>-BaP-d<sub>11</sub> which contains a nitro group perpendicular to the aromatic moiety<sup>39</sup>. In a previous study, a mixture of 1-NO<sub>2</sub>-BaP and 3-NO<sub>2</sub>-BaP was found to be 2.5 fold more mutagenic, with TA98, than 6-NO<sub>2</sub>-BaP<sup>7</sup>. Some studies reported that 1- and 3-NO<sub>2</sub>-BaP were direct-acting mutagens, in a Salmonella assay, but 6-NBaP was not<sup>40, 41</sup>. In a more recent study, 1- and 3-NO<sub>2</sub>-BaP were found to induce 713 and 1,931 revertants/nmol, respectively, in TA98, while 6-NO<sub>2</sub>-BaP induced less than 1 revertant/nmol<sup>38</sup>. However, the direct-acting mutagenicity of the NO<sub>2</sub> exposed BaP-d<sub>12</sub> extract was surprisingly low given that the same mono-NO<sub>2</sub>-BaP-d<sub>11</sub> products were measured as in the NO<sub>3</sub>/N<sub>2</sub>O<sub>5</sub> exposure (Figure 3.1 and 3.6A) and the percent NPAH formation was the highest (Appendix C.4). In addition, no cytotoxicity was found for the NO<sub>2</sub>-exposed BaP-d<sub>12</sub> extract. Therefore, the relatively high direct-acting mutagenicity of the NO<sub>3</sub>/N<sub>2</sub>O<sub>5</sub> exposed BaP-d<sub>12</sub> extract may also have been caused by the formation of other products.

For BghiP-d<sub>12</sub>, the direct-acting mutagenicity of the NO<sub>2</sub> and O<sub>3</sub> exposed extracts were not significantly different from the unexposed extracts. This finding was consistent with the chemical analysis which showed insignificant NPAH formation

after the NO<sub>2</sub> and O<sub>3</sub> exposures. However, there were 97 and 12 times increases in the direct-acting mutagenicity after BghiP-d<sub>12</sub> was exposed to NO<sub>3</sub>/N<sub>2</sub>O<sub>5</sub> and OH radicals, respectively (Figure 3.6A), corresponding to the formation of mono-NO<sub>2</sub>-BghiP-d<sub>11</sub> products. Of the three identified mono-NO<sub>2</sub>-BghiP-d<sub>11</sub> products, 7-NO<sub>2</sub>-BghiP-d<sub>11</sub> is expected to contribute the least to the direct-acting mutagenicity due to the NO<sub>2</sub> orientation (Appendix C.6). Dose-response profiles of non-deuterated 5-NO<sub>2</sub>-BghiP and 7-NO<sub>2</sub>-BghiP standards show that both are non-mutagenic (< 1 rev/nmol) (Appendix C.5).

Changes in direct-acting mutagenicity of DaiP-d<sub>14</sub> and DalP with the different exposures were less pronounced after NO<sub>3</sub>/N<sub>2</sub>O<sub>5</sub> (Figure 3.6A), suggesting that the single nitro product formed did not exhibit strong direct-acting mutagenicity. Previous studies suggested that NPAHs with a perpendicular orientation, have a high first half-wave reduction potential, which restricts the nitro-reduction process by bacteria<sup>38, 39</sup>. The orientation of nitro groups in both 5-NO<sub>2</sub>-DaiP-d<sub>14</sub> and 6-NO<sub>2</sub>-DalP, identified as the major products from all exposures, are nearly perpendicular to aromatic plane (Appendix C.6), causing these products to be less mutagenic. The 6- and 10-fold increases in the direct-acting mutagenicity of DaiP-d<sub>14</sub> and DalP, respectively, after NO<sub>3</sub>/N<sub>2</sub>O<sub>5</sub> exposure were due to the higher amounts of the nitro products formed when compared to O<sub>3</sub> and OH radical exposures. However, it suggested the potential formation of other unidentified degradation products with higher direct-acting mutagenicity when compared the direct-acting mutagenicity of DaiP-d<sub>14</sub> and DalP after NO<sub>3</sub>/N<sub>2</sub>O<sub>5</sub> exposure to that after NO<sub>2</sub> exposure.

***Indirect-acting mutagenicity*** Parent PAHs are known to be indirect-acting mutagens, which require metabolic activation to express mutagenicity, and unreacted parent PAHs may contribute to the indirect-acting mutagenicity of exposed extracts.

In addition, not all NPAHs are direct-acting mutagens. For example, 6-NO<sub>2</sub>-BaP was previously found to be an indirect-acting mutagen<sup>41, 42</sup> and some NPAHs, including 1-NO<sub>2</sub>-BaP and 3-NO<sub>2</sub>-BaP, exhibit both direct- and indirect-acting mutagenicity<sup>41</sup>. As shown in Figure 3.6B, the overall indirect-acting mutagenicity profile was similar to the direct-acting mutagenicity profile, with increased indirect-acting mutagenicity after NO<sub>3</sub>/N<sub>2</sub>O<sub>5</sub> exposure. This shows that NO<sub>3</sub>/N<sub>2</sub>O<sub>5</sub> are not only strong oxidants in transforming PAHs to NPAHs, but also in forming potential indirect-acting mutagens. In particular, BaP-d<sub>12</sub>, BkF-d<sub>12</sub>, and BghiP-d<sub>12</sub> appear to be degraded to both strong direct-acting and strong indirect-acting products. BkF-d<sub>12</sub> and BghiP-d<sub>12</sub> were the only two compounds that induced indirect-acting mutagenic activities significantly higher than the background after OH radical exposure (Figure 3.6B and Appendix C.7). Dose-response profiles of non-deuterated 7-NO<sub>2</sub>-BkF and 3,7-NO<sub>2</sub>-BkF standards showed that the 3,7-NO<sub>2</sub>-BkF exhibits both direct- and indirect-acting mutagenicity (96 and 513 rev/nmol, respectively), while 7-NO<sub>2</sub>-BkF are not mutagenic in both assays (Appendix C.5). This implies that the presence of the five di-NO<sub>2</sub>-BkF-d<sub>11</sub> products in the NO<sub>3</sub>/N<sub>2</sub>O<sub>5</sub> exposed extract contributed significantly to the direct-acting mutagenicity, as well as the indirect-acting mutagenicity. On the other hand, 5-NO<sub>2</sub>-BghiP is mutagenic to TA98 with S9 (27 rev/nmol), while 7-NO<sub>2</sub>-BghiP is not (Appendix C.5). For all PAHs tested, no significant increases in indirect-acting mutagenicity were observed after O<sub>3</sub> exposure, consistent with the absence of NPAH formation.

***Deuterium Isotope Effect*** The results from deuterium isotope effect mutagenicity studies for BaP/BaP-d<sub>12</sub>, 6-NO<sub>2</sub>-BaP/6-NO<sub>2</sub>-BaPd<sub>11</sub>, PYR/PYR-d<sub>10</sub> and 1-NO<sub>2</sub>-PYR/1-NO<sub>2</sub>-PYR-d<sub>9</sub> are shown in Figures 3.7 (A-D) and Figures 3.8 (A-D). There was no statistically significant deuterium isotope effect ( $p > 0.05$ ) for the parent

BaP and BaP-d<sub>12</sub> and PYR and PYR-d<sub>10</sub> in the assay without S9 (Figure 3.7A and Figure 3.8A). However, a statistically significant deuterium isotope effect ( $p < 0.05$ ) was observed for 6-NO<sub>2</sub>-BaP and 6-NO<sub>2</sub>-BaP-d<sub>11</sub> (Figures 3.7C). While 6-NO<sub>2</sub>-BaP exhibited a weak direct-acting mutagenicity, the activity of 6-NO<sub>2</sub>-BaP-d<sub>11</sub> was comparable to the background response. In the case of 1-NO<sub>2</sub>-PYR and 1-NO<sub>2</sub>-PYR-d<sub>9</sub>, the results were not conclusive because there was only one tested concentration with a statistically significant p-value ( $p < 0.05$ ), however both 1-NO<sub>2</sub>-PYR and 1-NO<sub>2</sub>-PYR-d<sub>9</sub> were mutagenic. In the Salmonella assay without metabolic activation, the metabolism of NPAHs proceeds through nitroreduction to form DNA adducts<sup>43</sup>. Isomeric NPAHs with lower reduction potentials have been shown to be direct-acting mutagens and their reduction potentials indicate the electron affinity of NPAHs<sup>38</sup>. A study on unsubstituted PAHs found that the deuterated PAHs had higher reduction potentials<sup>44</sup>. Therefore, the decreased mutagenicity of 6-NO<sub>2</sub>-BaP-d<sub>11</sub>, compared to 6-NO<sub>2</sub>-BaP, may be because of its higher reduction potential, inhibiting the nitroreduction process.

In the Salmonella assay with metabolic activation, no statistically significant deuterium isotope effect was observed for the parent BaP/BaP-d<sub>12</sub> and PYR/PYR-d<sub>10</sub> (Figure 3.7B and Figures 3.8B). The S9-mediated metabolism of aromatic compounds were proposed to occur via 1) arene oxidation or 2) nonconcerted addition of an iron(IV) oxyl species<sup>45</sup>. Both pathways are followed by the so-called “NIH shift”, involving a shift of hydrogen or deuterium to an adjacent position during hydroxylation reaction<sup>45</sup>. Because the substitution of deuterium for hydrogen did not result in different mutagenic activity for deuterated and non-deuterated pairs, it suggested that a step prior to the ring oxidation may be the rate-limiting step. However, a statistically significant deuterium isotope effect was observed for 6-

**Figure 3.7:** Mean ( $\pm 95\%$  confidence interval) direct- and indirect-acting mutagenic activities of BaP vs BaP-d<sub>12</sub> and 6-NBaP vs 6-NBaP-d<sub>11</sub>. P-values are derived from the two sample t-test. A number in bold indicates statistically significant difference ( $p < 0.05$ ).

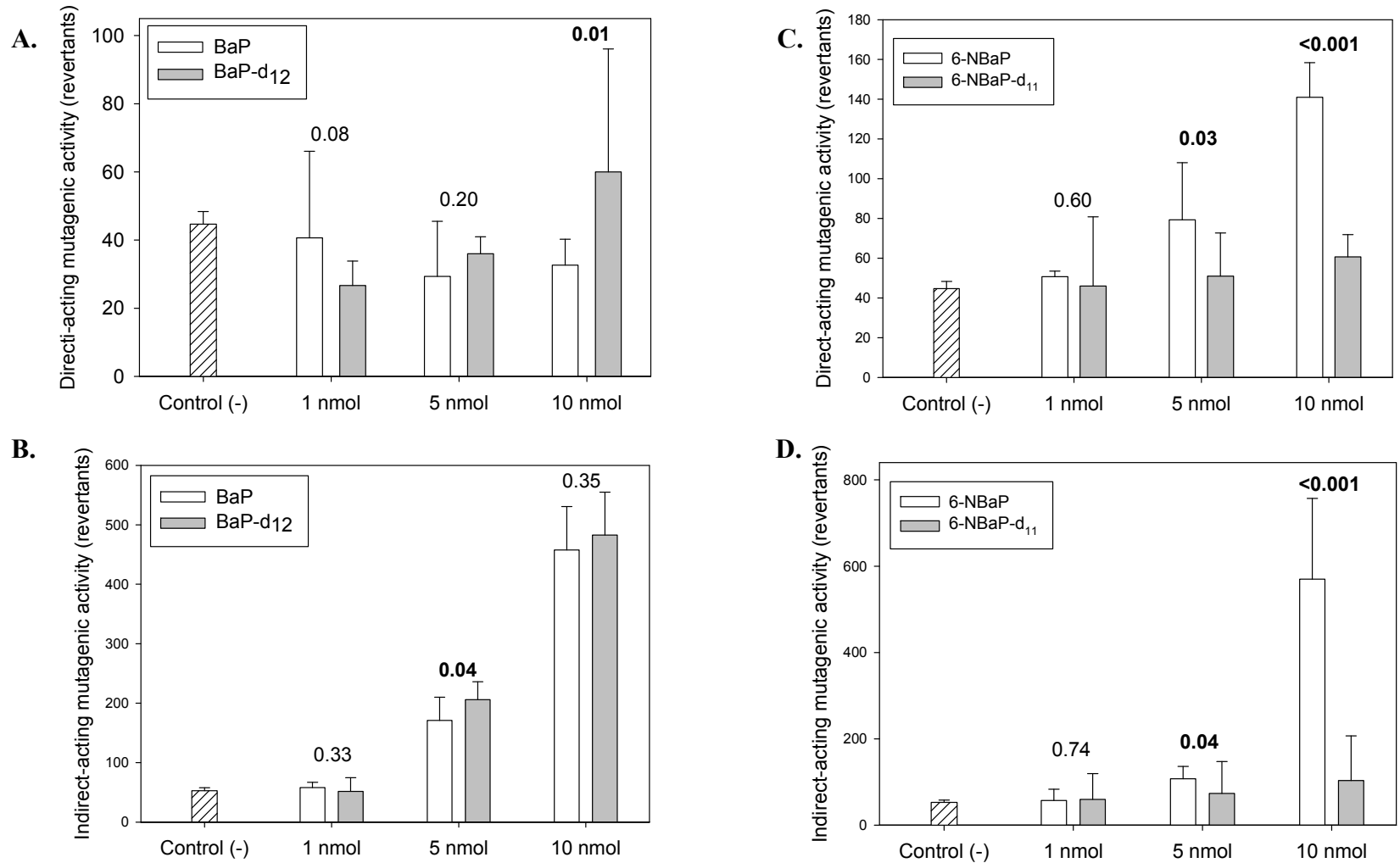
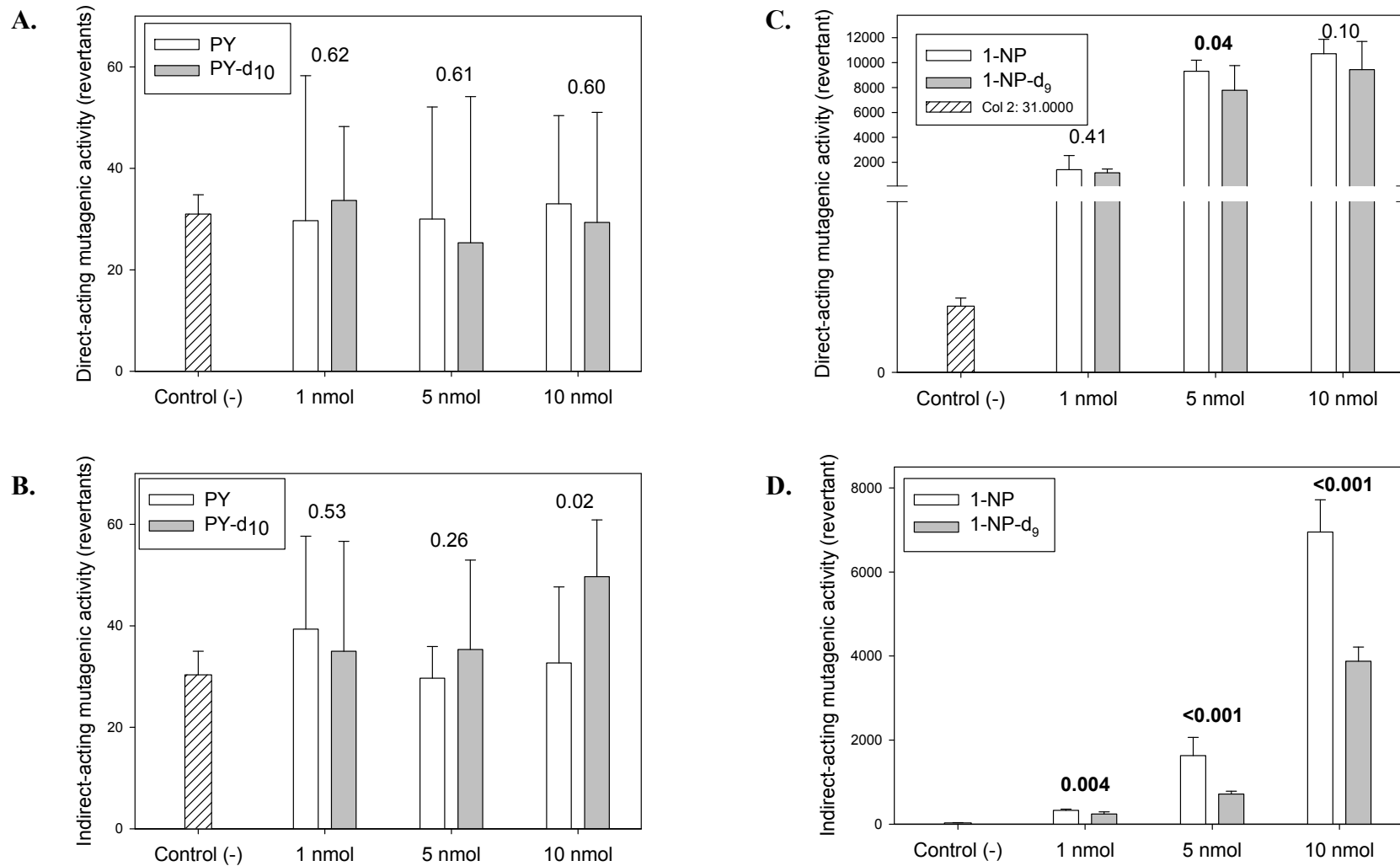


**Figure 3.8:** Mean ( $\pm 95\%$  confidence interval) direct- and indirect-acting mutagenic activities of PYR vs PYR-d<sub>10</sub> and 1-NP vs 1-NP-d<sub>9</sub>. P-values were derived from the two sample t-test. A number in bold indicates statistically significant difference ( $p < 0.05$ ).





NBaP/6-NBaPd<sub>11</sub> and 1-NO<sub>2</sub>-PYR/1-NO<sub>2</sub>-PYR-d<sub>9</sub> and substitution of deuterium for hydrogen lowered the mutagenicity (Figure 3.7D and Figure 3.8D). It should be noted that, while 6-NO<sub>2</sub>-BaP-d<sub>11</sub> was not mutagenic in the assays with S9, 1-NO<sub>2</sub>-PYR-d<sub>9</sub> was mutagenic but induced lower colony counts than the non-deuterated analog. In the presence of metabolic activation, more metabolic pathways, including nitroreduction, ring-oxidation followed by nitroreduction, and a ring-oxidation followed by nitroreduction and esterification, can be involved in metabolizing NPAHs in an S9-mediated assay<sup>46</sup>. If the ring oxidation was the only metabolic pathway responsible for converting 6-NO<sub>2</sub>-BaP/6-NO<sub>2</sub>-BaPd<sub>11</sub>, and 1-NO<sub>2</sub>-PYR/1-NO<sub>2</sub>-PYR-d<sub>9</sub> to a mutagenic form, the same result as the parent BaP/BaP-d<sub>12</sub> and PYR/PYR-d<sub>10</sub> would have been expected. And if the nitroreduction alone was the major metabolic pathway, the deuterium isotope effect would not be expected from 1-NO<sub>2</sub>-PYR/1-NO<sub>2</sub>-PYR-d<sub>9</sub>, because the deuterium isotope effect was not apparent in the absence of metabolic activation. However, in the case of 6-NBaP/6-NBaPd<sub>11</sub>, the deuterium isotope effect was observed in both assays (with and without metabolic activation). This suggested that several co-metabolic pathways, possibly selective for each NPAH, may be involved in the metabolism of nitro products when exogenous bioactivation is present.

When considering the impact of the deuterium isotope effect on our mutagenicity analysis, the results suggest that an increase in mutagenicity after exposure was expected. However, the magnitude of mutagenicity could be underestimated because the nitro products were deuterated. Future research should focus on the synthesis and testing of individual NO<sub>2</sub>-PAH isomers where commercial standards are not currently available, as well as the identification of oxy- and hydroxy-PAHs in the exposed extracts.

### **3.4 Acknowledgements**

This publication was made possible in part by grant number P30ES00210 from the National Institute of Environmental Health Sciences (NIEHS), NIH and NIEHS Grant P42 ES016465, and the U.S. National Science Foundation (ATM-0841165). Its contents are solely the responsibility of the authors and do not necessarily represent the official view of the NIEHS, NIH. Salmonella assays were conducted in the Cancer Chemoprotection Program (CCP) Core Laboratory of the Linus Pauling Institute, Oregon State University.

### 3.5 References

1. Atkinson, R.; Arey, J., Atmospheric Chemistry of Gas-Phase Polycyclic Aromatic Hydrocarbons: Formation of Atmospheric Mutagens. *Environ. Health Perspect.* **1994**, *102*, 117-126.
2. Durant, J. L.; Lafleur, A. L.; Plummer, E. F.; Taghizadeh, K.; Busby, W. F.; Thilly, W. G., Human Lymphoblast Mutagens in Urban Airborne Particles. *Environ. Sci. Technol.* **1998**, *32*, (13), 1894-1906.
3. Purohit, V.; Basu, A. K., Mutagenicity of Nitroaromatic Compounds. *Chem. Res. Toxicol.* **2000**, *13*, (8), 673-692.
4. Atkinson, R.; Arey, J.; Zielinska, B.; Aschmann, S. M., Kinetics and Nitro-Products of the Gas-Phase OH and NO<sub>3</sub> Radical-Initiated Reactions of Naphthalene-d<sub>8</sub>, Fluoranthene-d<sub>10</sub>, and Pyrene. *Int. J. Chem. Kinet.* **1990**, *22*, 999-1014.
5. Zielinska, B.; Arey, J.; Atkinson, R.; Ramdahl, T.; Winer, A. M.; Pitts, J. N., Reaction of dinitrogen pentoxide with fluoranthene. *J. Am. Chem. Soc.* **1986**, *108*, (14), 4126-4132.
6. Zimmermann, K.; Atkinson, R.; Arey, J.; Kojima, Y.; Inazu, K., Isomer distributions of molecular weight 247 and 273 nitro-PAHs in ambient samples, NIST diesel SRM, and from radical-initiated chamber reactions. *Atmos. Environ.* **2012**, *55*, (0), 431-439.
7. Pitts Jr, J. N.; Van Cauwenberghe, K. A.; Grosjean, D.; Schmid, J. P.; Fitz, D. R.; Belser, W.; Knudson, G.; Hynds, P. M., Atmospheric reactions of polycyclic aromatic hydrocarbons: facile formation of mutagenic nitro derivatives. *Science (New York, NY)* **1978**, *202*, (4367), 515.
8. Kamens, R. M.; Guo, J.; Guo, Z.; McDow, S. R., Polynuclear aromatic hydrocarbon degradation by heterogeneous reactions with N<sub>2</sub>O<sub>5</sub> on atmospheric particles. *Atmospheric Environment. Part A. General Topics* **1990**, *24*, (5), 1161-1173.
9. Esteve, W.; Budzinski, H.; Villenave, E., Relative rate constants for the heterogeneous reactions of NO<sub>2</sub> and OH radicals with polycyclic aromatic hydrocarbons adsorbed on carbonaceous particles. Part 2: PAHs adsorbed on diesel particulate exhaust SRM 1650a. *Atmos. Environ.* **2006**, *40*, (2), 201-211.
10. Pitts Jr, J. N.; Zielinska, B.; Sweetman, J. A.; Atkinson, R.; Winer, A. M., Reactions of adsorbed pyrene and perylene with gaseous N<sub>2</sub>O<sub>5</sub> under simulated atmospheric conditions. *Atmospheric Environment (1967)* **1985**, *19*, (6), 911-915.
11. Pitts, J. N.; Sweetman, J. A.; Zielinska, B.; Atkinson, R.; Winer, A. M.; Harger, W. P., Formation of nitroarenes from the reaction of polycyclic aromatic hydrocarbons with dinitrogen pentoxide. *Environmental Science & Technology* **1985**, *19*, (11), 1115-1121.
12. Miet, K.; Le Menach, K.; Flaud, P. M.; Budzinski, H.; Villenave, E., Heterogeneous reactivity of pyrene and 1-nitropyrene with NO<sub>2</sub>: Kinetics, product yields and mechanism. *Atmos. Environ.* **2009**, *43*, (4), 837-843.
13. Carrara, M.; Wolf, J.-C.; Niessner, R., Nitro-PAH formation studied by interacting artificially PAH-coated soot aerosol with NO<sub>2</sub> in the temperature range of 295-523 K. *Atmos. Environ.* **2010**, *44*, (32), 3878-3885.
14. Delmas, S.; Muller, J. F.; Atkinson, R., Use of FTMS laser microprobe for the in situ characterization of nitro-PAHs on particles. *Analisis* **1992**, *20*, 165-170.

15. Bamford, H. A.; Baker, J. E., Nitro-polycyclic aromatic hydrocarbon concentrations and sources in urban and suburban atmospheres of the Mid-Atlantic region. *Atmos. Environ.* **2003**, *37*, (15), 2077-2091.
16. Albinet, A.; Leoz-Garziandia, E.; Budzinski, H.; Villenave, E., Polycyclic aromatic hydrocarbons (PAHs), nitrated PAHs and oxygenated PAHs in ambient air of the Marseilles area (South of France): Concentrations and sources. *Sci. Total Environ.* **2007**, *384*, (1-3), 280-292.
17. Hattori, T.; Tang, N.; Tamura, K.; Hokoda, A.; Yang, X.; Igarashi, K.; Ohno, M.; Okada, Y.; Kameda, T.; Toriba, A., Particulate polycyclic aromatic hydrocarbons and their nitrated derivatives in three cities in Liaoning Province, China. *Environmental Forensics* **2007**, *8*, (1-2), 165-172.
18. Cho, B. P.; Kim, M.; Harvey, R. G., Synthesis and conformational analysis of nitropolycyclic fluoranthenes. *The Journal of Organic Chemistry* **1993**, *58*, (21), 5788-5796.
19. Vance, W. A.; Levin, D. E., Structural features of nitroaromatics that determine mutagenic activity in Salmonella typhimurium. *Environmental mutagenesis* **1984**, *6*, (6), 797-811.
20. Campbell, J.; Crumplin, G.; Garner, J. V.; Garner, R. C.; Martin, C. N.; Rutter, A., Nitrated polycyclic aromatic hydrocarbons: potent bacterial mutagens and stimulators of DNA repair synthesis in cultured human cells. *Carcinogenesis* **1981**, *2*, (6), 559-565.
21. Johansen, E.; Sydnes, L. K.; Greibrokk, T., Separation and Characterization of Mononitro Derivatives of Benzo [a] pyrene, Benzo [e] pyrene and Benzo [ghi] perylene. *Acta Chemica Scandinavia D'* **1984**, *38*, 309-318.
22. Sasaki, J.; Arey, J.; Harger, W. P., Formation of Mutagens from the Photooxidations of 2-4-Ring PAH. *Environ. Sci. Technol.* **1995**, *29*, (5), 1324-1335.
23. Nishino, N.; Atkinson, R.; Arey, J., Formation of Nitro Products from the Gas-Phase OH Radical-Initiated Reactions of Toluene, Naphthalene, and Biphenyl: Effect of NO<sub>2</sub> Concentration. *Environ. Sci. Technol.* **2008**, *42*, (24), 9203-9209.
24. Arey, J.; Zielinska, B.; Atkinson, R.; Aschmann, S. M., Nitroarene products from the gas-phase reactions of volatile polycyclic aromatic hydrocarbons with the OH radical and N<sub>2</sub>O<sub>5</sub>. *International Journal of Chemical Kinetics* **1989**, *21*, (9), 775-799.
25. Sasaki, J.; Aschmann, S. M.; Kwok, E. S. C.; Atkinson, R.; Arey, J., Products of the Gas-Phase OH and NO<sub>3</sub> Radical-Initiated Reactions of Naphthalene. *Environ. Sci. Technol.* **1997**, *31*, (11), 3173-3179.
26. Atkinson, R.; Baulch, D.; Cox, R.; Crowley, J.; Hampson, R.; Hynes, R.; Jenkin, M.; Rossi, M.; Troe, J., Evaluated kinetic and photochemical data for atmospheric chemistry: Volume I-gas phase reactions of O<sub>x</sub>, HO<sub>x</sub>, NO<sub>x</sub> and SO<sub>x</sub> species. *Atmos. Chem. Phys.* **2004**, *4*, (6), 1461-1738.
27. Wang, W.; Jariyasopit, N.; Schrlau, J.; Jia, Y.; Tao, S.; Yu, T.-W.; Dashwood, R. H.; Zhang, W.; Wang, X.; Simonich, S. L. M., Concentration and Photochemistry of PAHs, NPAHs, and OPAHs and Toxicity of PM<sub>2.5</sub> during the Beijing Olympic Games. *Environ. Sci. Technol.* **2011**, *45*, (16), 6887-6895.
28. Maron, D. M.; Ames, B. N., Revised methods for the Salmonella mutagenicity test. *Mutation Research/Environmental Mutagenesis and Related Subjects* **1983**, *113*, (3-4), 173-215.

29. Pitts Jr, J. N.; Sweetman, J. A.; Zielinska, B.; Winer, A. M.; Atkinson, R., Determination of 2-nitrofluoranthene and 2-nitropyrene in ambient particulate organic matter: Evidence for atmospheric reactions. *Atmospheric Environment (1967)* **1985**, *19*, (10), 1601-1608.
30. Zimmermann, K.; Atkinson, R.; Arey, J., Effect of NO<sub>2</sub> Concentration on Dimethylnitronaphthalene Yields and Isomer Distribution Patterns from the Gas-Phase OH Radical-Initiated Reactions of Selected Dimethylnaphthalenes. *Environ. Sci. Technol.* **2012**, *46*, (14), 7535-7542.
31. Miet, K.; Le Menach, K.; Flaud, P. M.; Budzinski, H.; Villenave, E., Heterogeneous reactions of ozone with pyrene, 1-hydroxypyrene and 1-nitropyrene adsorbed on particles. *Atmos. Environ.* **2009**, *43*, (24), 3699-3707.
32. White, C.; Robbat, A.; Hoes, R., Gas chromatographic retention characteristics of nitrated polycyclic aromatic hydrocarbons on SE-52. *Chromatographia* **1983**, *17*, (11), 605-612.
33. Schauer, C.; Niessner, R.; Pöschl, U., Analysis of nitrated polycyclic aromatic hydrocarbons by liquid chromatography with fluorescence and mass spectrometry detection: air particulate matter, soot, and reaction product studies. *Anal. Bioanal. Chem.* **2004**, *378*, (3), 725-736.
34. Ringuet, J.; Albinet, A.; Leoz-Garziandia, E.; Budzinski, H.; Villenave, E., Diurnal/nocturnal concentrations and sources of particulate-bound PAHs, OPAHs and NPAHs at traffic and suburban sites in the region of Paris (France). *Sci. Total Environ.* **2012**, *437*, 297-305.
35. Dewar, M.; Mole, T.; Urch, D.; Warford, E., 689. Electrophilic substitution. Part IV. The nitration of diphenyl, chrysene, benzo [a] pyrene, and anthanthrene. *J. Chem. Soc.* **1956**, 3572-3575.
36. Bamford, H. A.; Bezabeh, D. Z.; Schantz, M. M.; Wise, S. A.; Baker, J. E., Determination and comparison of nitrated-polycyclic aromatic hydrocarbons measured in air and diesel particulate reference materials. *Chemosphere* **2003**, *50*, (5), 575-587.
37. Zimmermann, K.; Jariyasopit, N.; Simonich, S. L.; Tao, S.; Atkinson, R.; Arey, J., Formation of nitro-PAHs from the heterogeneous reaction of ambient particle-bound PAHs with N<sub>2</sub>O<sub>5</sub>/NO<sub>3</sub>/NO<sub>2</sub>. *Environ. Sci. Technol.* **2013**.
38. Jung, H.; Heflich, R. H.; Fu, P. P.; Shaikh, A. U.; Hartman, P., Nitro group orientation, reduction potential, and direct-acting mutagenicity of nitro-polycyclic aromatic hydrocarbons. *Environ. Mol. Mutagen.* **1991**, *17*, (3), 169-180.
39. Fu, P. P.; Qui, F. Y.; Jung, H.; Von Tungeln, L. S.; Zhan, D. J.; Lee, M. J.; Wu, Y. S.; Heflich, R. H., Metabolism of isomeric nitrobenzo [a] pyrenes leading to DNA adducts and mutagenesis. *Mutation Research/Fundamental and Molecular Mechanisms of Mutagenesis* **1997**, *376*, (1), 43-51.
40. Chou, M.; Heflich, R.; Casciano, D.; Miller, D.; Freeman, J.; Evans, F.; Fu, P., Synthesis, spectral analysis, and mutagenicity of 1-, 3-, and 6-nitrobenzo [a] pyrene. *J. Med. Chem.* **1984**, *27*, (9), 1156-1161.
41. Pitts Jr, J. N.; Zielinska, B.; Harger, W. P., Isomeric mononitrobenzo [a] pyrenes: synthesis, identification and mutagenic activities. *Mutat. Res.* **1984**, *140*, (2-3), 81-85.
42. Rosenkranz, H. S.; Mermelstein, R., The mutagenic and carcinogenic properties of nitrated polycyclic aromatic hydrocarbons. In White, C. M., Ed. Huethig: Heidelberg, 1985; pp 267-297.

43. Fu, P. P.; Herreno-Saenz, D.; Von Tungeln, L. S.; Hart, R. W.; Lin, S.-D., DNA adducts and carcinogenicity of nitro-polycyclic aromatic hydrocarbons. *Polycyclic Aromat. Compd.* **1994**, *6*, (1-4), 71-78.
44. Goodnow, T. T.; Kaifer, A. E., Does isotopic substitution affect the reduction potential of aromatic molecules? *J. Phys. Chem.* **1990**, *94*, (19), 7682-7683.
45. Meunier, B.; De Visser, S. P.; Shaik, S., Mechanism of oxidation reactions catalyzed by cytochrome P450 enzymes. *Chemical Reviews-Columbus* **2004**, *104*, (9), 3947-3980.
46. Fu, P. P., Metabolism of nitro-polycyclic aromatic hydrocarbons. *Drug metabolism reviews* **1990**, *22*, (2-3), 209-268.

**CHAPTER 4: HETEROGENEOUS REACTIONS OF PM-BOUND  
PAHs AND NPAHs WITH NO<sub>3</sub>/N<sub>2</sub>O<sub>5</sub>, OH RADICALS, AND O<sub>3</sub>  
UNDER SIMULATED LONG-RANGE ATMOSPHERIC  
TRANSPORT CONDITIONS: REACTIVITY AND MUTAGENICITY**

NARUMOL JARIYASOPIT<sup>1</sup>, KATHRYN ZIMMERMANN<sup>2</sup>, JANET AREY<sup>2</sup>, ROGER  
ATKINSON<sup>2</sup>, TIAN-WEI YU<sup>3</sup>, RODERICK H. DASHWOOD<sup>3,4</sup>, SHU TAO<sup>5</sup>, STACI L.  
MASSEY SIMONICH<sup>1,4\*</sup>

<sup>1</sup>Department of Chemistry, Oregon State University, Corvallis, Oregon USA 97331;

<sup>2</sup>Air Pollution Research Center, University of California, Riverside;

<sup>3</sup>Linus Pauling Institute, Oregon State University, Corvallis, Oregon USA, 97331;

<sup>4</sup>Environmental and Molecular Toxicology, Oregon State University, Corvallis, Oregon,  
USA, 97331;

<sup>5</sup>College of Urban and Environmental Science, Peking University, Beijing, China,  
100871.

\*Corresponding author e-mail: [staci.simonich@orst.edu](mailto:staci.simonich@orst.edu); phone: (541) 737-9194; fax:  
(541) 737-0497

## ABSTRACT

The heterogeneous reactions of particulate matter (PM)-bound polycyclic aromatic hydrocarbons (PAHs) and nitro-PAHs (NPAHs) with  $\text{NO}_3/\text{N}_2\text{O}_5$ , OH radicals, and  $\text{O}_3$  were studied in a laboratory photochemical chamber. Ambient  $\text{PM}_{2.5}$  and  $\text{PM}_{10}$  samples were collected from Beijing, China and Riverside, California and exposed under simulated trans-Pacific atmospheric transport conditions. Changes in the masses of 30 PAHs and 27 NPAHs, as well as the direct and indirect-acting mutagenicity of the PM using the Salmonella mutagenicity assay with strain TA98 strain, were determined with and without photochemical reaction. Although there was a general trend of decreasing percent reactivity with increasing organic carbon or black carbon concentration in the Beijing PM samples after exposure to  $\text{NO}_3/\text{N}_2\text{O}_5$  and OH radical, the correlations were not statistically significant. In general,  $\text{O}_3$  was most effective in degrading PM-bound PAHs with more than four rings, except for benzo[a]pyrene which was degraded by  $\text{O}_3$  and  $\text{NO}_3/\text{N}_2\text{O}_5$  equally well. However, the NPAHs were most effectively formed during the  $\text{NO}_3/\text{N}_2\text{O}_5$  exposure. No significant formation of 2-nitrofluoranthene and 2-nitropyrene was observed in any of the exposures, suggesting that the PM-bound PAHs underwent heterogeneous reaction rather than gas-phase reaction. For the  $\text{NO}_3/\text{N}_2\text{O}_5$  exposure, the increase in direct-acting mutagenicity was associated with the formation of mutagenic NPAHs. The reactivity, based on 1-nitropyrene formation, of Beijing PM after  $\text{NO}_3/\text{N}_2\text{O}_5$  and OH radical exposures was higher than that of the Riverside PM in which no NPAH formation was observed in any of the exposures. The decreased reactivity of the Riverside PM was likely due to the accumulation of degradation products on the surface of PM decreasing the availability of PAHs for reaction.



## 4.1 Introduction

The long range atmospheric transport of PM-bound PAHs and NPAHs to remote sites, including mountains in France<sup>1</sup>, Norway<sup>2</sup>, Sweden<sup>2</sup>, Czech Republic<sup>3</sup>, the Canadian Arctic<sup>4</sup>, the Olympic Peninsula of Washington<sup>5, 6</sup>, and mountains in Oregon<sup>6, 7</sup> has been documented. Once emitted from combustion sources, some PAHs undergo reaction with OH radicals, NO<sub>3</sub> radicals, N<sub>2</sub>O<sub>5</sub> and O<sub>3</sub>, converting the parent PAHs to more polar species, including NPAHs. The transformation of PAHs occurs locally, near emission sources, and/or enroute to downwind receptor sites. Human exposure to PAH derivatives, including NPAHs, is of interest because some of them are more mutagenic than the parent PAHs<sup>8, 9</sup> and have been detected at many sites throughout the world<sup>10-14</sup>. A number of NPAHs are classified as “probable or possible human carcinogens”<sup>15</sup> and have been identified as a major contributor to the overall mutagenicity of PM despite their relatively low concentrations in the environment compared to parent PAHs<sup>16</sup>.

The reactivity of PM-bound PAHs varies, to some extent, with the composition of the particles<sup>17-21</sup>. The microenvironment of the particles, including the mineral content, organic and black carbon concentrations, as well as the ambient humidity, physical state of the organic layer surrounding the core of the particles and surface coverage all influence the reactivity of PM-bound PAHs<sup>19, 22-25</sup>. Various artificial substrates, including silica, graphite, diesel soot, fly ash, wood smoke and kerosene soot, have been used in laboratory experiments to simulate PM-bound PAH reactions and resulted in different heterogeneous rate constants<sup>17, 20, 26-30</sup>. Kamens et al.<sup>20</sup> reported larger rate constants for the reaction of N<sub>2</sub>O<sub>5</sub> with PAHs on diesel soot, compared to wood soot. Esteve et al.<sup>21</sup> found that the reaction of PAHs adsorbed on graphite particles with OH radicals

exhibited higher pseudo first-order rate constants than the reaction with PAHs adsorbed on diesel particles. We previously reported that PAHs sorbed to a glass fiber filter were effectively transformed to NPAHs by reaction with  $\text{NO}_3/\text{N}_2\text{O}_5$  (Chapter 3). However, few laboratory studies have been conducted on the transformation of PAHs and NPAHs on ambient PM. Recently, the reactivity of PM-bound PAHs was studied using a fast flow reactor using  $\text{O}_3$ , OH radicals and  $\text{NO}_2/\text{O}_3$ <sup>31</sup>.

The objectives of this research were to study the heterogeneous reactivity of PM-bound PAHs and NPAHs with  $\text{NO}_3/\text{N}_2\text{O}_5$ , OH radicals, and  $\text{O}_3$  under simulated long-range atmospheric transport conditions and determine the effect of these reaction products on the mutagenicity of the PM. Ambient PM samples tested were collected in Beijing, China and Riverside, CA. Both sampling sites have distinct characteristics. While Beijing PM is highly loaded with PAHs, suggesting strong primary emissions<sup>14</sup>, Riverside PM is dominated partly by chemically aged PM transported from Los Angeles, in addition to local primary emissions<sup>10</sup>. The PAH and NPAH measurements were carried out using GC-MS and the Salmonella mutagenicity assay (with and without S9). Based on these findings, the reactivity of the PM-bound PAHs is discussed with respect to the BC and OC concentration of the PM, as well as the significance of transformation reactions for atmospheric long range transport of PM-bound PAHs.

## **4.2 Experimental**

### **4.2.1 Chemicals**

All of the 30 parent PAHs and 27 NPAHs measured (and their abbreviations) are listed in Appendix D.1. Deuterium-labeled PAHs and NPAHs were purchased from CDN

Isotopes (Point-Claire, Quebec, Canada) and Cambridge Isotope Laboratories (Andover, MA). The isotopically labeled recovery PAH and NPAH surrogates included d<sub>10</sub>-fluorene, d<sub>10</sub>-phenanthrene, d<sub>10</sub>-pyrene, d<sub>12</sub>-triphenylene, d<sub>12</sub>-benzo[a]pyrene, d<sub>12</sub>-benzo[ghi]perylene, d<sub>7</sub>-1-nitronaphthalene, d<sub>9</sub>-5-nitroacenaphthene, d<sub>9</sub>-9-nitroanthracene, d<sub>9</sub>-3-nitrofluoranthene, d<sub>9</sub>-1-nitropyrene and d<sub>11</sub>-6-nitrochrysene. The labeled PAH and NPAH internal standards included d<sub>10</sub>-acenaphthene, d<sub>10</sub>-fluoranthene, d<sub>12</sub>-benzo[k]fluoranthene, d<sub>9</sub>-2-nitrobiphenyl and d<sub>9</sub>-2-nitrofluorene.

#### 4.2.2 Sampling

**Beijing, China** The Beijing sampling site was located on the roof of the 7-story (about 25 meters above ground) Geology Building on the Peking University Campus (PKU)<sup>14, 32</sup>. This site is located in Northwestern Beijing and is primarily a residential and commercial area. Dominant PAH emission sources near the site include vehicular traffic and fuel combustion for cooking. PM<sub>2.5</sub> and PM<sub>10</sub> were collected on pre-baked (350°C) quartz fiber filters (No.1851-865, Tisch Environmental, Cleves, OH) using a High Volume Cascade Impactor (Series 230, Tisch Environmental, Cleves, OH). PM samples were collected continuously over 24 h periods with the sampler being changed over in the late morning. The average flow rate was ~1.0 m<sup>3</sup> min<sup>-1</sup>. PM<sub>10</sub> and PM<sub>2.5</sub> samples were collected from May 2009 to February 2010 and in April 2011, respectively (Appendix D.2).

**Riverside, California** The Riverside sampling site was located at the University of California Air Pollution Research Center on the University of California-Riverside campus, approximately 90 km downwind of Los Angeles. PM<sub>2.5</sub> samples were collected

on a Teflon-impregnated glass fiber (TIGF) filters (Pallflex T60A20, 8 in  $\times$  10 in) using high-volume (Hi-vol) sampling devices during May 1997<sup>33</sup> (Appendix D.2). The average flow rate was  $\sim 0.6 \text{ m}^3 \text{ min}^{-1}$ .

#### 4.2.3 Filter Preparation and Exposures

The PAH and NPAH concentrations on Beijing PM vary significantly day to day<sup>14</sup>. In order to measure changes in the PAH and NPAH concentrations with and without exposure in the chamber, in the chemical study, 20.4 cm  $\times$  25.5 cm filters were cut into six equal portions of 8.5 cm  $\times$  10.2 cm (Appendix D.3). Three 8.5 cm  $\times$  10.2 cm portions were exposed in the chamber and the remaining three 8.5 cm  $\times$  10.2 cm portions were used as unexposed controls. In order to measure changes in the mutagenicity of the PM with and without exposure in the chamber, in the mutagenicity study, 20.4 cm  $\times$  25.5 cm filters were cut into four equal portions of 10.2 cm  $\times$  12.7 cm because the Salmonella assay did not adequately measure the mutagenicity of the 8.5 cm  $\times$  10.2 cm portions (Appendix D.3). Two 10.2 cm  $\times$  12.7 cm portions were exposed in the chamber and the remaining two 10.2 cm  $\times$  12.7 cm portions were used as unexposed controls. The PAH and NPAH concentrations of the exposed and unexposed 10.2 cm  $\times$  12.7 cm portions used in the mutagenicity study were also measured and directly compared to the results of the Salmonella assay. The PM<sub>2.5</sub> and PM<sub>10</sub> filters were exposed to NO<sub>3</sub>/N<sub>2</sub>O<sub>5</sub>, OH radicals, and O<sub>3</sub> in a  $\sim 7000$  L indoor collapsible Teflon chamber equipped with two parallel banks of blacklamps and a Teflon-coated fan at room temperature ( $\sim 296$  K) and  $\sim 735$  Torr<sup>34,35</sup>. The filters were placed on a standing, rotating apparatus within the Teflon chamber (Appendix D.4). For all exposure experiments, blank, clean filters were placed

in the Teflon chamber to test for background contamination in the chemistry and mutagenicity.

***NO<sub>3</sub>/N<sub>2</sub>O<sub>5</sub> Exposure*** NO<sub>3</sub> radicals were generated in the dark by the thermal decomposition of gaseous N<sub>2</sub>O<sub>5</sub> in the presence of added NO<sub>2</sub><sup>36, 37</sup>. Because this reaction is reversible, NO<sub>2</sub> was added in order to achieve the desired NO<sub>3</sub> concentration and the chamber was continuously flushed to avoid the build-up of NO<sub>2</sub>. One addition of ~0.40 – 0.46 ppm N<sub>2</sub>O<sub>5</sub> and ~1 ppm NO<sub>2</sub> were made every hour by flushing them into the chamber with a stream of N<sub>2</sub> over the 8 h exposure period. The average NO<sub>3</sub> concentration was ~420 ppt after adjusting for wall losses and flushing. The total exposure period was equivalent to exposing the PM to an average ambient NO<sub>3</sub> concentration of 45 ppt for seven 12-hour nights. Trans-Pacific atmospheric transport from Asia to the West Coast has been shown to occur in as little as 6 days during the Spring of the year<sup>38</sup>.

***OH radical Exposure*** The photolysis of methylnitrite (CH<sub>3</sub>ONO), at wavelength > 300 nm in the presence of NO, was used to generate OH radicals<sup>35, 39</sup>. Irradiations were carried out at 20% of the maximum light intensity. Initial CH<sub>3</sub>ONO and NO concentrations of 1 ppm were flushed with a stream of N<sub>2</sub> into the chamber. The chamber was operated continuously in the flush mode to avoid the build-up of NO<sub>2</sub> and HNO<sub>3</sub>. However, a minor amount of HNO<sub>3</sub> was expected to form and could have nitrated the PAHs. One addition of CH<sub>3</sub>ONO and NO was made every hour, leading to an hourly OH radical concentration of  $2 \times 10^7$  molecule cm<sup>-3</sup> (~0.8 ppt) for a total 8 h exposure time. The total OH radical concentration was equivalent to exposing the PM to an average

tropospheric OH radical concentration ( $1.0 \times 10^6$  molecule  $\text{cm}^{-3}$ ) for ~6.7 days (24-hour day) in order to simulate trans-Pacific atmospheric transport of PM-bound PAHs during the springtime<sup>6,7</sup>.

***O<sub>3</sub> Exposure*** Ozone was generated by a Welsbach T-408 O<sub>3</sub> generator and introduced into the chamber with a stream of N<sub>2</sub>. The exposure was conducted in the dark and the chamber was not flushed. The average O<sub>3</sub> concentration was ~800 ppb over the 9.5 h exposure period, which was equivalent to exposing the PM to an average ambient O<sub>3</sub> concentration of 40 ppb for 8 days (24-hour day). Ozone concentrations exceeding 100 ppb have been measured during trans-Pacific atmospheric transport events<sup>40</sup>.

#### **4.2.4 Sample Extraction and Analysis**

Details of the sample extraction and analysis have been previously described<sup>14</sup>. In brief, prior to extraction, the ambient PM filters used in the chemical study were spiked with perdeuterated PAH and NPAH surrogates. No perdeuterated surrogates were spiked onto the PM filters that were used for the mutagenicity testing because we wanted to eliminate a mutagenic response due to the surrogates. All PM filters were extracted at 100°C and 1500 psi twice with dichloromethane using pressurized liquid extraction and the two fractions were combined. The extracts used for the Salmonella assay were evaporated to dryness under a gentle N<sub>2</sub> stream. The residue was dissolved in 500  $\mu\text{l}$  dimethylsulfoxide (DMSO). The extracts used for the chemical analysis were purified using 20-g silica columns prior to chemical analysis (Mega BE-SI, Agilent Technologies, New Castle, DE). PAHs and NPAHs were eluted in the dichloromethane fraction and spiked with perdeuterated PAH and NPAH internal standards. PAHs were analyzed by

gas chromatographic mass spectrometry (Agilent 6890 GC coupled with an Agilent 5973N MSD) in selected ion monitoring using electron impact ionization, while NPAHs were analyzed using negative chemical ionization (NCI) with a programmed temperature vaporization (PTV) inlet (Gerstel, Germany)<sup>14</sup>. Both PAHs and NPAHs were separated on a 5% phenyl substituted methylpolysiloxane GC column (DB-5MS, 30m×0.25mm I.D., 0.25 µm film thickness, J&W Scientific, USA). The separation of 2-NF and 3-NF was achieved on a 50% phenyl substituted methylpolysiloxane GC column (DB-17MS, 30m×0.25mm I.D., 0.25 µm film thickness, J&W Scientific, USA).

#### **4.2.5 Salmonella Mutagenicity Assay**

The basic methodology followed that reported by Maron and Ames<sup>41</sup> and used *Salmonella typhimurium* strain TA98 was used in the study. The experimental details have been described elsewhere<sup>14</sup>. The positive control doses were 2 µg of 2-aminoanthracene (2-AA) and 20 µg of 4-nitro-1,2-phenylenediamine (NPD) for assays with and without metabolic activation (rat S9 mix), respectively. The negative control (DMSO) dose was 30 µl. All filter extracts were tested in triplicate.

Based on preliminary studies and the limit of detection in the Salmonella assay, only the Beijing PM samples were tested for mutagenic activity (Appendix D.2). Twenty µg of NPD and two µg of 2-AA gave mean revertant counts of ~3500/plate and ~1000/plate, respectively. The average background revertant count (DMSO) was ~25/plate for both assays. The revertant counts for the control blanks were comparable to the background revertant count, indicating no interference from the purified air in the chamber. It should be noted that different sets of filters were used for the mutagenicity and chemical studies (Appendix D.3) and that the PAH and NPAH concentrations of the

PM samples used for the mutagenicity testing were measured and directly compared to the results from the Salmonella assay.

## 4.3 Results and Discussion

### 4.3.1 Chemical Study

*Beijing, China PM* Using the paired cut-outs of the same PM filter (shown in Appendix D.3), the measured mass of individual PAHs and NPAHs on the exposed filter ( $\text{PAH}_{\text{exposed}}$  and  $\text{NPAH}_{\text{exposed}}$ ) was divided by the measured mass of the individual PAHs and NPAHs on the unexposed filter ( $\text{PAH}_{\text{unexposed}}$  and  $\text{NPAH}_{\text{unexposed}}$ ) in order to determine the amount of PAH or NPAH degraded or formed after exposure to  $\text{NO}_3/\text{N}_2\text{O}_5$ , OH radicals, and  $\text{O}_3$ . A ratio close to 1 suggested limited net degradation or formation of a given PAH or NPAH after exposure to the various oxidants. The  $\text{PAH}_{\text{exposed}}/\text{PAH}_{\text{unexposed}}$  ratios and the  $\text{NPAH}_{\text{exposed}}/\text{NPAH}_{\text{unexposed}}$  ratios for the Beijing PM samples after exposure to  $\text{NO}_3/\text{N}_2\text{O}_5$ , OH radicals, and  $\text{O}_3$  are shown in Figures 4.1A and 4.1B, respectively. An asterisk indicates the statistically significant difference in mass after exposure to the various oxidants ( $p\text{-value} < 0.05$ ). The means and standard errors of PAH and NPAH masses measured in Beijing filters with and without exposure to the various oxidants are given in Appendix D.5 to Appendix D.7. Because 2- to 4-ring PAHs exist in both the gas and particulate phases in the atmosphere at ambient air temperatures<sup>42</sup>, it is possible that a portion of the PAH sorbed to the PM desorbed from the PM into the gas phase of the reactor during the experiment. However, because the air temperature in the reactor was relatively constant during the different exposures ( $\sim 296$  K), the formation of NPAHs due to gas-phase reactions was minimal (see below), and the blank filters installed in the

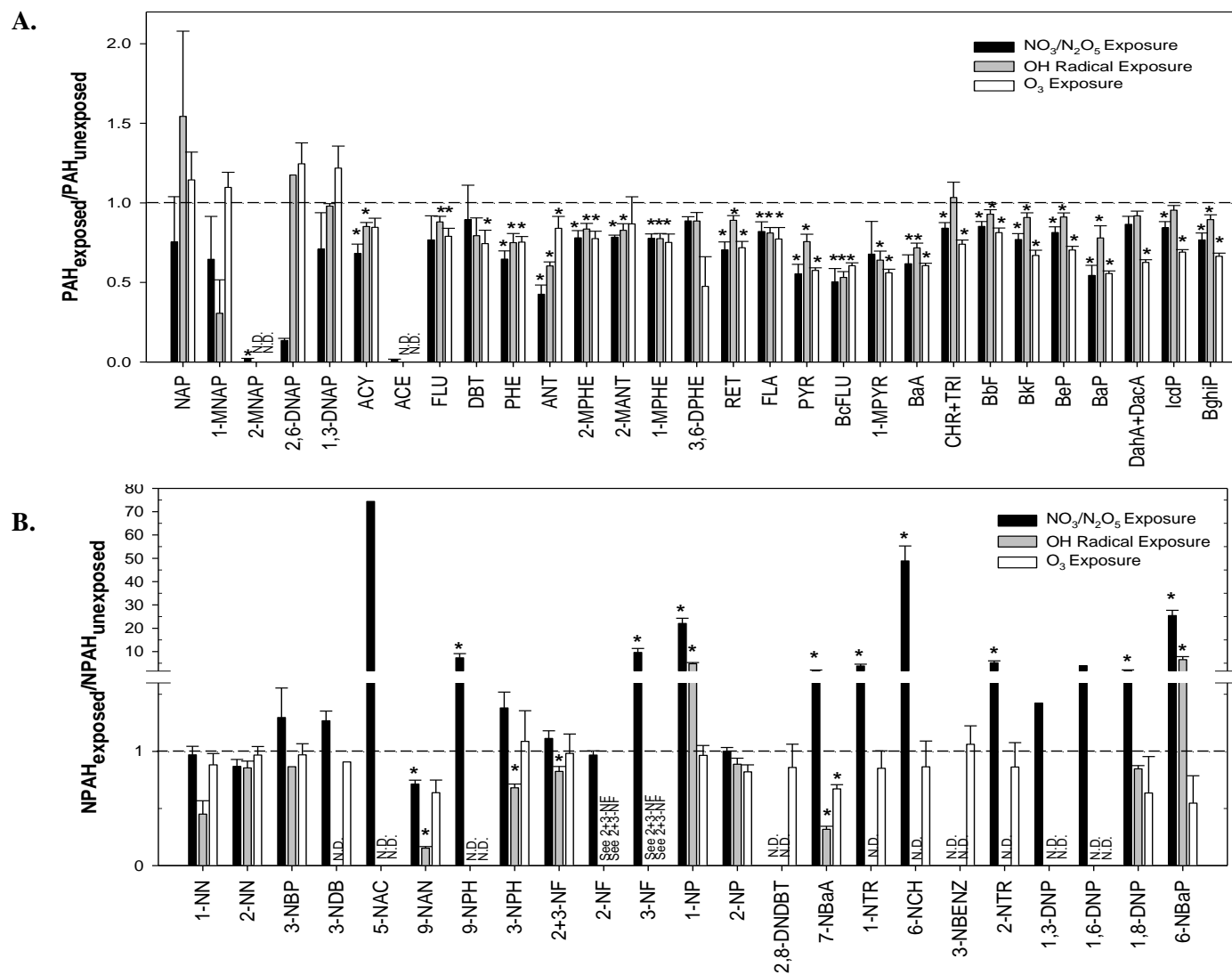


reactor at the same time as the PM had PAH concentrations below the detection limit, we believe that volatilization of these compounds from the PM was minimal during the course of the experiment.

For the Beijing PM, changes in the mass of NAP, methylnaphthalenes (MNAPs), and dimethylnaphthalenes (DNAPs) during exposure to  $\text{NO}_3/\text{N}_2\text{O}_5$ , OH radicals, and  $\text{O}_3$  were not statistically significant, except for the degradation of 2-MNAP during the  $\text{NO}_3/\text{N}_2\text{O}_5$  exposure (Figure 4.1 and Appendix D.5). The mass of 3- and 4-ring PAHs on the Beijing PM were significantly reduced during exposure to  $\text{NO}_3/\text{N}_2\text{O}_5$ , except for ACE, FLU, DBT, 3,6-DPHE and 1-MPYR (Appendix D.5). Among the measured 3- and 4-ring PAHs, ANT was the most reactive toward  $\text{NO}_3/\text{N}_2\text{O}_5$  reaction, followed by BcFLU and PYR (Figure 4.1A). Similar to the  $\text{NO}_3/\text{N}_2\text{O}_5$  exposure, most of the 3- and 4-ring PAHs on the Beijing PM were significantly degraded during exposure to OH radicals, except for DBT, 3,6-DPHE, and CHR+TRI (Appendix D.5). ANT was not degraded during the OH radical exposure (40%) as much as it was degraded in the  $\text{NO}_3/\text{N}_2\text{O}_5$  exposure (57%) (Appendix D.5 and Appendix D.6). During the OH radical exposure, BcFLU was degraded the most (47%), followed by ANT and 1-MPYR (40% and 36%) (Appendix D.6).

The exposure of Beijing PM to  $\text{O}_3$  also resulted in significant degradation of the 3- and 4-ring PAHs, except for ACY, 2-MANT and 3,6-DPHE. PYR, BcFLU, 1-MPYR, and BaA were all significantly degraded after exposure to  $\text{O}_3$  (Figure 4.1A and Appendix D.7). After exposure to ~800 ppb  $\text{O}_3$  for 9.5 h, the remaining fractions of PYR (58%)

**Figure 4.1** A.  $PAH_{\text{exposed}}/PAH_{\text{unexposed}}$  and B.  $NPAH_{\text{exposed}}/NPAH_{\text{unexposed}}$  of Beijing PM filters (n=3) used for the chemical study. An asterisk denotes the statistically significant difference between the unexposed and exposed masses. (N.D. = Not detected)



and BaA (61%) (Appendix D.7) on the Beijing PM were similar to a previous study where ambient PM was exposed to  $\sim 4$  ppm for 60 min<sup>31</sup>. This previous study reported that PYR and BaA concentrations plateaued at  $\sim 70\%$  of the initial concentrations<sup>31</sup> following exposure to O<sub>3</sub>. Combined, these data suggest that the degradation of PAHs sorbed to ambient PM plateaus after a period of time. In contrast, a previous study found that PYR coated on silica particles decayed completely after exposure to  $\sim 1.3$  ppm of O<sub>3</sub> within 10 minutes in a flow reactor<sup>26</sup>. This suggests that the reactivity of particle-bound PAHs is substrate-specific and is inhibited by the decreased availability of these PAHs on the surface of ambient PM.

The PAH<sub>exposed</sub> /PAH<sub>unexposed</sub> ratios of the PAHs with more than four rings that partition primarily to the particulate phase in the atmosphere, ranged from 0.54 to 0.86 (mean of 0.78), 0.78 to 0.95 (mean of 0.90), and 0.56 to 0.81 (mean of 0.67) for NO<sub>3</sub>/N<sub>2</sub>O<sub>5</sub>, OH radical and O<sub>3</sub> exposures, respectively (Figure 4.1A). These results show that all of the PAHs with more than four rings sorbed to Beijing PM were at least partially degraded during the OH radical exposure (Figure 4.1A and Appendix D.6). However, in general, O<sub>3</sub> was more effective in degrading these higher-ring PAHs than OH radicals and NO<sub>3</sub>/N<sub>2</sub>O<sub>5</sub> (Figure 4.1A, Appendix D.6, and Appendix D.7). Only BaP was degraded to a similar degree during exposure to O<sub>3</sub> and NO<sub>3</sub>/N<sub>2</sub>O<sub>5</sub> (Figure 4.1A and Appendix D.5 and Appendix D.7) and, of the higher-ring PAHs measured on the Beijing PM, BaP degraded the most during exposure to NO<sub>3</sub>/N<sub>2</sub>O<sub>5</sub>, OH radicals, and O<sub>3</sub> (Figure 4.1A). The high photochemical reactivity of BaP has been previously reported, including reaction with N<sub>2</sub>O<sub>5</sub>, O<sub>3</sub> and NO<sub>2</sub><sup>28, 43-45</sup>. Abelic-Juretic et al. found that, among the five PAHs sorbed to silica, perylene was the most reactive toward O<sub>3</sub>, followed by BaP<sup>46</sup>. On ambient PM,

BaP was also identified to be the most reactive PAH toward O<sub>3</sub>, OH radicals, and NO<sub>2</sub>/O<sub>3</sub><sup>31</sup>. Excluding BaP, the other higher-ring PAHs were degraded to a similar extent, with average percent degradation ranging from 5% to 11% (Appendix D.6), during OH radical exposure (Figure 4.1A). This suggests that higher-ring PAHs sorbed to ambient PM were not significantly degraded during exposure to OH radicals. Comparable heterogeneous pseudo-first-order rate constants, ranging from 0.010 to 0.016 s<sup>-1</sup>, for benzofluoranthenes, BaP, BeP and IcdP on diesel particles (NIST SRM 1650a) with OH radicals were previously reported at OH radical concentration of 3.4 × 10<sup>10</sup> molecule cm<sup>-3</sup><sup>21</sup>.

Figure 4.1B shows the NPAH<sub>exposed</sub> /NPAH<sub>unexposed</sub> ratios for the Beijing PM samples. The means and standard errors of NPAH masses measured on the Beijing PM samples, with and without exposure to the various oxidants, are given in Appendix D.5 to Appendix D.7. 2-NF and 3-NF were chromatographically separated and quantified using a 30 m DB-17 GC column for all NO<sub>3</sub>/N<sub>2</sub>O<sub>5</sub> unexposed and exposed Beijing PM samples and for one-third of the OH radical and O<sub>3</sub> unexposed and exposed Beijing PM samples because the 3-NF concentrations in the OH radical and O<sub>3</sub> unexposed and exposed PM samples were below the detection limit. For all exposures, there was no significant increase in the mass of 2-NF and 2-NP, which are products of gas-phase reactions<sup>47</sup>. This provides further evidence that there was no significant volatilization of 4-ring PAHs from the ambient PM into the gas-phase of the reactor and implies that the increase in the mass of other nitro-PAHs during the exposure experiments was likely due to heterogeneous reactions.

NPAHs were formed to a significant degree, with average percent formation ranging from 91% to 4,878%, during the  $\text{NO}_3/\text{N}_2\text{O}_5$  exposure (Figure 4.1B and Appendix D.5). While 1-NP and 6-NBaP were formed in both  $\text{NO}_3/\text{N}_2\text{O}_5$  and OH radical exposures, 9-NPH, 3-NF, 7-NBaA, 1-NTR, 6-NCH, 2-NTR and 1,8-DNP were only formed during the  $\text{NO}_3/\text{N}_2\text{O}_5$  exposure (Figure 4.1B). Our measured formation of 3-NF and 1-NP is consistent with the results from previous studies on the reaction of PAHs adsorbed on filters with gaseous  $\text{N}_2\text{O}_5$ <sup>34, 44</sup>. These previous studies found that 3-, 8-, 7- and 1-NF, along with 1-NP, were the major NPAH products formed by the heterogeneous reaction of FLA and PYR with  $\text{N}_2\text{O}_5$ . These isomers were indicative of heterogeneous reaction with  $\text{N}_2\text{O}_5$  and not  $\text{NO}_3$  radicals.  $\text{NO}_3$ -radical initiated reactions with FLA and PYR have been previously shown to form 2-NF and 2-NP as the major NPAH products via a different mechanism<sup>34</sup>. In the radical initiated reaction,  $\text{NO}_3$  radical attacks FLA or PYR at the highest electron density position, followed by  $\text{NO}_2$  addition at the *ortho* position<sup>48</sup>. In contrast, major NPAH isomers formed by heterogeneous reaction have the  $\text{NO}_2$  group added to the most thermodynamically stable position of OH-PAH adducts (see Chapter 3 of the thesis). Moreover, at equilibrium the  $\text{N}_2\text{O}_5$  concentration in the chamber was significantly higher than the  $\text{NO}_3$  concentration (~420 ppt). In contrast to PYR and FLA, the heterogeneous and gas-phase reactions of TRI were previously reported to both form 1- and 2-NTR<sup>34</sup>. In this study, 1-NTR and 2-NTR were equally formed after exposure to  $\text{NO}_3/\text{N}_2\text{O}_5$  (Figure 4.1B). Our measured formation of 7-NBaA, 6-NCH and 6-NBaP (Figure 4.1B) was in agreement with previous results showing their formation when PAHs associated with diesel soot were reacted with  $\text{N}_2\text{O}_5$ <sup>20</sup>.

High  $1\text{-NP}_{\text{exposed}}/1\text{-NP}_{\text{unexposed}}$  (mean of 4.8) and  $6\text{-NBaP}_{\text{exposed}}/6\text{-NBaP}_{\text{unexposed}}$  (mean of 6.5) ratios were also measured after the Beijing PM was exposed to OH radicals (Figure 4.1B). However, it was unlikely that these NPAHs were formed by reaction of the parent PAH with OH radical because OH radical reactions with PYR and BaP are expected to form 2-NP<sup>47</sup> and 2-NBaP (See Chapter 1 of the thesis) as major products, respectively. It is more likely that 1-NP and 6-NBaP formed in the OH radical exposure experiment by the heterogeneous nitration of parent PAHs by HNO<sub>3</sub>/NO<sub>2</sub>. The NO<sub>2</sub> concentrations in the chamber during the OH radical exposure experiment ranged from 0.5-2.2 ppm and was the product of the photolysis of methylnitrite to form OH radical. On the other hand, 3-NPH and 2+3-NF, and especially 9-NAN and 7-NBaA, were degraded during the OH radical exposure (Figure 4.1B). Because these same NPAHs were not as significantly degraded during the dark exposure with O<sub>3</sub> (Figure 4.1B), it is possible that the degradation observed during the OH radical exposure could be due, in part, to direct photolysis. Previously, Pitts et al. observed the direct photolysis of 9-NAN adsorbed on silica gel and identified quinones as the degradation products<sup>18</sup>. In another study, the direct photolysis of 7-NBaA resulted in increased direct-acting mutagenicity to TA98 in the Salmonella assay with increasing irradiation time<sup>49</sup>. The orientation of the nitro group has been related to the photochemical stability of NPAH<sup>50</sup>. Both 9-NAN and 7-NBaA have nitro group orientations that are out of the aromatic plane, reducing the steric effects exerted by two peri hydrogens. This structure makes these PAHs less photochemically stable and may explain their significant degradation during the OH radical exposure (Figure 4.1B)<sup>50</sup>. However, 6-NBaP also has a structure where the nitro group is out of the aromatic plane but showed significant net formation after exposure to

OH radical (mean  $\text{NPAH}_{\text{exposed}} / \text{NPAH}_{\text{unexposed}} = 6.5$ ) (Figure 4.1B). Exposure of the Beijing PM to  $\text{O}_3$  did not lead to significant NPAH formation (Figure 4.1B and Appendix D.7) and, except for the degradation of 7-NBaA, the NPAHs sorbed to Beijing PM were not significantly degraded during  $\text{O}_3$  exposure (Table 1B).

Because 1-NP was consistently formed from heterogeneous reaction of PYR adsorbed to a surface or particles<sup>51, 52</sup>, 1-NP was used as a representative NPAH to describe the reactivity of the Beijing PM to NPAH formation<sup>51</sup>. The percent reactivity of each of the paired PM samples, used in both the chemical and mutagenicity studies, was calculated as:

$$\% \text{ Reactivity} = \frac{\Delta[1\text{-NP}]}{[\text{PYR}]_0} \times 100 \quad (1)$$

where  $\Delta[1\text{-NP}] = 1\text{-NP}_{\text{exposed}} - 1\text{-NP}_{\text{unexposed}}$  and  $[\text{PYR}]_0 = [\text{PYR}]_{\text{unexposed}}$ <sup>51</sup>. We also calculated the 2-NF/BeP ratio of the unexposed samples as a measure of the degree to which the PM had undergone atmospheric processing (or aging) prior to collection at the Beijing sampling site<sup>51</sup>. 2-NF is formed from the gas-phase reaction of FLA with OH and  $\text{NO}_3$  radicals<sup>47</sup>, while BeP is resistant to atmospheric chemical degradation<sup>53</sup>. The correlation between percent reactivity and 2-NF/BeP ratio of Beijing PM samples exposed to  $\text{NO}_3/\text{N}_2\text{O}_5$  (Figure 4.2) shows the reactivity reduces exponentially when the 2-NF/BeP ratio decreases ( $R^2 = 0.79$ ,  $p\text{-value} < 0.0001$ ). Beijing PM samples with reduced reactivity had high 2-NF/BeP ratios, suggesting that the PAHs sorbed to Beijing PM that had undergone significant aging in the atmosphere were less available for reaction with  $\text{NO}_3/\text{N}_2\text{O}_5$ . Although there was a general trend of decreasing percent reactivity with

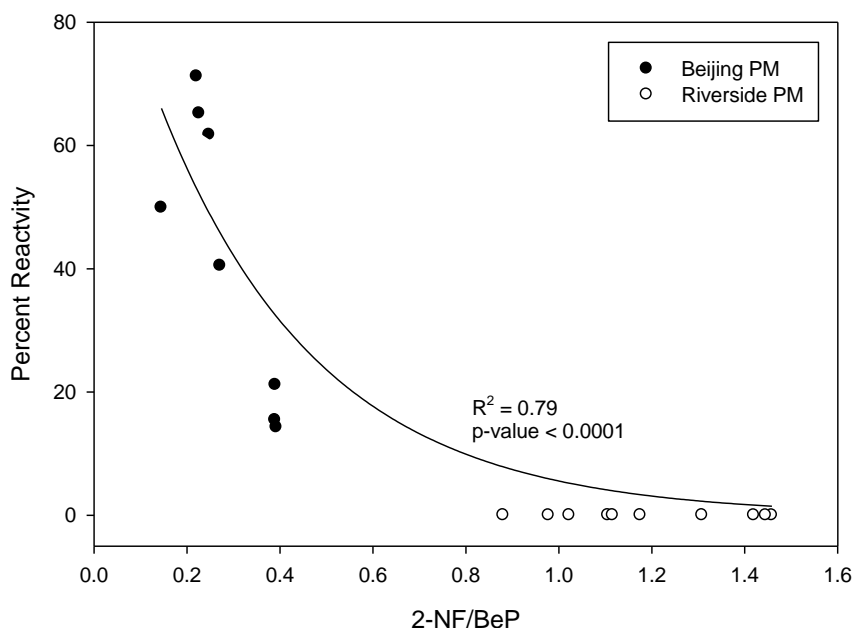


**Figure 4.2** Correlation between percent reactivity of the Beijing and Riverside PM samples exposed to  $\text{NO}_3/\text{N}_2\text{O}_5$  to  $2\text{-NF}_{\text{unexposed}}$  concentrations normalized to  $\text{BeP}_{\text{unexposed}}$ .

increasing OC or BC concentration in the Beijing PM samples after exposure to  $\text{NO}_3/\text{N}_2\text{O}_5$  and OH radical, the correlations were not statistically significant.

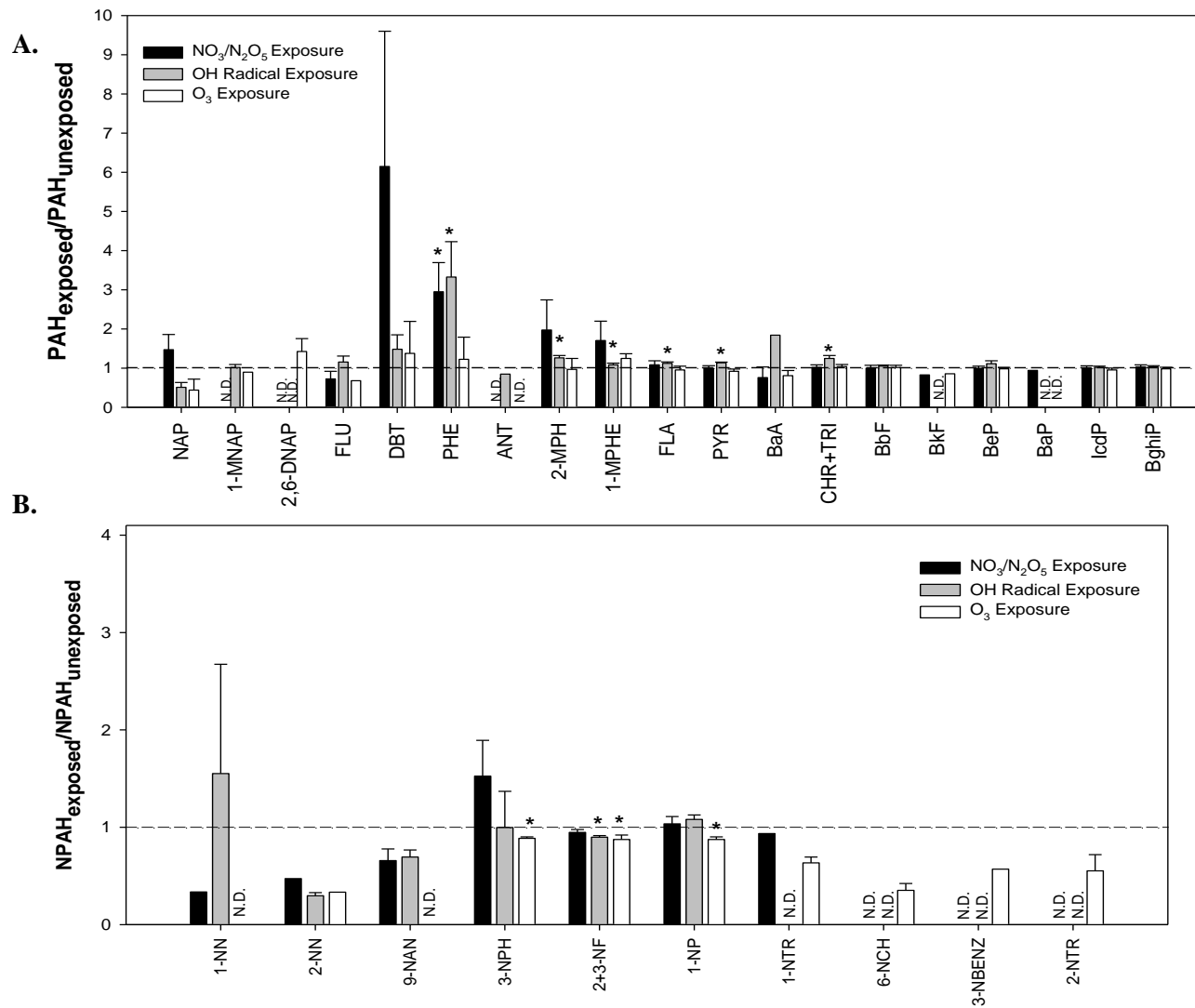
**Riverside, California PM** The  $\text{PAH}_{\text{exposed}}/\text{PAH}_{\text{unexposed}}$  ratios and the  $\text{NPAH}_{\text{exposed}}/\text{NPAH}_{\text{unexposed}}$  ratios for the Riverside PM samples after exposure to  $\text{NO}_3/\text{N}_2\text{O}_5$ , OH radicals, and  $\text{O}_3$  are shown in Figures 4.3A and 4.3B, respectively. The means and standard errors of PAH and NPAH masses measured in Riverside filters with and without exposure to the various oxidants are given in Appendix D.8 to Appendix D.10. Compared to the Beijing PM samples, a smaller number of individual PAH and NPAH were measured in the Riverside PM samples above their detection limit (Figures 4.1 and 4.3). Small, but statistically significant, formation of 2-MPH, 1-MPH, FLA, PYR, and CHR+TRI was measured after the exposure of Riverside PM to OH radicals,



and to a larger degree, PHE was measured after the exposure to  $\text{NO}_3/\text{N}_2\text{O}_5$  and OH radicals (Figure 4.3A). However, these small changes in mass (Appendix D.8) may fall within the experimental uncertainty. Compared to the Beijing PM samples, the higher-ring PAHs, including PYR and BaP, in the Riverside PM samples appeared to be more resistant to degradation during the  $\text{NO}_3/\text{N}_2\text{O}_5$  and OH radical exposures (Figures 4.1A and 4.3A). Exposure of the Riverside PM samples to  $\text{O}_3$  did not result in significant degradation of PAHs, including the higher-ring PAHs (Figures 4.3A). Consistent with the absence of significant degradation of PAHs sorbed to the Riverside PM, there was no significant formation of NPAHs in any of the exposures (Figure 4.3B). A small, but statistically significant reduction in mass was measured for 2+3-NF after exposure to OH radicals and for 3-NPH, 2+3-NF and 1-NP after exposure to  $\text{O}_3$  (Figure 4.3B). The correlation between percent reactivity and ratio of 2-NF to BeP of the Riverside samples exposed to  $\text{NO}_3/\text{N}_2\text{O}_5$  exposure is shown in Figure 4.2. The low percent reactivity of the Riverside samples was explained by high 2-NF/BeP ratio, indicating that the Riverside PM had undergone more aging than the Beijing PM.

These results suggest that the PAHs and NPAHs sorbed to the Riverside PM were less available for reaction compared to the PAHs and NPAHs sorbed to the Beijing PM. The decreased reactivity of the Riverside PM, compared to the Beijing PM, may be because the Riverside sampling site is located downwind of Los Angeles and receives photochemically “aged” air masses from this major source region. In contrast, the Beijing sampling site is surrounded by major PAH sources and receives air masses that are not as photochemically aged, in comparison. The accumulation of degradation products on the surface of Riverside PM could inhibit further atmospheric degradation of parent PAHs.

**Figure 4.3** A.  $PAH_{\text{exposed}}/PAH_{\text{unexposed}}$  and B.  $NPAH_{\text{exposed}}/NPAH_{\text{unexposed}}$  of Riverside PM filters (n=3) used for the chemical study. An asterisk denotes the statistically significant difference between the unexposed and exposed masses. (N.D. = Not detected)

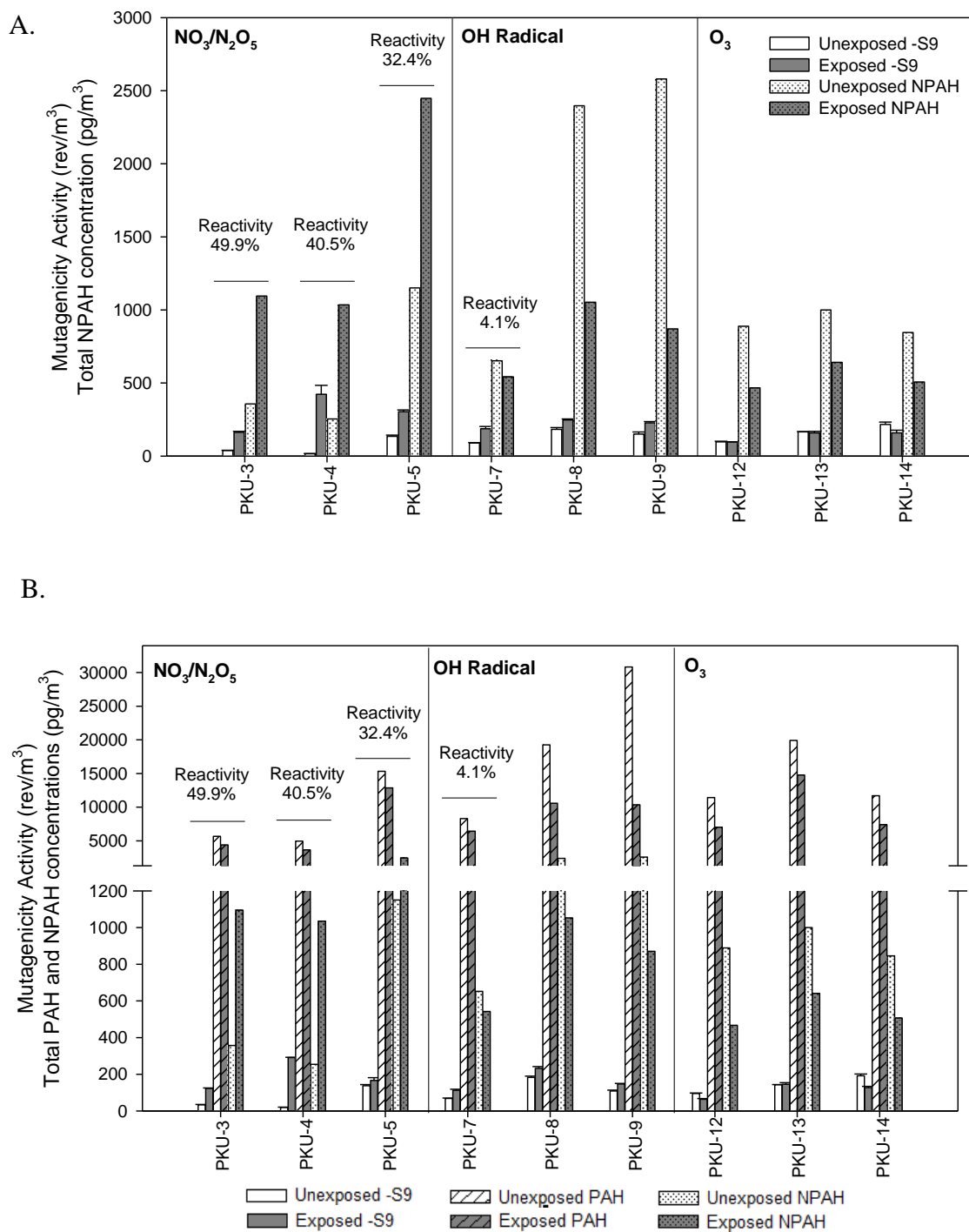


### 4.3.2 Mutagenicity Study

***Direct-acting Mutagenicity*** Most NPAHs are known to be direct-acting mutagens, requiring no exogenous bioactivation to convert them into the active form<sup>54</sup>. The direct-acting mutagenic activity of the unexposed and exposed paired Beijing PM samples is shown in Figure 4.4A, along with the percent reactivity of the PM tested. Appendix D.11 shows the  $PAH_{\text{exposed}}/PAH_{\text{unexposed}}$  ratios and the  $NPAH_{\text{exposed}}/NPAH_{\text{unexposed}}$  ratios for the Beijing PM samples used in the mutagenicity assay after exposure to  $NO_3/N_2O_5$ , OH radicals, and  $O_3$ . In general, the results were comparable to the Beijing PM samples used in the chemical study (Figures 4.1A and 4.1B) in that there was significant formation of NPAHs via heterogeneous reaction of the Beijing PM-bound PAHs with  $NO_3/N_2O_5$  (Figure 4.1B and Appendix D.11).

Minimal direct-acting activity was determined in the two unexposed Beijing extracts with lower NPAH concentrations (PKU-3 and PKU-4), compared to the unexposed Beijing PM extract with higher NPAH concentrations (PKU-5) (Figure 4.4A and Appendix D.12). This is consistent with a previous study from our laboratory that showed significant daily variation in the direct-acting mutagenicity, and corresponding NPAH concentrations, of Beijing PM<sup>14</sup>. After  $NO_3/N_2O_5$  exposure, the direct-acting mutagenicity of the Beijing PM increased 2- to 26-fold (Figure 4.4A). Of the Beijing PM samples exposed to  $NO_3/N_2O_5$ , the sharpest increase in direct-acting mutagenicity (26-fold) was attributed to sample PKU-4 that had the highest increases in 1,3-, 1,6-, and 1,8-DNP mass after exposure to  $NO_3/N_2O_5$  (Appendix D.12). Among these DNPs, 1,8-DNP resulted in the greatest percent increase in mass (10.2 ng) (Appendix D.12). The 1,8-DNP

**Figure 4.4** Comparison of A. direct-acting mutagenicity, total NPAH concentration and B. indirect-acting mutagenicity, total PAH and NPAH concentrations of exposed and unexposed Beijing PM samples. Percent reactivity is shown when the value is greater than zero (See text for description of percent reactivity).



concentrations measured in the other two mutagenicity study samples exposed to  $\text{NO}_3/\text{N}_2\text{O}_5$  (PKU-3 and PKU-5) were either below the detection limit or three times less than that measured in the PKU-4 sample. In other mutagenicity assays, DNPs, especially 1,8-DNP, were found to be powerful direct-acting mutagens<sup>55</sup>. Small amounts of DNPs have been shown to contribute significantly to the total direct-acting mutagenicity of diesel particles<sup>16</sup>.

For the OH radical exposure in the direct-acting mutagenicity study, two of the Beijing PM samples had zero percent reactivity (PKU-8 and PKU-9) and one sample had only 4.1% reactivity (PKU-7) (Figure 4.4A and Appendix D.13). This is consistent with the results from the chemical study that showed that the OH radical exposure did not result in the heterogeneous nitration of PM-bound PAHs to a significant degree (Figure 4.1B and Appendix D.11). Overall, the enhancement in direct-acting mutagenicity after OH radical exposure (mean of 1.7-fold) was lower than the enhancement in direct-acting mutagenicity after  $\text{NO}_3/\text{N}_2\text{O}_5$  exposure (mean of 11-fold). The  $\text{NPAH}_{\text{exposed}}/\text{NPAH}_{\text{unexposed}}$  profiles, from both the mutagenicity study and chemical study, showed the formation of 1-NP and 6-NBaP from OH radical exposure (Figure 4.1B and Appendix D.11). Given the significant 6-NBaP formation in all of the Beijing PM samples from exposure to OH radicals (Figure 4.1B and Appendix D.13), and the minimal corresponding increase in direct-acting mutagenicity of these same samples, 6-NBaP does not appear to contribute significantly to the overall direct-acting mutagenicity of the Beijing PM. This is consistent with the structure of 6-NBaP, with a  $\text{NO}_2$  group nearly perpendicular to the aromatic ring that does not allow for favorable nitro-reduction<sup>55</sup>. However, an increase in direct-acting mutagenicity and a decrease in total NPAH mass, as well as a decrease in

mutagenic 1-NP mass, was observed after PKU-8 and PKU-9 were exposed to OH radicals (Figure 4.4A). This suggests that other mutagenic degradation products, not measured in this study or below the detection limit of our analytical method, may have contributed to the enhanced direct-acting mutagenicity of the Beijing PM after exposure to OH radicals.

The percent reactivity of Beijing PM samples exposed to O<sub>3</sub> was zero (Figure 4.4A). Appendix D.11 shows that 2-NN, 3-NBP, 9-NAN, 3-NPH, 2+3-NF, 1-NP and 2-NP were degraded significantly during the O<sub>3</sub> exposure for the mutagenicity study, while only 7-NBaA was significantly degraded during the O<sub>3</sub> exposure for the chemical study (Figure 4.1B). Interestingly, only PKU-14 showed a significant decrease in direct-acting mutagenicity of the Beijing PM after exposure to O<sub>3</sub>, consistent with the corresponding decrease in the total NPAH mass (Figure 4.4A and Appendix D.14).

***Indirect-acting Mutagenicity*** Some parent PAHs and NPAHs, including 6-NBaP and 1-nitrocoronene, contribute to the indirect-acting mutagenicity of PM<sup>56</sup>. On average, there was a ~7-fold and ~1.4-fold increase in the indirect-acting mutagenicity of the Beijing PM after exposure to NO<sub>3</sub>/N<sub>2</sub>O<sub>5</sub> and OH radicals, respectively (Figure 4.4B). Because most parent PAHs were degraded after exposure to NO<sub>3</sub>/N<sub>2</sub>O<sub>5</sub> and OH radicals (Figure 4.4B, Appendix D.11 to D.13), it is possible that the NPAHs formed contributed to the increase in indirect-acting mutagenicity. Increased indirect-acting mutagenicity after parent PAH exposure to NO<sub>3</sub>/N<sub>2</sub>O<sub>5</sub> and OH radicals was observed in our previous studies (see Chapter 3 of the thesis). In addition, Kamens et al<sup>8</sup> found that the exposure of wood soot NO<sub>2</sub> and O<sub>3</sub> resulted in an increase in both direct- and indirect-acting

mutagenicity of the NPAH fraction. In the same study, the most polar fraction made the largest contribution to the total indirect-acting mutagenicity. This suggests that the other, more polar, transformation products may also contribute significantly to the indirect-acting mutagenicity of the crude extracts. Moreover, the high molecular weight PAHs (MW 302), including dibenzo[a,l]pyrene which is 30 times more toxic than BaP<sup>57</sup>, may also play a significant role in the indirect-acting mutagenicity and they are a significant contributor to inhalation cancer risk in Beijing air<sup>58</sup>. The results of our previous study on the heterogeneous nitration of dibenzo[a,l]pyrene adsorbed on filter showed that the indirect-acting mutagenicity increased 2.5-fold after the NO<sub>3</sub>/N<sub>2</sub>O<sub>5</sub> exposure and 6-nitrodibenzo[a,l]pyrene was the only nitro product identified (see Chapter 3).

For the O<sub>3</sub> exposure, the PAH<sub>exposed</sub>/PAH<sub>unexposed</sub> profile of Beijing PM samples were comparable for the mutagenicity and chemical studies (Figure 4.1A and Appendix D.11). The reduction in mutagenicity (33%) of the two Beijing samples exposed to O<sub>3</sub> (PKU-12 and PKU-14) may be associated with the degradation of the total parent PAH and NPAH masses (Figure 4.4B). However, there was no significant change in indirect-acting mutagenicity in PKU-13 when total PAH and NPAH masses decreased (Figure 4.4B).

The extent of PAH transformation observed in this study may be limited by the multilayer coverage of the ambient PM on the filters. In reality, the transformation of PAHs on PM may be more significant in the atmosphere, where the PAHs are present on individual particles, than on the filters we exposed under the current laboratory conditions. However, the resistance of the Riverside PM samples to chemical reaction

suggests that secondary pollutant formation may also play an important role in shielding PM-bound PAHs from transformation reactions, making them less available for chemical reactions. Overall, these results suggest that PAH and NPAH degradation and formation are likely to occur predominantly near emission sources where the concentrations of oxidants are relatively high.

#### **4.4 Acknowledgements**

This publication was made possible in part by grant number P30ES00210 from the National Institute of Environmental Health Sciences (NIEHS), NIH and NIEHS Grant P42 ES016465, and the U.S. National Science Foundation (ATM-0841165). Its contents are solely the responsibility of the authors and do not necessarily represent the official view of the NIEHS, NIH. Salmonella assays were conducted in the Cancer Chemoprotection Program (CCP) Core Laboratory of the Linus Pauling Institute, Oregon State University.



## 4.5 References

1. Albinet, A.; Leoz-Garziandia, E.; Budzinski, H.; Villenave, E.; Jaffrezo, J. L., Nitrated and oxygenated derivatives of polycyclic aromatic hydrocarbons in the ambient air of two French alpine valleys: Part 1: Concentrations, sources and gas/particle partitioning. *Atmos. Environ.* **2008**, *42*, (1), 43-54.
2. Björseth, A.; Lunde, G.; Lindskog, A., Long-range transport of polycyclic aromatic hydrocarbons. *Atmospheric Environment (1967)* **1979**, *13*, (1), 45-53.
3. Lammel, G.; Novák, J.; Landlová, L.; Dvorská, A.; Klánová, J.; Čupr, P.; Kohoutek, J.; Reimer, E.; Škrdlíková, L., Sources and distributions of polycyclic aromatic hydrocarbons and toxicity of polluted atmosphere aerosols. *Urban Airborne Particulate Matter* **2011**, 39-62.
4. Welch, H. E.; Muir, D. C. G.; Billeck, B. N.; Lockhart, W. L.; Brunskill, G. J.; Kling, H. J.; Olson, M. P.; Lemoine, R. M., Brown snow: a long-range transport event in the Canadian Arctic. *Environ. Sci. Technol.* **1991**, *25*, (2), 280-286.
5. Killin, R. K.; Simonich, S. L.; Jaffe, D. A.; DeForest, C. L.; Wilson, G. R., Transpacific and regional atmospheric transport of anthropogenic semivolatile organic compounds to Cheeka Peak Observatory during the spring of 2002. *Journal of geophysical research* **2004**, *109*, (D23), D23S15.
6. Genualdi, S. A.; Killin, R. K.; Woods, J.; Wilson, G.; Schmedding, D.; Simonich, S. L. M., Trans-Pacific and Regional Atmospheric Transport of Polycyclic Aromatic Hydrocarbons and Pesticides in Biomass Burning Emissions to Western North America. *Environ. Sci. Technol.* **2009**, *43*, (4), 1061-1066.
7. Primbs, T.; Piekarz, A.; Wilson, G.; Schmedding, D.; Higginbotham, C.; Field, J.; Simonich, S. M., Influence of Asian and Western United States Urban Areas and Fires on the Atmospheric Transport of Polycyclic Aromatic Hydrocarbons, Polychlorinated Biphenyls, and Fluorotelomer Alcohols in the Western United States. *Environ. Sci. Technol.* **2008**, *42*, (17), 6385-6391.
8. Kamens, R.; Bell, D.; Dietrich, A.; Perry, J.; Goodman, R.; Claxton, L.; Tejada, S., Mutagenic transformations of dilute wood smoke systems in the presence of ozone and nitrogen dioxide. Analysis of selected high-pressure liquid chromatography fractions from wood smoke particle extracts. *Environ. Sci. Technol.* **1985**, *19*, (1), 63-69.
9. Yang, X.-Y.; Igarashi, K.; Tang, N.; Lin, J.-M.; Wang, W.; Kameda, T.; Toriba, A.; Hayakawa, K., Indirect- and direct-acting mutagenicity of diesel, coal and wood burning-derived particulates and contribution of polycyclic aromatic hydrocarbons and nitropolycyclic aromatic hydrocarbons. *Mutation Research/Genetic Toxicology and Environmental Mutagenesis* **2010**, *695*, (1-2), 29-34.
10. Reisen, F.; Arey, J., Atmospheric Reactions Influence Seasonal PAH and Nitro-PAH Concentrations in the Los Angeles Basin. *Environ. Sci. Technol.* **2004**, *39*, (1), 64-73.
11. Dimashki, M.; Harrad, S.; Harrison, R. M., Measurements of nitro-PAH in the atmospheres of two cities. *Atmos. Environ.* **2000**, *34*, (15), 2459-2469.
12. Bamford, H. A.; Baker, J. E., Nitro-polycyclic aromatic hydrocarbon concentrations and sources in urban and suburban atmospheres of the Mid-Atlantic region. *Atmos. Environ.* **2003**, *37*, (15), 2077-2091.

13. Albinet, A.; Leoz-Garziandia, E.; Budzinski, H.; Villenave, E., Polycyclic aromatic hydrocarbons (PAHs), nitrated PAHs and oxygenated PAHs in ambient air of the Marseilles area (South of France): Concentrations and sources. *Sci. Total Environ.* **2007**, *384*, (1-3), 280-292.
14. Wang, W.; Jariyasopit, N.; Schrlau, J.; Jia, Y.; Tao, S.; Yu, T.-W.; Dashwood, R. H.; Zhang, W.; Wang, X.; Simonich, S. L. M., Concentration and Photochemistry of PAHs, NPAHs, and OPAHs and Toxicity of PM<sub>2.5</sub> during the Beijing Olympic Games. *Environ. Sci. Technol.* **2011**, *45*, (16), 6887-6895.
15. IARC Monograph in the series *Evaluation of Carcinogenic Risks to Humans: Vol 105, Diesel and gasoline engine exhausts and some nitroarenes*; World Health Organization: Lyon, 2012 (in prep).
16. Hayakawa, K.; Nakamura, A.; Terai, N.; Kizu, R.; Ando, K., Nitroarene Concentration and Direct-acting Mutagenicity of Diesel Exhaust Particulates Fractionated by Silica-Gel Column Chromatography. *Chem. Pharm. Bull.* **1997**, *45*, (11), 1820-1822.
17. Grosjean, D.; Fung, K.; Harrison, J., Interactions of polycyclic aromatic hydrocarbons with atmospheric pollutants. *Environ. Sci. Technol.* **1983**, *17*, (11), 673-679.
18. Pitts Jr, J. N.; Van Cauwenberghe, K. A.; Grosjean, D.; Schmid, J. P.; Fitz, D. R.; Belser, W.; Knudson, G.; Hynds, P. M., Atmospheric reactions of polycyclic aromatic hydrocarbons: facile formation of mutagenic nitro derivatives. *Science (New York, NY)* **1978**, *202*, (4367), 515.
19. McDow, S. R.; Sun, Q.; Vartiainen, M.; Hong, Y.; Yao, Y.; Fister, T.; Yao, R.; Kamens, R. M., Effect of composition and state of organic components on polycyclic aromatic hydrocarbon decay in atmospheric aerosols. *Environ. Sci. Technol.* **1994**, *28*, (12), 2147-2153.
20. Kamens, R. M.; Guo, J.; Guo, Z.; McDow, S. R., Polynuclear aromatic hydrocarbon degradation by heterogeneous reactions with N<sub>2</sub>O<sub>5</sub> on atmospheric particles. *Atmospheric Environment. Part A. General Topics* **1990**, *24*, (5), 1161-1173.
21. Esteve, W.; Budzinski, H.; Villenave, E., Relative rate constants for the heterogeneous reactions of NO<sub>2</sub> and OH radicals with polycyclic aromatic hydrocarbons adsorbed on carbonaceous particles. Part 2: PAHs adsorbed on diesel particulate exhaust SRM 1650a. *Atmos. Environ.* **2006**, *40*, (2), 201-211.
22. Behymer, T. D.; Hites, R. A., Photolysis of polycyclic aromatic hydrocarbons adsorbed on simulated atmospheric particulates. *Environ. Sci. Technol.* **1985**, *19*, (10), 1004-1006.
23. Zhou, S.; Lee, A.; McWhinney, R.; Abbatt, J., Burial Effects of Organic Coatings on the Heterogeneous Reactivity of Particle-Borne Benzo [a] pyrene (BaP) toward Ozone. *The Journal of Physical Chemistry A* **2012**, *116*, (26), 7050-7056.
24. Pöschl, U.; Letzel, T.; Schauer, C.; Niessner, R., Interaction of ozone and water vapor with spark discharge soot aerosol particles coated with benzo [a] pyrene: O<sub>3</sub> and H<sub>2</sub>O adsorption, benzo [a] pyrene degradation, and atmospheric implications. *The Journal of Physical Chemistry A* **2001**, *105*, (16), 4029-4041.
25. Kwamena, N. O. A.; Thornton, J. A.; Abbatt, J. P. D., Kinetics of surface-bound benzo [a] pyrene and ozone on solid organic and salt aerosols. *The Journal of Physical Chemistry A* **2004**, *108*, (52), 11626-11634.

26. Miet, K.; Le Menach, K.; Flaud, P. M.; Budzinski, H.; Villenave, E., Heterogeneous reactions of ozone with pyrene, 1-hydroxypyrene and 1-nitropyrene adsorbed on particles. *Atmos. Environ.* **2009**, *43*, (24), 3699-3707.
27. Esteve, W.; Budzinski, H.; Villenave, E., Relative rate constants for the heterogeneous reactions of OH, NO<sub>2</sub> and NO radicals with polycyclic aromatic hydrocarbons adsorbed on carbonaceous particles. Part 1: PAHs adsorbed on 1-2 μm calibrated graphite particles. *Atmos. Environ.* **2004**, *38*, (35), 6063-6072.
28. Perraudin, E.; Budzinski, H.; Villenave, E., Kinetic study of the reactions of ozone with polycyclic aromatic hydrocarbons adsorbed on atmospheric model particles. *J. Atmos. Chem.* **2007**, *56*, (1), 57-82.
29. Nguyen, M.; Bedjanian, Y.; Guilloteau, A., Kinetics of the reactions of soot surface-bound polycyclic aromatic hydrocarbons with NO<sub>2</sub>. *J. Atmos. Chem.* **2009**, *62*, (2), 139-150.
30. Bedjanian, Y.; Nguyen, M. L.; Le Bras, G., Kinetics of the reactions of soot surface-bound polycyclic aromatic hydrocarbons with the OH radicals. *Atmos. Environ.* **2010**, *44*, (14), 1754-1760.
31. Ringuet, J.; Albinet, A.; Leoz-Garziandia, E.; Budzinski, H. I. n.; Villenave, E., Reactivity of polycyclic aromatic compounds (PAHs, NPAHs and OPAHs) adsorbed on natural aerosol particles exposed to atmospheric oxidants. *Atmos. Environ.* **2012**.
32. Wang, W.; Primbs, T.; Tao, S.; Simonich, S. L. M., Atmospheric Particulate Matter Pollution during the 2008 Beijing Olympics. *Environ. Sci. Technol.* **2009**, *43*, (14), 5314-5320.
33. Atkinson, R.; Arey, J.; Dodge, M. C.; Harger, W. P.; McElroy, P.; Phouongphouang, P. T. Yields and Reactions of Intermediate Compounds Formed from the Initial Atmospheric Reactions of Selected VOCs. 2001.
34. Zimmermann, K.; Atkinson, R.; Arey, J.; Kojima, Y.; Inazu, K., Isomer distributions of molecular weight 247 and 273 nitro-PAHs in ambient samples, NIST diesel SRM, and from radical-initiated chamber reactions. *Atmos. Environ.* **2012**, *55*, (0), 431-439.
35. Nishino, N.; Atkinson, R.; Arey, J., Formation of Nitro Products from the Gas-Phase OH Radical-Initiated Reactions of Toluene, Naphthalene, and Biphenyl: Effect of NO<sub>2</sub> Concentration. *Environ. Sci. Technol.* **2008**, *42*, (24), 9203-9209.
36. Arey, J.; Zielinska, B.; Atkinson, R.; Aschmann, S. M., Nitroarene Products from the Gas-Phase Reactions of Volatile Polycyclic Aromatic Hydrocarbons with the OH Radical and N<sub>2</sub>O<sub>5</sub>. *Int. J. Chem. Kinet.* **1989**, *21*, 775-799.
37. Sasaki, J.; Aschmann, S. M.; Kwok, E. S. C.; Atkinson, R.; Arey, J., Products of the Gas-Phase OH and NO<sub>3</sub> Radical-Initiated Reactions of Naphthalene. *Environ. Sci. Technol.* **1997**, *31*, (11), 3173-3179.
38. Jaffe, D.; Anderson, T.; Cover, D.; Kotchenruther, R.; Trost, B.; Danielson, J.; Simpson, W.; Bernstein, T.; Karlsdottir, S.; Blake, D.; Harris, J.; Carmichael, G.; Uno, I., Transport of Asian Air Pollution to North America. *Geophys. Res. Lett.* **1999**, *26*, (6), 711-714.
39. Sasaki, J.; Arey, J.; Harger, W. P., Formation of Mutagens from the Photooxidations of 2-4-Ring PAH. *Environ. Sci. Technol.* **1995**, *29*, (5), 1324-1335.

40. Bertschi, I. T.; Jaffe, D. A., Long-range transport of ozone, carbon monoxide, and aerosols to the NE Pacific troposphere during the summer of 2003: Observations of smoke plumes from Asian boreal fires. *J. Geophys. Res.* **2005**, *110*, (D5), D05303.
41. Maron, D. M.; Ames, B. N., Revised methods for the Salmonella mutagenicity test. *Mutation Research/Environmental Mutagenesis and Related Subjects* **1983**, *113*, (3-4), 173-215.
42. Finlayson-Pitts, B. J.; Pitts Jr, J. N., *Chemistry of the upper and lower atmosphere*. 1st ed.; Academic Press: San Diego, 2000.
43. Behymer, T. D.; Hites, R. A., Photolysis of polycyclic aromatic hydrocarbons adsorbed on simulated atmospheric particulates. *Environ. Sci. Technol.* **1985**, *19*, (10), 1004-1006.
44. Pitts, J. N.; Sweetman, J. A.; Zielinska, B.; Atkinson, R.; Winer, A. M.; Harger, W. P., Formation of nitroarenes from the reaction of polycyclic aromatic hydrocarbons with dinitrogen pentoxide. *Environ. Sci. Technol.* **1985**, *19*, (11), 1115-1121.
45. Carrara, M.; Wolf, J.-C.; Niessner, R., Nitro-PAH formation studied by interacting artificially PAH-coated soot aerosol with NO<sub>2</sub> in the temperature range of 295-523 K. *Atmos. Environ.* **2010**, *44*, (32), 3878-3885.
46. Alebic-Juretic, A.; Cvitas, T.; Klasinc, L., Heterogeneous polycyclic aromatic hydrocarbon degradation with ozone on silica gel carrier. *Environ. Sci. Technol.* **1990**, *24*, (1), 62-66.
47. Atkinson, R.; Arey, J.; Zielinska, B.; Aschmann, S. M., Kinetics and Nitro-Products of the Gas-Phase OH and NO<sub>3</sub> Radical-Initiated Reactions of Naphthalene-d<sub>8</sub>, Fluoranthene-d<sub>10</sub>, and Pyrene. *Int. J. Chem. Kinet.* **1990**, *22*, 999-1014.
48. Pitts Jr, J. N.; Sweetman, J. A.; Zielinska, B.; Winer, A. M.; Atkinson, R., Determination of 2-nitrofluoranthene and 2-nitropyrene in ambient particulate organic matter: Evidence for atmospheric reactions. *Atmospheric Environment (1967)* **1985**, *19*, (10), 1601-1608.
49. White, G.; Fu, P.; Heflich, R., Effect of nitro substitution on the light-mediated mutagenicity of polycyclic aromatic hydrocarbons in Salmonella typhimurium TA 98. *Mutat. Res.* **1985**, *144*, (1), 1-7.
50. Fan, Z.; Kamens, R. M.; Hu, J.; Zhang, J.; McDow, S., Photostability of Nitro-Polycyclic Aromatic Hydrocarbons on Combustion Soot Particles in Sunlight. *Environ. Sci. Technol.* **1996**, *30*, (4), 1358-1364.
51. Zimmermann, K.; Jariyasopit, N.; Simonich, S. L.; Tao, S.; Atkinson, R.; Arey, J., Formation of nitro-PAHs from the heterogeneous reaction of ambient particle-bound PAHs with N<sub>2</sub>O<sub>5</sub>/NO<sub>3</sub>/NO<sub>2</sub>. *Environ. Sci. Technol.* **2013**.
52. Miet, K.; Le Menach, K.; Flaud, P. M.; Budzinski, H.; Villenave, E., Heterogeneous reactivity of pyrene and 1-nitropyrene with NO<sub>2</sub>: Kinetics, product yields and mechanism. *Atmos. Environ.* **2009**, *43*, (4), 837-843.
53. van Pinxteren, D.; Brüggemann, E.; Gnauk, T.; Iinuma, Y.; Müller, K.; Nowak, A.; Achtert, P.; Wiedensohler, A.; Herrmann, H., Size- and time-resolved chemical particle characterization during CAREBeijing-2006: Different pollution regimes and diurnal profiles. *Journal of Geophysical Research-Atmospheres* **2009**, *114*, D00G09.
54. Fu, P. P., Metabolism of nitro-polycyclic aromatic hydrocarbons. *Drug metabolism reviews* **1990**, *22*, (2-3), 209-268.

55. Jung, H.; Heflich, R. H.; Fu, P. P.; Shaikh, A. U.; Hartman, P., Nitro group orientation, reduction potential, and direct-acting mutagenicity of nitro-polycyclic aromatic hydrocarbons. *Environ. Mol. Mutagen.* **1991**, *17*, (3), 169-180.
56. Rosenkranz, H. S.; Mermelstein, R., The mutagenic and carcinogenic properties of nitrated polycyclic aromatic hydrocarbons. In White, C. M., Ed. Huethig: Heidelberg, 1985; pp 267-297.
57. USEPA *Development of a Relative Potency Factor (RPF) Approach for Polycyclic Aromatic Hydrocarbon (PAH) Mixtures, an external review draft*; U.S. Environmental Protection Agency, Intergrated Risk Information System (IRIS): Washington, DC, 2010.
58. Jia, Y.; Stone, D.; Wang, W.; Schrlau, J.; Tao, S.; Massey Simonich, S. L., Estimated Reduction in Cancer Risk due to PAH Exposures if Source Control Measures during the 2008 Beijing Olympics were Sustained. *Environ. Health Perspect.* **2011**.

## CHAPTER 5. CONCLUSIONS

In Chapter 2 of the thesis, the concentrations of polycyclic aromatic hydrocarbons (PAHs), nitrated-PAHs (NPAHs), and oxy-PAHs (OPAHs) and mutagenicity of Beijing particulate matter with aerodynamic diameters  $< 2.5 \mu\text{m}$  ( $\text{PM}_{2.5}$ ) were investigated during the 2008 Olympic Summer Games. The sampling period included the non-source control period and the source control period. In general, local black carbon (BC) and PAH emission sources, within 1 km of PKU, included vehicular traffic and fuel combustion for cooking. During the non-source control period, daily averages of PAHs, 302PAHs, NPAHs and OPAHs were 22.1, 4.6, 0.8 and 1.0  $\text{ng}/\text{m}^3$ , respectively. Significant reductions in BC (45%), OC (31%), molecular weight (MW)  $< 300$  PAH (26% - 73%), MW 302 PAH (22% - 77%), NPAH (15% - 68%) and OPAH (25% - 53%) concentrations were measured during the source control period.

The 2-nitrofluoranthene (2-NF)/1-nitropyrene (1-NP) and 2-NF/2-nitropyrene (2-NP) in the Beijing PM suggested a predominance of photochemical formation of NPAHs through OH-radical initiated reaction in the atmosphere. The correlations of PAH and derivative concentrations, and gas pollutants ( $\text{NO}$ ,  $\text{CO}$ ,  $\text{SO}_2$ ) were used to determine the origin of emission sources in Beijing. While PAH concentrations were associated with both local and regional emissions, the concentration of their derivatives were associated only with  $\text{NO}$ , a short-lived species, indicating that the PAH derivatives were primarily associated with local emissions. The  $\text{PM}_{2.5}$  crude extracts were tested for mutagenicity by the Salmonella mutagenicity assay using the *Salmonella typhimurium* strain TA98 with and without S9 mix. The mutagenicity data showed a small mass percent of the  $\Sigma\text{NPAH}$  and  $\Sigma\text{OPAH}$  potentially contributed to significant portion of the overall mutagenicity of

PM<sub>2.5</sub> in Beijing.

However, the PAH, NPAH, and OPAH composition of the PM<sub>2.5</sub> was similar throughout the sampling period, suggesting similar sources. For all periods, the general trend in concentration was benzo[b]fluoranthene (BbF) > benzo[e]pyrene (BaP) ~ indeno[1,2,3-cd]pyrene (IcdP) ~ benzo[ghi]perylene (BghiP) > fluoranthene (FLA) > pyrene (PYR) ~ benzo[k]fluoranthene (BkF) ~ benzo[a]pyrene (BaP) > chrysene+triphenylene (CHR+TRI) ~ benzo[a]anthracene (BaA). Regardless of pollution control measures, PAHs with 4-6 rings dominated the PAHs of PM<sub>2.5</sub>. These PAHs are primarily associated with the particulate phase, allowing them to effectively undergo long range transport.

To further understand the heterogeneous nitration of the higher molecular weight PAHs, five PAHs were tested in an indoor reaction chamber, as described in Chapter 3 of the thesis. These PAHs were deposited onto the quartz fiber filters and exposed to NO<sub>2</sub>, NO<sub>3</sub>/N<sub>2</sub>O<sub>5</sub>, O<sub>3</sub>, and OH radicals. In parallel to the laboratory experiments, a theoretical study was conducted to assist in determining the formation of NPAH isomers based on the OH-radical initiated reaction. The thermodynamic stability of the OH-PAH intermediates was used to rationalize the formation of NPAH isomers. As a consequence, the distribution of the NPAH isomers formed by heterogeneous reaction was predicted. Under the experimental conditions, exposures of NO<sub>2</sub> and NO<sub>3</sub>/N<sub>2</sub>O<sub>5</sub> effectively transformed surface-bound PAHs to NPAHs. Of the studied PAHs, the reaction of relatively lower MW PAHs, including benzo[a]pyrene-d<sub>12</sub> (BaP-d<sub>12</sub>), benzo[k]fluoranthene-d<sub>12</sub> (BkF-d<sub>12</sub>), and benzo[ghi]perylene (BghiP-d<sub>12</sub>), yielded more than one mono-nitro isomer product after the NO<sub>2</sub> and NO<sub>3</sub>/N<sub>2</sub>O<sub>5</sub> exposures, except for

the exposure of BghiP-d<sub>12</sub> with NO<sub>2</sub> which did not form any nitro products. Dinitro isomers were only detected after the exposure of surface-bound BkF-d<sub>12</sub> to NO<sub>3</sub>/N<sub>2</sub>O<sub>5</sub>. In contrast, only one mono-nitro isomer product was observed from the heterogeneous nitration of dibenzo[a,i]pyrene (DaiP-d<sub>14</sub>) and dibenzo[a,l]pyrene (DalP) with NO<sub>3</sub> and NO<sub>3</sub>/N<sub>2</sub>O<sub>5</sub>. These results may be because the differences in free energy between the first and second most favorable OH-PAH adducts of the higher MW PAHs were larger. The estimated percent of NPAH product formation relative to the amount of unexposed parent PAH suggested that BaP-d<sub>12</sub> was most readily nitrated in comparison to the other PAHs. Among the various exposures, the percent NPAH product formation was highest for the NO<sub>2</sub> exposure.

Changes in the indirect- and direct-acting mutagenicity, using the Salmonella assay with and without S9, of the PAHs deposited on filters were determined with and without photochemical reaction. Corresponding to the di-NO<sub>2</sub>-BkF-d<sub>11</sub> formation, the direct-acting mutagenicity sharply increased after the NO<sub>3</sub>/N<sub>2</sub>O<sub>5</sub> exposure, suggesting strong mutagenic potency of the di-NO<sub>2</sub>-BkF-d<sub>11</sub> isomers. The changes in direct-acting mutagenicity of higher MW PAH-exposed extracts were not as high as those of the lower MW PAHs. This may be because of the structures of the nitro PAH products, 5-NO<sub>2</sub>-DaiP-d<sub>14</sub> and 6-NO<sub>2</sub>-DalP, which contain a nitro group that is nearly perpendicular to the aromatic moiety. Such NO<sub>2</sub> group orientation was previously shown to reduce the mutagenic potency in the Salmonella assay testing. Because the deuterated parent PAHs were used in this study, except DalP, deuterium isotope effect was expected to underestimate the mutagenic activities of the exposed extracts, containing deuterated nitro PAH products.



Chamber experiments were also carried out to study the transformation of PM-bound PAHs under simulated atmospheric transport and are described in Chapter 4 of the thesis. Beijing, China and Riverside, California PM were exposed to various oxidants including  $\text{NO}_3/\text{N}_2\text{O}_5$ , OH radicals, and  $\text{O}_3$ . While Beijing has strong local emission sources, Riverside, a downwind receptor site of Los Angeles, receives photochemically-aged air masses in addition to local emissions.

The chemical study showed that  $\text{O}_3$  was more effective in degrading Beijing PM-bound PAHs with more than four rings compared to OH radicals and  $\text{NO}_3/\text{N}_2\text{O}_5$ , except for BaP which was degraded equally by  $\text{O}_3$  and  $\text{NO}_3/\text{N}_2\text{O}_5$ . Excluding BaP which was reactive in all exposures, the other PAHs with more than four rings were degraded to a similar extent during the OH radical exposure. Heterogeneous nitration only occurred significantly after  $\text{NO}_3/\text{N}_2\text{O}_5$  exposure. Multiple nitro-products, including 9-nitrophenanthrene (9-NPH), 3-nitrofluoranthene (3-NF), 7-nitrobenzo[a]anthracene (7-NBaA), 1-nitrotriphenylene (1-NTR), 6-nitrochrysene (6-NCH), 2-nitrotriphenylene (2-NTR), and 1,8-dinitropyrene (1,8-DNP), were only formed during the  $\text{NO}_3/\text{N}_2\text{O}_5$  exposure, while 1-nitropyrene (1-NP) and 6-nitrobenzo[a]pyrene (6-NBaP) were formed in both  $\text{NO}_3/\text{N}_2\text{O}_5$  and OH radical exposures. The dominant nitro PAH isomers formed by the exposure of PM-bound PAHs to  $\text{NO}_3/\text{N}_2\text{O}_5$  were consistent with previous studies on the heterogeneous nitration by  $\text{N}_2\text{O}_5$ , indicating that  $\text{N}_2\text{O}_5$  was likely responsible for the nitro PAH product formation in the reaction study. Besides the formation of 1-NP and 6-NBaP, no other NPAHs were formed during OH radical exposure. Substantial degradation of 9-nitroanthracene (9-NAN) and 7-NBaA was observed after the OH radical exposure and was likely due to direct photolysis. Exposure of the Beijing PM to

O<sub>3</sub> did not lead to significant NPAH formation but NPAH degradation was measured during the chemical and mutagenicity studies.

The effect of photochemical aging of the PM on the reactivity of the PM in the chamber was investigated using the ratio of 2-NF, which is primarily formed by reaction with OH radicals- and NO<sub>3</sub> radicals-initiated reactions, to benzo[e]pyrene (BeP), a relatively stable PAH. The higher percent reactivity of PAHs on the Beijing PM compared to the Riverside PM exposed to NO<sub>3</sub>/N<sub>2</sub>O<sub>5</sub> was attributed to the filters with lower 2-NF/BeP ratios. In addition, the exposure of the Riverside PM, which had relatively higher 2-NF/BeP ratio than Beijing PM, to NO<sub>3</sub>/N<sub>2</sub>O<sub>5</sub> did not result in significant NPAH formation, or almost zero percent reactivity. This indicated that higher degree of photochemical degradation the ambient PM had undergone, resulting in the reduced availability of parent PAHs for further oxidation, prior to sampling affected the reactivity of PAHs in the chamber. Riverside sampling site is located downwind of Los Angeles and Riverside receives photochemically aged air masses from this major source region.

Freshly-emitted PM is dominated by hydrophobic PAHs that more readily undergo transformation reactions that result in more hydrophilic compounds. These secondary pollutants are likely to partition into the particulate phase. A chamber study of the gas-phase reaction of phenanthrene with OH radicals found that several products, including NPAHs and OPAHs, existed primarily in the particle phase<sup>1</sup>. Adsorption/absorption into the particle phase shields the parent PAHs from further oxidation. The effect of degradation product formation was used to explain the plateau observed in the decay profiles of particle-bound PAHs<sup>2,3</sup>. Moreover, the physical state of

the organic matter on PM was also found to affect the reactivity. A recent study on the kinetics of heterogeneous reaction of BaP with O<sub>3</sub> on liquid and solid organic coatings showed that the solid coating could substantially suppress the heterogeneous reactivity of particle-bound BaP compared to the liquid coating<sup>4</sup>.

The effects of exposure of Beijing PM to NO<sub>3</sub>/N<sub>2</sub>O<sub>5</sub>, O<sub>3</sub> and OH radical on both direct- and indirect-acting mutagenicity were explored. After NO<sub>3</sub>/N<sub>2</sub>O<sub>5</sub> exposure, the direct-acting mutagenic activities increased proportionately with NPAH formation. The sharpest increase in direct-acting mutagenicity occurred when the mass of dinitropyrenes increased the most after the NO<sub>3</sub>/N<sub>2</sub>O<sub>5</sub> exposure. The indirect-acting mutagenicity of the Beijing PM increased after exposure to NO<sub>3</sub>/N<sub>2</sub>O<sub>5</sub> and OH radical, consistent with the results from Chapter 3 of the thesis. Besides some NPAHs that exhibit indirect-acting mutagenicity (e.g. 6-NBaP and 6-nitrodibenzo[a,l]pyrene), other more polar degradation products, not identified in this study, could significantly contribute to the increased indirect-acting mutagenicity. After exposure to O<sub>3</sub>, two out of three Beijing PM samples showed decreases in PAH and NPAH concentrations, and also indirect-acting mutagenicity.

The relationship between the percent reactivity of Beijing PM and the black carbon (BC) and organic carbon (OC) concentrations of Beijing PM was investigated. Although there was a general trend of decreasing percent reactivity with increasing OC or BC concentration in the Beijing PM samples after exposure to NO<sub>3</sub>/N<sub>2</sub>O<sub>5</sub> and OH radical, the correlations were not statistically significant. High concentrations of BC and OC in PM<sub>2.5</sub> may serve to protect PAHs from reacting with photochemical oxidants.

The results reported in Chapters 3 and 4 showed that  $\text{N}_2\text{O}_5$  was the most effective oxidant in transforming the surface-bound PAHs to NPAHs in the reaction chamber. However, these experimental results may not yield the same results during trans-Pacific atmospheric transport of PAHs. In the ambient environment, many reactions are occurring simultaneously including the formation of  $\text{N}_2\text{O}_5$  and competing reactions for  $\text{NO}_3$ .

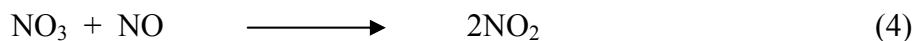
Generally,  $\text{N}_2\text{O}_5$  exists in equilibrium with  $\text{NO}_3$  and  $\text{NO}_2$ :



where M is third body molecule that takes excess energy away in order for the reaction to occur.  $\text{N}_2\text{O}_5$  is thermally unstable and hence the formation of  $\text{N}_2\text{O}_5$  increases at low temperatures. The concentration of  $\text{N}_2\text{O}_5$  is dependent on the production of  $\text{NO}_3$  and  $\text{NO}_2$ .  $\text{NO}_3$  radicals are slowly generated by



The production of  $\text{NO}_3$  is highly variable as it requires coexistence of two species<sup>5</sup>. At the same time, the  $\text{NO}_3$  removal processes, which decrease the formation of  $\text{N}_2\text{O}_5$ , are the direct photolysis of  $\text{NO}_3$  and the rapid reaction of  $\text{NO}_3$  with  $\text{NO}$ ;



Thus,  $\text{N}_2\text{O}_5$  is concentrated in polluted areas during the nighttime, when sunlight is absent and sources of  $\text{NO}$  are reduced. The nighttime average continental  $\text{NO}_3$  concentration were reported to be ~15 ppt in Hefei, China<sup>6</sup> and ~20 ppt in Riverside,

CA<sup>5</sup>. Variation of NO<sub>3</sub> concentration of several hundreds ppt have been measured in some polluted areas<sup>7</sup>. NO<sub>3</sub> and N<sub>2</sub>O<sub>5</sub> concentrations were also measured in the marine atmosphere in clean air masses. The NO<sub>3</sub> concentration was found to be as low as 1-5 ppt over west coast of Ireland<sup>8</sup> and N<sub>2</sub>O<sub>5</sub> concentrations were below the detection limit of 2 ppt near Fairbanks, Alaska<sup>9</sup>. In addition to the lack of N<sub>2</sub>O<sub>5</sub> sources over the marine boundary layer, the uptake coefficient of N<sub>2</sub>O<sub>5</sub> for continent aerosols was at least 10 times smaller than that for sea-salt particles. Moreover, the N<sub>2</sub>O<sub>5</sub> formation reaction has to compete with a reaction between NO<sub>3</sub> and dimethylsulfide, which has been reported to account for 80% of NO<sub>3</sub> removal processes<sup>8</sup>. A more recent study of the reactive uptake of NO<sub>3</sub>, N<sub>2</sub>O<sub>5</sub>, NO<sub>2</sub>, HNO<sub>3</sub> and O<sub>3</sub> on PAH surfaces suggested that heterogeneous formation of NPAHs via reaction with N<sub>2</sub>O<sub>5</sub> was not important due to the extremely small reactive uptake coefficient<sup>10</sup>. In the same study, the reaction of NO<sub>3</sub> radicals with PAHs coated on glass surface yielded a much larger reactive uptake coefficient, however, the study did not include product identification. Consequently, air masses over the ocean are not likely to form N<sub>2</sub>O<sub>5</sub> that will subsequently react with PAHs during trans-Pacific transport. However, it is possible that NPAHs that are formed near major source regions in Asia, such as Beijing, undergo trans-Pacific transport.

The fate of PM-bound PAHs would be mainly governed by transformation occurring near emission sources. As shown in Chapter 2, there was a significantly positive correlation between NPAH and OPAH concentrations of Beijing PM and NO concentrations. This implied that PAH and NPAH degradation and formation occurs predominantly near emission sources where the concentrations of gaseous oxidants are sufficiently high. Similar to N<sub>2</sub>O<sub>5</sub> reaction, NO<sub>2</sub>, NO<sub>3</sub> radical, and OH radical reactions

would be less important over the marine boundary layer due to a lack of sources. Nitrogen oxide emissions are primarily associated with anthropogenic sources and oceans are not a significant source<sup>11</sup>. On the other hand, the production of OH radicals is dependent on photolysis of O<sub>3</sub> and the presence of water vapor which exhibits a strong vertical gradient<sup>12</sup>. At higher altitudes, OH radical concentrations are expected to be lower and therefore, PAH degradation via reaction with OH radical should decrease. As a result, after PM undergoes atmospheric transport away from emission sources, the photochemistry and reaction with O<sub>3</sub> would become more important degradation pathways for PAHs adsorbed on PM during the trans-Pacific transport. O<sub>3</sub> concentrations have been shown to be enhanced during the trans-Pacific transport events. At the top of Mt. Bachelor (2763 m above sea level) in Oregon, USA, the average O<sub>3</sub> concentrations were 40 ppb and 54 ppb when the site received regional airflow and Asian outflow, respectively<sup>12</sup>. In the same study, the highest hourly average of O<sub>3</sub> concentration was 78 ppb. Higher O<sub>3</sub> concentration (exceeding 100 ppb) has been reported in another Asian long range transport campaign using a small aircraft<sup>13</sup>. This implies that the results from our O<sub>3</sub> chamber exposure, in which the concentration was equivalent to exposing the PM to an average ambient O<sub>3</sub> concentration of 40 ppb for 8 days, could be realistic given that the O<sub>3</sub> concentration is fairly substantial in remote areas.

A number of studies were carried out to investigate the atmospheric degradation of particle-associated PAH derivatives as a function of sunlight<sup>14-18</sup> and ozone<sup>3, 19, 20</sup>, using single component substrate or combustion-derived soot. Results showed that photodegradation was likely to be the dominant degradation pathway of particle NPAHs<sup>21</sup>. Photodegradation studies of NPAHs dissolved in organic solvents<sup>15, 22-24</sup> and

deposited on particles<sup>17, 18, 21, 23</sup> have also been conducted and showed the main breakdown products included hydroxy, quinone, nitrohydroxy and dihydroxy compounds<sup>18, 21-23</sup>.

Two major factors affecting the effectiveness of NPAH degradation are the orientation of NO<sub>2</sub> group and the particle composition. The NPAH containing a perpendicular NO<sub>2</sub> group readily undergoes nitro-nitrite rearrangement upon irradiation<sup>25</sup>, making it more susceptible to photochemistry. The particle constituents were found to either suppress or accelerate the degradation processes. The photochemical reaction of 1-nitropyrene could be suppressed by the highly carbonaceous fraction of particles<sup>14</sup>, while certain methoxyphenols and OPAHs, present abundantly in wood combustion soot, were found to accelerate PAH and NPAH photodegradation<sup>15, 24, 26-28</sup>. For OPAHs, only the compounds with an  $n\pi^*$  excited triplet state, for example anthraquinone and 9,10-phenanthrenedione, were capable of accelerating the photolytic process, in organic solution, through production of radical species. Fan et al. suggested the significance of these factors were dependent on the physical properties of media; in solution, the compound structure is the dominant factor while on PM, the chemical components have more effect on photodegradation<sup>21</sup>. However, the experimental results showed that NPAHs were generally less reactive relatively to their parent PAHs<sup>3, 14, 20, 29, 30</sup>.

In contrast to NPAHs, degradation of OPAHs has been less studied and there was experimental variation between different OPAHs. Grosjean et al. did not observe significant loss of anthraquinone from the 24-hour exposure with ~10 ppm of O<sub>3</sub><sup>31</sup>. Similarly, benzanthrone was relatively stable toward ozone reaction (0.16 to 0.25 ppm) in the dark<sup>32</sup>. Cope and Kalkwolf exposed pyrenequinones to O<sub>3</sub> at 0.16 ppm and found that

in the presence of light the reaction rate was about 15 times the rate constant for the dark reaction<sup>33</sup>. Also, cyclopenta[def]phenanthrene, benzanthrone, OH-fluorenone, and anthraldehyde were found to be stable at mid-day and in low ozone concentration (<0.06 ppm)<sup>32</sup>. However, a half-life of 80 to 200 min was determined for benzo[a]fluoranthene (BaF), BkF, BaP and BghiP exposed to sunlight and 0.2 ppm of ozone<sup>32</sup>. As mentioned above, the photostability of OPAHs is, in part, dependent on the electronic configuration of the excited triplet, attributing to the ability to abstract hydrogen. Nonetheless, the fact that OPAHs can be dynamically formed and degraded upon photoreaction makes it challenging to model the atmospheric fate of OPAHs during long range atmospheric transport.

Next steps for this research should include the measurement of OPAHs formed by the heterogeneous reaction of PM-bound PAHs with the respect to oxidants, along with the associated mutagenicity. In addition, field measurements of NPAHs and OPAHs at Mt. Bachelor Observatory during spring, when the trans-Pacific transport events occur, will allow us to determine which NPAH and OPAH undergo trans-Pacific transport. Combined, these data will help us understand if trans-Pacific atmospheric transport results in an increase in the concentrations of mutagenic NPAHs and OPAHs in the Western U.S.



## REFERENCES

1. Lee, J.; Lane, D. A., Formation of oxidized products from the reaction of gaseous phenanthrene with the OH radical in a reaction chamber. *Atmos. Environ.* **2010**, *44* (20), 2469-2477.
2. Pöschl, U., Formation and decomposition of hazardous chemical components contained in atmospheric aerosol particles. *Journal of aerosol medicine* **2002**, *15* (2), 203-212.
3. Miet, K.; Le Menach, K.; Flaud, P. M.; Budzinski, H.; Villenave, E., Heterogeneous reactions of ozone with pyrene, 1-hydroxypyrene and 1-nitropyrene adsorbed on particles. *Atmos. Environ.* **2009**, *43* (24), 3699-3707.
4. Zhou, S.; Lee, A.; McWhinney, R.; Abbatt, J., Burial Effects of Organic Coatings on the Heterogeneous Reactivity of Particle-Borne Benzo [a] pyrene (BaP) toward Ozone. *The Journal of Physical Chemistry A* **2012**, *116* (26), 7050-7056.
5. Atkinson, R.; Arey, J., Mechanisms of the gas-phase reactions of aromatic hydrocarbons and PAHs with OH and NO<sub>3</sub> radicals. *Polycyclic Aromat. Compd.* **2007**, *27* (1), 15-40.
6. Li, S.; Liu, W.; Xie, P.; Li, A.; Qin, M.; Peng, F.; Zhu, Y., Observation of the nighttime nitrate radical in Hefei, China. *Journal of Environmental Sciences* **2008**, *20* (1), 45-49.
7. Penkett, S. A.; Burgess, R. A.; Coe, H.; Coll, I.; Hov, Å.; Lindskog, A.; Schmidbauer, N.; Solberg, S.; Roemer, M.; Thijsse, T.; Beck, J.; Reeves, C. E., Evidence for large average concentrations of the nitrate radical (NO<sub>3</sub>) in Western Europe from the HANSA hydrocarbon database. *Atmos. Environ.* **2007**, *41* (16), 3465-3478.
8. Allan, B. J.; McFiggans, G.; Plane, J. M. C.; Coe, H.; McFadyen, G. G., The nitrate radical in the remote marine boundary layer. *Journal of geophysical research* **2000**, *105* (D19), 24191-24,204.
9. Ayers, J. D.; Simpson, W. R., Measurements of N<sub>2</sub>O<sub>5</sub> near Fairbanks, Alaska. *Journal of geophysical research* **2006**, *111* (D14), D14309.
10. Gross, S.; Bertram, A. K., Reactive uptake of NO<sub>3</sub>, N<sub>2</sub>O<sub>5</sub>, NO<sub>2</sub>, HNO<sub>3</sub>, and O<sub>3</sub> on three types of polycyclic aromatic hydrocarbon surfaces. *The Journal of Physical Chemistry A* **2008**, *112* (14), 3104-3113.
11. Finlayson-Pitts, B. J.; Pitts Jr, J. N., *Chemistry of the upper and lower atmosphere*. 1st ed.; Academic Press: San Diego, 2000.
12. Weiss-Penzias, P.; Jaffe, D. A.; Swartzendruber, P.; Dennison, J. B.; Chand, D.; Hafner, W.; Prestbo, E., Observations of Asian air pollution in the free troposphere at Mount Bachelor Observatory during the spring of 2004. *Journal of Geophysical Research* **2006**, *111* (D10), D10304.
13. Bertschi, I. T.; Jaffe, D. A., Long-range transport of ozone, carbon monoxide, and aerosols to the NE Pacific troposphere during the summer of 2003: Observations of smoke plumes from Asian boreal fires. *J. Geophys. Res.* **2005**, *110* (D5), D05303.
14. Holder, P. S.; Wehry, E. L.; Mamantov, G., Photochemical Transformation of 1-Nitropyrene Sorbed on Coal Fly Ash Fractions. *Polycyclic Aromat. Compd.* **1994**, *4* (3), 135-139.

15. Feilberg, A.; Nielsen, T., Effect of aerosol chemical composition on the photodegradation of nitro-polycyclic aromatic hydrocarbons. *Environ. Sci. Technol.* **2000**, *34* (5), 789-797.
16. Feilberg, A.; Ohura, T.; Nielsen, T.; Poulsen, M. W. B.; Amagai, T., Occurrence and photostability of 3-nitrobenzanthrone associated with atmospheric particles. *Atmos. Environ.* **2002**, *36* (22), 3591-3600.
17. Fan, Z.; Chen, D.; Birla, P.; Kamens, R. M., Modeling of nitro-polycyclic aromatic hydrocarbon formation and decay in the atmosphere. *Atmos. Environ.* **1995**, *29* (10), 1171-1181.
18. Benson, J. M.; Brooks, A. L.; Cheng, Y. S.; Henderson, T. R.; White, J. E., Environmental transformation of 1-nitropyrene on glass surfaces. *Atmospheric Environment (1967)* **1985**, *19* (7), 1169-1174.
19. Kwamena, N.-O. A.; Earp, M. E.; Young, C. J.; Abbatt, J. P. D., Kinetic and Product Yield Study of the Heterogeneous Gas-Surface Reaction of Anthracene and Ozone. *The Journal of Physical Chemistry A* **2006**, *110* (10), 3638-3646.
20. Fan, Z.; Kamens, R. M.; Zhang, J.; Hu, J., Ozone-Nitrogen Dioxide-NPAH Heterogeneous Soot Particle Reactions and Modeling NPAH in the Atmosphere. *Environ. Sci. Technol.* **1996**, *30* (9), 2821-2827.
21. Fan, Z.; Kamens, R. M.; Hu, J.; Zhang, J.; McDow, S., Photostability of Nitro-Polycyclic Aromatic Hydrocarbons on Combustion Soot Particles in Sunlight. *Environ. Sci. Technol.* **1996**, *30* (4), 1358-1364.
22. Arce, R.; Pino, E. F.; Valle, C.; Algreja, J., Photophysics and Photochemistry of 1-nitropyrene. *The Journal of Physical Chemistry A* **2008**, *112* (41), 10294-10304.
23. Holloway, M. P.; Biaglow, M. C.; McCoy, E. C.; Anders, M.; Rosenkranz, H. S.; Howard, P. C., Photochemical instability of 1-nitropyrene, 3-nitrofluoranthene, 1,8-dinitropyrene and their parent polycyclic aromatic hydrocarbons. *Mutation Research/Genetic Toxicology* **1987**, *187* (4), 199-207.
24. McDow, S. R.; Sun, Q.; Vartiainen, M.; Hong, Y.; Yao, Y.; Fister, T.; Yao, R.; Kamens, R. M., Effect of composition and state of organic components on polycyclic aromatic hydrocarbon decay in atmospheric aerosols. *Environ. Sci. Technol.* **1994**, *28* (12), 2147-2153.
25. Chapman, O.; Heckert, D.; Reasoner, J.; Thackaberry, S., Photochemical Studies on 9-Nitroanthracene. *J. Am. Chem. Soc.* **1966**, *88* (23), 5550-5554.
26. Jang, M.; McDow, S. R., Benz [a] anthracene photodegradation in the presence of known organic constituents of atmospheric aerosols. *Environ. Sci. Technol.* **1995**, *29* (10), 2654-2660.
27. Odum, J. R.; McDow, S. R.; Kamens, R. M., Mechanistic and kinetic studies of the photodegradation of benz [a] anthracene in the presence of methoxyphenols. *Environ. Sci. Technol.* **1994**, *28* (7), 1285-1290.
28. Feilberg, A.; Nielsen, T., Photodegradation of nitro-PAHs in viscous organic media used as models of organic aerosols. *Environ. Sci. Technol.* **2001**, *35* (1), 108-113.
29. Miet, K.; Le Menach, K.; Flaud, P. M.; Budzinski, H.; Villenave, E., Heterogeneous reactivity of pyrene and 1-nitropyrene with NO<sub>2</sub>: Kinetics, product yields and mechanism. *Atmos. Environ.* **2009**, *43* (4), 837-843.

30. Kamens, R. M.; Guo, J.; Guo, Z.; McDow, S. R., Polynuclear aromatic hydrocarbon degradation by heterogeneous reactions with N<sub>2</sub>O<sub>5</sub> on atmospheric particles. *Atmospheric Environment. Part A. General Topics* **1990**, *24* (5), 1161-1173.
31. Grosjean, D.; Whitmore, P. M.; De Moor, C. P.; Cass, G. R.; Druzik, J. R., Fading of alizarin and related artists' pigments by atmospheric ozone: Reaction products and mechanisms. *Environ. Sci. Technol.* **1987**, *21* (7), 635-643.
32. Kamens, R. M.; Karam, H.; Guo, J.; Perry, J. M.; Stockburger, L., The behavior of oxygenated polycyclic aromatic hydrocarbons on atmospheric soot particles. *Environ. Sci. Technol.* **1989**, *23* (7), 801-806.
33. Cope, V. W.; Kalkwarf, D. R., Photooxidation of selected polycyclic aromatic hydrocarbons and pyrenequinones coated on glass surfaces. *Environ. Sci. Technol.* **1987**, *21* (7), 643-648.

**APPENDIX A**

**Appendix A.1:** PAHs, NPAHs, OPAHs classified by the IARC monographs. Group 1 indicates “Carcinogenic to humans”, Group 2A indicates “Probably carcinogenic to humans”, Group 2B = “Possibly carcinogenic to humans”, Group 3 indicates “Not classifiable as to its carcinogenicity to humans”.

PAH	Group	Reference <sup>a</sup>
<b><u>Mutagenic</u></b>		
Naphthalene	2B	82
Benzo[c]phenanthrene	2B	92
Benzo[a]anthracene	2B	3, 32, 92
Chrysene	2B	92
5-Methylchrysene	2B	32, 92
Benzo[j]aceanthrylene	2B	92
Benzo[b]fluoranthene	2B	3, 32, 92
Benzo[j]fluoranthene	2B	3, 32, 92
Benzo[k]fluoranthene	2B	32, 92
Cyclopenta[cd]pyrene	2A	92
Benzo[a]pyrene	1	3, 92, 100F
Dibenz[a,h]anthracene	2A	3, 32, 92
Indeno[1,2,3-cd]pyrene	2B	3, 32, 92
Dibenzo[a,h]pyrene	2B	3, 32, 92
Dibenzo[a,i]pyrene	2B	3, 32, 92
Dibenzo[a,l]pyrene	2A	92
5-Nitroacenaphthene	2B	16
2-Nitrofluorene	2B	46, 105
1-Nitropyrene	2A	46, 105
4-Nitropyrene	2B	46, 105
1,3-Dinitropyrene	2B	46, 105
1,6-Dinitropyrene	2B	46, 105
1,8-Dinitropyrene	2B	46, 105
3,7-Dinitrofluoranthene	2B	65, 105
3,9-Dinitrofluoranthene	2B	65, 105
6-Nitrochrysene	2A	46, 105
3-Nitrobenzanthrone	2B	105
Anthraquinone	2B	101
2-Methyl-1-nitroanthraquinone	2B	27
<b><u>Non-Mutagenic (Group 3)</u></b>		
Acenaphthene		92
Fluorene		32, 92
Anthracene		32, 92
Phenanthrene		32, 92

**Appendix A.1 (continued)**

<b>PAH</b>	<b>Group</b>	<b>Reference<sup>a</sup></b>
1-Methylphenanthrene		32, 92
1,4-Dimethylphenanthrene		92
Fluoranthene		32
2-Methylfluoranthene		92
3-Methylfluoranthene		32, 92
Pyrene		32, 92
Triphenylene		32, 92
1-, 2-, 3-, 4-, and 6-Methylchrysenes		32, 92
Benzo[a]fluorene		32, 92
Benzo[b]fluorene		32, 92
Benzo[c]fluorene		32, 92
11H-benz[bc]aceanthrylene		92
Acepyrene		92
Benzo[a]fluoranthene		92
Benzo[ghi]fluoranthene		32, 92
13H-Dibenzo[a,g]fluorene		92
4H-cyclopenta[def]chrysene		92
5,6-Cyclopenteno-1,2-benzanthracene		92
Perylene		32, 92
Picene		92
Benzo[e]pyrene		3, 32, 92
Benzo[b]chrysene		92
Dibenz[a,c]anthracene		32, 92
Dibenz[a,j]anthracene		32, 92
Benzo[g]chrysene		92
Dibenzo[a,e]fluoranthene		32, 92
Naphthol[2,1]fluoranthene		92
Anthanthrene		32, 92
Benzo[ghi]perylene		32, 92
Dibenzo[e,l]pyrene		92
Dibenzo[a,e]pyrene		92
Naphthol[1,2-a]fluoranthene		92
Naphthol[1,2-b]fluoranthene		92
Naphthol[2,3-e]pyrene		92
Coronene		32
Dibenzo(h,rst)pentaphene		3, 92
1-Nitronaphthalene		46
2-Nitronaphthalene		46
4-nitrobiphenyl		3

**Appendix A.1 (continued)**

<b>PAH</b>	<b>Group</b>	<b>Reference<sup>a</sup></b>
9-nitroanthracene		33
3-nitrofluoranthene		33
2-nitropyrene		46
6-Nitrobenzo(a)pyrene		46
7-Nitrobenz(a)anthracene		46
3-Nitroperylene		46

<sup>a</sup>International Agency for Research on Cancer Monograph Vol.3 (1973), Vol.16(1987), Vol 27 (1987)Vol. 32 (1983), Vol.33(1984), 46 (1989), 65 (1996), 82 (2002), 92 (2010), 100F (2012), 101 (in prep), and 105 (in prep).

**APPENDIX B**



### Appendix B.1: MW 302 PAH Analysis

The identification and quantification of 15 MW 302 PAHs (N23aP, N23eP, N12bF, DBaeF, DBbkF, DBelP, DBakF, DBjIF, N23jF, N23bF, N23kF, BbPer, DBaiP, DBaeP, DBalP, DBahP and coronene (MW 300) was based on authentic standards. The identification of 7 other MW 302 isomers (DBbeF, N12eP, N12aP, N21aP, and three unknown isomers) was based on the comparison with their mass spectra and retention indices of the same isomers in NIST SRM 1597 by Schubert et al.<sup>1</sup> because there were no commercially available standards (Appendix B.2). We used the retention index (RI) method introduced by Lee et al.<sup>2</sup> and Bemgård et al.<sup>3</sup> which uses PAHs with an increasing number of aromatic rings as retention markers to calculate the RIs of an unknown chemical based on the following equation:

$$RI = 100 \frac{T_{R(unk)} - T_{R(C_z)}}{T_{R(C_{z+1})} - T_{R(C_z)}} + 100Z$$

Where  $T_{R(unk)}$  is the retention time of the unknown,  $T_{R(C_z)}$  and  $T_{R(C_{z+1})}$  are the retention times of the PAH retention markers which bracket the unknown's retention time, and  $Z$  is the number of rings in the PAH that elutes just prior to the unknown. Picene and coronene were used as retention markers for MW 302 PAHs and reference RI values were assigned based on Schubert et al.<sup>1</sup>.

Quantification of the MW 302 PAHs was based on the relative response ratio of the deuterated surrogate to the analyte standard with a nine point calibration curve (R-square > 0.99). For the quantification of known MW 302 isomers without commercially available standards (DBbeF, N12eP, N12aP, and N21aP) and unknown MW 302 isomers, a response factor of 1.01 relative to N23eP was used because of the similar response

among the MW 302 isomers (errors <5%)<sup>1</sup>.

The average recovery of the benzo[ghi]perylene-d<sub>12</sub> was 82%, with a standard deviation of 10%. The detection limits of individual MW 302 PAHs and coronene ranged from 3.4 to 33.3 pg/μL and all MW 302 PAHs were below the detection limit in the six field blanks. For method validation, the NIST coal tar extract SRM 1597a was measured and the concentrations of 15 MW 302 PAH isomers and coronene were within 30% of both the certified and reference values (Appendix B.2).

**Appendix B.2:** Retention time (RT) and retention index (RI) of MW 302 PAHs measured in a standard and SRM 1597a.

Compound	Peak No. <sup>a</sup>	Abbreviation	This Study				Schubert et al.(1)	
			RT of Standards (min)	Measured RT in SRM1597a (min)	Calculated RI of Standards	Calculated RI in SRM 1597a	RI of Reference Standards	RI in SRM 1597a
<i>Retention markers</i>								
Picene (MW=278)	-		71.76	71.68	500.0	500.0	500	500
Coronene (MW=300)	Cor	Cor	106.93	106.85	532.9	532.6	532.9	532.6
<i>MW 302 isomers</i>								
Naphtho[1,2-b]fluoranthene	3	N12bF	92.13	92.11	519.1	518.9	519.1	518.9
Naphtho[2,3-j]fluoranthene/Naphtho[1,2-k]fluoranthene	4	N23jF/N12kF	93.2	92.85	520.1	519.6	520	519.8
Naphtho[2,3-b]fluoranthene	5	N23bF	93.93	93.82	520.7	520.5	520.6	520.5
Dibenzo[a,e]fluoranthene/Dibenzo[b,k]fluoranthene	6	DBaeF/DBbkF	94.45	94.4	521.2	521.1	521.1	521.1
Dibenzo[a,k]fluoranthene	7	DBakF	95.18	95.1	521.9	521.7	521.9	521.7
Dibenzo[j,l]fluoranthene	8	DBjIF	96.13	95.99	522.8	522.5	522.6	522.5
Dibenzo[a,l]pyrene	10	DBalP	97.08	96.96	523.7	523.4	523.5	523.5
Naphtho[2,3-k]fluoranthene	12	N23kF	98.6	98.52	525.1	524.9	525	524.9
Naphtho[2,3-e]pyrene	15	N23eP	102.32	102.21	528.6	528.3	528.5	528.3
Dibenzo[a,e]pyrene	16	DBaeP	105.8	105.72	531.8	531.6	531.8	531.5
Dibenzo[e,l]pyrene	18	DBelP	108.58	108.46	534.4	534.1	534.1	531.4
Naphtho[2,3-a]pyrene	19	N23aP	109.55	109.44	535.4	535.0	535.1	535
Benzo[b]perylene	20	BbPer	110.65	110.6	536.4	536.1	536.2	536.1
Dibenzo[a,i]pyrene	21	DBaiP	111.41	111.27	537.1	536.7	536.9	536.7
Dibenzo[a,h]pyrene	22	DBahP	114.77	114.63	540.2	539.8	540.1	539.8
Dibenzo[b,e]fluoranthene*	1	DBbeF	-	89.4	-	516.4	516.5	516.5
Unknown peak 1*	2	U1	-	90.44	-	517.4		517.5
Naphtho[1,2-e]pyrene*	9	N12eP	-	96.35	-	522.9	522.8	522.9
Unknown peak2*	11	U2	-	97.6	-	524.0		524.1
Naphtho[1,2-a]pyrene*	13	N12aP	-	99.1	-	525.4	525.3	525.4
Unknown peak3*	14	U3	-	100.11	-	526.4		526.4
Naphtho[2,1-a]pyrene*	17	N21aP	-	108.01	-	533.7	533.9	533.7

\* Isomers without standards but identified according to Schubert et al.<sup>1</sup>

<sup>a</sup> Peak numbers based on elution order on DB-17MS

**Appendix B.3:** Concentrations of MW 302 PAH isomers and coronene (MW 300) in SRM 1597a (coal tar extract) (mg/kg)

	NIST <sup>a</sup>	This Study (n=3)	Schubert et al.(1) (n=3)
DBbkF	11.2 ± 0.8	11.19 ± 0.19	11.4 ± 0.3
DBaeP	9.08 ± 0.39	7.65 ± 0.13	8.82 ± 0.4
DBahP	2.57 ± 0.3	3.19 ± 0.09	2.72 ± 0.07
Cor	8.7 ± 1.8	7.51 ± 0.24	8.39 ± 0.38
N12bF	8.6 ± 2.0	10.79 ± 0.26	10.4 ± 0.2
N12kF/N23jF <sup>b</sup>	10.7 ± 1.2	13.14 ± 0.18	11.0 ± 0.3
N23bF	3.52 ± 0.30	2.64 ± 0.08	3.11 ± 0.06
DBakF	3.21 ± 0.31	2.34 ± 0.05	3.27 ± 0.07
DBjlF	6.5 ± 1.4	5.82 ± 0.16	7.72 ± 0.23
DBalP	1.12 ± 0.17	1.10 ± 0.10	1.21 ± 0.03
N23eP	4.31 ± 0.44	4.84 ± 0.16	4.32 ± 0.12
DBelP	2.72 ± 0.17	3.26 ± 0.27	2.76 ± 0.20
N23aP	4.29 ± 0.89	4.83 ± 0.15	5.58 ± 0.17
BbPer	9.04 ± 0.99	9.75 ± 0.23	9.65 ± 0.33
N23kF	2.07 ± 0.06	2.26 ± 0.25	2.11 ± 0.02
DBaiP	3.87 ± 0.34	4.97 ± 0.03	4.28 ± 0.13

<sup>a</sup> DBbkF, DBaeP, and DBahP are NIST certified concentrations, all others are NIST reference concentrations.

<sup>b</sup> N12kF and N23jF co-eluted. The NIST concentration was based on the identification of N12kF, while in this study and Schubert et al.<sup>1</sup> it was based on both compounds.

**Appendix B.4: NPAH and OPAH Analysis and Method Validation**

The DB-5 column GC oven temperature program was 60°C for 1 min, ramped at 40°C/min to 150 °C (held 5 min), ramped at 4°C/min to 300 °C (held for 15 min), for a total run time of 60.75 min, while the DB-17 column oven temperature program was 50°C for 1 min, ramped at 45°C/min to 150 °C (held 10 min), ramped at 5°C/min to 300 °C (held 15 min), for a total runtime of 58.22 min. The programmed temperature vaporization (PTV) inlet temperature program was 40 °C, ramped at 600 °C/min to 350 °C. The selected ion monitoring programs are given in Appendix B.5.

The NPAH and OPAH recoveries over the entire analytical method were determined in triplicate. A known concentration of the NPAHs and OPAHs were spiked onto blank filters prior to extraction and the isotopically labeled surrogates were spiked into the extract following silica solid phase extraction. Using the difference between the spiked concentration and the measured concentration, the recovery of the analyte was calculated and is shown in Appendix B.5. Excluding BENZ, the mean recovery was 84.4%, with an average relative standard deviation (%RSD) of 4.9%. The percent recoveries ranged from 51.1% of 1-NN to 105.0% of 2-MANQ. The low recovery of 1-NN was likely due to its relatively high vapor pressure and loss due to volatilization during extract concentration by evaporation. In addition, the low BENZ recovery is due to its elution in both the DCM and ethyl acetate fractions of the silica solid phase extraction.

The limit of quantitation (LOQ) was defined as a signal-to-noise ratio of 10:1. Measured concentrations were only reported when the concentration was greater than the LOQ, unless specified otherwise. The estimated detection limits (EDLs) are reported in Appendix B.5 and were defined as a signal-to-noise ratio of 3:1 in the sample matrix. The EDLs are reported in Appendix B.5 to allow comparison to

previous NPAH and OPAH methods. However, the LOQs were used to report the NPAH and OPAH concentrations in this study.

**Appendix B.5:** Selected ion monitoring (SIM), quantitation, method recovery and estimated detection limit [EDL] for OPAH and NPAH measured by Electron Capture Ionization GC/MS.

Compound	Abbrev.	Retention Time DB-5	Retention Time DB-17	Quantitation Ion (m/z)	Confirmation Ion (m/z)	Quantitation Compound	% Recovery	% RSD	EDL (pg/ $\mu$ L)
<b>SIM Window 1</b>									
d7-1-Nitronaphthalene		9.19	17.71	180.20	181.20	Surrogate	102.9%	1.9%	-
1-Nitronaphthalene	1-NN	9.25	17.85	173.10	174.10	d7-Nitronaphthalene	51.1%	17.1%	0.93
2-Nitronaphthalene	2-NN	10.26	18.99	173.10	174.10	d7-Nitronaphthalene	53.6%	14.7%	0.70
d9-2-Nitrobiphenyl		11.18	20.48	208.30	209.20	Internal Standard	100.0%	0.0%	-
9-Fluorenone	9-FLU	12.50	21.80	180.10	181.10	d7-Nitronaphthalene	58.4%	10.5%	2.57
3-Nitrobiphenyl	3-NBP	14.64	23.63	199.10	200.10	d7-Nitronaphthalene	65.8%	6.1%	1.68
<b>SIM Window 2</b>									
9,10-Anthraquinone	ANQ	18.26	28.33	208.10	209.10	d7-Nitronaphthalene	85.7%	9.2%	92.43
3-Nitrodibenzofuran	3-NDF	18.63	27.89	213.10	214.10	d7-Nitronaphthalene	79.5%	3.4%	9.43
d9-5-Nitroacenaphthene		18.86	28.91	208.20	209.20	Surrogate	103.9%	2.3%	-
5-Nitroacenaphthene	5-NAC	19.03	29.11	199.10	200.10	d9-Nitroacenaphthene	77.1%	3.5%	0.10
<b>SIM Window 3</b>									
d9-2-Nitrofluorene		21.27	30.89	220.20	221.20	Internal Standard	100%	0%	-
2-Methylanthraquinone	2-MANQ	21.44	30.83	222.10	223.10	d9-5-Nitroacenaphthene	101.6%	14.1%	14.00
d9-9-Nitroanthracene		21.86	31.61	232.20	233.20	Surrogate	105.3%	1.1%	-
9-Nitroanthracene	9-NAN	21.95	31.71	223.10	224.10	d9-9-Nitroanthracene	78.3%	2.8%	3.83
3-Nitrophenanthrene	3-NPH	24.76	34.02	223.10	224.10	d9-9-Nitroanthracene	87.4%	1.1%	1.08
<b>SIM Window 4</b>									
Benanthrone	BENZ	29.61	39.02	230.20	231.10	d9-9-Nitroanthracene	16.9%	31.7%	11.64
d9-3-Nitrofluoranthene		30.54	39.40	256.10	257.30	Surrogate	105.3%	0.8%	-
2-Nitrofluoranthene	2-NF	30.60	39.04	247.10	248.20	d9-3-Nitrofluoranthene	98.8%	1.4%	14.29
Benz[a]anthracene-7,12-dione	BaAD	31.48	40.18	258.10	259.10	d9-3-Nitrofluoranthene	92.3%	1.5%	8.00
d9-1-Nitropyrene		31.59	40.64	256.20	257.20	Surrogate	104.4%	0.5%	-
1-Nitropyrene	1-NP	31.65	40.72	247.10	248.10	d9-1-Nitropyrene	93.9%	1.6%	3.14

**Appendix A.5 (continued):**

Analyte	Abbrev.	Retention Time DB-5	Retention Time DB-17	Quantitation Ion (m/z)	Confirmation Ion (m/z)	Quantitation Compound	% Recovery	% RSD	EDL (pg/ $\mu$ L)
<b>SIM Window 4</b>									
2-Nitropyrene	2-NP	32.09	41.00	247.10	248.10	d9-1-Nitropyrene	94.1%	1.0%	28.47
7-Nitrobenz[a]anthracene	7-NBaA	35.22	43.26	273.10	274.20	d9-1-Nitropyrene	95.2%	0.4%	20.81
d11-6-Nitrochrysene		36.69	44.71	284.20	285.10	Surrogate	104.6%	1.1%	-



**Appendix B.6:** Parent PAH, NPAH, OPAH, OC, and BC concentration during source control and non-source control periods, t-test results, and the reduction in concentration (pg/m<sup>3</sup>) (\*: p<0.05).

	Source control Period (n=46)			Non-Source control Period (n=17)			T-test (p_value)	Reduction	
	Mean (± sd)	Min.	Max.	Mean (± sd)	Min.	Max.		Conc.	(%)
<b><i>MW&lt;300 PAHs</i></b>									
Naphthalene	22.3±8.3	10.3	43.5	32.4±13.3	9.8	47.6	<b>0.013*</b>	10.1	31.2%
2-Methylnaphthalene	31.6±9.5	16.7	63.1	43.1±16.1	15.1	70.2	<b>0.018*</b>	11.5	26.6%
1-Methylnaphthalene	21.4±5.9	11.8	40.4	22.4±7.5	9.4	34.6	0.611	1.0	4.4%
2,6-Dimethylnaphthalene	16.0±3.9	9.0	29.5	17.5±6.6	7.5	27.9	0.397	1.6	9.0%
1,3-Dimethylnaphthalene	23.5±6.5	12.8	45.8	24.1±7.9	11.0	35.2	0.769	0.6	2.5%
Acenaphthylene	13.7±4.6	6.8	26.5	29.0±15.1	11.4	58.0	<b>&lt;0.001*</b>	15.4	53.0%
Fluorene	28.7±10.7	13.9	59.1	50.4±21.1	16.8	85.9	<b>&lt;0.001*</b>	21.8	43.2%
Dibenzothiophene	20.5±7.8	3.6	42.3	43.0±22.3	14.1	87.6	<b>&lt;0.001*</b>	22.5	52.3%
Phenanthrene	259.6±83.5	143.4	515.5	536.1±275.4	150.9	1007.6	<b>0.002*</b>	276.5	51.6%
Anthracene	44.3±33.3	13.7	175.1	69.5±30.9	22.2	121.1	<b>0.014*</b>	25.2	36.3%
2-Methylphenanthrene	92.9±30.7	49.6	187.5	154.8±67.6	50.8	262.1	<b>0.003*</b>	62.0	40.0%
2-Methylanthracene	19.4±8.0	7.7	57.5	31.5±12.2	11.1	50.2	<b>0.002*</b>	12.1	38.3%
1-Methylphenanthrene	51.2±19.4	25.6	113.3	94.7±40.5	25.0	165.4	<b>&lt;0.001*</b>	43.6	46.0%
3,6-Dimethylphenanthrene	8.0±2.0	3.2	13.5	11.4±4.0	4.1	19.5	<b>0.006*</b>	3.3	29.3%
Fluoranthene	854.7±294.2	347.1	1552.1	1549.6±798.8	299.3	2931.5	<b>0.005*</b>	694.9	44.8%
Pyrene	578.7±187.1	255.1	1002.5	1065.5±536.2	185.5	1965.0	<b>0.004*</b>	486.9	45.7%
Retene	69.0±19.6	18.8	119.2	138.0±66.4	31.6	252.5	<b>&lt;0.001*</b>	68.9	50.0%
1-Methylpyrene	66.5±18.7	36.8	102.8	113.7±48.0	22.7	190.9	<b>0.002*</b>	47.2	41.5%
Benz(a)anthracene	374.2±140.5	175.8	800.3	956.5±565.2	220.3	1915.1	<b>&lt;0.001*</b>	582.2	60.9%

## Appendix B.6 (continued)

	Source control Period (n=46)			Non-Source control Period (n=17)			T-test (p_value)	Reduction	
	Mean ( $\pm$ sd)	Min.	Max.	Mean ( $\pm$ sd)	Min.	Max.		Conc.	(%)
Chrysene + Triphenylene	379.6 $\pm$ 169.1	134.3	789.8	1106.9 $\pm$ 747.1	201.4	2520.2	<b>0.002*</b>	727.3	65.7%
6-Methylchrysene	49.3 $\pm$ 21.5	19.3	110.5	118.1 $\pm$ 62.5	28.9	223.0	<b>&lt;0.001*</b>	68.8	58.3%
Benzo(b)fluoranthene	2224.7 $\pm$ 1057.9	980.8	4784.9	4658.2 $\pm$ 2960.1	1002.2	11019.3	<b>0.007*</b>	2433.5	52.2%
Benzo(k)fluoranthene	569.7 $\pm$ 276.4	252.5	1388.5	2582.9 $\pm$ 3152.7	261.1	9780.2	<b>0.027*</b>	2013.2	77.9%
Benzo(e)pyrene	1162.8 $\pm$ 526.9	507.5	2421.5	2286.9 $\pm$ 1411.7	489.1	5096.9	<b>0.009*</b>	1124.1	49.2%
Benzo(a)pyrene	708.9 $\pm$ 367.3	297.6	1874.7	1659.4 $\pm$ 1028.7	397.9	3834.1	<b>0.003*</b>	950.4	57.3%
Indeno(1,2,3-cd)pyrene	1322.6 $\pm$ 607.2	609.9	3051.7	2161.7 $\pm$ 1249.5	587.1	4772.3	<b>0.024*</b>	839.0	38.8%
Dibenz(a,h)anthracene	210.3 $\pm$ 83.0	103.4	439.0	334.0 $\pm$ 180.7	96.4	704.4	<b>0.021*</b>	123.6	37.0%
Benzo(ghi)perylene	1320.4 $\pm$ 623.0	588.6	3025.6	2180.8 $\pm$ 1244.6	579.1	4773.2	<b>0.02*</b>	860.4	39.5%
$\Sigma$ PAH <sub>2ring</sub>	177.1 $\pm$ 39.2	111.7	286.8	262.0 $\pm$ 92.8	114.2	394.8	<b>0.003*</b>	84.9	32.4%
$\Sigma$ PAH <sub>3ring</sub>	1399.1 $\pm$ 428.4	682.8	2525.7	2585.6 $\pm$ 1259.2	595.0	4681.3	<b>0.003*</b>	1186.5	45.9%
$\Sigma$ PAH <sub>4ring</sub>	4242.6 $\pm$ 1766.1	1911.5	8715.6	10601.7 $\pm$ 7720.6	1922.0	27582.4	<b>0.007*</b>	6359.1	60.0%
$\Sigma$ PAH <sub>56ring</sub>	4725.1 $\pm$ 2183.7	2155.9	10812.4	8622.6 $\pm$ 5022.4	2172.9	19180.9	<b>0.01*</b>	3897.6	45.2%
$\Sigma$ PAH <sub>16-US Priority</sub> (ng/m <sup>3</sup> )	8.9 $\pm$ 3.6	4.3	18.5	19.0 $\pm$ 12.2	4.1	45.5	<b>0.007*</b>	10.1	53.2%
$\Sigma$ PAH <sub>28</sub> (ng/m <sup>3</sup> )	10.5 $\pm$ 4.2	5.1	21.6	22.1 $\pm$ 13.9	4.9	51.8	<b>0.006*</b>	11.6	52.5%
BaP-TEQ <sup>a</sup> (ng/m <sup>3</sup> )	1.4 $\pm$ 0.7	0.7	3.4	3.1 $\pm$ 2.0	0.7	7.4	<b>&lt;0.001*</b>	1.7	54.7%
<b><i>MW 302 PAHs</i></b>									
N12bF	408.4 $\pm$ 152.6	184.4	733.2	546.0 $\pm$ 281.6	174.9	1097.1	<b>0.011*</b>	137.6	25%
N23jF/N[12k]F	412.7 $\pm$ 138.6	205.5	726.9	531.0 $\pm$ 242.2	199.1	991.4	<b>0.013*</b>	118.4	22%
DBaeF/DBbkF	352.0 $\pm$ 132.4	169.5	638.4	483.0 $\pm$ 239.6	160.1	956.6	<b>0.006*</b>	131.0	27%

## Appendix B.6 (continued)

	Source control Period (n=46)			Non-Source control Period (n=17)			T-test (p_value)	Reduction	
	Mean ( $\pm$ sd)	Min.	Max.	Mean ( $\pm$ sd)	Min.	Max.		Conc.	(%)
DBakF	32.4 $\pm$ 13.8	13.2	70.2	56.1 $\pm$ 28.2	17.5	122.3	<0.001*	21.0	37%
DBjlF	221.2 $\pm$ 88.9	102.8	423.9	312.3 $\pm$ 162.7	96.5	638.2	0.005*	91.1	29%
DBalP	30.5 $\pm$ 11.1	BDL	54.8	48.6 $\pm$ 19.4	23.7	94.9	<0.001*	18.1	37%
N23bF	118.7 $\pm$ 51.4	44.3	235.3	173.3 $\pm$ 87.6	53.3	341.9	0.003*	54.5	31%
N23kF	41.1 $\pm$ 20.8	BDL	87.9	69.5 $\pm$ 37.5	19.9	152.7	<0.001*	28.4	41%
N23eP	144.8 $\pm$ 60.5	66.6	287.9	197.5 $\pm$ 98.6	62.2	394.4	0.010*	52.6	27%
DBaeP	171.5 $\pm$ 68.5	86.6	316.9	255.0 $\pm$ 128.0	75.7	523.8	0.001*	83.6	33%
DBelP	326.0 $\pm$ 122.3	140.8	571.7	441.8 $\pm$ 238.3	128.6	924.2	0.010*	115.8	26%
N23aP	9.5 $\pm$ 13.9	BDL	49.4	40.4 $\pm$ 36.8	BDL	116.6	<0.001*	30.9	77%
BbPer	73.7 $\pm$ 40.3	18.5	171.8	145.8 $\pm$ 78.3	30.1	309.5	<0.001*	72.2	49%
DBaiP	58.9 $\pm$ 30.2	BDL	124.2	110.7 $\pm$ 58.3	26.5	244.8	<0.001*	51.8	47%
DBahP	5.9 $\pm$ 8.2	BDL	31.6	24.8 $\pm$ 19.9	BDL	64.6	<0.001*	18.8	76%
DBbeF*	64.2 $\pm$ 24.6	29.1	116.4	95.3 $\pm$ 50.7	24.8	184.3	0.002*	31.1	33%
U1*	97.6 $\pm$ 38.8	46.6	184.2	147.4 $\pm$ 79.6	39.1	292.6	0.001*	49.8	34%
N12eP*	83.5 $\pm$ 34.7	38.6	171.0	114.9 $\pm$ 61.8	28.5	217.1	0.010*	31.4	27%
U2*	176.8 $\pm$ 70.7	75.5	340.1	257.8 $\pm$ 139.2	67.5	513.6	0.003*	81.0	31%
N12aP*	69.7 $\pm$ 32.3	31.7	158.1	120.9 $\pm$ 64.0	31.3	255.5	<0.001*	51.2	42%
U3*	19.2 $\pm$ 9.9	BDL	45.1	36.0 $\pm$ 18.7	BDL	76.8	<0.001*	16.8	47%
N21aP*	256.0 $\pm$ 116.3	113.5	540.5	440.6 $\pm$ 232.3	118.5	921.2	<0.001*	184.6	42%
$\Sigma$ DBP	266.9 $\pm$ 108.7	88.6	500.9	439.1 $\pm$ 217.4	125.9	928.1	<0.001*	172.2	39%
$\Sigma$ 302PAH (ng/m3)	3.2 $\pm$ 1.2	1.6	5.9	4.6 $\pm$ 2.3	1.4	9.4	<0.001*	1.4	32%

## Appendix B.6 (continued)

	Source control Period (n=46)			Non-Source control Period (n=17)			T-test (p_value)	Reduction	
	Mean ( $\pm$ sd)	Min.	Max.	Mean ( $\pm$ sd)	Min.	Max.		Conc.	(%)
$\Sigma$ 302PAH <sub>mut</sub> (ng/m3)	2.0 $\pm$ 0.8	1.0	3.6	2.9 $\pm$ 1.4	0.9	5.9	<b>0.001*</b>	0.9	31%
<b><i>NPAHs</i></b>									
1-nitronaphthalene	5.8 $\pm$ 3.1	2.1	16.0	4.7 $\pm$ 1.6	2.9	8.5	0.952	-1.1	-24.5%
2-nitronaphthalene	3.2 $\pm$ 0.5	1.8	4.1	3.8 $\pm$ 0.5	3.3	4.8	<b>0.010*</b>	0.6	15.1%
3-nitrobiphenyl	2.5 $\pm$ 0.0	2.5	2.5	3.4 $\pm$ 0.7	2.6	4.4	n/a	0.9	27.6%
3-nitrobenzofuran	9.8 $\pm$ 0.0	9.8	9.8	12.4 $\pm$ 5.6	4.7	19.7	n/a	2.6	20.7%
5-nitroacenaphthene	3.6 $\pm$ 1.0	2.8	5.0	4.8 $\pm$ 2.4	2.8	9.0	0.170	1.1	24.1%
9-nitroanthracene	173.1 $\pm$ 133.5	21.7	543.9	247.4 $\pm$ 144.3	57.4	489.6	<b>0.047*</b>	74.4	30.1%
3-nitrophenanthrene	7.1 $\pm$ 4.0	2.5	17.7	9.0 $\pm$ 4.1	2.8	15.2	0.089	1.9	21.0%
2-nitrofluoranthene	145.9 $\pm$ 108.7	30.6	433.4	336.3 $\pm$ 295.4	25.1	1,015.9	<b>0.014*</b>	190.4	56.6%
1-nitropyrene	8.3 $\pm$ 0.7	7.8	8.8	10.2 $\pm$ 1.5	7.4	11.9	<b>0.029*</b>	1.9	18.4%
2-nitropyrene	44.9 $\pm$ 18.7	19.2	88.8	80.7 $\pm$ 40.0	23.1	152.8	<b>0.006*</b>	35.8	44.4%
7-nitrobenz[a]anthracene	78.9 $\pm$ 70.1	11.4	267.6	115.3 $\pm$ 87.3	17.4	314.2	0.085	36.4	31.6%
$\Sigma$ NPAH	421.3 $\pm$ 306.8	68.1	1,288.6	792.1 $\pm$ 552.4	135.8	1,721.1	<b>0.012*</b>	370.8	46.8%
<b><i>OPAHs</i></b>									
9-fluorenone	68.8 $\pm$ 30.3	1.9	122.5	128.8 $\pm$ 53.3	33.1	219.6	<b>&lt;0.001*</b>	60.0	46.6%
9,10-anthraquinone	267.5 $\pm$ 90.1	75.1	476.1	355.7 $\pm$ 105.2	96.7	503.8	<b>0.004*</b>	88.2	24.8%
2-methyl-9,10-anthraquinone	120.8 $\pm$ 49.2	45.9	240.2	236.6 $\pm$ 264.8	36.3	1174.0	0.057	115.8	49.0%
Benzanthrone	31.5 $\pm$ 31.3	5.3	112.5	30.6 $\pm$ 24.5	11.5	73.2	0.527	-0.9	-3.0%
Benz[a]anthracene-7,12-dione	221.6 $\pm$ 104.4	79.7	436.7	301.0 $\pm$ 186.6	79.8	549.1	0.068	79.3	26.4%
$\Sigma$ OPAH	694.9 $\pm$ 250.1	205.3	1,241.1	1,032.3 $\pm$ 466.9	245.9	2,198.1	<b>0.008*</b>	337.4	32.7%

**Appendix B.6 (continued)**

	Source control Period (n=46)			Non-Source control Period (n=17)			T-test (p_value)	Reduction	
	Mean ( $\pm$ sd)	Min.	Max.	Mean ( $\pm$ sd)	Min.	Max.		Conc.	(%)
PM <sub>2.5</sub> ( $\mu\text{g}/\text{m}^3$ )	81.3 $\pm$ 43.2	28.2	205.9	97.2 $\pm$ 59.8	28.7	214.4	0.277	15.9	16.4%
OC ( $\mu\text{g}/\text{m}^3$ )	9.9 $\pm$ 2.9	4.9	16.3	14.4 $\pm$ 7.5	4.9	25.6	<b>0.038*</b>	4.5	31.1%
BC ( $\mu\text{g}/\text{m}^3$ )	1.7 $\pm$ 0.7	0.7	3.7	3.1 $\pm$ 1.7	0.8	6.4	<b>0.008*</b>	1.4	45.5%
OC/BC	6.2 $\pm$ 1.2	3.9	9.3	4.9 $\pm$ 0.9	3.9	6.9	<b>&lt;0.001*</b>	-1.3	-26.9%
OC/(OC+BC)	85.8 $\pm$ 2.4%	79.5%	90.3%	82.8 $\pm$ 2.3%	79.5%	87.3%	<b>&lt;0.001*</b>	-3.0%	-3.7%
2-NF/1-NP	38.7 $\pm$ 15.2			46.1 $\pm$ 23.7			<b>0.001*</b>		16%
2-NF/2-NP	4.5 $\pm$ 1.9			4.7 $\pm$ 1.8			0.073		5%

<sup>a</sup>: Including Naphthalene, Acenaphthylene, Fluorene, Phenanthrene, Anthracene, Fluoranthene, Pyrene, Benz(a)anthracene, Chrysene, Benzo(b)fluoranthene, Benzo(k)fluoranthene, Benzo(a)pyrene, Indeno(1,2,3-cd)pyrene, Dibenz(a,h)anthracene, Benzo(ghi)perylene for BaP<sub>-TEQ</sub> calculation.

**Appendix B.7:** Parent PAH, NPAH, OPAH, OC, and BC concentration during Olympic and non-Olympic periods, t-test results, and the reduction in concentration (pg/m<sup>3</sup>) (\*: p<0.05).

	Olympic Period (n=17)			Non-Olympic Period (n=46)			T-test (p_value)	Reduction	
	Mean (± sd)	Min.	Max.	Mean (± sd)	Min.	Max.		Con.	(%)
<i>MW&lt;300 PAHs</i>									
Naphthalene	20.9±8.4	10.3	43.5	26.6±11.2	9.8	47.6	0.071	5.7	21.5%
2-Methylnaphthalene	33.0±9.8	21.7	63.1	35.4±13.6	15.1	70.2	0.452	2.5	7.0%
1-Methylnaphthalene	21.9±6.0	13.9	40.4	21.6±6.5	9.4	34.6	0.887	-0.3	-1.2%
2,6-Dimethylnaphthalene	16.3±4.2	10.5	29.5	16.4±5.0	7.5	27.9	0.937	0.1	0.7%
1,3-Dimethylnaphthalene	24.5±7.1	14.4	45.8	23.4±6.8	11.0	35.2	0.595	-1.1	-4.6%
Acenaphthylene	11.2±2.3	6.8	15.8	20.4±12.0	6.8	58.0	<0.001*	9.2	45.0%
Fluorene	23.6±6.7	13.9	45.0	38.9±18.0	16.8	85.9	<0.001*	15.3	39.4%
Dibenzothiophene	14.7±5.6	3.6	25.8	31.1±17.1	14.1	87.6	<0.001*	16.4	52.7%
Phenanthrene	208.3±54.8	143.4	367.4	383.8±213.8	150.9	1007.6	<0.001*	175.5	45.7%
Anthracene	50.6±50.5	13.7	175.1	51.2±26.1	20.9	121.1	0.961	0.7	1.3%
2-Methylphenanthrene	74.5±19.3	49.6	120.6	123.4±53.3	50.8	262.1	<0.001*	48.9	39.6%
2-Methylantracene	16.5±4.5	7.7	25.6	25.2±11.5	11.1	57.5	<0.001*	8.7	34.6%
1-Methylphenanthrene	39.7±9.3	25.6	57.5	72.1±34.2	25.0	165.4	<0.001*	32.4	45.0%
3,6-Dimethylphenanthrene	7.1±2.2	3.2	13.5	9.6±3.1	4.1	19.5	0.004*	2.5	26.0%
Fluoranthene	666.0±173.3	347.1	1009.6	1190.7±601.3	299.3	2931.5	<0.001*	524.7	44.1%
Pyrene	470.9±109.7	255.1	680.9	804.4±410.6	185.5	1965.0	<0.001*	333.5	41.5%
Retene	63.5±20.9	18.8	112.2	97.1±53.1	31.6	252.5	<0.001*	33.6	34.6%
1-Methylpyrene	56.2±11.4	36.8	73.7	88.3±38.2	22.7	190.9	<0.001*	32.1	36.3%
Benz(a)anthracene	284±55.2	175.8	372.4	628.7±440.9	203.7	1915.1	<0.001*	344.7	54.8%

### Appendix B.7 (continued)

	Olympic Period (n=17)			Non-Olympic Period (n=46)			T-test (p_value)	Reduction	
	Mean ( $\pm$ sd)	Min.	Max.	Mean ( $\pm$ sd)	Min.	Max.		Con.	(%)
Chrysene + Triphenylene	260.8 $\pm$ 63.3	134.3	396.4	699.8 $\pm$ 566.2	189.5	2520.2	<0.001*	439.0	62.7%
6-Methylchrysene	35.3 $\pm$ 8.0	19.3	48.0	80.7 $\pm$ 50.8	24.6	223.0	<0.001*	45.4	56.2%
Benzo(b)fluoranthene	1482.4 $\pm$ 420.5	980.8	2492.9	3434.2 $\pm$ 2185.5	1002.2	11019.3	<0.001*	1951.8	56.8%
Benzo(k)fluoranthene	386.4 $\pm$ 120.2	252.5	674.1	1398 $\pm$ 2117.1	261.1	9780.2	0.005*	1011.6	72.4%
Benzo(e)pyrene	784.3 $\pm$ 220.4	507.5	1319.2	1735.7 $\pm$ 1035.4	489.1	5096.9	<0.001*	951.4	54.8%
Benzo(a)pyrene	459.6 $\pm$ 133.8	297.6	742.1	1165.1 $\pm$ 787.3	374.1	3834.1	<0.001*	705.5	60.6%
Indeno(1,2,3-cd)pyrene	930.7 $\pm$ 239.9	609.9	1469.5	1794.0 $\pm$ 946.7	587.1	4772.3	<0.001*	863.3	48.1%
Dibenz(a,h)anthracene	157.0 $\pm$ 40.5	103.4	254.1	278.0 $\pm$ 134.8	96.4	704.4	<0.001*	121.0	43.5%
Benzo(ghi)perylene	915.6 $\pm$ 249.2	588.6	1481.8	1805 $\pm$ 952.3	579.1	4773.2	<0.001*	889.4	49.3%
$\Sigma$ PAH <sub>2ring</sub>	165.0 $\pm$ 38.8	111.7	286.8	213.8 $\pm$ 73.6	112.7	394.8	0.002*	48.8	22.8%
$\Sigma$ PAH <sub>3ring</sub>	1126.2 $\pm$ 281.4	682.8	1738.1	1953.2 $\pm$ 960.7	595.0	4681.3	<0.001*	827.0	42.3%
$\Sigma$ PAH <sub>4ring</sub>	2975.9 $\pm$ 638.5	1911.5	4264.5	7134 $\pm$ 5546.2	1922.0	27582.4	<0.001*	4158.1	58.3%
$\Sigma$ PAH <sub>5ring</sub>	3247.2 $\pm$ 851.3	2155.9	5266.6	6777.8 $\pm$ 3780.5	2172.9	19180.9	<0.001*	3530.6	52.1%
$\Sigma$ PAH <sub>16-US Priority</sub> (ng/m <sup>3</sup> )	6.3 $\pm$ 1.3	4.3	9.0	13.7 $\pm$ 8.9	4.1	45.5	<0.001*	7.4	54.0%
$\Sigma$ PAH <sub>28</sub> (ng/m <sup>3</sup> )	7.5 $\pm$ 1.6	5.1	10.8	16.1 $\pm$ 10.1	4.9	51.8	<0.001*	8.6	53.4%
BaP- <sub>TEQ</sub> <sup>a</sup> (ng/m <sup>3</sup> )	0.9 $\pm$ 0.2	0.7	1.5	2.2 $\pm$ 1.5	0.7	7.4	<0.001*	1.3	57.3%
<b>MW 302 PAHs</b>									
N12bF	296.4 $\pm$ 64.6	184.4	417.3	504.8 $\pm$ 208.2	174.9	1097.1	<0.001*	208.5	41%

## Appendix B.7 (continued)

	Olympic Period (n=17)			Non-Olympic Period (n=46)			T-test (p_value)	Reduction	
	Mean ( $\pm$ sd)	Min.	Max.	Mean ( $\pm$ sd)	Min.	Max.		Con.	(%)
N23jF/N[12k]F	311.0 $\pm$ 62.3	205.5	425.0	497.7 $\pm$ 181.6	199.1	991.4	< <b>0.001</b> *	186.7	38%
N23bF	86.2 $\pm$ 23.8	52.8	137.4	152.2 $\pm$ 69.3	44.3	341.9	< <b>0.001</b> *	66.1	43%
DBaeF/DBbkF	261.1 $\pm$ 60.3	169.5	374.3	437.5 $\pm$ 181.4	160.1	956.6	< <b>0.001</b> *	176.4	40%
DBakF	25.7 $\pm$ 6.4	13.2	38.2	46.7 $\pm$ 21.5	17.5	122.3	< <b>0.001</b> *	21.0	45%
DBjIF	160.8 $\pm$ 35.7	102.8	234.6	279.5 $\pm$ 123.7	96.5	638.2	< <b>0.001</b> *	118.8	42%
DBalP	26.5 $\pm$ 8.1	BDL	39.2	38.9 $\pm$ 16.8	BDL	94.9	<b>0.003</b> *	12.4	32%
N23kF	30.2 $\pm$ 10.3	12.4	50.6	56.1 $\pm$ 30.7	BDL	152.7	<b>0.001</b> *	25.9	46%
N23eP	103.2 $\pm$ 27.0	66.6	159.0	181.2 $\pm$ 77.2	62.2	394.4	< <b>0.001</b> *	78.0	43%
DBaeP	123.8 $\pm$ 28.8	86.6	179.6	221.9 $\pm$ 97.6	75.7	523.8	< <b>0.001</b> *	98.1	44%
DBelP	233.9 $\pm$ 56.4	140.8	314.7	406.3 $\pm$ 172.0	128.6	924.2	< <b>0.001</b> *	172.3	42%
N23aP	8.4 $\pm$ 11.0	BDL	30.2	21.5 $\pm$ 29.3	BDL	116.6	<b>0.044</b> *	13.1	61%
BbPer	52.5 $\pm$ 22.4	18.5	91.1	109.2 $\pm$ 64.7	21.6	309.5	<b>0.001</b> *	56.7	52%
DBaiP	44.4 $\pm$ 17.2	15.9	73.5	84.1 $\pm$ 48.3	BDL	244.8	<b>0.001</b> *	39.7	47%
DBahP	4.5 $\pm$ 5.8	BDL	16.2	13.6 $\pm$ 16.5	BDL	64.6	<b>0.019</b> *	9.1	67%
DBbeF*	46.2 $\pm$ 9.6	29.1	63.8	83.0 $\pm$ 37.2	24.8	184.3	< <b>0.001</b> *	36.8	44%
U1*	70.2 $\pm$ 13.6	46.6	93.3	127.2 $\pm$ 59.1	39.1	292.6	< <b>0.001</b> *	57.0	45%
N12eP*	59.2 $\pm$ 11.7	38.6	79.9	105.0 $\pm$ 47.1	28.5	217.1	< <b>0.001</b> *	45.8	44%
U2*	126.0 $\pm$ 28.1	75.5	178.1	227.5 $\pm$ 103.0	67.5	513.6	< <b>0.001</b> *	101.5	45%
N12aP*	48.5 $\pm$ 13.3	31.7	76.6	97.4 $\pm$ 50.1	31.3	255.5	< <b>0.001</b> *	48.8	50%
U3*	13.2 $\pm$ 4.8	BDL	22.6	27.9 $\pm$ 15.3	BDL	76.8	< <b>0.001</b> *	14.7	53%
N21aP*	178.0 $\pm$ 49.9	113.5	279.8	356.4 $\pm$ 180.4	118.5	921.2	< <b>0.001</b> *	178.4	50%



### Appendix B.7 (continued)

	Olympic Period (n=17)			Non-Olympic Period (n=46)			T-test (p_value)	Reduction	
	Mean ( $\pm$ sd)	Min.	Max.	Mean ( $\pm$ sd)	Min.	Max.		Con.	(%)
$\Sigma$ DBP	199.2 $\pm$ 50.3	130.6	301.8	358.5 $\pm$ 170.3	88.6	928.1	<0.001*	159.3	44%
$\Sigma$ 302PAH (ng/m3)	2.3 $\pm$ 0.5	1.6	3.3	4.1 $\pm$ 1.7	1.4	9.4	<0.001*	1.8	43%
$\Sigma$ 302PAHmut a(ng/m3)	1.5 $\pm$ 0.3	1.0	2.1	2.5 $\pm$ 1.1	0.9	5.9	<0.001*	1.0	43%
<b><i>NPAHs</i></b>									
1-nitronaphthalene	5.4 $\pm$ 3.7	2.2	16.0	5.5 $\pm$ 2.4	2.1	12.9	0.466	0.1	1.7%
2-nitronaphthalene	2.6 $\pm$ 0.5	1.8	3.0	3.6 $\pm$ 0.4	2.7	4.8	<b>0.002*</b>	1.0	28.0%
3-nitrobiphenyl	1.7 <sup>b</sup>	-	-	3.3 $\pm$ 0.7	2.5	4.4	n/a	3.3	57.6%
3-nitrodibenzofuran	9.4 <sup>b</sup>	-	-	12.0 $\pm$ 5.2	4.7	19.7	n/a	12.0	34.2%
5-nitroacenaphthene	1.0 <sup>b</sup>	-	-	4.3 $\pm$ 2.0	2.8	9.0	n/a	2.0	81.4%
9-nitroanthracene	130.6 $\pm$ 113.2	21.7	414.0	217.9 $\pm$ 142.0	51.4	543.9	<b>0.011*</b>	87.4	40.1%
3-nitrophenanthrene	4.7 $\pm$ 2.1	2.5	10.0	8.7 $\pm$ 4.2	2.8	17.7	<0.001*	4.0	45.7%
2-nitrofluoranthene	78.0 $\pm$ 34.7	30.6	152.5	244.4 $\pm$ 212.3	25.1	1,015.9	<0.001*	166.4	68.1%
1-nitropyrene	3.1 <sup>b</sup>	-	-	9.8 $\pm$ 1.5	7.4	11.9	n/a	9.8	73.4%
2-nitropyrene	31.3 $\pm$ 11.1	19.2	45.5	62 $\pm$ 32.5	22.4	152.8	<0.001*	30.7	49.5%
7-nitrobenz[a]anthracene	45.4 $\pm$ 46.8	11.4	153.0	109.6 $\pm$ 79.8	12.4	314.2	<0.001*	64.2	58.5%
$\Sigma$ NPAH	270.0 $\pm$ 192.1	68.1	761.3	620.8 $\pm$ 441.0	94.7	1,721.1	<0.001*	350.8	56.5%

**Appendix B.7 (continued)**

	Olympic Period (n=17)			Non-Olympic Period (n=46)			T-test (p_value)	Reduction	
	Mean ( $\pm$ sd)	Min.	Max.	Mean ( $\pm$ sd)	Min.	Max.		Con.	(%)
<b>OPAHs</b>									
9-fluorenone	50.1 $\pm$ 29.5	3.1	122.5	98.8 $\pm$ 44.2	1.9	219.6	<0.001*	48.6	49.2%
9,10-anthraquinone	206.4 $\pm$ 82.2	75.1	365.5	325.0 $\pm$ 88.1	96.7	503.8	<0.001*	118.6	36.5%
2-methyl-9,10-anthraquinone	14.7 $\pm$ 5.6	3.6	25.8	31.1 $\pm$ 17.1	14.1	87.6	<0.001*	16.4	52.7%
Benzanthrone	91.9 $\pm$ 41.9	45.9	204.5	175.8 $\pm$ 169.4	36.3	1,174.0	0.003	83.9	47.7%
Benz[a]anthracene-7,12-dione	142.3 $\pm$ 53.2	79.7	279.7	283.1 $\pm$ 136.2	79.8	549.1	<0.001*	140.8	49.7%
$\Sigma$ OPAH	504.6 $\pm$ 195.4	205.3	882.1	897.5 $\pm$ 338.4	245.9	2,198.1	<0.001*	392.9	43.8%
PM <sub>2.5</sub> ( $\mu$ g/m <sup>3</sup> )	64.7 $\pm$ 36.3	28.2	147.4	93.9 $\pm$ 50.2	28.7	214.4	0.039*	29.2	31.1%
OC ( $\mu$ g/m <sup>3</sup> )	8.4 $\pm$ 2.0	4.9	12.1	12.2 $\pm$ 5.3	4.9	25.6	<0.001*	3.8	31.5%
BC ( $\mu$ g/m <sup>3</sup> )	1.3 $\pm$ 0.4	0.7	1.9	2.4 $\pm$ 1.3	0.8	6.4	<0.001*	1.1	44.8%
OC/BC	6.7 $\pm$ 1.3	4.5	9.3	5.6 $\pm$ 1.1	3.9	7.8	0.003*	-1.1	-20.0%
OC/(OC+BC)	86.58% $\pm$ 2.42%	81.85%	90.33%	84.32% $\pm$ 2.62%	79.46%	88.65%	0.004*	-2.3%	-2.7%
2-NF/1-NP	25.2			44.9 $\pm$ 22.1			-		-
2-NF/2-NP	3.4 $\pm$ 1.1			4.8 $\pm$ 1.8			<0.001*		30%

<sup>a</sup>: Including Naphthalene, Acenaphthylene, Fluorene, Phenanthrene, Anthracene, Fluoranthene, Pyrene, Benz(a)anthracene, Chrysene, Benzo(b)fluoranthene, Benzo(k)fluoranthene, Benzo(a)pyrene, Indeno(1,2,3-cd)pyrene, Dibenz(a,h)anthracene, Benzo(ghi)perylene for BaP<sub>-TEQ</sub> calculation.

<sup>b</sup>: Concentrations with S/N greater than LOD but less than LOQ.

**Appendix B.8:** Comparison of mean OC and BC concentrations, OC/BC ratios, for the Beijing PM2.5 samples during the summer months. <sup>a</sup>OC/BC ratio was calculated from the published concentrations. \*\*p < 0.01.

Sampling period	OC Concentration ( $\mu\text{g}/\text{m}^3$ )		BC Concentration ( $\mu\text{g}/\text{m}^3$ )		OC/BC		R value	R <sup>2</sup>	Reference	
	Mean	SD	Mean	SD	Mean	SD				
Jul-Oct 2008	All periods	11.10	4.94	2.06	1.23	5.88	1.28	0.90**	0.89	This study
	Source control period	9.90	2.93	1.68	0.68	6.23	1.22	0.88**	0.06	
	Non source control period	14.38	7.47	3.09	1.75	4.91	0.91	0.97**	0.92	
	Olympic period	8.36	2.03	1.31	0.41	6.67	1.34	0.67**	0.49	
	Non-Olympic period	12.20	5.34	2.36	1.32	5.56	1.12	0.89**	0.40	
Jul-Sep 2008	Olympic period			2.3						Wang et al. <sup>4</sup>
	Non Olympic period			3.5						
Aug 2007				6.2						Wang et al. <sup>4</sup>
Aug 2003		19.7		6.7		3.0				Chan et al. <sup>5</sup>
Jun-Jul 2002		10.7	3.6	5.7	2.9	2.2				Dan et al. <sup>6</sup>
Summer 2002	Traffic site	11.5	3.7	5.2	2.4	2.2 <sup>a</sup>				Sun et al. <sup>7</sup>
	Industrial site	9.3	3.2	6.6	3.2	1.4 <sup>a</sup>				
	Residential site	11.2	3.8	5.9	2.6	1.9 <sup>a</sup>				
Summer 1999-2000		13.42		6.27		2.14 <sup>a</sup>				He et al. <sup>8</sup>

**Appendix B.9:** Cross-correlation matrix (r values) of individual MW<300 parent PAH, ΣPAH<sub>28</sub>, and Σ PAH<sub>16-US</sub> Priority concentrations. \* indicates p<0.05. \*\* indicates p<0.01.

	NAP	2-MNAP	1-MNAP	2,6-DMNAP	1,3-DMNAP	ACY	FLO	DBT	PHE	ANT	2-MPHE	2-MANT	1-MPHE	3,6-DMPHE	FLA	PYR
NAP	1															
2-MNAP	0.90**	1														
1-MNAP	0.75**	0.90**	1													
2,6-DMNAP	0.83**	0.91**	0.93**	1												
1,3-DMNAP	0.79**	0.90**	0.95**	0.95**	1											
ACY	0.62**	0.52**	0.30*	0.39**	0.26	1										
FLO	0.54**	0.39**	0.16	0.28*	0.17	0.90**	1									
DBT	0.31*	0.19	0.04	0.11	0.04	0.72**	0.78**	1								
PHE	0.60**	0.48**	0.25	0.35**	0.24	0.91**	0.94**	0.85**	1							
ANT	0.47**	0.40**	0.21	0.31*	0.26	0.73**	0.71**	0.51**	0.66**	1						
2-MPHE	0.56**	0.44**	0.24	0.32*	0.24	0.89**	0.93**	0.84**	0.98**	0.68**	1					
2-MANT	0.47**	0.45**	0.30**	0.34**	0.28**	0.85**	0.79**	0.61**	0.76**	0.77**	0.80**	1				
1-MPHE	0.48**	0.39**	0.18	0.24	0.16	0.90**	0.92**	0.86**	0.96**	0.72**	0.98**	0.84**	1			
3,6-DMPHE	0.47**	0.43**	0.31**	0.34*	0.29*	0.83**	0.85**	0.68**	0.84**	0.68**	0.89**	0.83**	0.88**	1		
FLA	0.42**	0.34**	0.16	0.24	0.15	0.77**	0.81**	0.83**	0.93**	0.58**	0.91**	0.66**	0.91**	0.76**	1	
PYR	0.45**	0.38**	0.20	0.28**	0.19	0.80**	0.81**	0.81**	0.93**	0.62**	0.91**	0.71**	0.92**	0.77**	0.98**	1
RET	0.54**	0.52**	0.35**	0.39**	0.33*	0.78**	0.74**	0.47**	0.75**	0.71**	0.74**	0.80**	0.77**	0.83**	0.65**	0.72**
1-MPYR	0.36**	0.32*	0.17	0.22	0.13	0.83**	0.79**	0.75**	0.85**	0.69**	0.85**	0.83**	0.90**	0.80**	0.88**	0.93**
BaA	0.49**	0.41**	0.18	0.27**	0.15	0.90**	0.84**	0.79**	0.89**	0.70**	0.86**	0.83**	0.90**	0.77**	0.85**	0.89**
CHR+TRI	0.57**	0.45**	0.21	0.33*	0.19	0.90**	0.88**	0.83**	0.95**	0.63**	0.91**	0.74**	0.91**	0.76**	0.91**	0.93**
6-MCHR	0.50**	0.37**	0.16	0.28**	0.13	0.91**	0.86**	0.76**	0.86**	0.69**	0.83**	0.81**	0.87**	0.77**	0.75**	0.79**
BbF	0.53**	0.36**	0.17	0.32*	0.14	0.88**	0.85**	0.77**	0.88**	0.62**	0.84**	0.69**	0.83**	0.73**	0.81**	0.82**
BkF	0.53**	0.40**	0.20	0.32*	0.17	0.85**	0.80**	0.75**	0.85**	0.62**	0.81**	0.69**	0.80**	0.71**	0.77**	0.80**
BeP	0.53**	0.36**	0.17	0.32*	0.15	0.88**	0.84**	0.77**	0.87**	0.62**	0.84**	0.70**	0.83**	0.73**	0.80**	0.82**
BaP	0.53**	0.39**	0.19	0.31*	0.16	0.89**	0.83**	0.77**	0.86**	0.62**	0.83**	0.78**	0.85**	0.73**	0.79**	0.82**
IcdP	0.53**	0.34*	0.18	0.35**	0.17	0.81**	0.77**	0.70**	0.79**	0.57**	0.77**	0.63**	0.75**	0.64**	0.72**	0.76**
DahA	0.50**	0.33*	0.17	0.33*	0.15	0.85**	0.81**	0.73**	0.81**	0.61**	0.80**	0.69**	0.79**	0.69**	0.73**	0.77**
BghiP	0.53**	0.33*	0.17	0.34**	0.16	0.82**	0.77**	0.70**	0.79**	0.57**	0.77**	0.63**	0.75**	0.65**	0.72**	0.75**
ΣPAH <sub>28</sub>	0.55**	0.40**	0.20	0.33*	0.17	0.90**	0.87**	0.79**	0.91**	0.65**	0.88**	0.73**	0.87**	0.76**	0.85**	0.87**
ΣPAH <sub>16-US</sub>	0.55**	0.39**	0.20	0.33*	0.17	0.90**	0.86**	0.79**	0.91**	0.65**	0.88**	0.73**	0.87**	0.75**	0.85**	0.88**

Appendix B.9 (continued)

	RET	1-MPYR	BaA	CHR+TRI	6-MCHR	BbF	BkF	BeP	BaP	IcdP	DahA	BghiP
NAP												
2-MNAP												
1-MNAP												
2,6-DMNAP												
1,3-DMNAP												
ACY												
FLO												
DBT												
PHE												
ANT												
2-MPHE												
2-MANT												
1-MPHE												
3,6-DMPHE												
FLA												
PYR												
RET	1											
1-MPYR	0.81**	1										
BaA	0.82**	0.94**	1									
CHR+TRI	0.75**	0.88**	0.96**	1								
6-MCHR	0.82**	0.88**	0.96**	0.91**	1							
BbF	0.71**	0.82**	0.90**	0.94**	0.93**	1						
BkF	0.73**	0.81**	0.91**	0.91**	0.90**	0.94**	1					
BeP	0.70**	0.82**	0.89**	0.94**	0.93**	1.00**	0.93**	1				
BaP	0.76**	0.87**	0.95**	0.94**	0.96**	0.96**	0.92**	0.96**	1			
IcdP	0.65**	0.76**	0.84**	0.88**	0.89**	0.98**	0.91**	0.98**	0.94**	1		
DahA	0.67**	0.79**	0.86**	0.88**	0.91**	0.98**	0.92**	0.98**	0.94**	0.99**	1	
BghiP	0.65**	0.76**	0.84**	0.87**	0.90**	0.98**	0.91**	0.98**	0.94**	1.00**	0.99**	1
ΣPAH <sub>28</sub>	0.75**	0.87**	0.94**	0.97**	0.94**	0.99**	0.96**	0.99**	0.97**	0.96**	0.97**	0.96**
ΣPAH <sub>16-US</sub>	0.75**	0.87**	0.94**	0.97**	0.94**	0.99**	0.96**	0.99**	0.97**	0.96**	0.97**	0.96**

**Appendix B.10:** Cross-correlation matrix (r values) of individual MW 302 PAH concentrations. All p-value < 0.01 except for correlation between N23aP and N12eP (p-value=0.03).

	N12bF	N23jF N12kF	N23bF	DBaeF DBbkF	DBakF	DBjlF	DBalP	N23kF	N23eF	DBaeP	DBelP	N23aP	BbPer	DBaiP	DBahP	DBbeF	U1	N12eP	U2	N12aP	U3	N21aP	
N12bF	1.00																						
N23jF/N12kF	1.00	1.00																					
N23bF	0.97	0.98	1.00																				
DBaeF/DBbkF	0.99	0.99	0.98	1.00																			
DBakF	0.90	0.91	0.94	0.91	1.00																		
DBjlF	0.99	0.99	0.98	1.00	0.92	1.00																	
DBalP	0.81	0.82	0.89	0.85	0.90	0.86	1.00																
N23kF	0.85	0.87	0.93	0.87	0.96	0.88	0.90	1.00															
N23eF	0.98	0.99	0.99	0.99	0.93	0.99	0.86	0.91	1.00														
DBaeP	0.97	0.98	0.98	0.98	0.96	0.99	0.89	0.92	0.98	1.00													
DBelP	0.96	0.95	0.90	0.95	0.87	0.94	0.75	0.80	0.92	0.95	1.00												
N23aP	0.40	0.43	0.52	0.44	0.72	0.45	0.65	0.75	0.48	0.56	0.44	1.00											
BbPer	0.81	0.83	0.89	0.83	0.97	0.84	0.90	0.98	0.87	0.91	0.78	0.81	1.00										
DBaiP	0.81	0.83	0.89	0.84	0.97	0.85	0.90	0.98	0.87	0.91	0.79	0.80	0.99	1.00									
DBahP	0.47	0.50	0.58	0.50	0.76	0.51	0.70	0.79	0.54	0.62	0.50	0.98	0.85	0.85	1.00								
DBbeF	0.93	0.92	0.89	0.92	0.84	0.92	0.76	0.78	0.90	0.90	0.88	0.37	0.74	0.75	0.43	1.00							
U1	0.93	0.92	0.90	0.93	0.84	0.93	0.77	0.79	0.91	0.90	0.88	0.37	0.75	0.75	0.43	1.00	1.00						
N12eP	0.93	0.92	0.89	0.92	0.81	0.92	0.74	0.75	0.91	0.88	0.85	0.29	0.70	0.70	0.35	0.98	0.99	1.00					
U2	0.94	0.94	0.91	0.94	0.85	0.94	0.76	0.80	0.92	0.91	0.90	0.38	0.76	0.77	0.44	0.99	0.99	0.98	1.00				
N12aP	0.93	0.93	0.95	0.94	0.93	0.95	0.88	0.90	0.94	0.95	0.87	0.54	0.88	0.88	0.60	0.96	0.97	0.94	0.97	1.00			
U3	0.84	0.86	0.91	0.86	0.94	0.87	0.88	0.93	0.89	0.91	0.79	0.68	0.93	0.93	0.72	0.89	0.89	0.86	0.89	0.97	1.00		
N21aP	0.92	0.92	0.94	0.93	0.93	0.93	0.86	0.91	0.93	0.94	0.87	0.57	0.88	0.89	0.63	0.96	0.96	0.93	0.97	0.99	0.97	1.00	

**Appendix B.11:** Cross-correlation matrix (r values) of individual NPAH,  $\Sigma$ NPAH, OPAH and  $\Sigma$ OPAH concentrations. \* indicates  $p < 0.05$ . \*\* indicates  $p < 0.01$ .

	1-NN	2-NN	3-NBP	3-NBF	5-NAC	9-NAN	3-NPH	2-NF	1-NP	2-NP	7-NBaA	9-FLU	ANQ	2-MANQ	BENZ	BaAD
1-NN	1															
2-NN	0.09	1														
3-NBP	-0.18	0.36	1													
3-NBF	-0.43	0.71	0.66	1												
5-NAC	0.30	0.93**	n/a	n/a	1											
9-NAN	0.64**	0.45*	0.21	0.21	0.37	1										
3-NPH	0.64**	0.55**	0.21	0.43	0.68*	0.72**	1									
2-NF	0.58**	0.70**	0.61	0.93**	0.66*	0.74**	0.88**	1								
1-NP	0.33	0.27	0.46	0.37	0.66	0.51	0.56	0.63*	1							
2-NP	0.27	0.50*	0.39	0.29	0.54	0.67**	0.70**	0.84**	0.59*	1						
7-NBaA	0.53**	0.55**	0.07	0.25	0.62	0.91**	0.78**	0.80**	0.23	0.73**	1					
$\Sigma$ NPAH	0.64**	0.59**	0.43	0.32	0.56	0.94**	0.83**	0.91**	0.66*	0.86	0.94	0.64**	0.59**	0.72**	0.31	0.84**
9-FLU	0.31*	0.56**	0.86*	0.71	0.50	0.56**	0.71**	0.63**	0.78**	0.77**	0.56**	1				
ANQ	0.34*	0.47*	0.61	0.36	0.08	0.70**	0.66**	0.51**	0.43	0.74**	0.64**	0.83**	1			
2-MANQ	0.40**	0.54**	0.07	0.25	0.09	0.80**	0.67**	0.59**	0.27	0.81**	0.72**	0.76**	0.93**	1		
BENZ	0.14	0.35	n/a	n/a	-0.40	0.25	0.32	0.32	0	0.20	0.46*	0.35	0.34	0.43*	1	
BaAD	0.52**	0.74**	0.61	0.93**	0.68*	0.76**	0.88**	0.89**	0.59**	0.84**	0.88**	0.63**	0.62	0.60	0.23	1
$\Sigma$ OPAH	0.47**	0.57**	0.32	0.61	0.62	0.82**	0.80**	0.77**	0.58*	0.87**	0.83**	0.85**	0.91**	0.91**	0.41*	0.86**

**Appendix B.12:** Cross-correlation matrix (r values) of individual MW<300 parent PAH, ΣPAH<sub>28</sub>, ΣPAH<sub>16-US</sub> Priority, NPAH, ΣNPAH, OPAH and ΣOPAH concentrations. \* indicates p<0.05. \*\* indicates p<0.01.

	1-NN	2-NN	3-NBP	3-NBF	5-NAC	9-NAN	3-NPH	2-NF	1-NP	2-NP	7-NBaA	9-FLU	ANQ	2-MANQ	BENZ	BaAD
NAP	0.37**	0.47*	0.71	0.64	0.47	0.40**	0.46**	0.48**	0.87**	0.39*	0.43**	0.42**	0.29*	0.37**	0.12	0.42**
2-MNAP	0.27	0.34	0.43	0.29	0.33	0.25	0.33*	0.33*	0.87**	0.39*	0.25	0.31*	0.20	0.29*	0.08	0.25
1-MNAP	0.36**	0.23	0.32	0.14	0.03	0.17	0.29*	0.23	0.81**	0.27	0.17	0.21	0.15	0.20	0.16	0.21
2,6-DMNAP	0.40**	0.30	0.43	0.57	0.35	0.33*	0.40**	0.36**	0.73**	0.32	0.32*	0.30*	0.22	0.31*	0.17	0.34**
1,3-DMNAP	0.33*	0.27	0.64	0.79*	0.26	0.19	0.27	0.23	0.75**	0.22	0.17	0.17	0.09	0.18	0.20	0.21
ACY	0.38**	0.70**	0.32	0.43	0.32	0.70**	0.73**	0.74**	0.68*	0.84**	0.73**	0.75**	0.70**	0.75**	0.28	0.72**
FLO	0.23	0.67**	0.71	0.89**	0.62	0.61**	0.60**	0.66**	0.73**	0.71**	0.62**	0.72**	0.58**	0.63**	0.08	0.63**
DBT	0.07	0.58**	0.46	0.82*	0.5	0.37**	0.58**	0.58**	0.72**	0.70**	0.50**	0.78**	0.58**	0.53**	0.25	0.60**
PHE	0.27	0.76**	0.79*	0.93**	0.42	0.51**	0.68**	0.68**	0.81**	0.78**	0.53**	0.81**	0.60**	0.63**	0.23	0.65**
ANT	0.14	0.37	0.54	0.43	0.39	0.51**	0.44**	0.51**	0.74**	0.53**	0.50**	0.47**	0.48**	0.56**	0.12	0.51**
2-MPHE	0.24	0.77**	0.75	0.93**	0.42	0.48**	0.66**	0.67**	0.75**	0.76**	0.51**	0.77**	0.59**	0.60**	0.08	0.67**
2-MANT	0.13	0.52**	0.46	0.29	-0.12	0.47**	0.44**	0.50**	0.46	0.69**	0.49**	0.58**	0.55**	0.61**	-0.03	0.53**
1-MPHE	0.16	0.74**	0.71	0.89**	0.20	0.44**	0.63**	0.62**	0.71*	0.79**	0.46**	0.75**	0.59**	0.60**	0.10	0.60**
3,6-DMPHE	0.23	0.64**	0.54	0.43	0.47	0.51**	0.55**	0.54**	0.73**	0.76**	0.55**	0.72**	0.68**	0.69**	0.12	0.59**
FLA	0.20	0.64**	0.57	0.79*	0.31	0.36**	0.59**	0.61**	0.66*	0.58**	0.39**	0.78**	0.51**	0.49**	0.38	0.55**
PYR	0.23	0.64**	0.75	0.89**	0.10	0.38**	0.65**	0.65**	0.73**	0.68**	0.41**	0.76**	0.50**	0.52**	0.34	0.58**
RET	0.24	0.43*	0.64	0.43	-0.05	0.53**	0.58**	0.52**	0.49	0.71**	0.51**	0.55**	0.57**	0.63**	0.08	0.52**
1-MPYR	0.17	0.63**	0.64	0.39	-0.01	0.45**	0.61**	0.62**	0.56	0.70**	0.44**	0.68**	0.54**	0.58**	0.30	0.58**
BaA	0.23	0.68**	0.75	0.54	0.04	0.54**	0.66**	0.68**	0.60*	0.81**	0.56**	0.71**	0.59**	0.64**	0.21	0.64**
CHR+TRI	0.31*	0.72**	0.57	0.43	0.37	0.55**	0.72**	0.75**	0.77**	0.84**	0.59**	0.78**	0.59**	0.63**	0.23	0.70**
6-MCHR	0.29*	0.68**	0.64	0.39	0.18	0.69**	0.73**	0.73**	0.65*	0.87**	0.73**	0.74**	0.73**	0.79**	0.33	0.75**
BbF	0.39**	0.71**	0.75	0.89**	0.55	0.73**	0.82**	0.84**	0.74**	0.91**	0.80**	0.74**	0.68**	0.73**	0.33	0.88**
BkF	0.39**	0.72**	0.89**	0.75	0.47	0.73**	0.82**	0.82**	0.80**	0.90**	0.81**	0.71**	0.68**	0.73**	0.30	0.88**
BeP	0.37**	0.73**	0.57	0.79*	0.55	0.72**	0.81**	0.83**	0.72**	0.90**	0.80**	0.73**	0.67**	0.73**	0.34	0.88**
BaP	0.34*	0.71**	0.79*	0.57	0.15	0.68**	0.75**	0.76**	0.69*	0.89**	0.74**	0.71**	0.66**	0.71**	0.38	0.76**
IcdP	0.41**	0.72**	0.89**	0.82*	0.55	0.73**	0.85**	0.85**	0.75**	0.90**	0.82**	0.67**	0.63**	0.69**	0.29	0.89**
DahA	0.39**	0.75**	0.82*	0.82*	0.55	0.74**	0.82**	0.82**	0.74**	0.90**	0.84**	0.66**	0.64**	0.70**	0.29	0.89**
BghiP	0.40**	0.72**	0.82*	0.82*	0.55	0.74**	0.84**	0.85**	0.67*	0.90**	0.83**	0.66**	0.63**	0.70**	0.30	0.89**
ΣPAH <sub>16-US</sub>	0.37**	0.75**	0.89**	0.75	0.47	0.69**	0.81**	0.82**	0.80**	0.89**	0.75**	0.74**	0.66**	0.71**	0.32	0.83**
ΣPAH <sub>27</sub>	0.37**	0.76**	0.89**	0.75	0.47	0.70**	0.81**	0.82**	0.80**	0.89**	0.75**	0.75**	0.67**	0.72**	0.31	0.84**



**Appendix B.13:** Correlation of parent PAH, NPAH, and OPAH with PM<sub>2.5</sub>, OC, BC and gas pollutant concentrations.

	PM <sub>2.5</sub>	OC	BC	OC/BC	NO	NO <sub>2</sub>	NO <sub>x</sub>	CO	SO <sub>2</sub>	O <sub>3</sub>
<i>MW&lt;300 PAHs</i>										
NAP	0.31*	0.59**	0.56**	-0.34**	0.23	0.30	0.30	0.16	0.30	0.07
2-MNAP	0.31*	0.59**	0.56**	-0.34**	-0.04	-0.05	-0.05	-0.08	0.05	0.14
1-MNAP	0.21	0.42**	0.41**	-0.25	-0.15	-0.26	-0.27	-0.10	-0.02	0.18
2,6-DMNAP	0.13	0.25	0.21	-0.12	0.04	0.05	0.04	-0.14	0.03	0.12
1,3-DMNAP	0.23	0.41**	0.36**	-0.12	-0.04	-0.10	-0.10	-0.11	0.04	0.12
ACY	0.15	0.28**	0.22	-0.12	0.61**	0.58**	0.59**	0.41**	0.26	-0.34*
FLO	0.25	0.55**	0.60**	-0.58**	0.70**	0.73**	0.73**	0.35*	0.28	-0.32
DBT	0.45**	0.56**	0.66**	-	0.38*	0.47**	0.46**	0.52**	0.44**	0.05
PHE	0.21	0.51**	0.56**	-0.48**	0.56**	0.60**	0.60**	0.58**	0.52**	-0.08
ANT	0.40**	0.60**	0.65**	-0.60**	0.50**	0.49**	0.49**	0.34*	0.12	-0.43**
2-MPHE	0.05	0.31**	0.35**	-0.37**	0.51**	0.52**	0.52**	0.61**	0.47**	-0.11
2-MANT	0.40**	0.55**	0.60**	-0.57**	0.41**	0.32*	0.33*	0.30	0.09	-0.39*
1-MPHE	0.10	0.30**	0.37**	-0.43**	0.52**	0.51**	0.52**	0.60**	0.43**	-0.20
3,6-DMPHE	0.31*	0.47**	0.54**	-0.61**	0.45**	0.32*	0.33*	0.37*	0.24	-0.31
FLA	0.16	0.31*	0.36**	-0.43**	0.38*	0.46**	0.45**	0.56**	0.58**	-0.02
PYR	0.44**	0.49**	0.53**	-0.54**	0.37*	0.47**	0.47**	0.61**	0.62**	-0.03
RET	0.42**	0.49**	0.53**	-0.60**	0.27	0.27	0.26	0.22	0.22	-0.10
1-MPYR	0.04	0.29*	0.32*	-0.35**	0.40**	0.42**	0.42**	0.54**	0.36*	-0.27
BaA	0.22	0.34*	0.41**	-0.55**	0.51**	0.52**	0.53**	0.59**	0.44**	-0.31
CHR+TRI	0.27*	0.49**	0.57**	-0.60**	0.54**	0.61**	0.61**	0.61**	0.62**	-0.11
6-MCHR	0.42**	0.63**	0.68**	-0.61**	0.62**	0.64**	0.64**	0.47**	0.26	-0.48**
BbF	0.19	0.49**	0.57**	-0.55**	0.63**	0.69**	0.69**	0.45**	0.46**	-0.31
BkF	0.35**	0.62**	0.64**	-0.50**	0.61**	0.64**	0.64**	0.47**	0.45**	-0.30
BeP	0.34*	0.61**	0.64**	-0.51**	0.64**	0.65**	0.66**	0.45**	0.44**	-0.32
BaP	0.34*	0.60**	0.62**	-0.51**	0.52**	0.55**	0.55**	0.52**	0.42**	-0.21
IcdP	0.32*	0.57**	0.63**	-0.58**	0.56**	0.64**	0.63**	0.43**	0.39*	-0.31
DahA	0.38**	0.63**	0.64**	-0.46**	0.59**	0.63**	0.63**	0.45**	0.36*	-0.38*
BghiP	0.33*	0.59**	0.61**	-0.49**	0.60**	0.65**	0.65**	0.41	0.37*	-0.34*
ΣPAH <sub>2ring</sub>	0.33*	0.59**	0.62**	-0.42**	0.36*	0.33*	0.32*	0.28	0.30	-0.06
ΣPAH <sub>3ring</sub>	0.40**	0.52**	0.57**	-0.58**	0.45**	0.52**	0.51**	0.61**	0.55**	-0.08
ΣPAH <sub>4ring</sub>	0.36**	0.61**	0.65**	-0.56**	0.60**	0.67**	0.66**	0.52**	0.51**	-0.25

**Appendix B.13 (continued)**

	PM <sub>2.5</sub>	OC	BC	OC/BC	NO	NO <sub>2</sub>	NO <sub>x</sub>	CO	SO <sub>2</sub>	O <sub>3</sub>
ΣPAH <sub>56ring</sub>	0.35**	0.61**	0.65**	-0.50**	0.60**	0.64**	0.64**	0.46**	0.40**	-0.31
ΣPAH <sub>28</sub>	0.34**	0.63**	0.70**	-0.55**	0.62**	0.68**	0.67**	0.50**	0.47**	-0.27
ΣPAH <sub>16-USPriority</sub>	0.37**	0.65**	0.71**	-0.55**	0.60**	0.67**	0.66**	0.52**	0.50**	-0.25
<b><i>MW 302 PAHs</i></b>										
N12bF	0.50**	0.69**	0.69**	-0.47**	0.52**	0.63**	0.64**	0.50**	0.47**	-0.21
N23jF/N12kF	0.47**	0.65**	0.66**	-0.47**	0.49**	0.59**	0.60**	0.49**	0.44**	-0.24
N23bF	0.35**	0.60**	0.63**	-0.47**	0.54**	0.63**	0.64**	0.44**	0.32*	-0.36*
DBaeF/DBbkF	0.46**	0.67**	0.68**	-0.49**	0.54**	0.66**	0.66**	0.51**	0.46**	-0.25
DBakF	0.30*	0.52**	0.56**	-0.48**	0.52**	0.57**	0.58**	0.54**	0.27*	-0.37*
DBjIF	0.45**	0.67**	0.68**	-0.48**	0.56**	0.67**	0.68**	0.49**	0.44**	-0.28
DBalP	0.16	0.49**	0.54**	-0.47**	0.61**	0.68**	0.69**	0.36*	0.19	-0.44**
N23kF	0.23	0.45**	0.48**	-0.44**	0.38*	0.42**	0.43**	0.43**	0.12	-0.29
N23eF	0.38**	0.61**	0.62**	-0.46**	0.54**	0.62**	0.63**	0.45**	0.36*	-0.33*
DBaeP	0.39**	0.61**	0.64**	-0.50**	0.57**	0.65**	0.66**	0.53**	0.40*	-0.33*
DBelP	0.54**	0.67**	0.67**	-0.49**	0.48**	0.58**	0.59**	0.63**	0.52**	-0.09
N23aP	-0.12	0.05	0.12	-0.26	0.07	-0.05	-0.03	0.21	-0.40*	-0.15
BbPer	0.19*	0.42**	0.48**	-0.46**	0.43**	0.44**	0.45**	0.50**	0.11	-0.39*
DBaiP	0.19	0.43**	0.48**	-0.45**	0.42**	0.42**	0.43**	0.45**	0.05	-0.38*
DBahP	-0.06	0.13	0.20	-0.30*	0.08	-0.05	-0.03	0.23	-0.32*	-0.22
DBbeF*	0.49**	0.65**	0.67**	-0.50**	0.51**	0.63**	0.63**	0.52**	0.48**	-0.20
U1*	0.50**	0.66**	0.68**	-0.49**	0.50**	0.62**	0.62**	0.48**	0.47**	-0.20
N12eP*	0.47**	0.64**	0.64**	-0.45**	0.50**	0.60**	0.61**	0.42**	0.44**	-0.24
U2*	0.49**	0.65**	0.66**	-0.48**	0.50**	0.60**	0.60**	0.47**	0.46**	-0.20
N12aP*	0.38**	0.61**	0.64**	-0.51**	0.53**	0.61**	0.62**	0.47**	0.36*	-0.32
U3*	0.24	0.47**	0.52**	-0.49**	0.51**	0.57**	0.58**	0.48**	0.21	-0.41*
N21aP*	0.37**	0.58**	0.62**	-0.50**	0.51**	0.58**	0.59**	0.47**	0.35*	-0.29
Σ302PAH	0.43**	0.64**	0.66**	-0.50**	0.53**	0.62**	0.63**	0.52**	0.41**	-0.27
Σ302PAH <sub>mut</sub> <sup>a</sup> (ng/m <sup>3</sup> )	0.42**	0.63**	0.65**	-0.50**	0.53**	0.62**	0.62**	0.53**	0.40**	-0.27

Appendix B.13 (continued)

	PM <sub>2.5</sub>	OC	BC	OC/BC	NO	NO <sub>2</sub>	NO <sub>x</sub>	CO	SO <sub>2</sub>	O <sub>3</sub>
<i>NPAHs</i>										
1-NN	0.18	0.40**	0.35*	-0.08	0.28	0.21	0.22	-0.02	0.14	0.06
2-NN	0.50**	0.59**	0.70**	-0.68**	0.47*	0.45*	0.50*	0.36	0.42	-0.20
3-NBP	0.32	0.43	0.29	-0.14	n/a	n/a	n/a	n/a	n/a	n/a
3-NDF	0.54	0.54	0.46	-0.29	n/a	n/a	n/a	n/a	n/a	n/a
5-NAC	0.88**	0.79**	0.58	-0.31	0.70	0.50	0.50	-0.10	-0.10	0.10
9-NAN	-0.09	0.37**	0.36**	-0.18	0.44**	0.34*	0.37*	-0.12	-0.05	-0.22
3-NPH	0.36*	0.66**	0.60**	-0.38**	0.33*	0.43**	0.42**	0.21	0.30	0.00
2-NF	0.41**	0.69**	0.72**	-0.44**	0.50**	0.59**	0.59**	0.32*	0.36*	-0.10
1-NP	0.52	0.61*	0.73**	-0.22	n/a	n/a	n/a	n/a	n/a	n/a
2-NP	0.27	0.53	0.64**	-0.51**	0.49*	0.33	0.38	0.15	0.14	-0.31
7-NBaA	0.26	0.63**	0.59**	-0.35*	0.44*	0.30	0.33	0.13	0.10	-0.22
ΣNPAH	0.15	0.57**	0.58**	-0.33*	0.54**	0.51**	0.53**	0.09	0.14	-0.21
<i>OPAHs</i>										
9-FLU	0.30*	0.52**	0.57**	-0.46**	0.49**	0.44**	0.47**	0.25	0.20	0.01
ANQ	0.01	0.30*	0.35**	-0.30*	0.46**	0.26	0.30	0.13	-0.01	-0.19
2-MANQ	-0.08	0.29*	0.34**	-0.30*	0.48**	0.32*	0.36*	0.11	-0.03	-0.31*
BENZ <sup>a</sup>	0.05	0.19	0.29	-0.27	0.19	0.19	0.16	0.02	0.48*	0.10
BaAD	0.37**	0.67**	0.64**	-0.34*	0.45**	0.44**	0.45**	0.34*	0.22	-0.15
ΣOPAH	0.55**	0.55**	0.57**	-0.39**	0.54**	0.56**	0.57**	0.25	0.20	-0.28
<b>BC</b>	0.74**	0.90**	-	-0.78**	0.14	0.36*	0.33	0.69**	0.71**	0.31
<b>OC</b>	0.77**	-	0.90**	-0.49**	0.19	0.44**	0.40**	0.60**	0.61**	0.35*
<b>OC/BC</b>	-0.48**	-	-	-	-0.00	-0.11	-0.10	-0.61**	-0.63**	-0.26
<b>PM<sub>2.5</sub></b>	-	0.77**	0.74**	-0.48**	-0.25	-0.02	-0.06	0.67**	0.63**	0.55**

\*Correlation is significant at the 0.05 level (2-tailed).

\*\* Correlation is significant at the 0.01 level (2-tailed).

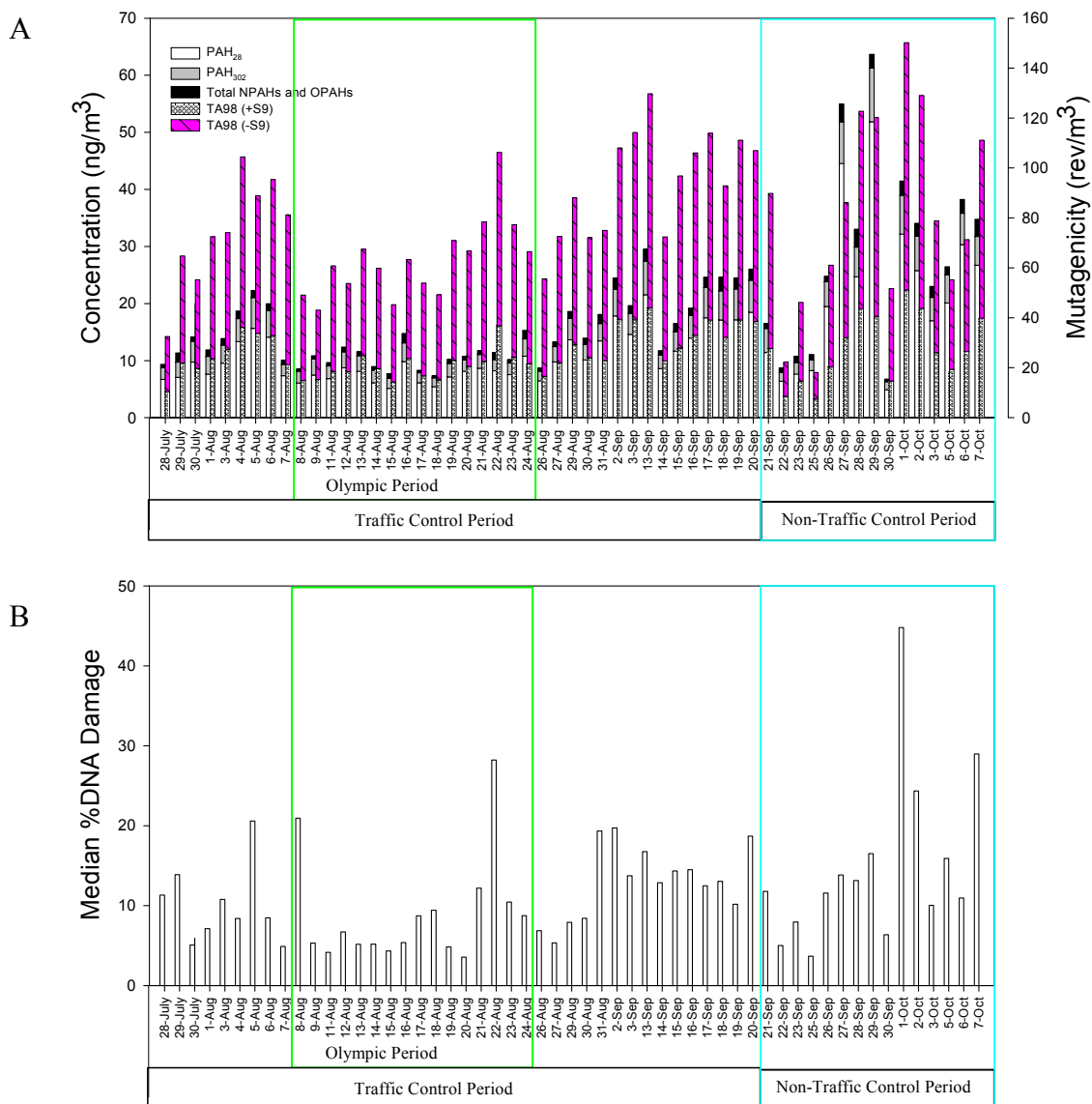
<sup>a</sup>Possibly underestimated by this method.

n/a – not available due to small data set. Possibly underestimated by this method.

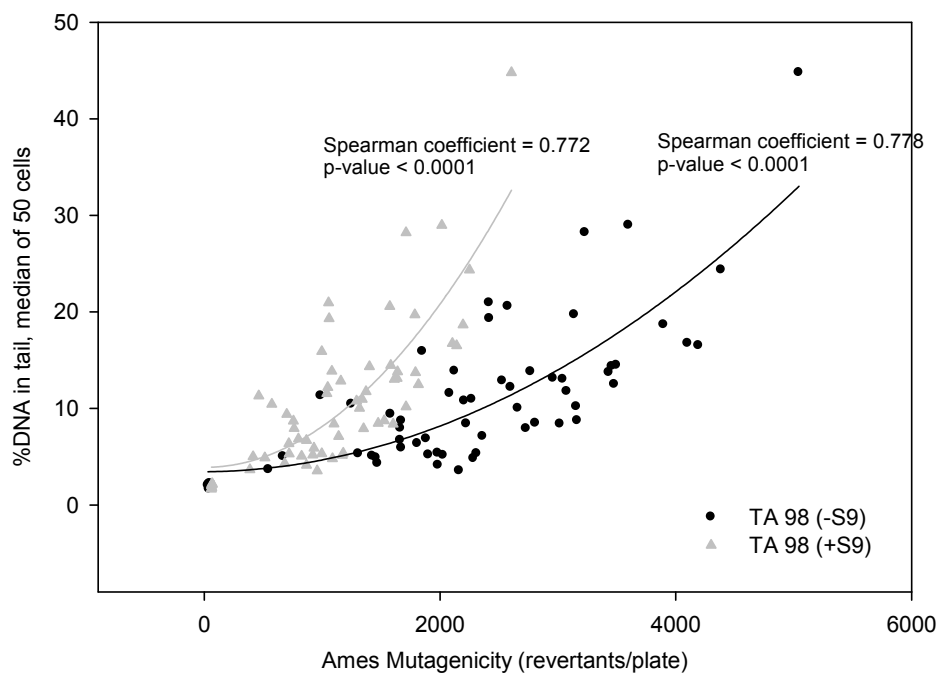
**Appendix B.14:** Mean, standard deviation and t-test results for different diagnostic PAH ratios.

<b>Ratios</b>	<b>Fla/Fla+Pyr</b>	<b>IcdP/Bghip+Icdp</b>	<b>BeP/BaP+BeP</b>	<b>IcdP/IcdP+BeP</b>
<b>All Periods</b>				
All Ave	0.59	0.50	0.61	0.52
All Std	0.02	0.01	0.05	0.03
Min	0.54	0.49	0.50	0.42
Max	0.64	0.52	0.74	0.56
<b>Source control period</b>				
Source Ave	0.59	0.50	0.63	0.53
Source Std	0.02	0.01	0.04	0.02
Min	0.54	0.49	0.56	0.47
Max	0.64	0.52	0.74	0.56
<b>Non source control period</b>				
Non-Source Ave	0.59	0.50	0.58	0.49
Non-Source Std	0.02	0.01	0.05	0.04
Min	0.54	0.49	0.50	0.42
Max	0.64	0.51	0.65	0.55
<b>T-test (p value)</b>	0.80	0.07	<b>&lt;0.001</b>	<b>&lt;0.001</b>
<b>Olympic period</b>				
Oly Ave	0.58	0.50	0.63	0.54
Oly Std	0.02	0.01	0.05	0.02
Min	0.54	0.50	0.56	0.51
Max	0.62	0.52	0.74	0.56
<b>Non-Olympic period</b>				
NonOly Ave	0.60	0.50	0.61	0.51
NonOly Std	0.02	0.01	0.04	0.03
Min	0.54	0.49	0.50	0.42
Max	0.64	0.51	0.69	0.56
<b>T-test (p value)</b>	0.04	0.01	0.089	<b>&lt;0.001</b>

**Appendix B.15:** A. Daily  $\Sigma\text{PAH}_{28}$ ,  $\Sigma 302\text{PAH}$ , and sum of  $\Sigma\text{NPAH}$  and  $\Sigma\text{OPAH}$  concentration and corresponding total direct-acting and indirect-acting mutagen density for the sample extract. B. Daily median %DNA damage for the PM crude extracts.



**Appendix B.16:** Spearman correlation between direct-acting and indirect-acting Ames mutagenicities and percent DNA damage in the Comet assay.



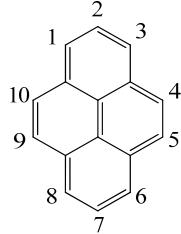
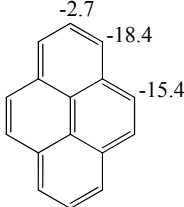
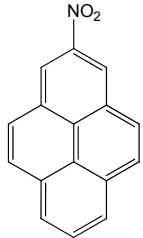
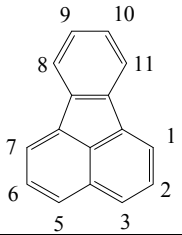
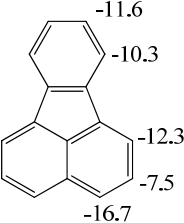
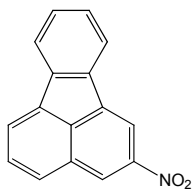
## References

1. Schubert, P.; Schantz, M. M.; Sander, L. C.; Wise, S. A., Determination of Polycyclic Aromatic Hydrocarbons with Molecular Weight 300 and 302 in Environmental-Matrix Standard Reference Materials by Gas Chromatography/Mass Spectrometry. *Anal. Chem.* **2003**, *75*, (2), 234-246.
2. Lee, M. L.; Vassilaros, D. L.; White, C. M., Retention indices for programmed-temperature capillary-column gas chromatography of polycyclic aromatic hydrocarbons. *Anal. Chem.* **1979**, *51*, (6), 768-773.
3. Bengård, A.; Colmsjö, A.; Lundmark, B.-O., Gas chromatographic analysis of high-molecular-mass polycyclic aromatic hydrocarbons : II. Polycyclic aromatic hydrocarbons with relative molecular masses exceeding 328. *Journal of Chromatography A* **1993**, *630*, (1-2), 287-295.
4. Wang, X.; Westerdahl, D.; Chen, L. C.; Wu, Y.; Hao, J.; Pan, X.; Guo, X.; Zhang, K. M., Evaluating the air quality impacts of the 2008 Beijing Olympic Games: On-road emission factors and black carbon profiles. *Atmos. Environ.* **2009**, *43*, (30), 4535-4543.
5. Chan, C. K.; Yao, X., Air pollution in mega cities in China. *Atmos. Environ.* **2008**, *42*, (1), 1-42.
6. Dan, M.; Zhuang, G. S.; Li, X. X.; Tao, H. R.; Zhuang, Y. H., The characteristics of carbonaceous species and their sources in PM<sub>2.5</sub> in Beijing. *Atmos. Environ.* **2004**, *38*, (21), 3443-3452.
7. Sun, Y. L.; Zhuang, G. S.; Ying, W.; Han, L. H.; Guo, J. H.; Mo, D.; Zhang, W. J.; Wang, Z. F.; Hao, Z. P., The air-borne particulate pollution in Beijing - concentration, composition, distribution and sources. *Atmos. Environ.* **2004**, *38*, (35), 5991-6004.
8. He, K. B.; Yang, F. M.; Ma, Y. L.; Zhang, Q.; Yao, X. H.; Chan, C. K.; Cadle, S.; Chan, T.; Mulawa, P., The characteristics of PM<sub>2.5</sub> in Beijing, China. *Atmos. Environ.* **2001**, *35*, (29), 4959-4970.

**APPENDIX C**



**Appendix C.1:** Free energies ( $\Delta G_{\text{rxn}}$ ) of OH-PAH adducts calculated using density functional theory (B3LYP) and the 6-31G(d) basis set compared to NPAH isomers identified in a previous gas-phase OH-radical chamber study.

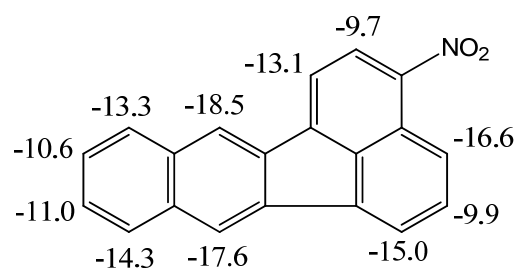
Parent PAH	Numbering Scheme	OH-PAH-Adduct $\Delta G_{\text{rxn}}$ (Kcal/mol)	Theoretical NPAH formed in gas phase	Chamber NPAH measured (%yield) <sup>a</sup>
1. Pyrene				2-nitropyrene (~0.5%) 4-nitropyrene (~0.06%)
2. Fluoranthene				2-nitrofluoranthene (~3%) 7-nitrofluoranthene (~1%) 8-nitrofluoranthene (~0.3%)

<sup>a</sup>Atkinson, R.; Arey, J.; Zielinska, B.; Aschmann, S. M., Kinetics and Nitro-Products of the Gas-Phase OH and NO<sub>3</sub> Radical-Initiated Reactions of Naphthalene-d<sub>8</sub>, Fluoranthene-d<sub>10</sub>, and Pyrene. *International Journal of Chemical Kinetics* 1990, 22, 999-101.

**Appendix C.2:** Calculated dipole moments of NPAHs identified in the chamber studies and predicted GC retention orders.

<b>NPAH</b>	<b>Calculated Dipole Moment (Debye)</b>	<b>Predicted Retention order</b>
6-NBaP	4.85	1
1-NBaP	6.06	2
3-NBaP	6.16	3
7-NBkF	4.02	1
1-NBkF	4.68	2
8-NBkF	5.00	3
3-NBkF	5.94	4
9-NBkF	6.61	5
7-NBghiP	4.51	1
4-NBghiP	5.75	4
5-NBghiP	6.03	5

**Appendix C.3:** Free energies ( $\Delta G_{\text{rxn}}$ ) of OH-3-NO<sub>2</sub>-BkF adduct calculated using density functional theory (B3LYP) and the 6-31G(d) basis set.



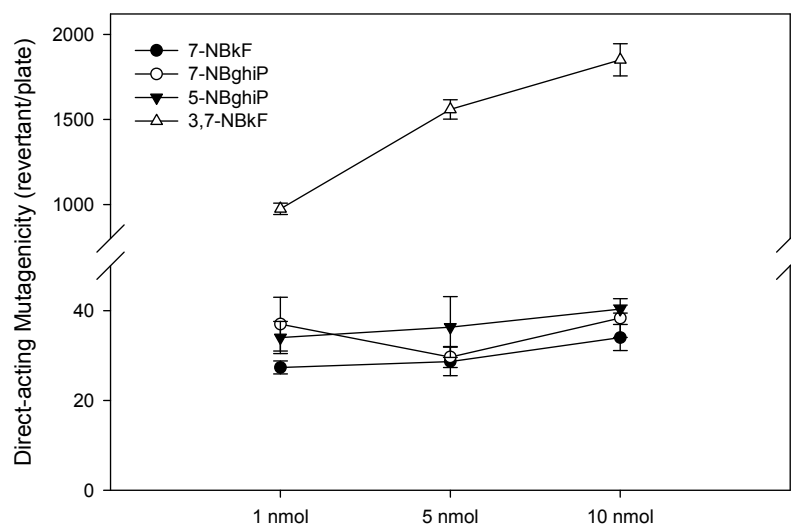
**Appendix C.4:** Estimated percent nitro PAH product formation relative to the amount of unexposed parent PAH.

	<b>NO<sub>2</sub></b>	<b>NO<sub>3</sub>/N<sub>2</sub>O<sub>5</sub></b>	<b>O<sub>3</sub></b>	<b>OH</b>
BaP-d <sub>12</sub>	181%	82%	0%	40%
BkF-d <sub>12</sub>	a	60%	0%	1%
BghiP-d <sub>12</sub>	0%	8%	0%	1%
DaiP-d <sub>14</sub>	46%	6%	0%	0%
DalP	38%	9%	0%	0%

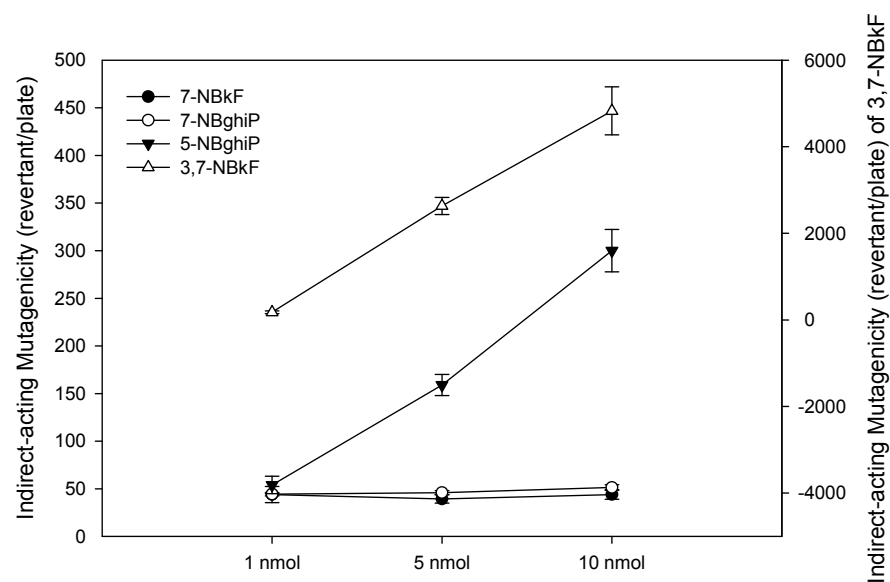
a: unable to determine fraction due to a significant loss during sample preparation

**Appendix C.5:** Dose response profiles of 7-NBkF, 3,7-DNBkF, 5-NBghiP and 7-NBghiP in A. TA98 (-S9) B. TA98 (+S9).

A.



B.

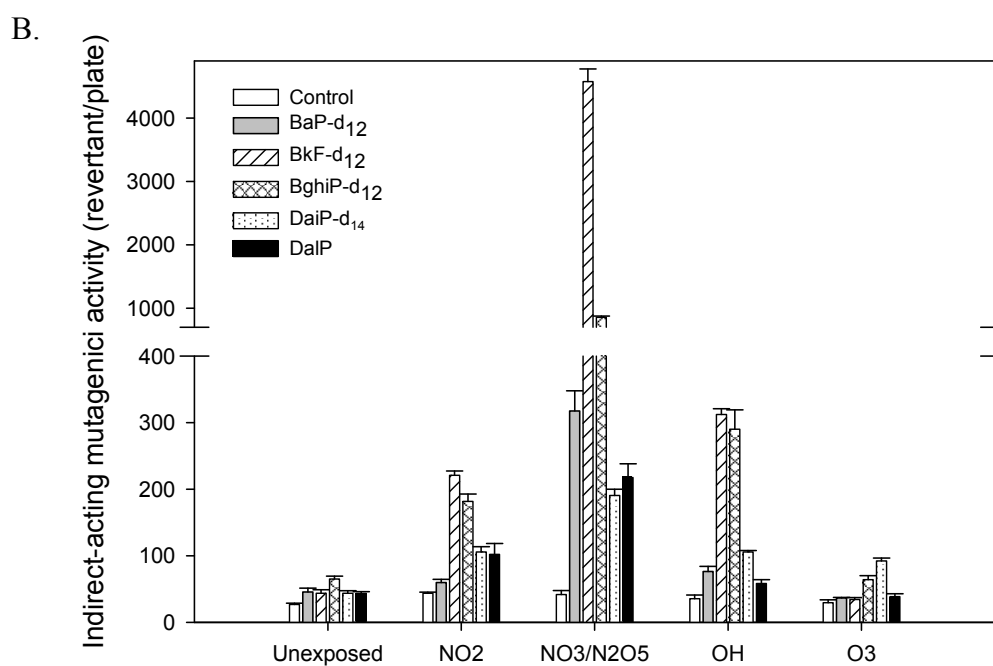
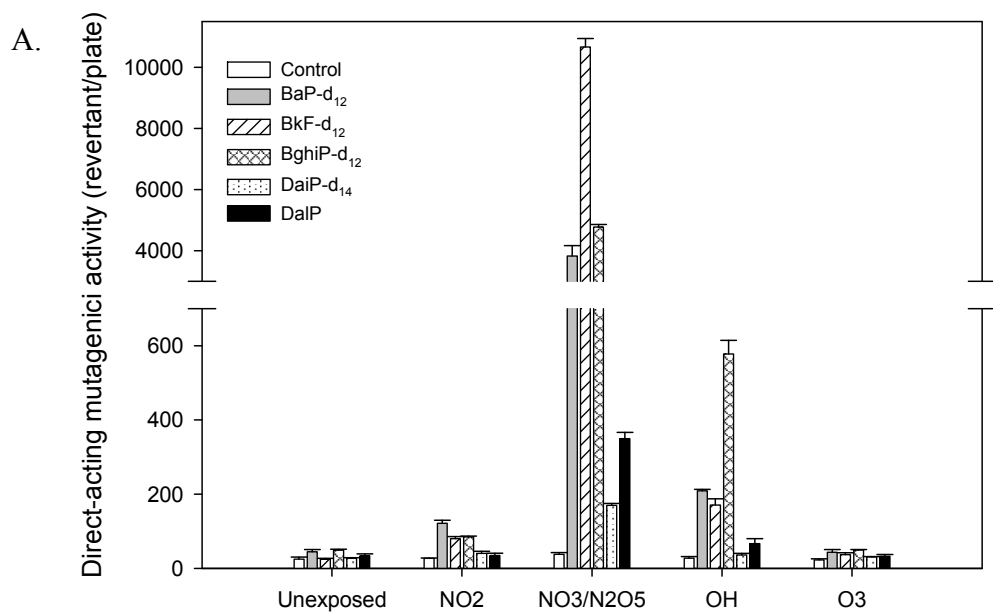


Compound	TA 98 (-S9) rev/nmol	TA (+S9) rev/nmol
7-NO <sub>2</sub> -BkF	< 1	< 1
3,7-NO <sub>2</sub> -BkF	96	513
5-NO <sub>2</sub> -BghiP	< 1	27
7-NO <sub>2</sub> -BghiP	< 1	< 1

**Appendix C.6:** C-C-N-O dihedral angles of NPAHs, computed using density functional theory (B3LYP) and the 6-31G(d) basis set.

<b>NPAHs</b>	<b>Angle</b>
1-NBaP	22.4
2-NBaP	24.7
6-NBaP	54.7
1-NBkF	19.7
3-NBkF	3.6
7-NBkF	51.4
8-NBkF	24.6
9-NBkF	0.0
4-NBghiP	26.2
5-NBghiP	25.1
7-NBghiP	53.2
5-NDaiP	55.5
6-NDalP	53.7

**Appendix C.7:** Mean ( $\pm$  standard error) of A. direct- and B. indirect-acting mutagenicities (revertants/nmol) of filter extracts. All extracts were tested in triplicate for mutagenic activity.



**APPENDIX D**



**Appendix D.1:** List of parent PAHs and NPAHs (and their abbreviations) measured in this study.

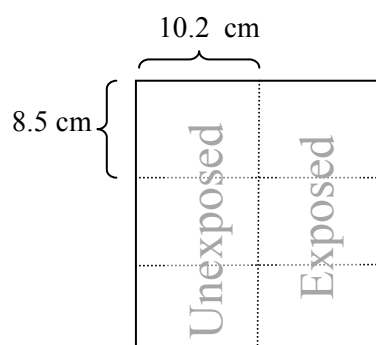
#	Compound	Abbreviation	#	Compound	Abbreviation
<b>PAHs<sup>1</sup></b>			<b>NPAHs<sup>2</sup></b>		
1	naphthalene	NAP	1	1-nitronaphthalene	1-NN
2	2-methylnaphthalene	2-MNAP	2	2-nitronaphthalene	2-NN
3	1-methylnaphthalene	1-MNAP	3	2-nitrobiphenyl	2-NBP
4	2,6-dimethylnaphthalene	2,6-DNAP	4	3-nitrobiphenyl	3-NBP
5	1,3-dimethylnaphthalene	1,3-DNAP	5	4-nitrobiphenyl	4-NBP
6	acenaphthylene	ACY	6	3-nitrodibenzofuran	3-NDF
7	acenaphthene	ACE	7	5-nitroacenaphthalene	5-NAC
8	fluorene	FLU	8	2-nitrofluorene	2-NFL
9	phenanthrene	PHE	9	9-nitroanthracene	9-NAN
10	anthracene	ANT	10	9-nitrophenanthrene	9-NPH
11	2-methylphenanthrene	2-MPHE	11	2-nitrodibenzothiophene	2-NDBT
12	2-methylanthracene	2-MANT	12	3-nitrophenanthrene	3-NPH
13	1-methylphenanthrene	1-MPHE	13	2-nitroanthracene	2-NAN
14	3,6-dimethylphenanthrene	3,6-DPHE	14	2-nitrofluoranthene	2-NF
15	dibenzothiophene	DBT	15	3-nitrofluoranthene	3-NF
16	fluoranthene	FLA	16	1-nitropyrene	1-NP
17	pyrene	PYR	17	2-nitropyrene	2-NP
18	retene	RET	18	7-nitrobenz(a)anthracene	7-NBaA
19	Benz[c]fluorene	BcFLU	19	1-nitrotriphenylene	1-NTR
20	1-methylpyrene	1-MPYR	20	2,8-dinitrodibenzothiophene	2,8-DNDBT
21	benz[a]anthracene	BaA	21	6-nitrochrysene	6-NCH
22	chrysene + triphylene	CHR+TRI	22	3-nitrobenzathrone	3-NBENZ
23	6-methylchrysene	6-MCHR	23	2-nitrotriphenylene	2-NTR
24	benzo(b)fluoranthene	BbF	24	1,3-dinitropyrene	1,3-DNP
25	benzo(k)fluoranthene	BkF	25	1,6-dinitropyrene	1,6-DNP
26	benzo[e]pyrene	BeP	26	1,8-dinitropyrene	1,8-DNP
27	benzo[a]pyrene	BaP	27	6-nitrobenzo[a]pyrene	6-NBaP
28	indeno[1,2,3-cd]pyrene	IcdP			
29	dibenz[a,h]+(a,c)anthracene	DahA+DacA			
30	benzo[g,h,i]perylene	BghiP			

<sup>1</sup>Purchased from AccuStandard (New Haven, CT) and Chem Service (West Chester, PA)

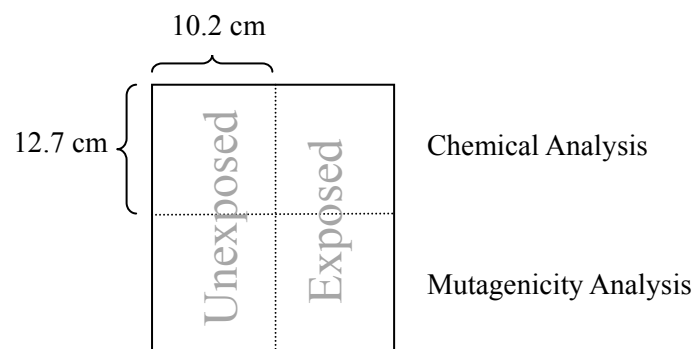
<sup>2</sup>Purchased from Chiron AS (Norway), AccuStandard (New Haven, CT), Chem Service (West Chester, PA) and Sigma-Aldrich Corp. Cambridge Isotope Laboratories (Andover, MA)

**Appendix D.2:** Sampling details for the PM filters used in the exposure experiments.

Filter Code	PM Size	Location	Sampling Date	Duration	Exposure	Experiment
PKU-1	PM <sub>2.5</sub>	Beijing	4/20/11	24 h	NO <sub>3</sub> /N <sub>2</sub> O <sub>5</sub>	Chemistry
PKU-2	PM <sub>2.5</sub>	Beijing	4/21/11	24 h	NO <sub>3</sub> /N <sub>2</sub> O <sub>5</sub>	Chemistry
PKU A	PM <sub>10</sub>	Beijing	May 09- Feb 10	24 h	NO <sub>3</sub> /N <sub>2</sub> O <sub>5</sub>	Chemistry
PKU-3	PM <sub>2.5</sub>	Beijing	4/22/11	24 h	NO <sub>3</sub> /N <sub>2</sub> O <sub>5</sub>	Mutagenicity
PKU-4	PM <sub>2.5</sub>	Beijing	4/23/11	24 h	NO <sub>3</sub> /N <sub>2</sub> O <sub>5</sub>	Mutagenicity
PKU-5	PM <sub>2.5</sub>	Beijing	4/25/11	24 h	NO <sub>3</sub> /N <sub>2</sub> O <sub>5</sub>	Mutagenicity
PKU-6	PM <sub>2.5</sub>	Beijing	4/26/11	24 h	OH Radical	Chemistry
PKU B	PM <sub>10</sub>	Beijing	May 09- Feb 10	24 h	OH Radical	Chemistry
PKU C	PM <sub>10</sub>	Beijing	May 09- Feb 10	24 h	OH Radical	Chemistry
PKU-7	PM <sub>2.5</sub>	Beijing	4/27/11	24 h	OH Radical	Mutagenicity
PKU-8	PM <sub>2.5</sub>	Beijing	4/28/11	24 h	OH Radical	Mutagenicity
PKU-9	PM <sub>2.5</sub>	Beijing	4/29/11	24 h	OH Radical	Mutagenicity
PKU-10	PM <sub>2.5</sub>	Beijing	4/14/11	24 h	O <sub>3</sub>	Chemistry
PKU-11	PM <sub>2.5</sub>	Beijing	4/16/11	24 h	O <sub>3</sub>	Chemistry
PKU D	PM <sub>10</sub>	Beijing	May 09- Feb 10	24 h	O <sub>3</sub>	Chemistry
PKU-12	PM <sub>2.5</sub>	Beijing	4/18/11	24 h	O <sub>3</sub>	Mutagenicity
PKU-13	PM <sub>2.5</sub>	Beijing	4/19/11	24 h	O <sub>3</sub>	Mutagenicity
PKU-14	PM <sub>2.5</sub>	Beijing	4/13/11	24 h	O <sub>3</sub>	Mutagenicity
MT97-67 Q3	PM <sub>2.5</sub>	Riverside	10/4/97	7 h (daytime)	NO <sub>3</sub> /N <sub>2</sub> O <sub>5</sub>	Chemistry
MT97-66 Q2	PM <sub>2.5</sub>	Riverside	10/4/97	7 h (daytime)	OH Radical	Chemistry
MT97-65 Q1	PM <sub>2.5</sub>	Riverside	10/4/97	7 h (daytime)	O <sub>3</sub>	Chemistry

**Appendix D.3:** Cutting of the filters used in the chemical and mutagenicity studies.

Chemical Study



Mutagenicity Study

**Appendix D.4:** Rotating apparatus placed inside the Teflon chamber for exposing cut PM filters.



**Appendix D.5:** Means and standard errors of PAH and NPAH masses (ng) measured in PKU filters used for the chemical study of NO<sub>3</sub>/N<sub>2</sub>O<sub>5</sub> exposure. In the case that a compound was not detected in all samples, superscript denotes number of samples detected. Numbers in bold are estimated detection limits. An asterisk indicates the statistically significant difference in mass (p-value < 0.05).

Compound	PKU A (n=3)		PKU-1 (n=3)		PKU-2 (n=3)		Avg. %change
	Unexposed	Exposed	Unexposed	Exposed	Unexposed	Exposed	
<b>PAHs</b>							
NAP	14.5 ± 2.2	13.7 ± 0.5	637.3 ± 310.2	11.4 ± 0.4	3.8 ± 0.6	3.8 ± 2.8	-25% ± 28%
2-MNAP			289.8 ± 14.1 <sup>2</sup>	<b>6.2</b>			-98% ± 0.1%*
1-MNAP			93.1 ± 42.1	6.3 ± 1.9	4.1 ± 0.3 <sup>2</sup>	4.2 ± 0.8 <sup>2</sup>	-35% ± 27%
2,6-DMNAP			29.5 ± 2.4 <sup>2</sup>	<b>3.9</b>			-87% ± 1%
1,3-DMNAP	4.3 ± 0.4	4.5 ± 0.6	38.0 ± 16.3	<b>4.8</b>			-29% ± 23%
ACY	4.3 ± 0.2	3.1 ± 0.1	6.8 ± 0.4	4.3 ± 0.5			-32% ± 6%*
ACE			207.2 ± 14.9	<b>3.4</b>			-98 ± 0.1%
FLU	6.8 ± 0.5	5.7 ± 0.6	97.1 ± 41.6	10.8 ± 0.1	5.0 ± 0.4	5.9 ± 1.3	-23% ± 15%
DBT	6.3 ± 0.8	5.0 ± 0.3	24.5 ± 6.0	11.1 ± 1.4	2.3 ± 0.5	2.5 ± 0.8	-11% ± 22%
PHE	81.5 ± 4.4	59.6 ± 7.2	243.7 ± 38.9	111.8 ± 2.9	31.3 ± 0.2	22.8 ± 1.5	-35% ± 5%*
ANT	8.2 ± 0.2	4.1 ± 0.3	16.4 ± 3.7	<b>4.9</b>			-57% ± 6%*
2-MPHE	28.3 ± 1.6	20.7 ± 2.3	66.4 ± 2.8	55.0 ± 3.9			-22% ± 5%*
2-MANT	3.9 ± 0.1	<b>3.1</b>					-22% ± 1%*
1-MPHE	17.4 ± 1.0	12.0 ± 1.2	40.9 ± 0.4	33.5 ± 0.9	13.1 ± 0.5	10.9 ± 0.9	-22% ± 3%*
3,6-DPHE	3.0 ± 0.1 <sup>2</sup>	<b>2.7</b>	5.7 <sup>1</sup>	4.9 <sup>1</sup>			-11% ± 3%
RET	47.6 ± 3.7	36.0 ± 4.8	50.6 ± 0.8	41.1 ± 1.3	23.8 ± 0.9	13.0 ± 0.6	-29% ± 5%*
FLA	318.7 ± 17.7	202.0 ± 22.3	550.4 ± 22.6	540.1 ± 22.6	124.4 ± 3.4	105.5 ± 12.6	-18% ± 6%*
PYR	220.6 ± 13.6	122.1 ± 14.6	369.2 ± 7.5	278.3 ± 11.0	94.1 ± 3.1	33.7 ± 1.0	-45% ± 6%*
BcFLU			80.3 ± 0.8	45.9 ± 13.3	24.2 ± 0.7	10.5 ± 0.8	-50% ± 8%*
1-MPYR	21.1 ± 1.2	10.4 ± 1.1	30.0 ± 0.2	35.2 ± 17.0	10.6 ± 0.3	3.9 ± 0.04	-32% ± 21%
BaA	132.3 ± 6.9	67.1 ± 6.9	177.8 ± 5.4	146.3 ± 12.1	52.5 ± 3.6	27.7 ± 2.8	-38% ± 6%*
CHR + TRI	184.3 ± 13.4	143.4 ± 21.2	223.9 ± 4.6	207.8 ± 10.0	64.2 ± 1.4	52.8 ± 0.7	-16% ± 4%*
BbF	743.3 ± 48.8	595.2 ± 81.4	630.6 ± 8.3	596.5 ± 9.8	276.6 ± 4.5	225.6 ± 1.2	-15% ± 3%*

Appendix D.5 (continued)

Compound	Uncoded A (n=3)		PKU-1 (n=3)		PKU-2 (n=3)		Avg. %change
	Unexposed	Exposed	Unexposed	Exposed	Unexposed	Exposed	
IcdP	366.3 ± 21.8	284.2 ± 36.7	368.1 ± 3.0	367.7 ± 5.9	152.8 ± 4.3	118.6 ± 1.7	-16% ± 4%
BghiP	370.4 ± 22.8	249.0 ± 32.6	382.7 ± 3.0	352.8 ± 9.2	157.2 ± 4.2	112.1 ± 1.5	-23% ± 4%
<b>NPAHs</b>							
1-NN			0.7 ± 0.1	0.6 ± 0.04	0.2 ± 0.01	0.3 ± 0.02	-3% ± 8%
2-NN			1.1 ± 0.1	0.9 ± 0.1	0.5 ± 0.01	0.4 ± 0.1	-13% ± 6%
3-NBP	0.88 <sup>1</sup>	1.82 <sup>1</sup>	1.3 ± 0.1	1.3 ± 0.1			30% ± 26%
3-NDB			2.7 ± 0.1	3.4 ± 0.2			27% ± 9%
5-NAC	0.2 <sup>1</sup>	17.1 <sup>1</sup>					7340%
9-NAN	110.0 ± 7.0	64.4 ± 1.0	123.1 ± 2.4	100.0 ± 1.2	31.7 ± 1.7	23.5 ± 0.9	-29% ± 3%*
9-NPH			<b>0.5</b>	4.8 ± 1.7	<b>0.5</b>	2.7 ± 0.1	633% ± 177%*
3-NPH	4.1 ± 0.6	3.8 ± 0.1	2.7 ± 0.1	4.0 ± 0.7	1.2 ± 0.04	2.0 ± 0.1	38% ± 14%
2-NF	257.9 ± 15.5	231.1 ± 3.4	139.8 ± 2.1	141.3 ± 11.6	32.4 ± 2.1	32.0 ± 2.7	-3% ± 4%
3-NF	<b>0.9</b>	14.7 ± 0.8	<b>1.1</b>	6.7 ± 1.4	<b>1.1</b>	6.7 ± 0.5	862% ± 173%*
1-NP	3.1 ± 0.5	64.1 ± 2.7	4.3 ± 0.1	67.2 ± 9.3	2.2 ± 0.03	64.2 ± 0.9	2104% ± 224%*
2-NP			12.0 ± 0.4	12.1 ± 0.4	10.1 ± 0.2	10.0 ± 0.5	0.2% ± 3%
7-NBaA	29.4 ± 2.4	48.5 ± 0.8	24.5 ± 0.9	34.8 ± 2.2	12.4 ± 0.3	32.7 ± 0.4	91% ± 19%*
1-NTR	<b>0.6</b>	3.7 ± 0.2	<b>0.6</b>	1.1 ± 0.2	<b>0.6</b>	1.8 ± 0.4	278% ± 78%*
6-NCH	<b>0.8</b>	25.0 ± 0.8	<b>0.2</b>	6.9 ± 1.5	<b>0.2</b>	11.3 ± 1.0	4878% ± 644%*
2-NTR	<b>0.7</b>	5.9 ± 0.3	0.5 ± 0.03	1.5 ± 0.3	<b>0.4</b>	1.6 ± 0.1	420% ± 80%*
1,3-DNP			0.7 <sup>1</sup>	1.1 <sup>1</sup>			42%
1,6-DNP			0.6 <sup>1</sup>	2.5 <sup>1</sup>			296%
1,8-DNP			2.6 ± 0.04	5.3 ± 0.8	1.6 <sup>1</sup>	2.5 <sup>1</sup>	91% ± 23%*
6-NBaP	<b>5.3</b>	91.4 ± 1.8	<b>6.1</b>	191.3 ± 6.6	<b>6.1</b>	171.2 ± 15.6	2445% ± 226%*

**Appendix D.6:** Means and standard errors of PAH and NPAH masses (ng) measured in PKU filters used for the chemical study of OH radical exposure. In the case that a compound was not detected in all samples, superscript denotes number of samples detected. Numbers in bold are estimated detection limits. An asterisk indicates the statistically significant difference in mass (p-value < 0.05).

Compound	PKU B (n=3)		PKU C (n=3)		PKU-6 (n=3)		Avg. %change
	Unexposed	Exposed	Unexposed	Exposed	Unexposed	Exposed	
<b>PAHs</b>							
NAP	1.0 ± 0.4 <sup>2</sup>	<b>0.5</b>	17.5 ± 2.2	17.3 ± 1.9	3.2 ± 2.1 <sup>2</sup>	5.6 ± 0.4 <sup>2</sup>	58% ± 47%
1-MNAP					<b>3.8</b>	4.5 ± 1.2 <sup>2</sup>	38% ± 35%
2,6-DMNAP					3.9 <sup>1</sup>	4.6 <sup>1</sup>	17%
1,3-DMNAP	4.0 ± 0.2	3.8 ± 0.2	3.9 ± 0.2	3.9 ± 0.1			-2% ± 2%
ACY	5.2 ± 0.2	4.2 ± 0.2	5.3 ± 0.2	4.6 ± 0.3	4.3 ± 0.03 <sup>2</sup>	3.9 ± 0.3 <sup>2</sup>	-15% ± 3%*
FLU	8.5 ± 0.3	8.2 ± 0.3	8.7 ± 0.5	7.6 ± 0.4	6.8 ± 0.3	5.5 ± 0.4	-12% ± 4%*
DBT	7.6 ± 0.7	6.4 ± 0.3	6.7 ± 0.5	6.1 ± 0.5	3.5 ± 0.1	2.1 ± 1.1	-21% ± 11%
PHE	96.4 ± 4.2	86.0 ± 3.8	102.4 ± 7.8	82.2 ± 5.0	60.4 ± 1.7	33.1 ± 1.4	-25% ± 6%*
ANT	8.1 ± 0.6	4.7 ± 0.03	8.9 ± 0.8	5.7 ± 0.2	9.2 ± 0.2	5.3 ± 0.3	-40% ± 3%*
2-MPHE	31.5 ± 1.4	27.8 ± 1.0	33.9 ± 2.8	26.1 ± 1.3	29.7 ± 0.6	25.3 ± 3.0	-16% ± 4%*
2-MANT	3.7 ± 0.2	<b>3.1</b>	3.9 ± 0.4	<b>3.1</b>			-17% ± 4%*
1-MPHE	19.9 ± 1.1	16.7 ± 0.7	21.0 ± 1.8	15.9 ± 0.4	19.8 ± 0.6	14.3 ± 1.5	-22% ± 3%*
3,6-DPHE	2.8 ± 0.1 <sup>2</sup>	2.5 ± 0.2 <sup>2</sup>	3.2 ± 0.1 <sup>2</sup>	<b>2.7</b>	6.5 ± 0.8 <sup>2</sup>	6.0 ± 0.3 <sup>2</sup>	-11% ± 5%
RET	31.0 ± 1.2	29.1 ± 1.5	32.5 ± 2.2	26.5 ± 1.8	44.3 ± 2.2	40.6 ± 3.7	-11% ± 3%*
FLA	379.6 ± 22.8	336.9 ± 13.0	432.9 ± 37.4	319.3 ± 20.9	195.2 ± 2.9	156.1 ± 14.4	-19% ± 3%*
PYR	250.0 ± 10.9	216.0 ± 9.2	265.7 ± 19.3	210.6 ± 12.1	142.3 ± 3.5	86.0 ± 8.0	-24% ± 5%*
BcFLU					39.5 ± 1.0	21.1 ± 1.9	-47% ± 4%*
1-MPYR	21.5 ± 1.4	17.0 ± 0.3	23.1 ± 1.4	15.9 ± 1.0	18.9 ± 0.4	8.2 ± 0.8	-36% ± 6%*
BaA	130.2 ± 5.4	99.3 ± 2.5	135.8 ± 9.4	102.3 ± 4.6	133.2 ± 4.6	83.8 ± 4.9	-28% ± 3%*
CHR + TRI	138.6 ± 5.8	139.4 ± 6.6	149.2 ± 11.1	132.8 ± 7.9	98.0 ± 18.4	106.9 ± 3.6	3% ± 10%
BbF	650.0 ± 33.8	641.8 ± 27.3	668.5 ± 44.4	590.7 ± 29.5	440.8 ± 6.0	440.0 ± 9.9	-7% ± 3%*
BkF	179.0 ± 10.7	172.4 ± 7.9	182.5 ± 14.5	154.7 ± 9.5	146.8 ± 2.1	132.1 ± 2.9	-9% ± 3%*
BeP	342.7 ± 16.6	327.4 ± 12.3	353.0 ± 24.7	309.4 ± 16.1	236.5 ± 2.7	210.9 ± 5.8	-9% ± 3%*
BaP	230.6 ± 11.2	231.9 ± 9.4	245.8 ± 18.2	197.5 ± 10.4	178.8 ± 3.6	93.0 ± 4.6	-22% ± 8%*
DahA+DacA	71.6 ± 3.7	70.3 ± 2.5	75.0 ± 5.4	67.4 ± 3.9	17.8 ± 0.3	15.4 ± 0.6	-8% ± 3%

Appendix D.6 (continued)

Compound	PKU B (n=3)		PKU C (n=3)		PKU-6 (n=3)		Avg. %change
	Unexposed	Exposed	Unexposed	Exposed	Unexposed	Exposed	
IcdP	481.8 ± 22.1	486.6 ± 21.4	497.5 ± 34.5	462.1 ± 30.3	242.9 ± 1.6	222.2 ± 5.4	-5% ± 3%
BghiP	494.8 ± 26.9	468.8 ± 19.4	508.9 ± 37.7	445.8 ± 29.2	255.1 ± 0.9	216.2 ± 7.7	-11% ± 3%*
<b>NPAHs</b>							
1-NN	0.7 ± 0.4	<b>0.5</b>			0.4 ± 0.1	0.1 ± 0.0	143% ± 198%
2-NN	0.7 <sup>1</sup>	0.7 <sup>1</sup>			0.6 ± 0.1	0.5 ± 0.01	-14% ± 6%
3-NBP					0.8 <sup>1</sup>	0.7 <sup>1</sup>	-13%
9-NAN	54.6 ± 3.4	10.7 ± 1.7	72.2 ± 7.3	8.8 ± 0.7	49.5 ± 1.7	6.9 ± 0.9	-85% ± 1%*
3-NPH	5.0 ± 0.4	3.9 ± 0.1	6.0 ± 0.6	3.8 ± 0.5	1.4 ± 0.04	0.9 ± 0.1	-32% ± 3%*
2-+3-NF	90.2 ± 7.0	85.7 ± 1.4	114.5 ± 10.5	82.5 ± 7.3	49.5 ± 0.8	39.2 ± 2.1	-18% ± 4%*
1-NP	0.9 ± 0.2	3.8 ± 0.2	0.7 ± 0.03	4.0 ± 0.3	3.3 ± 0.04	12.1 ± 1.9	376% ± 54%*
2-NP	17.4 ± 1.2	17.0 ± 0.8	17.1 ± 2.0	15.4 ± 1.3	11.2 ± 0.2	8.6 ± 1.1	-11% ± 5%
7-NBaA	18.5 ± 1.2	6.6 ± 1.0	18.0 ± 1.5	5.3 ± 0.4	21.6 ± 0.4	6.3 ± 0.4	-68% ± 3%*
6-NBaP	<b>5.3</b>	52.8 ± 11.2	<b>5.3</b>	21.4 ± 5.8 <sup>2</sup>	<b>6.1</b>	29.1 ± 7.6	552% ± 131%*



**Appendix D.7:** Means and standard errors of PAH and NPAH masses (ng) measured in PKU filters used for the chemical study of O<sub>3</sub> exposure. In the case that a compound was not detected in all samples, superscript denotes number of samples detected. Numbers in bold are estimated detection limits. An asterisk indicates the statistically significant difference in mass (p-value < 0.05).

Compound	PKU D (n=2)		PKU-10 (n=3)		PKU-11 (n=3)		Avg. %change
	Unexposed	Exposed	Unexposed	Exposed	Unexposed	Exposed	
<b>PAHs</b>							
NAP	27.0 ± 4.5	20.2 ± 0.6	9.6 ± 2.9	10.2 ± 2.1	12.4 ± 0.6	15.8 ± 3.5	14% ± 17%
1-MNAP			8.1 ± 1.0	9.0 ± 0.8	9.6 ± 0.5	10.1 ± 1.5	10% ± 10%
2,6-DMNAP			4.5 ± 0.6 <sup>2</sup>	5.8 ± 0.6 <sup>2</sup>	5.2 ± 0.5 <sup>2</sup>	4.1 ± 2.1 <sup>2</sup>	25% - 13%
1,3-DMNAP	7.5 ± 2.5	5.7 ± 2.0	6.0 ± 0.9	8.6 ± 1.1	8.0 ± 1.1	9.8 ± 0.4	22% ± 14%
ACY	6.5 ± 0.4	5.3 ± 1.1	3.9 ± 0.1 <sup>2</sup>	3.8 ± 0.6 <sup>2</sup>	5.4 ± 0.3	4.2 ± 0.7	-15% ± 6%
FLU	13.5 ± 2.4	9.9 ± 0.5	11.1 ± 1.0	9.2 ± 1.3	14.1 ± 0.9	10.8 ± 1.4	-21% ± 5%*
DBT	11.0 ± 1.5	10.1 ± 1.4	11.9 ± 0.1	9.0 ± 1.0	15.4 ± 0.7	9.0 ± 1.1	-26% ± 8%*
PHE	147.6 ± 21.4	98.0 ± 4.8	104.9 ± 6.8	85.5 ± 7.4	161.2 ± 11.7	119.1 ± 7.2	-25% ± 4%*
ANT	10.7 ± 0.7	8.6 ± 0.1	9.0 ± 1.0	8.0 ± 1.2	13.3 ± 1.0	10.4 ± 0.8	-16% ± 8%*
2-MPHE	48.0 ± 10.3	34.7 ± 1.3	51.0 ± 3.1	42.3 ± 3.0	67.2 ± 3.3	48.8 ± 4.0	-22% ± 5%*
2-MANT	5.1 ± 0.3	4.4 ± 0.6					
1-MPHE	27.7 ± 5.6	19.0 ± 1.5	36.4 ± 2.2	30.8 ± 1.1	45.8 ± 0.8	30.7 ± 3.2	-25% ± 5%*
3,6-DPHE	3.7 ± 0.6	<b>2.7</b>			10.3 ± 4.0 <sup>2</sup>	<b>5.7</b>	-30% ± 12%
RET	43.2 ± 9.9	24.5 ± 1.8	100.5 ± 8.5	74.9 ± 8.3	72.2 ± 7.5	56.6 ± 8.3	-28% ± 4%*
FLA	527.1 ± 156.7	389.2 ± 47.5	250.4 ± 14.2	204.5 ± 12.4	498.7 ± 14.4	341.1 ± 26.6	-23% ± 7%*
PYR	313.5 ± 45.2	186.6 ± 8.0	147.5 ± 6.3	83.1 ± 6.3	252.0 ± 9.1	143.4 ± 7.4	-42% ± 2%*
BcFLU			34.9 ± 1.7	21.8 ± 1.5	48.4 ± 1.8	28.5 ± 1.9	-39% ± 2%*
1-MPYR	24.2 ± 3.6	13.4 ± 0.1	15.9 ± 1.2	9.0 ± 0.7	20.8 ± 1.2	11.5 ± 0.9	-44% ± 2%*
BaA	154.0 ± 17.1	89.4 ± 2.4	75.5 ± 2.4	46.0 ± 3.4	103.3 ± 3.7	63.8 ± 3.7	-39% ± 1%*
CHR + TRI	219.8 ± 36.2	140.2 ± 8.9	89.8 ± 3.7	67.8 ± 4.0	133.5 ± 6.3	105.1 ± 5.6	-26% ± 3%*
BbF	848.2 ± 162.5	631.6 ± 16.0	261.5 ± 8.1	209.5 ± 9.2	336.5 ± 8.7	287.7 ± 10.7	-19% ± 3%*
BkF	223.1 ± 47.5	144.8 ± 4.7	69.7 ± 2.7	44.1 ± 2.5	96.2 ± 1.6	67.8 ± 5.7	-33% ± 3%*
BeP	438.5 ± 66.3	304.0 ± 7.6	138.9 ± 4.6	91.9 ± 4.9	184.0 ± 5.2	136.9 ± 6.8	-30% ± 2%*
BaP	250.3 ± 34.7	133.4 ± 4.9	85.1 ± 4.2	45.8 ± 2.8	124.0 ± 3.0	72.4 ± 3.3	-44% ± 2%*
DahA+DacA	83.4 ± 11.1	51.1 ± 3.5	9.5 ± 0.3	5.7 ± 0.3	12.4 ± 0.4	8.2 ± 0.5	-37% ± 2%*
IcdP	465.7 ± 62.0	303.3 ± 16.7	129.0 ± 3.8	87.2 ± 4.1	171.6 ± 4.6	124.8 ± 4.6	-31% ± 2%*

Appendix D.7 (continued)

Compound	PKU D (n=2)		PKU-10 (n=3)		PKU-11 (n=3)		Avg. %change
	Unexposed	Exposed	Unexposed	Exposed	Unexposed	Exposed	
BghiP	444.4 ± 77.8	279.5 ± 15.7	129.1 ± 4.1	82.1 ± 3.6	167.3 ± 5.2	118.3 ± 4.5	-34% ± 2%*
<b>NPAHs</b>							
1-NN	0.6 <sup>1</sup>	0.48 <sup>1</sup>	0.9 ± 0.1	1.0 ± 0.01	0.7 ± 0.1	0.5 ± 0.02	5% ± 19%
2-NN			0.8 ± 0.1	0.9 ± 0.03	0.8 ± 0.03	0.7 ± 0.02	-3% ± 7%
3-NBP			1.2 ± 0.1	1.3 ± 0.1	1.6 ± 0.1	1.3 ± 0.02	-3% ± 10%
3-NDB					2.8 <sup>1</sup>	2.5 <sup>1</sup>	-9%
9-NAN	79.7 ± 13.4	70.7 ± 22.3	32.5 ± 5.0	18.0 ± 1.6	16.1 ± 0.9	7.9 ± 0.4	-24% ± 15%
3-NPH	3.1 ± 1.1	4.37 ± 1.6	1.5 ± 0.3	1.3 ± 0.1	1.2 ± 0.1	1.0 ± 0.1	17% ± 26%
2-+3-NF	151.3 ± 25.0	203.3 ± 69.0	31.4 ± 2.9	24.8 ± 0.9	34.6 ± 1.8	29.2 ± 1.5	4% ± 17%
1-NP	1.9 ± 0.5	1.4 ± 0.4	6.6 ± 0.8	6.2 ± 0.6	5.9 ± 1.0	6.3 ± 0.3	1% ± 5%
2-NP			4.0 ± 0.5	3.1 ± 0.2	2.9 <sup>1</sup>	2.8 <sup>1</sup>	-18% ± 6%
2,8-DNDBT			1.7 ± 0.4 <sup>2</sup>	1.4 ± 0.04 <sup>2</sup>			-14% ± 20%
7-NBaA	16.1 ± 0.8	12.0 ± 0.9	11.0 ± 1.6	7.4 ± 0.8	3.4 ± 0.1	2.1 ± 0.01	-28% ± 8%*
1-NTR			1.7 ± 0.4	1.5 ± 0.5			-15% ± 15%
6-NCH			1.3 ± 0.2	1.2 ± 0.3			-13% ± 23%
3-NBENZ			1.2 ± 0.2 <sup>2</sup>	1.3 ± 0.03 <sup>2</sup>			
2-NTR			1.1 ± 0.2	1.0 ± 0.3			-14% ± 21%
1,8-DNP					1.7 ± 0.1 <sup>2</sup>	<b>1.6<sup>2</sup></b>	-5% ± 3%
6-NBaP	17.3 <sup>1</sup>	5.3 <sup>1</sup>			4.8 <sup>1</sup>	3.8 <sup>1</sup>	24% ± 45%

**Appendix D.8:** Means and standard errors of PAH and NPAH masses (ng) measured in Riverside filters used for the chemical study of NO<sub>3</sub>/N<sub>2</sub>O<sub>5</sub> exposure. In the case that a compound was not detected in all samples, superscript denotes number of samples detected. Numbers in bold are estimated detection limits. An asterisk indicates the statistically significant difference in mass (p-value < 0.05).

Compound	R-671 (n=3)		R-672 (n=3)		R-673 (n=3)		Avg. %change
	Unexposed	Exposed	Unexposed	Exposed	Unexposed	Exposed	
<b>PAHs</b>							
NAP	2.5 ± 0.7	1.7 ± 0.3	1.8 ± 0.2	4.3 ± 1.0	3.6 ± 0.3 <sup>2</sup>	3.9 ± 0.7 <sup>2</sup>	47% ± 39%
FLU	4.8 <sup>1</sup>	3.5 <sup>1</sup>	3.7 ± 0.2 <sup>2</sup>	2.1 ± 2.1 <sup>2</sup>	4.2 ± 0.1 <sup>2</sup>	<b>3.5</b>	-28% ± 20%
DBT	<b>0.6</b> <sup>2</sup>	1.8 ± 0.3 <sup>2</sup>	0.6 ± 0.02 <sup>2</sup>	2.3 ± 0.3 <sup>2</sup>	1.3 ± 0.3	6.8 ± 4.5	515% ± 345%
PHE	1.6 ± 0.5	3.0 ± 0.6	1.5 ± 0.3	4.8 ± 2.2	4.4 ± 0.5	10.0 ± 3.5	195% ± 74%*
2-MPHE			<b>5.0</b>	5.3 <sup>1</sup>	6.0 ± 0.6	13.0 ± 5.0	97% ± 77%
1-MPHE			<b>4.0</b>	5.9 <sup>1</sup>	4.1 ± 0.1	7.1 ± 2.7	70% ± 49%
FLA	5.3 ± 0.2	6.1 ± 0.4	4.9 ± 0.2	6.0 ± 0.5	8.0 ± 1.6	6.3 ± 1.0	8% ± 10%
PYR	4.4 ± 0.1	5.0 ± 0.1	4.5 ± 0.2	4.6 ± 0.4	6.0 ± 1.0	4.7 ± 0.03	-0.3% ± 6%
BaA	1.7 ± 0.5 <sup>2</sup>	1.6 ± 0.5 <sup>2</sup>			2.4 ± 0.1	<b>1.2</b>	-24% ± 27%
CHR + TRI	1.9 ± 0.1	2.1 ± 0.1	1.8 ± 0.1	1.9 ± 0.1	2.5 ± 0.5	2.1 ± 0.1	2% ± 6%
BbF	5.2 ± 0.5	5.7 ± 0.1	4.8 ± 0.1	5.2 ± 0.2	7.0 ± 1.7	5.2 ± 0.2	-0.02% ± 7%
BkF					2.7 <sup>1</sup>	2.2 <sup>1</sup>	-17%
BeP	4.2 ± 0.2	4.6 ± 0.1	4.0 ± 0.2	4.2 ± 0.2	5.1 ± 0.7	4.2 ± 0.1	-0.4% ± 5%
BaP					9.3 <sup>1</sup>	8.8 <sup>1</sup>	-6%
IcdP	3.6 ± 0.3	3.9 ± 0.2	3.4 ± 0.1	3.5 ± 0.1	4.4 ± 0.7	3.4 ± 0.1	-1% ± 6%
BghiP	5.6 ± 0.4	6.5 ± 0.01	5.7 ± 0.1	5.9 ± 0.3	6.7 ± 0.6	6.0 ± 0.2	3% ± 5%
<b>NPAHs</b>							
1-NN			0.4 <sup>1</sup>	<b>0.1</b>			-66%
2-NN			0.3 <sup>1</sup>	<b>0.2</b>			-53%
9-NAN	0.3 <sup>1</sup>	<b>0.2</b>			0.4 ± 0.1 <sup>2</sup>	<b>0.2</b>	-34% ± 12%
3-NPH	0.3 ± 0.1	0.3 ± 0.01	0.2 ± 0.1	0.3 ± 0.1	0.1 <sup>1</sup>	0.2 <sup>1</sup>	52% ± 37%
2-+3-NF	4.6 ± 0.2	4.2 ± 0.3	5.3 ± 0.3	4.9 ± 0.2	5.3 ± 0.3	5.2 ± 0.3	-5% ± 6%
1-NP	0.2 ± 0.1	0.2 ± 0.02	0.3 ± 0.1	0.3 ± 0.03	0.3 ± 0.04	0.3 ± 0.03	3% ± 8%
1-NTR	0.3 <sup>1</sup>	<b>0.2</b>					-7%

**Appendix D.9:** Means and standard errors of PAH and NPAH masses (ng) measured in Riverside filters used for the chemical study of OH radical exposure. In the case that a compound was not detected in all samples, superscript denotes number of samples detected. Numbers in bold are estimated detection limits. An asterisk indicates the statistically significant difference in mass (p-value < 0.05).

Compound	R-661 (n=3)		R-662 (n=3)		R-673 (n=3)		Avg. %change
	Unexposed	Exposed	Unexposed	Exposed	Unexposed	Exposed	
<b>PAHs</b>							
NAP	6.1 <sup>1</sup>	2.4 <sup>1</sup>			5.1 <sup>1</sup>	<b>3.2<sup>1</sup></b>	-49% ± 12%
1-MNAP	4.7 ± 0.2 <sup>2</sup>	5.4 ± 0.2 <sup>2</sup>	5.0 <sup>1</sup>	<b>4.1</b>	4.8 ± 0.4	4.7 ± 0.3	2% ± 8%
FLU	<b>3.5</b>	4.9 ± 0.9	3.7 <sup>1</sup>	<b>3.5</b>	3.9 ± 0.2 <sup>2</sup>	3.6 ± 0.1 <sup>2</sup>	16% ± 15%
DBT	0.6 <sup>1</sup>	1.1 <sup>1</sup>	0.8 ± 0.2 <sup>2</sup>	<b>0.6</b>	0.6 ± 0.2	0.8 ± 0.3	48% ± 37%
PHE	2.7 ± 0.7	11.0 ± 2.6	3.8 ± 1.1	5.3 ± 0.3	3.2 ± 1.1	6.1 ± 1.1	232% ± 90%*
ANT					1.3 <sup>1</sup>	1.4 <sup>1</sup>	-15% ± 73%
2-MPHE	6.0 ± 0.3	8.0 ± 0.3	5.9 ± 0.2	7.0 ± 0.7	5.4 ± 0.2	6.8 ± 0.3	26% ± 6%*
1-MPHE	<b>4.0</b>	4.4 ± 0.3	<b>4.0</b>	4.2 ± 0.2 <sup>2</sup>	<b>4.0</b>	4.0 <sup>1</sup>	8% ± 4%*
FLA	6.2 ± 0.2	7.6 ± 0.4	6.5 ± 0.1	6.6 ± 0.4	5.9 ± 0.3	6.6 ± 0.2	12% ± 4%*
PYR	5.1 ± 0.1	5.9 ± 0.2	5.6 ± 0.4	5.9 ± 0.4	5.1 ± 0.2	5.9 ± 0.2	14% ± 2%*
BaA	<b>1.2</b>	2.1					84%
CHR + TRI	2.0 ± 0.2	2.1 ± 0.1	2.1 ± 0.1	2.8 ± 0.2	1.8 ± 0.1	2.4 ± 0.2	25% ± 8%*
BbF	5.4 ± 0.2	5.5 ± 0.2	5.7 ± 0.2	6.2 ± 0.5	5.1 ± 0.3	5.3 ± 0.2	5% ± 3%
BeP	4.8 ± 0.1	5.3 ± 0.3	4.9 ± 0.2	5.3 ± 0.4	4.5 ± 0.3	5.1 ± 1.0	11% ± 7%
IcdP	4.1 ± 0.1	4.1 ± 0.2	4.1 ± 0.03	4.4 ± 0.3	4.0 ± 0.3	4.0 ± 0.2	2% ± 3%
BghiP	6.6 ± 0.1	6.5 ± 0.4	7.1 ± 0.4	7.4 ± 0.5	6.4 ± 0.3	6.8 ± 0.3	3% ± 3%
<b>NPAHs</b>							
1-NN	0.2 ± 0.1 <sup>2</sup>	<b>0.1</b>					55% ± 112%
2-NN	0.6 ± 0.1 <sup>2</sup>	<b>0.2</b>	0.4 <sup>1</sup>	0.2 <sup>1</sup>			-70% ± 3%
9-NAN	0.3 ± 0.03 <sup>2</sup>	<b>0.2</b>					-31% ± 7%
3-NPH	0.6 ± 0.1 <sup>2</sup>	0.2 ± 0.1 <sup>2</sup>	0.3 ± 0.1	0.4 ± 0.0	0.4 ± 0.1 <sup>2</sup>	0.2 ± 0.1 <sup>2</sup>	-0.2% ± 37%
2-+3-NF	4.9 ± 0.02	4.6 ± 0.1	5.4 ± 0.1	4.7 ± 0.1	4.5 ± 0.1	4.0 ± 0.1	-10% ± 2%*
1-NP	0.3 ± 0.04	0.3 ± 0.1	0.3 ± 0.03	0.3 ± 0.03	0.2 ± 0.02	0.3 ± 0.02	8% ± 5%

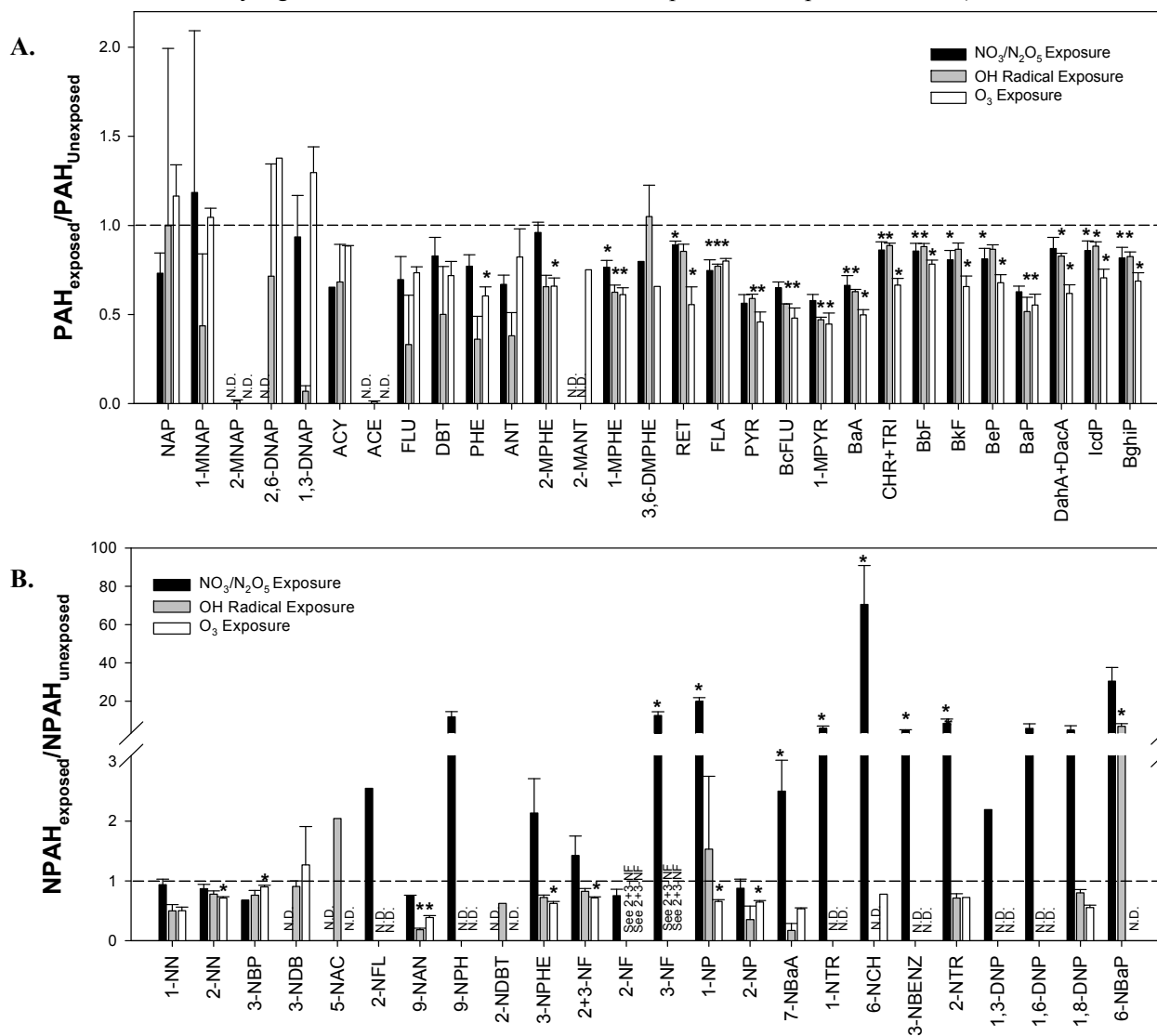
**Appendix D.10:** Means and standard errors of PAH and NPAH masses (ng) measured in Riverside filters used for the chemical study of O<sub>3</sub> exposure. In the case that a compound was not detected in all samples, superscript denotes number of samples detected. Numbers in bold are estimated detection limits. An asterisk indicates the statistically significant difference in mass (p-value < 0.05).

Compound	R-651 (n=3)		R-652 (n=3)		R-653 (n=3)		Avg. %change
	Unexposed	Exposed	Unexposed	Exposed	Unexposed	Exposed	
<b>PAHs</b>							
NAP	4.8 <sup>1</sup>	0.8 <sup>1</sup>	4.5 <sup>1</sup>	<b>3.2</b>			-56% ± 28%
1-MNAP	4.6 <sup>1</sup>	<b>4.1</b>					-11%
2,6-DMNAP			1.4 <sup>1</sup>	1.55 <sup>1</sup>			9%
FLU	5.2 <sup>1</sup>	<b>3.5</b>					-32%
DBT	3.9 ± 0.3 <sup>2</sup>	2.0 ± 1.5 <sup>2</sup>	1.9 ± 1.3 <sup>2</sup>	1.9 ± 1.3 <sup>2</sup>	3.7 ± 0.2 <sup>2</sup>	3.1 ± 0.01 <sup>2</sup>	38% ± 82%
PHE	5.7 ± 2.9 <sup>2</sup>	2.0 ± 0.6 <sup>2</sup>	2.7 ± 1.0	4.1 ± 1.8	3.0 ± 0.9	1.7 ± 0.7	22% ± 57%
ANT							
2-MPHE	6.7 ± 0.7 <sup>2</sup>	<b>5.0</b>	6.8 ± 1.8 <sup>2</sup>	8.3 ± 2.1 <sup>2</sup>	9.2 <sup>1</sup>	<b>5.0</b>	-3% ± 28%
1-MPHE			<b>4.0</b>	4.9 ± 0.5 <sup>2</sup>			
FLA	8.6 ± 2.7	6.0 ± 0.3	6.4 ± 0.8	6.5 ± 1.0	5.9 ± 0.2	5.7 ± 0.3	-5% ± 10%
PYR	6.4 ± 1.6	4.9 ± 0.2	5.4 ± 0.3	5.4 ± 0.7	5.2 ± 0.2	4.8 ± 0.1	-8% ± 6%
BaA	3.0 ± 0.6	2.0 ± 0.4	2.3 ± 0.1	1.8 ± 0.9	2.4 ± 0.04	2.3 ± 0.04	-19% ± 13%
CHR + TRI	2.5 ± 0.2	2.2 ± 0.1	2.3 ± 0.2	2.5 ± 0.3	2.1 ± 0.1	2.4 ± 0.1	4% ± 5%
BbF	6.9 ± 1.1	6.0 ± 0.2	6.0 ± 0.2	6.5 ± 0.8	5.8 ± 0.1	6.1 ± 0.1	2% ± 6%
BkF	2.6 <sup>1</sup>	2.2 <sup>1</sup>					-14%
BeP	5.4 ± 0.6	4.8 ± 0.1	5.0 ± 0.1	5.2 ± 0.5	4.8 ± 0.1	4.8 ± 0.1	-2% ± 4%
DahA+DacA							
IcdP	4.8 ± 0.6	4.0 ± 0.1	4.3 ± 0.2	4.6 ± 0.4	4.4 ± 0.2	4.1 ± 0.4	-5% ± 5%
BghiP	7.5 ± 0.6	6.8 ± 0.3	7.2 ± 0.4	7.6 ± 0.9	7.2 ± 0.1	7.0 ± 0.4	-2% ± 4%
<b>NPAHs</b>							
2-NN	0.5 <sup>1</sup>	0.2 <sup>1</sup>					-67%
3-NPH	0.4 ± 0.01	0.3 ± 0.01	0.4 ± 0.01	0.3 ± 0.01	0.4 ± 0.01	0.3 ± 0.00	-12% ± 2%*
2+3-NF	4.5 ± 0.1	4.6 ± 0.2	5.4 ± 0.5	4.1 ± 0.03	4.6 ± 0.1	3.9 ± 0.2	-13% ± 4%*
1-NP	0.3 ± 0.01	0.2 ± 0.01	0.2 ± 0.01	0.2 ± 0.01	0.2 ± 0.00	0.2 ± 0.01	-13% ± 3%*
1-NTR	0.5 ± 0.1 <sup>2</sup>	0.4 ± 0.1 <sup>2</sup>					-37% ± 6%

Appendix D.10 (continued)

Compound	R-651 (n=3)		R-652 (n=3)		R-653 (n=3)		Avg. %change
	Unexposed	Exposed	Unexposed	Exposed	Unexposed	Exposed	
6-NCH	0.3 ± 0.1 <sup>2</sup>	<b>0.1</b>					-65% ± 7%
3-NBENZ	0.8 <sup>1</sup>	0.5 <sup>1</sup>					-43%
2-NTR	0.7 ± 0.03 <sup>2</sup>	0.4 ± 0.1 <sup>2</sup>					-45% ± 17%

**Appendix D.11:** A.  $PAH_{\text{exposed}}/PAH_{\text{unexposed}}$  and B.  $NPAH_{\text{exposed}}/NPAH_{\text{unexposed}}$  of Beijing PM filters (n=3) used for the mutagenicity study. An asterisk denotes the statistically significant difference between the unexposed and exposed masses. (N.D. = Not detected)



**Appendix D.12:** Means and standard errors of PAH and NPAH masses (ng) measured in PKU filters used for the mutagenicity study of NO<sub>3</sub>/N<sub>2</sub>O<sub>5</sub> radical exposure. In the case that a compound was not detected in all samples, superscript denotes number of samples detected. Numbers in bold are estimated detection limits. An asterisk indicates the statistically significant difference in mass (p-value < 0.05).

Compound	PKU-3		PKU-4		PKU-5		Avg. %change
	Unexposed	Exposed	Unexposed	Exposed	Unexposed	Exposed	
<b>PAHs</b>							
NAP	8.8	5.7	8.2	7.9	22.2	13.1	-27% ± 11%
1-MNAP			<b>3.3</b>	6.8	11.8	<b>3.3</b>	19% ± 91%
1,3-DMNAP	5.3	5.9	<b>4.8</b>	5.9	10.1	<b>4.8</b>	-6% ± 23%
ACY					9.6	6.3	-35%
FLU	9.1	6.5	9.0	8.2	26.7	12.4	-30% ± 13%
DBT	7.9	7.2	7.3	7.0	23.7	14.7	-17% ± 11%
PHE	62.9	50.1	69.1	60.0	241.8	156.8	-23% ± 6%
ANT	7.4	5.4	6.9	<b>4.9</b>	20.5	11.6	-33% ± 5%
2-MPHE	34.4	33.6	35.0	36.8	95.7	81.5	-4% ± 6%
1-MPHE	24.3	19.1	26.8	18.6			-26% ± 5%*
3,6-DPHE					7.9	6.3	-20%
RET	73.9	62.7	92.9	85.8	70.5	63.4	-11% ± 2%*
FLA	167.4	116.0	212.6	144.9	619.5	536.7	-25% ± 6%*
PYR	110.0	52.3	153.0	87.4	382.5	246.1	-44% ± 5%
BcFLU	31.0	18.2	35.4	24.3	93.6	63.5	-35% ± 3%
1-MPYR	14.7	7.8	16.2	10.5	32.3	18.2	-42% ± 3%
BaA	86.4	53.5	83.6	50.1	109.9	147.5	-34% ± 5%*
CHR + TRI	85.6	75.8	82.8	64.0	246.6	228.7	-14% ± 5%*
BbF	380.9	328.1	280.1	218.6	786.4	729.5	-14% ± 4%*
BkF	107.6	86.9	78.7	56.2	257.3	231.0	-19% ± 5%*
BeP	200.6	163.0	149.3	105.9	440.1	402.3	-19% ± 6%*
BaP	123.5	70.1	102.6	65.6	320.3	216.3	-37% ± 3%
DahA+DacA	14.3	12.5	10.3	7.9	33.5	32.7	-13% ± 6%
IcdP	194.8	169.1	129.0	98.0	412.3	390.8	-14% ± 5%*



Appendix D.12 (continued)

Compound	PKU-3		PKU-4		PKU-5		Avg. %change
	Unexposed	Exposed	Unexposed	Exposed	Unexposed	Exposed	
BghiP	202.7	164.4	125.1	89.9	415.5	383.6	-18% ± 6%*
<b>NPAHs</b>							
1-NN	0.4	0.4	0.5	0.6	0.8	0.6	-6% ± 9%
2-NN	0.6	0.5	0.5	0.5	1.0	0.7	-13% ± 7%
3-NBP					1.3	0.9	-32%
2-NFL			<b>0.2</b>	0.6			155%
9-NAN	47.9	34.3	21.0	15.7	75.1	57.8	26% ± 2%
9-NPH	<b>0.5</b>	4.2	<b>0.5</b>	8.7	<b>0.5</b>	5.3	1090% ± 268%
3-NPH	1.4	2.6	1.2	3.7	3.4	4.5	114% ± 58%
2+3-NF	32.8	43.7	25.5	51.6	205.0	183.6	42.6% ± 32.7%
2-NF	29.1	25.7	40.5	21.9	199.9	167.0	-25% ± 11%
3-NF	<b>1.1</b>	10.3	<b>1.1</b>	17.5	<b>1.1</b>	12.5	1156% ± 199%*
1-NP	3.5	61.6	3.2	75.8	6.5	121.9	1896% ± 195%*
2-NP	10.4	7.5			31.0	32.0	-12.4% ± 16%
7-NBaA	19.1	39.4	8.0	28.2	26.8	51.2	150% 52%*
1-NTR	<b>0.6</b>	3.9	<b>0.6</b>	4.6	<b>0.6</b>	2.3	493% ± 114%*
6-NCH	<b>0.6</b>	19.8	0.3	25.5	<b>0.2</b>	16.3	6955% ± 2034%*
3-NBENZ	<b>0.6</b>	3.0	<b>1.0</b>	3.3	<b>1.0</b>	5.4	351% ± 63%*
2-NTR	<b>0.4</b>	3.1	<b>0.4</b>	5.0	<b>0.4</b>	2.9	840% ± 173%*
1,3-DNP			<b>0.7</b>	1.6			119%
1,6-DNP	<b>0.6</b>	2.1	<b>0.6</b>	6.7	<b>0.6</b>	2.2	483% ± 242%
1,8-DNP			<b>1.6</b>	11.8	<b>1.6</b>	4.2	389% ± 329%
6-NBaP	<b>6.1</b>	159.2	<b>6.1</b>	127.4	<b>6.1</b>	273.5	2946% ± 723%

**Appendix D.13:** Means and standard errors of PAH and NPAH masses (ng) measured in PKU filters used for the mutagenicity study of OH radical exposure. In the case that a compound was not detected in all samples, superscript denotes number of samples detected. Numbers in bold are estimated detection limits. An asterisk indicates the statistically significant difference in mass (p-value < 0.05).

Compound	PKU-7		PKU-8		PKU-9		Avg. %change
	Unexposed	Exposed	Unexposed	Exposed	Unexposed	Exposed	
<b>PAHs</b>							
NAP	3.8	11.5	968.7	6.2	2,086.3	3.5	0.1% ± 100%
2-MNAP			290.8	<b>6.2</b>	626.8	<b>6.2</b>	-98% ± 0.6%
1-MNAP	5.0	6.2	146.8	7.1	320.7	5.7	-56% ± 40%
2,6-DMNAP	<b>3.9</b>	7.8	63.0	9.2	141.1	<b>3.9</b>	-28% ± 63%
1,3-DMNAP			55.0	5.5	126.6	<b>4.8</b>	-93% ± 3%
ACY	4.5	5.0	9.5	4.8	11.9	5.3	-32% ± 21%
ACE			231.0	<b>3.4</b>	484.5	<b>3.4</b>	-99% ± 0.4%
FLU	8.3	7.3	123.4	8.4	311.3	12.6	-67% ± 28%
DBT	5.5	5.7	22.8	6.8	53.7	9.3	-50% ± 27%
PHE	99.7	61.2	248.2	68.2	390.4	75.6	-64% ± 13%
ANT	9.0	5.8	19.5	<b>4.9</b>	27.3	6.7	-62% ± 13%
2-MPHE	48.1	37.7	68.5	40.4	84.5	50.3	-34% ± 6%
1-MPHE	33.3	23.5	38.2	22.1	49.4	29.2	-37% ± 4%*
3,6-DPHE	<b>5.7</b>	6.7	6.9	8.8	8.1	<b>5.7</b>	5% ± 18%
RET	46.4	42.8	40.3	31.5	58.5	50.2	-15%
FLA	379.2	301.0	468.8	353.8	361.6	276.6	-23% ± 1%*
PYR	258.5	153.0	315.1	198.5	225.3	123.2	-41% ± 2%*
BcFLU	51.0	28.5	69.3	38.8	53.74	30.0	-44% ± 0.1*
1-MPYR	24.4	11.4	27.5	13.7	22.6	10.1	-53% ± 2*
BaA	124.7	75.8	159.0	99.6	110.69	72.0	-37% ± 1%*
CHR + TRI	136.9	118.9	219.0	200.3	165.01	144.5	-11% ± 1%*
BbF	403.8	363.1	753.0	676.5	630.9	533.9	-12% ± 2%*
BkF	126.8	116.9	252.8	220.9	208.8	167.8	-13% ± 3%
BeP	209.1	188.6	435.6	382.5	361.0	295.0	-13% ± 3%
BaP	163.5	59.0	300.0	187.7	217.8	122.4	-48% ± 8%*

Appendix D.13 (continued)

Compound	PKU-7		PKU-8		PKU-9		Avg. %change
	Unexposed	Exposed	Unexposed	Exposed	Unexposed	Exposed	
DahA+DacA	15.6	12.6	34.7	29.8	25.1	20.4	-17% ± 2%*
IcdP	227.0	196.6	422.6	393.9	337.4	287.3	-12% ± 3%*
BghiP	230.8	187.5	459.7	402.2	365.7	288.2	-17% ± 3%*
<b>NPAHs</b>							
1-NN	1.1	0.5	1.4	0.5	0.3	0.2	-50% ± 31%
2-NN	0.8	0.6	1.2	0.8	0.9	0.8	-22% ± 17%
3-NBP	1.2	0.9	1.7	1.0	1.3	1.2	-24% ± 25%
3-NDB			4.7	3.8	3.5	3.5	-9% ± 18%
5-NAC			0.4	0.9			
9-NAN	60.9	10.3	91.2	13.8	47.8	11.0	-82% ± 7%*
2-NDBT			0.5	0.3			-37%
3-NPH	1.5	1.2	3.5	2.3	3.0	2.1	-28% ± 12%
2-+3-NF	113.8	104.6	276.5	214.5	116.0	90.4	-18% ± 14%
1-NP	3.6	14.3	38.6	10.5	54.0	19.0	53% ± 366%
2-NP	8.0	6.4	154.5	21.3	210.7	24.4	-65% 68%
7-NBaA	9.0	3.7	193.4	10.5	208.7	10.3	-83% ± 35%
2-NTR			0.6	<b>0.4</b>	0.5	<b>0.4</b>	-29% ± 14%
1,8-DNP			3.2	2.8	2.8	2.1	-20% ± 11%
6-NBaP	<b>6.1</b>	28.8	<b>6.1</b>	58.1	8.6	56.7	591%* ± 418%*

**Appendix D.14:** Means and standard errors of PAH and NPAH masses (ng) measured in PKU filters used for the mutagenicity study of O<sub>3</sub> exposure. In the case that a compound was not detected in all samples, superscript denotes number of samples detected. Numbers in bold are estimated detection limits. An asterisk indicates the statistically significant difference in mass (p-value < 0.05).

Compound	PKU-12		PKU-13		PKU-14		Avg. %change
	Unexposed	Exposed	Unexposed	Exposed	Unexposed	Exposed	
<b>PAHs</b>							
NAP	12.14	15.0	17.1	24.4	12.0	9.9	16% ± 18%
1-MNAP	7.2	7.8	10.4	11.6	6.8	6.4	5% ± 5%
2,6-DMNAP			<b>3.9</b>	5.4			38%
1,3-DMNAP	<b>4.8</b>	5.5	7.1	10.3			30% ± 14%
ACY	4.9	4.3	9.4	8.3	4.9	4.4	-12% ± 0.2%
FLU	9.1	6.9	18.9	14.7	11.7	7.8	-27% ± 3%
DBT	8.6	7.0	23.7	13.4	12.1	9.4	-28% ± 8%
PHE	133.9	78.7	344.6	240.7	173.5	91.1	-40% ± 5%*
ANT	7.3	8.3	25.3	18.3	10.4	6.4	-18% ± 16%
2-MPHE	58.0	37.5	106.8	79.4	69.0	40.5	-34% ± 5%*
2-MANT			10.1	<b>7.6</b>			-25%
1-MPHE	42.6	26.5	80.3	54.0	45.2	24.4	-39% ± 4%*
3,6-DPHE			8.7	<b>5.7</b>			-34%
RET	89.3	39.8	100.7	75.7	71.4	33.6	-44% ± 10%*
FLA	463.3	367.9	1101.1	910.2	563.3	439.2	-20% ± 1%*
PYR	347.4	136.5	759.1	432.4	387.4	159.4	-54% ± 6%*
BcFLU	86.3	35.4	144.9	85.9	78.9	34.5	-52% ± 6%*
1-MPYR	38.8	14.4	61.8	35.2	32.9	13.1	-55% ± 6%*
BaA	221.5	101.6	372.6	207.3	190.6	91.3	-50% ± 3%*
CHR + TRI	221.1	139.7	446.5	330.6	235.6	146.7	-34% ± 4%*
BbF	598.9	451.6	1050.1	870.2	680.0	519.5	-22% ± 2%*
BkF	204.2	118.0	349.8	270.6	229.6	142.2	-34% ± 6%*
BeP	327.4	202.5	597.0	457.3	368.9	239.9	-32% ± 4%*
BaP	301.9	138.5	486.4	324.2	302.3	161.2	-45% ± 6%*
DahA+DacA	27.0	14.9	49.1	35.0	27.9	16.4	-38% ± 5%*
IcdP	363.3	234.9	593.8	476.1	413.2	276.2	-29% ± 5%*

Appendix D.14 (continued)

Compound	PKU-12		PKU-13		PKU-14		Avg. %change
	Unexposed	Exposed	Unexposed	Exposed	Unexposed	Exposed	
BghiP	390.1	244.1	635.8	494.7	426.0	280.8	-31% ± 5%*
<b>NPAHs</b>							
1-NN	1.4	0.6	1.9	1.2	2.8	1.2	-50% ± 6%
2-NN	0.9	0.6	1.4	1.0	1.5	1.0	-29 ± 2%*
3-NBP	2.1	1.8	3.4	3.2	2.1	2.0	-10% ± 3%*
3-NDB			5.9	5.1	<b>2.5</b>	4.4	31.4 ± 44%
9-NAN	121.4	42.2	120.0	54.5	83.9	29.7	-62% ± 3%*
3-NPH	3.6	2.0	2.8	1.9	3.1	2.0	-38% ± 3%*
2-+3-NF	112.9	77.7	188.5	141.5	172.5	121.4	-29% ± 2%*
1-NP	6.9	4.7	8.4	5.0	5.8	4.0	-34% ± 3%*
2-NP	16.3	10.0	18.4	12.8	17.4	10.8	-36% ± 3%*
7-NBaA	39.9	21.0	16.7	9.4	19.5	10.0	-47% ± 2%
6-NCH			0.2	<b>0.2</b>			-22%
2-NTR					0.5	<b>0.4</b>	-28%
1,8-DNP	3.4	<b>1.6</b>	4.9	3.0	3.1	1.8	-45% ± 4%

